Anastasia Malek *Editor*

Experimental Metastasis: Modeling and Analysis

Springer

Experimental Metastasis: Modeling and Analysis

Anastasia Malek
Editor

Experimental Metastasis: Modeling and Analysis

Springer

Editor
Anastasia Malek
Oncoendocrinology
Petrov Institute of Oncology
St Petersburg
Russia

ISBN 978-94-007-7834-4 ISBN 978-94-007-7835-1 (eBook)
DOI 10.1007/978-94-007-7835-1
Springer Dordrecht Heidelberg New York London

Library of Congress Control Number: 2013953922

Printed on acid-free paper

Springer is part of Springer Science+Business Media (www.springer.com)

Contents

Contributors

Alexander R. A. Anderson Integrated Mathematical Oncology, H. Lee Moffitt Cancer Center and Research Institute, Tampa, FL, USA

Niranjan Awasthi Department of Surgery, Division of Surgical Oncology, Hamon Center for Therapeutic Oncology Research, University of Texas, Southwestern, Dallas, USA

David Basanta Integrated Mathematical Oncology, H. Lee Moffitt Cancer Center and Research Institute, Tampa, FL, USA

Fariba Behbod Department of Pathology and Laboratory Medicine, The University of Kansas Medical Center, Kansas City, USA

Rolf A. Brekken Department of Surgery, Division of Surgical Oncology, Hamon Center for Therapeutic Oncology Research, University of Texas, Southwestern, Dallas, USA

Department of Pharmacology, Simmons Comprehensive Cancer Center, University of Texas, Southwestern, Dallas, USA

Ann F. Chambers London Regional Cancer Program and Department of Oncology, University of Western Ontario, London, Canada

Michael T. Dellinger Hamon Center for Therapeutic Oncology Research, University of Texas, Southwestern, Dallas, USA

Hanan Elsarraj Department of Pathology and Laboratory Medicine, The University of Kansas Medical Center, Kansas City, USA

Alexander G. Fletcher Wolfson Centre for Mathematical Biology, Mathematical Institute, Oxford University, Oxford, UK

Philip Gerlee Mathematical Sciences Division, University of Gothenburg, Gothenburg, Sweden

Chalmers University of Technology, Gothenburg, Sweden

Mark R. Gilbert Department of Otolaryngology-Head and Neck Surgery, School of Medicine, University of Pittsburgh, Pittsburgh, USA

Yvonne Kienast Pharma Research and Early Development, Roche Diagnostics GmbH, Penzberg, Germany

Seungwon Kim Department of Otolaryngology-Head and Neck Surgery, School of Medicine, University of Pittsburgh, Pittsburgh, USA

Chwee-Ming Lim Department of Otolaryngology Head and Neck Surgery, National University Health System Singapore, Singapore, Republic of Singapore

Philip K. Maini Wolfson Centre for Mathematical Biology, Mathematical Institute, Oxford University, Oxford, UK

Anastasia Malek Department of Oncoendocrinology, Petrov Institute of Oncology, Sankt-Petersburg, Russia

Antonia Marazioti Department of Physiology, Faculty of Medicine, University of Patras, Patras, Greece

Katherine T. Ostapoff Department of Surgery, Division of Surgical Oncology, Hamon Center for Therapeutic Oncology Research, University of Texas, Southwestern, Dallas, USA

Arindam Paul Department of Pathology and Laboratory Medicine, The University of Kansas Medical Center, Kansas City, USA

Roderich E. Schwarz IU Health Goshen Center for Cancer Care, Indiana University School of Medicine, Goshen, USA

Jacob G. Scott Integrated Mathematical Oncology, H. Lee Moffitt Cancer Center and Research Institute, Tampa, FL, USA

Wolfson Centre for Mathematical Biology, Mathematical Institute, Oxford University, Oxford, UK

Georgios T. Stathopoulos Department of Physiology, Faculty of Medicine, University of Patras, Patras, Greece

Shane Stecklein Department of Pathology and Laboratory Medicine, The University of Kansas Medical Center, Kansas City, USA

Jason L. Townson The University of New Mexico, Center for Micro-Engineered Materials, Albuquerque, USA

Kelli Valdez Department of Pathology and Laboratory Medicine, The University of Kansas Medical Center, Kansas City, USA

Chapter 1
Introduction: Experimental Metastasis

Anastasia Malek

Abstract The short introductory chapter is aimed to state importance of the cancer metastasis research, to review basic approach and to present content and structure of the book.

1.1 Metastases, the Hallmark of Cancer Disease

Metastatic spread is the most lethal aspect of cancer. The prognosis for cancer patients is determined by the speed and pattern of metastatic dissemination. For most tumour types, the diagnosis of metastatic cancer is regarded to indicate a terminal prognosis, and the effects of metastatic growth are thought to be responsible for more than 90 % of deaths of cancer patients [1, 2]. In contrast to therapy for local malignancies, therapeutic approaches to treat advanced cancer are significantly more variable and aggressive; therapy impacts many vital organs and produces significant side-effects. Currently, for most types of advanced cancers, therapeutic outcomes are disappointing. This situation induces development of palliative care approaches that can improve quality of life, and even prolong life, for cancer patients [3]. However, complete recovery remains a hope for all patients.

Intense study of the metastatic process is the only way to improve therapeutic results for patients with advanced cancer; therefore, it is an essential area of cancer research. Although development of metastases is a systemic disease process, the majority of research efforts have focused on understanding the process of local invasion. Changes in cell adhesion, activation of proteolysis, and the acquisition of motile properties by tumour cells are accepted as key events in local invasion. Upon detachment from the primary tumour and entry into the vascular system, survival of cancer cells is mediated by activation of endogenous morphogenetic processes such as epithelial-mesenchymal transition and resistance to anoikis. Further spread of cancer can follow various pathways, which are determined by many known as well as currently unknown factors.

A. Malek (✉)
Department of Oncoendocrinology, Petrov Institute of Oncology, Sankt-Petersburg, Russia
e-mail: anastasia@malek.com

A. Malek (ed.), *Experimental Metastasis: Modeling and Analysis,*
DOI 10.1007/978-94-007-7835-1_1,

Lymph node metastases represents the first step in tumor dissemination for many types of cancer, including head and neck, stomach, pancreas, colon, breast, cervix, and prostate. The presence of lymph node metastases is a key determinant in tumor staging, whereas spread of the tumor beyond regional lymph nodes is traditionally considered as indicator of poor prognosis. However, it is not simple penetration of lymphatic vessels by cancer cells; rather the lymphatic system plays an active role in the process of tumor dissemination. A primary tumor is considered to be capable of modifying the endothelium of adjacent lymph capillaries and inducing morphological alteration of lymph nodes even before metastases occur [4]. For instance, specific morphological changes have been observed in sentinel lymph nodes by growing melanoma. It has been suggested that these changes are induced by cancer cell–derived exosomes that "prepare" lymph nodes to accept of disseminating cancer cells [5]. Moreover, it is a well-known fact, that tumors can stimulate lymphogenesis around and inside the tumor mass. Despite the fact that intra-tumoural lymphatic vessels are considered to be non-functional, recent studies have revealed that their density strongly correlates with clinical parameters of cancers commonly considered to have a tendency for blood-mediated metastasis (i.e., lung carcinomas, kidney carcinomas, and neuroblastomas [6–8]. Lymph node colonization has been shown to be associated with distant organ metastasis in a rodent model [9]. As such, the role of the lymphatic system in cancer dissemination is not limited by implication of regional or distant lymph nodes; rather, it seems to have a general character. The role of particular molecular factors and whole regulatory network mediating interaction of tumors with the lymphatic system have been extensively reviewed [10, 11]. Keeping in mind the traditional "protective" anti-cancer function of the immune system, its role as an instigator for distant metastatic dissemination has been discussed in recent publications [12, 13].

The direction and efficacy of colonization to distant organs by cancer cells after they have entered the bloodstream is a major issue. In principle, circulating tumor cells have the potential to access many if not all organs of the body. Nevertheless, overt metastases do not necessarily form in all organs, and specific types of tumors exhibit preferential metastasis formation in certain organs. The lungs, liver, bone, and brain are frequent sites of metastasis formation by circulating tumor cells. Conversely, metastases virtually never form in skeletal muscle, despite its well-developed blood supply. A conceptual framework to understand these patterns of metastasis is provided by Paget's seed and soil hypothesis [14]. Various possible mechanisms may govern or at least simultaneously influence cancer dissemination. They include local vasculature structure, adhesion properties of endothelia, and the tissue environment supporting cancer cells proliferation. These aspects have been comprehensively reviewed in recent studies [2]. Investigation of the underlying molecular mechanisms of distant tumor dissemination via the bloodstream may result in new strategies to prevent or to treat metastatic disease.

1.2 Modelling Approaches

In order to study and accurately solve the complex interactions between tumor cells and the whole organism that occurs during metastatic dissemination, it is necessary to develop and to use appropriate models. It is an obvious fact that any experimental or computational model may reflect only certain features of the natural process. There are always factors missing or corrupted by modelling. Consideration of these aspects is an extremely important issue for conducting experiments, apply models, and extrapolating results.

In general, the metastatic process may be recapitulated in its entirety with in vivo models or may be dissected into single steps and assayed in vitro. Both approaches play essential roles, even considering that their results do not always correlate. Animal models obviously more closely reflect the actual process in humans; however, many factors cannot be controlled and may significantly impact the results. The in vitro approach also has shortcomings; it differs significantly from the actual metastatic process and can recapitulate only a single aspect of cancer cell vitality (i.e., proliferation rate, non-adherent growth ability, motility, invasiveness, and colony formation activity). Considering the genetic plasticity associated with cancer, tumor tissue is thought to be polyclonal and contains calls with various genetic alterations and at various states of proliferative activity. Cell lines established from tumor tissues and cultured in vitro for extended periods of time are established with the goal of being genetically uniform; however, the cell line may not permanently maintain the properties of the original tissue. For instance, correlations between the expression patterns of genes implicated in multi-drug resistance in clinical ovarian cancer samples and established cell lines have not been observed [15]. All the aspects differing cell culture experiments from the in vivo situation should be considered. In order to reduce the impact of in vitro culturing, preclinical studies are often performed using material obtained directly from patients and maintained ex vivo for as short a time period as possible [16].

Organotypic 3D co-culturing is an experimental approach that is (in terms of proximity to real situation) in between in vivo and in vitro models. By using various artificial substances such as Matrigel, Gelfoam, and Collagen Sponge, a three-dimensional culture mimicking specific tissue structure can be created. Co-culturing cancer cells in such a close-to-reality environment can combine the advantages of in vivo and in vitro methods and provide broad experimental resources.

1.3 The Book Content and Structure

The purpose of this book is to describe recent methodological approaches to cancer metastasis research. The focus of this book does not entail either methods of molecular biology or approaches to the general evaluation of metastatic properties of cancer cells. The issues regarding the study of the entire metastatic process and

relevant properties of cancer cells are addressed by an excellent laboratory manual written by D. R. Welsh [17]. Our book focuses on the study of advanced cancer biology with emphasis on certain clinically relevant pathways of cancer dissemination.

Chapter 2, 3, and 4 describe the methods applied to the investigation of head and neck, breast, and pancreatic cancers, respectively. The lymphatic system presents a primary dissemination pathway for these types of cancer; therefore, methods to evaluate lymphangitic spread of tumours are presented in detail. Each chapter begins with a short review of genetic and molecular features of certain cancer types; this aids in the assimilation of subsequent information. All chapters describe relevant in vivo models. In addition, Chap. 3 provides protocols for in vitro assays applicable to any cancer type. Some aspects of distant dissemination of pancreatic cancer are discussed in Chap. 4.

Metastatic spread targeting vital organs via the circulatory system is the focus of subsequent chapters. Chapter 5 and 6 are focused on approaches to the study of brain and lung metastases. These chapters include reviews of anatomic, morphologic, and molecular aspects implicated in colonization of these organs by circulating cancer cells. Relevant ex vivo and in vivo models are presented in detail, as well as advanced techniques to evaluate results of experiments. Thus, Chap. 5 presents a method of intravital multiphoton laser scanning microscopy that allows the observation of the process of metastasis formation at the single cell level. Chapter 6 presents the qPCR-based method for quantification of xenograft metastases burden with the limit of detection below 0.001 % of the total cell number. Both methods provide a novel opportunity to experimentally address unanswered questions of metastasis research and can be modified for other (in addition to brain and lung) applications.

Chapter 7 is devoted to metastasis via the portal vein system. The liver is a common site of metastases that originate from digestive system tumours. Considering the number of vital functions of this organ, its metastatic invasion is associated with profound morbidity and mortality. The unique anatomy of the liver and mechanisms of liver dissemination are discussed in the chapter, as well as relevant in vitro and in vivo experimental models.

Tumour dissemination within serous cavities (i.e., pleural and peritoneal) present a specific issue. This metastatic pathway is mediated by particular mechanisms; it has a typical clinical manifestations and assumes specific therapeutic approaches. Important aspects of malignant pleural effusion and relevant experimental models are presented in Chap. 8.

The book concludes with a review of a computational method to model and study the metastatic process. This last chapter has the focus of providing oncologists and cancer biologists with general concepts of the metastatic process from a mathematical point of view. As in many other areas of biological research, computational modelling has the potential potency to combine and clarify existing experimental data and to develop a hypothesis that can be further validated by experiments. Such combination of biological (in vitro and in vivo) and computational modelling appears to present the most effective approach for the study of the metastatic process.

Obviously, many important issues of experimental modelling are missing in each chapter as well as the book as whole. An extended references list, supplementing

each chapter, will facilitate retrieval of additional information. Moreover, many specific issues of experimental modelling such as models of prostate [18] or ovarian cancer [19] as well as modelling of bone metastasis [20] have been extensively reviewed in the literature. It is hoped that the theoretical and practical information presented here will provide a framework for an experimental approach to cancer metastasis research and aid researchers in the development of new models.

References

1. Sleeman J, Steeg PS (2010) Cancer metastasis as a therapeutic target. Eur J Cancer 46:1177–1180
2. Sleeman JP, Nazarenko I, Thiele W (2011) Do all roads lead to Rome? Routes to metastasis development. Int J Cancer 128:2511–2526
3. Gaertner J, Weingartner V, Wolf J, Voltz R (2013) Early palliative care for patients with advanced cancer: how to make it work? Curr Opin Oncol 25:342–352
4. Rinderknecht M, Detmar M (2008) Tumor lymphangiogenesis and melanoma metastasis. J Cell Physiol 216:347–354
5. Hood JL, San RS, Wickline SA (2011) Exosomes released by melanoma cells prepare sentinel lymph nodes for tumor metastasis. Cancer Res 71:3792–3801
6. Jin S, Zhu W, Shi Q, Zhang Z, Guo R (2012) Clinicopathological significance of lymphatic vessel density marked by D2–40 and E-cadherin expression in non-small-cell lung cancer. Med Oncol 29(5):3157–3161
7. Ozardili I, Guldur ME, Ciftci H, Bitiren M, Altunkol A (2012) Correlation between lymphangiogenesis and clinicopathological parameters in renal cell carcinom. Singapore Med J 53:332–335
8. Ramani P, Norton A, Somerville MS, May MT (2012) PROX1 lymphatic density correlates with adverse clinicopathological factors, lymph node metastases and survival in neuroblastomas. J Neurooncol 108(3):375–383
9. Hirakawa S, Brown LF, Kodama S, Paavonen K, Alitalo K et al (2007) VEGF-C-induced lymphangiogenesis in sentinel lymph nodes promotes tumor metastasis to distant sites. Blood 109:1010–1017
10. Achen MG, Stacker SA (2008) Molecular control of lymphatic metastasis. Ann N Y Acad Sci 1131:225–234
11. Schenck M, Rubben H, Gulbins E (2009) [Molecular aspects of lymph node metastasis]. Urologe A 48:6–11
12. Sleeman JP (2000) The lymph node as a bridgehead in the metastatic dissemination of tumors. Recent Results Cancer Res 157:55–81
13. Sleeman JP, Cady B, Pantel K (2012) The connectivity of lymphogenous and hematogenous tumor cell dissemination: biological insights and clinical implications. Clin Exp Metastasis 29:737–746
14. Paget S (1989) The distribution of secondary growths in cancer of the breast. 1889. Cancer Metastasis Rev 8:98–101
15. Gillet JP, Calcagno AM, Varma S, Marino M, Green LJ et al (2011) Redefining the relevance of established cancer cell lines to the study of mechanisms of clinical anti-cancer drug resistance. Proc Natl Acad Sci USA 108:18708–18713
16. Haglund C, Aleskog A, Nygren P, Gullbo J, Hoglund M et al (2012) In vitro evaluation of clinical activity and toxicity of anticancer drugs using tumor cells from patients and cells representing normal tissues. Cancer Chemother Pharmacol 69:697–707

17. Rusciano D, Welch DR, Burger MM (eds) (2000) Cancer metastasis: In vitro and in vivo experimental approaches. Laboratory techniques in biochemistry and molecular biology, vol 29. Elsevier B.V. (ISBN: 978-0-444-82372-4)
18. Chen L, Hann B, Wu L (2011) Experimental models to study lymphatic and blood vascular metastasis. J Surg Oncol 103:475–483
19. Fong MY, Kakar SS (2009) Ovarian cancer mouse models: a summary of current models and their limitations. J Ovarian Res 2:12
20. Rosol TJ, Tannehill-Gregg SH, LeRoy BE, Mandl S, Contag CH (2003) Animal models of bone metastasis. Cancer 97:748–757

Chapter 2
Head and Neck Cancer

Mark R. Gilbert, Chwee-Ming Lim and Seungwon Kim

Abstract Head and neck squamous cell carcinoma (HNSCC) is the sixth most common type of cancer worldwide. Although advance of conventional and development of new therapeutic approaches, including fractionated radiotherapy, targeted chemotherapy and concurrent radiotherapy and chemotherapy, the improvement in overall survival in patients with HNSCC is still low. HNSCCs often metastasize to locoregional lymph nodes, and lymph node involvement represents one of the most important prognostic factors of poor clinical outcome. Experimental models of the HNSCC and its spread via lymphatic system is an essential research tool used to study all steps of HNSCC progression and evaluation of new therapeutic approaches. This chapter provides with short review of molecular events implicated in metastatic spread of the HNSCC and presents experimental approaches with emphasis on in vivo models. Importantly, methods to model and to visualize the spread of HNSCC into sentinel lymph nodes are presented.

Abbreviations

HNSCC	head and neck squamous cell carcinoma
MMPs	metalloproteinases
HPV	human papillomavirus
ECM	extracellular matrix
UADT	upper aerodigestive tract
DMBA	dimethy-1,2 benzanthracene
4NQO	4-nitroquinoline 1-oxide
TPA	12-O-tetradecanoylphorbol-13-acetate

S. Kim (✉) · M. R. Gilbert
Department of Otolaryngology-Head and Neck Surgery, School of Medicine, University of Pittsburgh, Pittsburgh, USA
e-mail: kimsw2@upmc.edu

C.-M. Lim
Department of Otolaryngology Head and Neck Surgery, National University Health System Singapore, Singapore, Republic of Singapore

A. Malek (ed.), *Experimental Metastasis: Modeling and Analysis,*
DOI 10.1007/978-94-007-7835-1_2, © Springer Science+Business Media Dordrecht 2013

2.1 Introduction

Head and neck cancer, which generally comprises the cancers of the oral cavity, pharynx and larynx, affects 49,260 Americans each year, with an average five-year survival of approximately 61 % and an estimated 11,480 deaths a year [1]. The vast majority of these cancers is of squamous epithelial cell origin and is called head and neck squamous cell carcinomas (HNSCC *or* SCCHN) [2]. The major risk factors and causative etiologies for HNSCC are exposure to tobacco, alcohol, and, increasingly, the human papillomavirus (HPV). Metastatic spread is primarily lymphatic, with spread primarily to locoregional lymph nodes, although rarely distant organs [3], and locoregional metastasis is a very poor prognostic indicator [4]. While 5-year survival for cancer overall is improving over the past 3 decades, head and neck cancers survival has been stagnant [1], due in large measure to the difficulty in obtaining regional control of the disease and preventing metastasis. Furthermore, once metastasis or recurrence occurs, few treatment options exist beyond palliation, and those that exist have not been shown to be very effective [5]. Thus, having appropriate preclinical models for HNSCC metastasis is of vital importance for developing new strategies for preventing metastasis spread and improving locoregional control. In this chapter, we explore the research into various in vitro and in vivo HNSCC models and attempt to explain the advantages and limitations of each.

2.2 Molecular Mechanisms Of Local Invasion and Metastasis

Understanding the invasion-metastatic cascade provides a basic framework of analyzing the metastatic model of cancer, including HNSCC. This model depicts a succession of cellular-biologic changes, starting with dissociation of cells from their primary site followed by local invasion of cells into the nearby lymphatic or hematogenous system which allows these cells to extravasate into the distant host parenchyma [6]. These cancer cells interact with the host tissue and acquire a distinct tumor microenvironment which leads to autonomous growth of cancer from micrometastasis to clinically evident macrometastasis. The following discussion focuses on the various putative proteins and factors responsible for the metastatic cascade in HNSCC in the various stages of metastasis.

The ability of cancer cells to dissociate from their primary host tissue is a prerequisite for metastasis. E-cadherin is a key cell-to cell adhesion molecule which facilitates the formation of adheren junctions with adjacent epithelial cells and hence, maintains the quiescence of the cells within these sheets [7, 8]. Therefore, downregulation or dysfunction of E-cadherin results in a functional loss of E-cadherin–mediated cell adhesion and enhances the ability of cells to dissociate from the primary tumor. Moreover, it is evident that as carcinomas arising from epithelial tissues progressed to higher pathological grades of malignancy, they typically developed alterations in their shape as well as in their attachment to other cells and

to the extracellular matrix (ECM). Given these information, preclinical studies on HNSCC have demonstrated a link between downregulation of E-cadherin expression and metastasis by either correlating loss of expression in the primary tumor with positive lymph node status or by revealing a significant loss of expression in metastatic lymph nodes compared with primary tumors [9–12].

Dysadherin, a recently characterized cancer related glycoprotein, has been shown to down-regulate E-cadherin protein and thus, function as an"anti-adhesion" molecule [13]. This downregulation appears to occur in a post-transcriptional level without affecting the mRNA levels of the protein [6, 13, 14]. In HNSCC, dysadherin immunostaining is seen in the membranes of the cancerous cells and is predominantly localized in the intercellular borders of cancer cells and in poorly differentiated tumors [14, 15]. Muramatsou and colleagues established an association between dysadherin and prognosis of HNSCC patients treated with radiation therapy. They found that patients with tumors that expressed higher level of dysadherin achieved a statistically higher complete response rate compared to those with lower expression levels of dysadherin. This study also found that patients who showed high level of dysadherin and low levels of E-cadherin had higher risks of having cervical metastasis at the time of diagnosis.

The movement of cancer cells from the site of origin into lymphatic or vascular channels require the breakdown of ECM that normally acts to providing an anchoring mechanism. This process has been found to be dependent on metalloproteinases (MMPs), a family of zinc-dependent endopeptidases that degrade components of the basement membrane and ECM. All MMPs share the pro-domain and the catalytic domains, and can act on broad spectrum substrates within the ECM [7]. They are classified into secreted (soluble) and membrane-anchored MMPs; both types are initially synthesized as pro-enzymes, which then require activation either extracellularly or intracellularly. Among the 20 plus MMPs that have been characterized, MMP2 and MMP9 overexpression in HNSCC tumor samples has been correlated with invasion, metastasis, and poor prognosis [10, 16]. These studies also found that the expression of MMPs correlated inversely with the amount of ECM found around the tumor cells. Similarly, high protein expression levels of MT1-MMP, a membrane-bound metalloproteinase have also been linked to HNSCC metastasis. MT1-MMP itself has proteolytic activity against ECM components but is also important in the activation of MMP2 [12].

Although the mechanisms responsible for MMP upregulation and activation in HNSCC are not fully elucidated, interaction with tissue inhibitors of metalloproteinases (TIMPs) has been shown to be partly responsible in regulating the functional activity of MMP. The anti-invasive effects of TIMPs have been studied in HNSCC and levels of TIMP-1 have been found to be higher in HNSCC tumor specimens matched with non-metastatic cases than in metastatic cases [17]. More recently, MMP-10 has been shown to be functionally upregulated in metastatic HNSCC in an *in vitro* model [18]. In a study that utilized a combination of microarray and immunohistochemistry analysis, the overexpression of MMP-10 was found to promote the invasion of HNSCC cells *in vitro*. Conversely, the downregulation of MMP-10 resulted in the inhibition of invasion of HNSCC cells.

Vascular endothelial growth factor (VEGF) is classically thought of as a proangiogenic protein that is produced in response to hypoxia. Tumor-produced VEGF is responsible for promoting ingrowth of tumor vessels. Overexpression of VEGF has been reported in many solid tumors, including HNSCC, and is generally associated with increased tumor progression, increased resistance to chemotherapy, and poor prognosis. Although the VEGF family of cytokines modulate metastasis via the promotion of angiogenesis, recently studies have shown that VEGF may also have autocrine effects on tumor cells. Several tumor types, including HNSCC, have been found to express VEGFRs and the activation of tumoral VEGF/VEGFR axis has been shown to promotion of migration and invasion of the tumor cells [19]. Conversely, several studied have shown that the downregulation of VEGF leads to a decrease in invasion and migration, suggesting that VEGF acts to promote invasion and migration [7, 20, 21]. The promotion of migration and invasion of cancer cells by VEGF appears to be due to the ability of VEGF to promote epithelial-mesenchymal transition (EMT) [22]. A study by Bock et al showed that the overexpression of VEGF-C in HNSCC cell line SCC116 resulted in a 30% higher baseline rate of invasion compared with that in control cells, and that downregulation of VEGF-C expression by short hairpin RNA led to decreased invasion [23]. Given that hypoxia a stress condition for tumors cells, it not surprising that VEGF has an autocrine effect on tumor cells with the end-effect being the movement of the tumors cells away from areas of hypoxic stress.

Tumor angiogenesis is a critical aspect of tumor progression and various inhibitors of the VEGF pathway have been developed and have been approved for anticancer therapy. However, it should be pointed out that several preclinical studies have demonstrated increased metastasis of tumors after short-term administration of VEGF inhibitors [24, 25]. The mechanism behind this observation remains unclear but it is thought that the short-term administration of VEGF inhibitors leads to the production of cytokines in the host animal that ultimately results in a prometastatic condition [24, 25].

Cancer stem cells have attracted significant interest among researchers in recent years as evidence have suggested that a small tumor cell subpopulation among the primary tumor mass might be responsible for tumor initiation, growth, maintenance and spreading. These cells are therefore able to self-renew and have immense capability to self-propagate and seed once they are released from the primary host tumor [26]. While the cellular origin of CSC/CIC and the associated molecular pathways are still matter of discussion, there are evidence for the existence of primitive cancer stem cells (pCSC) which are responsible in the development of tumour neo-vasculogenesis [7, 27]. This is due to the fact that vascular endothelial derived growth factor receptor 2 (VEGFR-2) is considered to be the molecular marker of pCSCs [27, 28]. In breast cancer and lymphoma, the process of angiogenesis from bone marrow derived circulating endothelial progenitors have been implicated for sustaining tumor growth and metastasis. These pCSCs and CSCs have the potential of transforming into cells with endothelial characteristics. These observations have resulted increasingly research to extrapolate these observations in HNSCC. There have been some success in propagating and isolating CSCs in HNSCC and the

coming years will likely see a paradigm change in understanding how these CSCs acquire the metastatic features through the molecular signalling pathways.

2.3 In Vitro Models

In vitro models are extensively being used to study HNSCC. Several hundred HNSCC cell lines have been established by various investigators and used to study a broad spectrum of questions related to head and neck cancer. Moreover, several techniques exist for the culture of normal epithelial cells from the upper aerodigestive tract (UADT) and to model the multistep process of malignant transformation using HPV infection, oncogenes over-expression of and/or exposing to various carcinogens. This approach also allows for the comparison of cancerogenic effects of various irritants like tobacco smokes. In order to approximate experiental conditions to real tissue and to simulate histological complexity, three dimensional model systems are being applied.

Culture techniques for growing dissociated primary tumor cells for short term experimental analysis are being used as well. However, most experimental studies are being performed with established cell culture. Unlike many other cancer types, a wide variety of primary and metastatic HNSCC cell lines are available. An extended guide with classification of available cancer cell lines and discussion of important aspects of culturing is review of Dr. Charles J. Lin in "Head & Neck" 2007. All conventional cell culture techniques and assays, like colorimetric cell proliferation, wound-healing, trans-well, zymography assays as well as non-adherent culturing and cell sphere formation presented in other chapters of this issue are applicable for HNSCC research.

2.4 In Vivo Models

The use of an appropriate animal model which can accurately recapitulate the disease process is an essential aspect of anticancer drug discovery, as it allows easy, reproducible testing of agents or mechanistic hypotheses in a wholly intact biological system [29, 30]. One commonly used preclinical model is nude mice with subcutaneous cancer xenografts. However, such models lack the specific interactions that exist between the tumor cells and their native environment—interactions that influence the molecular, pathologic, and clinical features of the tumor [31–35]. Because these distinct interactions are lost or altered when the tumors are established in ectopic sites, it is preferable to establish tumors at orthotopic sites. Furthermore, since orthotopic models recreate the specific subsite and thus the pattern of spread distinct to the cancer of interest, they allow for study of metastasis and the effects of agent that inhibit metastasis. However, there are inherent drawbacks to orthotopic models as well. The cancer cell lines in orthotopic xenograft models already possess

a fully malignant potential when injected into the test animals—thus, orthotopic xenograft models do not allow modeling of the pre-neoplastic processes preceding full malignant transformation. Modeling of such premalignant process requires the use of transgenic (e.g. murine) models.

Additionally, in each of these models, there are a variety of potential methods for assessing both primary tumor burden and metastasis. Identification of the sentinel lymph node and non-invasive imaging of tumor cells which have metastasized to the lymphatics are two methods which are of increasing interest in animal models. These techniques allow the study of the process of metastasis in earlier stages than traditional histology, which may rely on metastatic tumors becoming grossly apparent, by which time the process of metastasis is very far along.

2.4.1 Carcinogen Induction Models

Carcinogenic agents offer a way to induce cancer in an animal model that is similar to the development of cancer in humans, and there are several models in existence. For example, polycyclic hydrocarbon 9,10 dimethy-1,2 benzanthracene (DMBA) may be dissolved in benzene or acetone and administered to the cheek pouch of hamsters. This model, in which DMBA is painted onto the buccal surface of the cheek pouch in hamsters, was first described by Salley [36]. It was later refined by Lin et al. [37] who showed that tumor incidence can be increased (up to 100%) by painting the pouch three times a week for eight weeks followed by painting with arecaidine six times a week for four weeks in order to promote the initial carcinogenesis. Other promotional agents that have been used after initial exposure to DMBA include 4-nitroquinoline 1-oxide (4NQO) and 12-O-tetradecanoylphorbol-13-acetate (TPA), which have been used to produce oral cancer with high frequency [38]. These tumors have been shown to possess many molecular changes seen in human oral cancer. They show increased expression of epidermal growth factor receptor (EGF), transforming growth factor receptor-*a* (TGF-*a*), and oncogenic proteins such as ras and p53, as well as an increase in low-molecular weight keratins and proliferative markers [39–43].

Chronic administration of 4NQO to rodents may also be used to produce oral cancer models [44]. 4NQO is a water soluble agent, and thus, it can easily be added to the drinking water of the rodents (requiring less effort than the painting technique above). This method has been shown to induce SCC of the palate, tongue, esophagus, and stomach. These tumors also display several of the molecular changes seen in human SCC, including increased expression of ras, p53, E-cadherin, Bcl-2 and Bax [45–48]. An advantage of this model is that it mimics the development of human oral cancer, with fully malignant SCC being clearly preceded by increasing grades of dysplastic changes. It thus becomes an ideal model for studying premalignant lesions and potential agents that can be used to reverse malignant transformation [49]. However, the reliable development of tumors requires the administration of 4NQO for extended periods lasting over two to three months [44].

One additional disadvantage to all the models above is that the carcinogen induction model does not allow for study of specific genes or protein expression in the process of oral carcinogenesis. For this purpose, xenograft or transgenic mouse models are necessary.

2.4.2 Orthotopic Models

The majority of orthotopic models of HNSCC are oral squamous cell carcinoma models in rodents. Fitch et al. first described orthotopic xenograft models of oral SCC in which SCC cells, aspirated from subcutaneous ectopic xenografts in nude mice, were subsequently injected into the tongues of nude mice [50]. Oral SCC cell lines have since been implanted by other means; for example, they may also be injected into the floor of mouth of nude mice transcutaneously [51]. In this technique, which was first reported by Dinesman et al., cells are injected via a submandibular route into the deep tissue surrounding the mylohyoid muscles within the floor of mouth. However, the authors found that almost 40 % of the mice developed pulmonary metastasis while only 5 % of the mice developed cervical lymphatic metastasis [51], numbers that do not replicate the more locoregional pattern of metastasis seen in human HNSCC [3]. One possible explanation for this observation is spillage of the injected tumor cells into the murine vasculature during injection, leading to pulmonary emboli of the tumor cells. Unfortunately, pulmonary lesions produced in this fashion have bypassed the normal process of metastasis in HNSCC and, thus, this model contradicts the concept of orthotopic model.

Myers et al. [52] described another orthotopic model of oral SCC that was produced by injection into the tongues of nude mice, similar to the model by Fitch et al. [50]. However, this model employed submucosal injection of oral cell lines directly into the dorsal tongue of nude mice. The resulting xenografts reproduced several features of human HNSCC (e.g. cervical lymphatic metastasis and disease specific symptoms such as dysphagia and weight loss). More importantly, oral cells injected into the tongues of nude mice had significantly higher tumorigenicity than oral SCC cells injected subcutaneously into the flank. This observation is significant for validating orthotopic xenograft models since the organ-specific tumor-stromal cell interaction that is thought to be lost in subcutaneous ectopic models was able to be reproduced. Similarly, Cabanillas et al. have produced a highly metastatic intraoral and submucosal model using the human glottis cancer line SCC 38 in nude mice, with a 100 % lymphatic and perineural invasion, and 22 % bone destruction and vascular invasion, and, similar to most HNSCC in humans, showed no hematogenous spread [53].

Although the above models all use mice to model oral SCC, other HNSCC models do exist. For example, Bao et al. produced a rat model of human HNSCC through subcutaneous injection of the human HNSCC cell line SCC-4 in athymic nude rats at the level of the scapulae, thus producing a non-oral HNSCC orthotopic model [54]. However, although the size of the animals in this model enabled the

easy use of ^{18}F-FDG PET imaging, no metastases, either cervical or distant, were reported, although this could be due to the particular cell line used.

This last example demonstrates point that it is helpful to use cell lines for in vivo models that have been associated with metastasis. Thus, the HNSCC cell lines used may be of particular interest for metastasis research, and may be from a variety of sources. Human cell lines have been developed from metastases from multiple head and neck squamous cell carcinoma subsites. For example, UM-22B cells were derived from lymph node metastases from hypopharyngeal cancer [55], PCI-37B cells were derived from laryngeal cancer lymph node metastases [56]. Detroit 562 cells were derived from a pharyngeal cancer lung metastasis and are still in use many years after their establishment [57, 58]. UMSCC2 and UMSCC17B lines have been shown to be highly metastatic to locoregional lymph nodes after injection into the tongue in a nude mouse model [59].

A disadvantage of the aforementioned xenograft models is that although the use of human cell lines is an attempt to more faithfully replicate human HNSCC, the use of such lines requires immunosuppression of the animal, typically using either athymic or severe combined immunodeficiency (SCID) mice. Indeed, the use of immunodeficient mice precludes the study of interactions between the host immune system and the tumor. O'Malley et al. [60] proposed bypassing this problem by injecting SCC VII , a murine SCC cell line, into the floor of mouth of syngeneic C3H/HeJ mice. In this way, xenografts have been produced in the floor of mouth that show local invasion into the mandible and mylohyoid muscle, with cervical lymphatic and pulmonary metastasis. However, SCC VII cell lines were later found to have originated not from the oral cavity, but from the abdominal wall of the C3H mouse [61]. Still, these cells are frequently used in head and neck cancer experiments because of their utility in replicating metastatic behavior in the head and neck. Behren et al. recently effectively used GFP transfected SCC VII cells in the floor-of-mouth of BALB/c-NU mice resulting in the formation of invasive tumors that metastasize to regional lymph nodes [62]. Similarly, Yu et al. successfully developed several highly metastatic cell lines through injection of SCC VII cells into mouse auricles and subsequent excision and serial passaging in culture [63]. Matsumoto et al. have taken a similar murine squamous cell line, NR-S1, which is usually poorly metastatic, and through in vivo selection, have developed the highly metastatic line NR-S1M which metastasizes rapidly to locoregional lymph nodes [64]. Judd et al. have since been able to combine both the carcinogen induction approach with the orthotopic xenograft approach and avoid the use of immunosuppression while still having an orthotopic model [65]. The authors used DMBA to produce murine OSCC lines in C57BL/6 mice that were then injected into the either the floor of mouth/buccal region or into the flank in syngeneic mice, and they were able to demonstrated cervical metastasis from orthotopic transplants at the same rate as metastasis to lymph nodes draining the flank [65]. Such combination models may hold promise as they lack some of the drawbacks to the individual models above.

2.4.3 Transgenic Models

Transgenic models hold the advantage of a stable introduction of cancer using specifically targeted oncogenic pathways within the animal of interest, allowing for an intact, relatively untampered biological system. These models allow to study initial steps of cancer development and local spreading, to consider host-tumor interaction and to estimate role of immune system.

There are multiple models that have been produced. The first model type involves the use of the keratin promoter, and there are two such models of oral cancer that have been described. These models utilize the keratin 5 (K5) or keratin 14 (K14) promoter to overexpress the oncogene K-*ras*^{G12D} in the oral epithelium of mice [66, 67]. These two promoters allow for specific orthotopic models due to differences in distribution: K5 is normally expressed both within the basal epithelium of the tongue and the forestomach, whereas K14 is mainly expressed in the basal layer of the oral mucosa and tongue [66]. Subsequently, either promoter is ideal for targeting transgenic expression within the oral cavity.

2.4.3.1 K-*ras*^{G12D}

Vitale-Cross et al. produced an animal model in which the expression of K-*ras*^{G12D} oncogene, driven by K5 promoter, was placed under the control of *tet*-responsive elements, and they were able to induce K-*ras*^{G12D} expression by the administration of doxycycline [67]. Furthermore, they found premalignant lesions of varying dysplasia as well as malignant SCC in the skin, oral mucosa, tongue, esophagus, forestomach, or uterine cervix of the mice [67]. In another model by Caulin et al. [66], the K-*ras*^{G12D} oncogene, this time driven by either K5 or K14 promoter, was placed under the control of a modified Cre recombinase fused to a deletion mutant of the human progesterone receptor. Administration of RU486 in this model resulted in K-*ras*^{G12D} oncogene induction in the oral epithelium of mice. In contrast to the previous model, only squamous papilloma formation was found within the oral cavity [66].

The K-*ras*^{G12D} oncogene has also been used to produce SCC exclusively within the oral cavity [68]. Mice carrying the K-*ras*^{G12D} oncogene construct, under the control of both K14 promoter and tamoxifen-inducible Cre recombinase, were crossed with p53 conditional knockout mice. As early as two weeks after the beginning of tamoxifen treatment, the resulting progeny mice had developed SCC exclusively in the oral cavity [68].

2.4.3.2 *Trp53* $^{F/F}$; K14Cre myrAkt

There are other oncogenes that may be manipulated as well to produce transgenic models. Constitutive activation of Akt along with downregulation of Trp53 has been

used to Moral et al. to produce an oral cancer models [69]. In this model, the K14 promoter is again used to target the expression specifically to the oral cavity, this time producing constitutively active Akt. The authors found that mice developed pre-neoplastic lesions which progressed to oral SCC which also demonstrated cervical lymphatic and pulmonary metastasis. Perhaps more importantly, the authors showed that the SCC tumors produced this way possessed many of the molecular changes frequently seen in human HNSCC, including the overexpression of epidermal growth factor receptor (EGFR) and Stat3.

It is important to keep in mind that there are several drawbacks to the use of transgenic models, despite the reproduction of some of the major clinical characteristics of head and neck cancer. First, the transgene expression is usually driven through the use of a heterologous promoter, meaning that there are non-physiologic levels of transgene product. Second, the tumor microenvironment in the transgenic mice is significantly different from typical carcinogenesis in that the stromal cells also carry the transgene, as opposed to the mutation only existing in tumor cells. True, the use of oral-mucosa specific promoters (e.g. K5, K14) minimizes the leakage of transgene expression, the intended tissue specificity is unfortunately not absolute. Finally, and most importantly, except in very rare cases, no single gene predominates the process of oral cancer carcinogenesis., and thus this is a flawed system that may have limited applicability. The use of one or two specific genes (e.g. K-*ras* or Akt) to drive the tumor formation will not necessarily reflect the carcinogenic process in humans. For instance, K-*ras* mutations in human head and neck cancer are relatively infrequent, although the presence of H-*ras* mutations in HNSCC has been previously demonstrated [70, 71].

2.5 Sentinel Lymph Node

One important aspect of metastasis modeling is the identification of the sentinel lymph node, whether in the search for early metastasis that is not apparent grossly or by the imaging methods below, or whether the process of lymphatic spread is being studied. Sentinel lymph node mapping for HNSCC is an investigational tool that is not routine in the clinical setting and currently is not the standard of care due to the lack of large randomized clinical trials [72]. However, several recent studies have shown that it has promise and may eventually become standard of care [73–76].

Lymph node identification in mice can be difficult due to their small size and lack of distinct features from surrounding tissue. However, two distinct groups of lymph nodes in the neck can be identified in mice: a superficial group and a deep group of cervical lymph nodes. The superficial group of cervical lymph nodes is located at the lateral border of the submandibular gland. There are two lymph nodes on each side. (Fig. 2.1a). Solitary lymph nodes can be also found under submandibular gland. (Fig. 2.1b). These lymph nodes are the ones most frequently involved in metastasis from tumor xenografts in the oral cavity such as the tongue, floor of

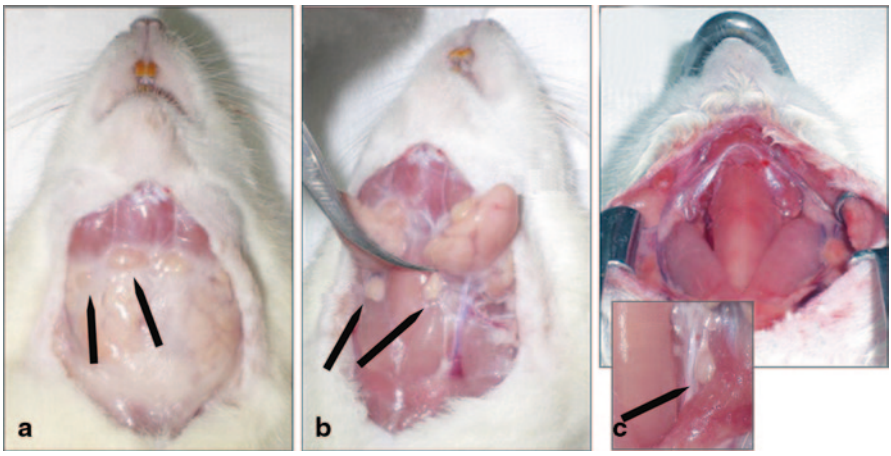

Fig. 2.1 Superficial group of cervical lymph nodes **a** When the skin of the anterior neck is reflected, the submandibular gland is immediately encountered. Two lymph nodes on are found on each side located on the superior-lateral border of the submandibular gland. **b** When capsulated glands are dislocated, singular or grouped lymph nodes can be identified. **c** In order to fond deep group of cervical lymph nodes, the submandibular glands should be completely removed, the trachea along with the sternocleidomastoid muscles are exposed. The deep group of cervical lymph nodes is located underneath the sternocleidomastoid muscles and can be visualized by reflecting the muscles laterally. In the inserted images, the right sternocleidomastoid muscles are removed. (The lymph nodes are marked by *arrows*). (Adopted with permission from [93], Journal of Neuroscience Methods)

mouth, or the buccal surface. The deep group of cervical lymph nodes is located deep to the sternocleidomastoid muscles, lateral to the tracheoesophageal complex (Fig. 2.1c). These lymph nodes are usually involved by metastasis from orthotopic thyroid tumor xenografts but are rarely involved in metastasis from tumor xenografts in the oral cavity.

Localization of sentinel lymph nodes is usually accomplished by means of 2% Evans blue dye into an anatomic area, which quickly collects in the lymphatic system and identifies the lymph nodes and vessels which drain that area. Harrell et al. have injected Evans blue dye into the tail or footpad in mice and rats and have mapped lymphatic drainage patterns to and from inguinal, popliteal, iliac, renal, and axillary lymph nodes [77]. Such mapping is helpful in assessing the location of probable sentinel lymph nodes associated with heterotopic tumor injection sites, and also provides a simple tool for rapidly identifying the likely drainage pathways. For example, dye may be injected into xenografted tumors once they are established and growing in animals, but it may be also injected as an adjunct to the tumor cells during implantation to suggest where the probable sentinel lymph node will be. Such prior identification of likely sentinel lymph nodes may also allow for the study of pre-metastatic lymph nodes and the "soil preparation" hypothesis, which proposes that there are changes in the sentinel lymph node induced by various unknown tumor-secreted cytokines in order to facilitate eventual metastasis to that node [78].

In addition to the aforementioned Evans blue dye, a variety of other dyes have shown promise in SLN detection in both human and animal studies. In clinical studies, Indocyanin Green, a fluorescent dye, has been used to identify sentinel lymph nodes in oropharyngeal cancer [79], and may hold promise as a dye for animal models. Methylene blue dye has also been safely and effectively used in clinical studies of sentinel lymph node identification in breast cancer [80], but has been found to be a poor SLN dye in an intradermal feline model of melanoma due to poor lymphatic uptake and increased staining of surrounding tissue [81], suggesting that it may be necessary to optimize the dye for the particular model. Cyalume is another fluorescent dye that was investigated in the feline melanoma model, and although it allowed easy lymphatic identification, it leaked into the surround interstitial space, causing the increased background fluorescence [81]. Isosulfan blue, in contrast, had minimal diffusion and was associated with rapid lymphatic identification [81]. Although this melanoma model is not a HNSCC model, melanoma is an epithelial malignancy like HNSCC and orthotopic intradermal injections are common to models of both, suggesting that these techniques may be transferable.

There are, however, few studies to date of sentinel lymph node identification in head and neck mouse models, none of which appear to investigate HNSCC. Rebhun et al. investigated the impact of sentinel lymph node excision in a murine model of melanoma by injection of a murine melanoma cell line B16-BL6 into the auricle of the ear (specifically, the ventral pinna) [82]. In order to demonstrate that sentinel lymph nodes would be identifiable, they first injected 2 % Evans blue dye into the ventral ear fold while observing the ventral cervical nodes where a surgical incision had been made. Rapid identification of the sentinel lymph nodes was made and the nodes were dissected away in this sham procedure. They then injected similarly melanoma cells which had been labeled prior to trypsinization with Vybrant DiI cell-labeling solution (Molecular Probes, Eugene, OR), allowing easy identification of sentinel lymph nodes and lymphatic drainage channels when metastasis occurred. Gross lymph node metastases were visible after four weeks in several mice that underwent wide local excision of the ear two weeks after injection, but not in any of those who also had sentinel lymphadenectomy and wide local excision, demonstrating the putative value of sentinel lymphadenectomy in this model [82].

Hoshida et al. published a very nice study which presents many of the possible experimental approaches to identifying sentinel lymph nodes in a head and neck model [83]. Expanding a mouse ear tumor model they had previously developed [84], they first performed lymphangiography of the peripheral ear with injections of Evan's blue dye and 2.5 % FITC-dextran, revealing the lymphatic network, a principal drainage vessel at the ear base, and the presumptive sentinel lymph node, which was a superficial cervical node [83]. Trypsinized tumor cell suspensions of GFP-expressing T241 fibrosarcoma which had previously been grown in the flank of several mice, were then injected into the ear. FITC-dextran was then injected into the tumor surface at 150mm^3 volumes, allowing lymphatic mapping with epifluorescence intravital microscopy (IVM) and/or multiphoton laser scanning IVM, and lymphatic size measurements were taken [83]. They were further able to measure

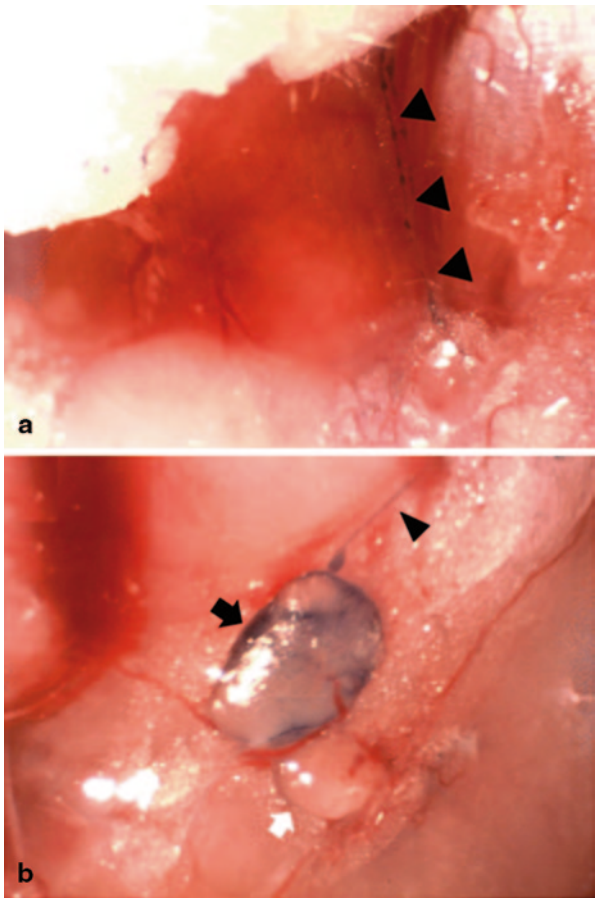

Fig. 2.2 Visualization of sentinel lymph node draining with Evans blue. The sentinel lymph node draining the oral cavity is usually found within the superficial group of lymph nodes adjacent to the submandibular gland. **a** 2% Evans blue dye injected into the buccal surface of athymic, nude mouse results in detection of lymphatic vessel draining the oral cavity into the cervical lymph nodes. The lymphatic vessels are marked by arrowheads. **b** A sentinel lymph node draining the oral cavity. The afferent lymphatic vessel is marked by the arrow head and the sentinel lymph node is marked by the black arrow. Note the adjacent lymph node (marked by an *open arrow*) that is not a sentinel lymph node despite its proximity to the actual sentinel lymph node

lymph fluid velocity using photobleaching and were able to monitor tumor cell arrival to the cervical lymph node with multiphoton laser scanning IVM following 1% TRITC-dextran injection into the tip of the ear [83]. Using these approaches Hoshida et al. were able to show that VEGF-C overexpression increases metastasis by increasing lymphatic vessel hyperplasia, lymphatic flow rate, and delivery of tumor cells to lymph nodes—effects they were able to abrogate with anti-VEGFR-3 antibody [83]. These approaches and results demonstrate the utility of a good SLN model in understanding metastasis and in developing potential therapies for inhibiting metastasis.

In our own experience, we have investigated the possibility of a HNSCC sentinel lymph node model by injected the buccal mucosa of the mouse with 2% Evans blue dye. Consistent with the above approaches, there is very rapid identification of lymphatic channels within minutes and consistent drainage to superficial cervical nodes, suggesting that such a sentinel lymph node model holds promise (Fig. 2.2).

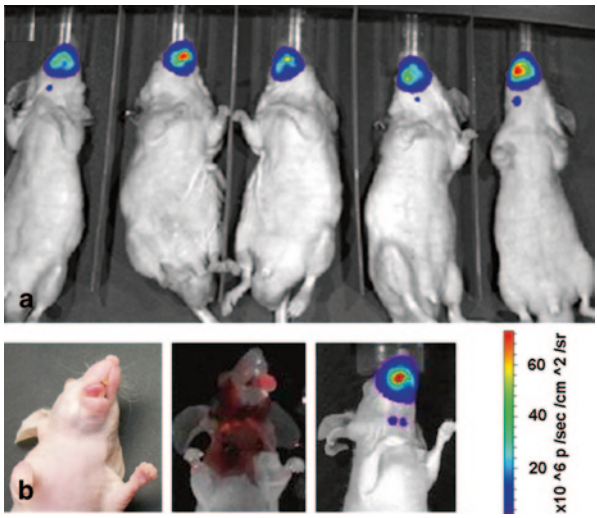

Fig. 2.3 Methods of xenograft tumor visualization. **a** Bioluminescent imaging of athymic mice bearing orthotopic tongue cancer xenografts. Color bar: Max 2,41e^5 Min 7,30e^6. (Photographs courtesy of Dr. Jeffrey N. Myers, MD Anderson Cancer Center, USA) **b** Detection of oral cancer using bioluminescent (BLU)—Luciferase activity and fluorescent (FLU)—near infrared (NIR), MMPSense680 imaging. (Adopted with permission from [94])

2.6 Imaging/Detection Methods

In an attempt to aid in the identification of cervical lymph nodes bearing metastatic deposits, various imaging methods have been propose. One of the first methods used for detecting cervical or distant metastasis in HNSCC xenografts was to engineer HNSCC cell lines to express fluorescent proteins (GFP or RFP) or enzyme luciferase. This can be accomplished by transfecting HNSCC cell lines with expression vectors such as lentiviral vectors that express these proteins.

The most frequently used system for *in vivo* imaging of tumor xenografts in mice including HNSCC is the use of bioluminescence imaging. The term bioluminescence refers to the process of light emission by living organism and utilizes the enzyme luciferase. Luciferase acts on its substrate, luciferin, to convert luciferin into oxyluciferin. The conversion reaction results in the formation of oxyluciferin in an electronically excited state. Relaxation of oxyluciferin to its relaxed state is then accompanied by release of photon of light. In this approach, tumor cell lines are engineered to express the enzyme luciferase by transfecting the cell lines with luciferase expression vector. Any xenografts produced from these cell lines can then be visualized by the intravenous administration of luciferin [85]. In a typical bioluminescent visualization of tumor xenografts, a photographic image of the animal is obtained first followed by a bioluminescent image. The two images are then superimposed to correlate the areas of bioluminescence with the anatomy of the animal (Fig. 2.3a). This method has been used for visualization of cervical lymphatic metastasis from oral cancer xenografts in several publications [86–88].

A more sophisticated approach is to take advantage of metabolic or protein expression differences between normal lymph nodes and tumor tissues to specifically target metastatic deposits for visualization. For example, various studies have taken

advantage of the fact that most HNSCC express high levels of the epidermal growth factor receptor (EGFR), GLUT-1 receptor or αvβ3 integrins to perform *in vivo* imaging of murine HNSCC xenografts. In addition, front of active tumor spread can be imaged using fluorescence agents that detect increased activity of enzymes that are mainly found in the invasive tumor front. These approaches involve the *in vivo* administration of a tumor-targeting ligand, which is conjugated to a detection agent. The agent then becomes concentrated at the site of target-molecule expression and thereby allows visualization of the tumors. Rosenthal et al studied the feasibility of using cetuximab, a humanized monoclonal antibody against EGFR, conjugated to Cy5.5 fluorochrome to visualize HNSCC xenografts [89]. Furthermore, the authors utilized the presence or absence of fluorescence in the surgical bed after resection of these xenografts to assess the adequacy of margin status. Keereweer et al. used tumor-specific near-infrared fluorescence agents against EGFR (fluorescently-labeled recombinant EGF) and the glucose transporter system (fluorescently-labeled 2-deoxyglucose, an analog of the tumor PET tracer 2-deoxy-2-(^{18}F)fluoro-D-glucose) to identify tumor margins and cervical metastasis in a mouse model of tongue cancer [90]. Using of combination of the bioluminescent and fluorescent imaging allows to detect metastatic focuses and tumor spread demarcation simultaneously (Fig. 2.3b).

Detection of radioactive nuclide of cooper presents another example of tumor imaging technique. For instance, panitumumab, a humanized monoclonal antibody against EGFR, conjugated to ^{64}CU-1,4,7,10-tetraazacyclododecane-N, N',N'',N'''-tetraacetic acid (DOTA) was administered to mice hearing HNSCC xenografts [91]. With the panitumumab-^{64}CU DOTA conjugate, the authors were able to visualize HNSCC xenografts using small animal PET. These authors have also utilized cetuximab conjugated to ^{64}CU DOTA to target HNSCC xenografts for imaging via small animal PET [92].

2.7 Conclusion

The availability of a proper model, whether *in vitro* or *in vivo*, is critical in studying the metastasis of head and neck cancer. The orthotopic model of head and neck cancer is particularly suitable in studying the process of metastasis in this disease. The establishment of tumor in their orthotopic location allows for proper reconstitution of the tumor-stromal interactions that exist in human tumors. Furthermore, the pattern of metastasis that is found in human head and neck cancer cannot be replicated without the use of the orthotopic model. The use of human cell lines in murine models is somewhat problematic in that the model assumes proper interaction between the murine and human ligands and their cognate receptors during the process of metastasis. In situations where this is a concern, the use of syngeneic head and neck cancer cell lines may be appropriate. None of models discussed in this review are without shortcomings and when a model is chosen, the appropriate uses and the various advantages and disadvantages of that model must be recognized. Until

a disease model with greatest resemblance to human cancer can be created, the advantages and disadvantages of each model should be considered carefully and utilized judiciously.

References

1. Altekruse S, Kosary C, Krapcho M, Neyman N, Aminou R et al (2010) SEER Cancer Statistics Review, 1975–2007. http://seer.cancer.gov/csr/1975_2007/: based on November 2009 SEER data submission, posted to the SEER web site
2. Davies L, Welch HG (2006) Epidemiology of head and neck cancer in the United States. Otolaryngol Head Neck Surg 135:451–457
3. Garavello W, Ciardo A, Spreafico R, Gaini RM (2006) Risk factors for distant metastases in head and neck squamous cell carcinoma. Arch Otolaryngol Head Neck Surg 132:762–766
4. Becker MT, Shores CG, Yu KK, Yarbrough WG (2004) Molecular assay to detect metastatic head and neck squamous cell carcinoma. Arch Otolaryngol Head Neck Surg 130:21–27
5. Vermorken JB, Specenier P (2010) Optimal treatment for recurrent/metastatic head and neck cancer. Ann Oncol 21(Suppl 7):vii252–261
6. Howell GM, Grandis JR (2005) Molecular mediators of metastasis in head and neck squamous cell carcinoma. Head Neck 27:710–717
7. Andrews NA, Jones AS, Helliwell TR, Kinsella AR (1997) Expression of the E-cadherin-catenin cell adhesion complex in primary squamous cell carcinomas of the head and neck and their nodal metastases. Br J Cancer 75:1474–1480
8. Cavallaro U, Christofori G (2004) Cell adhesion and signalling by cadherins and Ig-CAMs in cancer. Nat Rev Cancer 4:118–132
9. Ikebe T, Shinohara M, Takeuchi H, Beppu M, Kurahara S et al (1999) Gelatinolytic activity of matrix metalloproteinase in tumor tissues correlates with the invasiveness of oral cancer. Clin Exp Metastasis 17:315–323
10. Kurahara S, Shinohara M, Ikebe T, Nakamura S, Beppu M et al (1999) Expression of MMPS, MT-MMP, and TIMPs in squamous cell carcinoma of the oral cavity: correlations with tumor invasion and metastasis. Head Neck 21:627–638
11. Rodrigo JP, Dominguez F, Alvarez C, Manrique C, Herrero A et al (2002) Expression of E-cadherin in squamous cell carcinomas of the supraglottic larynx with correlations to clinicopathological features. Eur J Cancer 38:1059–1064
12. Sato H, Takino T, Okada Y, Cao J, Shinagawa A et al (1994) A matrix metalloproteinase expressed on the surface of invasive tumour cells. Nature 370:61–65
13. Nakanishi Y, Akimoto S, Sato Y, Kanai Y, Sakamoto M et al (2004) Prognostic significance of dysadherin expression in tongue cancer: immunohistochemical analysis of 91 cases. Appl Immunohistochem Mol Morphol 12:323–328
14. Muramatsu H, Akimoto T, Maebayashi K, Kita M, Mitsuhashi N (2008) Prognostic significance of dysadherin and E-cadherin expression in patients with head and neck cancer treated by radiation therapy. Anticancer Res 28:3859–3864
15. Kudo Y, Ogawa I, Kitajima S, Kitagawa M, Kawai H et al (2006) Periostin promotes invasion and anchorage-independent growth in the metastatic process of head and neck cancer. Cancer Res 66:6928–6935
16. Imanishi Y, Fujii M, Tokumaru Y, Tomita T, Kanke M et al (2000) Clinical significance of expression of membrane type 1 matrix metalloproteinase and matrix metalloproteinase-2 in human head and neck squamous cell carcinoma. Hum Pathol 31:895–904
17. Zhang X, Liu Y, Gilcrease MZ, Yuan XH, Clayman GL et al (2002) A lymph node metastatic mouse model reveals alterations of metastasis-related gene expression in metastatic human oral carcinoma sublines selected from a poorly metastatic parental cell line. Cancer 95:1663–1672

18. Deraz EM, Kudo Y, Yoshida M, Obayashi M, Tsunematsu T et al (2011) MMP-10/stromelysin-2 promotes invasion of head and neck cancer. PLoS One 6:e25438
19. Christopoulos A, Ahn SM, Klein JD, Kim S (2011) Biology of vascular endothelial growth factor and its receptors in head and neck cancer: beyond angiogenesis. Head Neck 33:1220–1229
20. Shemirani B, Crowe DL (2000) Head and neck squamous cell carcinoma lines produce biologically active angiogenic factors. Oral Oncol 36:61–66
21. Smith BD, Smith GL, Carter D, Sasaki CT, Haffty BG (2000) Prognostic significance of vascular endothelial growth factor protein levels in oral and oropharyngeal squamous cell carcinoma. J Clin Oncol 18:2046–2052
22. Ferrara N, Gerber HP, LeCouter J (2003) The biology of VEGF and its receptors. Nat Med 9:669–676
23. Bock JM, Sinclair LL, Bedford NS, Jackson RE, Lee JH et al (2008) Modulation of cellular invasion by VEGF-C expression in squamous cell carcinoma of the head and neck. Arch Otolaryngol Head Neck Surg 134:355–362
24. Ebos JM, Lee CR, Cruz-Munoz W, Bjarnason GA, Christensen JG et al (2009) Accelerated metastasis after short-term treatment with a potent inhibitor of tumor angiogenesis. Cancer Cell 15:232–239
25. Paez-Ribes M, Allen E, Hudock J, Takeda T, Okuyama H et al (2009) Antiangiogenic therapy elicits malignant progression of tumors to increased local invasion and distant metastasis. Cancer Cell 15:220–231
26. Bhaijee F, Pepper DJ, Pitman KT, Bell D (2011) Cancer stem cells in head and neck squamous cell carcinoma: A review of current knowledge and future applications. Head Neck 34(6):894–899
27. Shen R, Ye Y, Chen L, Yan Q, Barsky SH et al (2008) Precancerous stem cells can serve as tumor vasculogenic progenitors. PLoS One 3:e1652
28. Sayed SI, Dwivedi RC, Katna R, Garg A, Pathak KA et al (2011) Implications of understanding cancer stem cell (CSC) biology in head and neck squamous cell cancer. Oral Oncol 47:237–243
29. Fidler IJ (1986) Rationale and methods for the use of nude mice to study the biology and therapy of human cancer metastasis. Cancer Metastasis Rev 5:29–49
30. Killion JJ, Radinsky R, Fidler IJ (1998) Orthotopic models are necessary to predict therapy of transplantable tumors in mice. Cancer Metastasis Rev 17:279–284
31. Kubota T (1994) Metastatic models of human cancer xenografted in the nude mouse: the importance of orthotopic transplantation. J Cell Biochem 56:4–8
32. Singh RK, Bucana CD, Gutman M, Fan D, Wilson MR et al (1994) Organ site-dependent expression of basic fibroblast growth factor in human renal cell carcinoma cells. Am J Pathol 145:365–374
33. Fidler IJ, Wilmanns C, Staroselsky A, Radinsky R, Dong Z et al (1994) Modulation of tumor cell response to chemotherapy by the organ environment. Cancer Metastasis Rev 13:209–222
34. Dong Z, Radinsky R, Fan D, Tsan R, Bucana CD et al (1994) Organ-specific modulation of steady-state mdr gene expression and drug resistance in murine colon cancer cells. J Natl Cancer Inst 86:913–920
35. Radinsky R, Beltran PJ, Tsan R, Zhang R, Cone RD et al (1995) Transcriptional induction of the melanocyte-stimulating hormone receptor in brain metastases of murine K-1735 melanoma. Cancer Res 55:141–148
36. Salley JJ (1954) Experimental carcinogenesis in the cheek pouch of the Syrian hamster. J Dent Res 33:253–262
37. Lin LM, Chen YK, Lai DL, Huang YL (1996) Minimal arecaidine concentrations showing a promotion effect during DMBA-induced hamster cheek pouch carcinogenesis. J Oral Pathol Med 25:65–68
38. Kim TW, Chen Q, Shen X, Regezi JA, Ramos DM et al (2002) Oral mucosal carcinogenesis in SENCAR mice. Anticancer Res 22:2733–2740
39. Wong DT, Gallagher GT, Gertz R, Chang AL, Shklar G (1988) Transforming growth factor alpha in chemically transformed hamster oral keratinocytes. Cancer Res 48:3130–3134
40. Schwartz JL, Shklar G (1996) Glutathione inhibits experimental oral carcinogenesis, p53 expression, and angiogenesis. Nutr Cancer 26:229–236

41. Gimenez-Conti IB, Bianchi AB, Stockman SL, Conti CJ, Slaga TJ (1992) Activating mutation of the Ha-ras gene in chemically induced tumors of the hamster cheek pouch. Mol Carcinog 5:25–263
42. Robles AI, Gimenez-Conti IB, Roop D, Slaga TJ, Conti CJ (1993) Low frequency of codon 61 Ha-ras mutations and lack of keratin 13 expression in 7,12-dimethylbenz[a]-anthracene-induced hamster skin tumors. Mol Carcinog 7:94–98.
43. Schwartz JL, Antoniades DZ, Zhao S (1993) Molecular and biochemical reprogramming of oncogenesis through the activity of prooxidants and antioxidants. Ann N Y Acad Sci 686:262–278; discussion 278–269
44. Wallenius K, Lekholm U (1973) Oral cancer in rats induced by the water-soluble carcinogen 4-nitrochinoline N-oxide. Odontol Revy 24:39–48
45. Yuan B, Heniford BW, Ackermann DM, Hawkins BL, Hendler FJ (1994) Harvey ras (H-ras) point mutations are induced by 4-nitroquinoline-1-oxide in murine oral squamous epithelia, while squamous cell carcinomas and loss of heterozygosity occur without additional exposure. Cancer Res 54:5310–5317
46. Osugi Y (1996) p53 expression in various stages of 4-nitroquinoline 1-oxide induced carcinoma in the rat tongue. J Osaka Dent Univ 30:29–35
47. Sakaki T, Tamura I, Kadota H, Kakudo K (2003) Changing expression of E- and P-cadherin during rat tongue carcinogenesis induced by 4-nitroquinoline 1-oxide. J Oral Pathol Med 32:530–537
48. Nishimura A (1999) Changes in Bcl-2 and Bax expression in rat tongue during 4-nitroquinoline 1-oxide-induced carcinogenesis. J Dent Res 78:1264–1269
49. Nauta JM, Roodenburg JL, Nikkels PG, Witjes MJ, Vermey A (1995) Comparison of epithelial dysplasia–the 4NQO rat palate model and human oral mucosa. Int J Oral Maxillofac Surg 24:53–58
50. Fitch KA, Somers KD, Schechter GL (1988) The development of a head and neck tumor model in the nude mouse. In: Wolf GT, Carey TE (eds) Head and neck oncology research. Kugler & Ghedini, Amsterdam (Distributors for the U.S.A. and Canada, Kugler Publications). pp. 187–190
51. Dinesman A, Haughey B, Gates GA, Aufdemorte T, Von Hoff DD (1990) Development of a new in vivo model for head and neck cancer. Otolaryngol Head Neck Surg 103:766–774
52. Myers JN, Holsinger FC, Jasser SA, Bekele BN, Fidler IJ (2002) An orthotopic nude mouse model of oral tongue squamous cell carcinoma. Clin Cancer Res 8:293–298
53. Cabanillas R, Secades P, Rodrigo JP, Astudillo A, Suarez C et al (2005) [Orthotopic murine model of head and neck squamous cell carcinoma]. Acta otorrinolaringologica espanola 56:89–95
54. Bao A, Phillips WT, Goins B, McGuff HS, Zheng X et al (2006) Setup and characterization of a human head and neck squamous cell carcinoma xenograft model in nude rats. Otolaryngol Head Neck 135:853–857
55. Jetten AM, Kim JS, Sacks PG, Rearick JI, Lotan D et al (1990) Inhibition of growth and squamous-cell differentiation markers in cultured human head and neck squamous carcinoma cells by beta-all-trans retinoic acid. Int J Cancer 45:195–202
56. Heo DS, Snyderman C, Gollin SM, Pan S, Walker E et al (1989) Biology, cytogenetics, and sensitivity to immunological effector cells of new head and neck squamous cell carcinoma lines. Cancer Res 49:5167–5175
57. Matijevic T, Marjanovic M, Pavelic J (2009) Functionally active toll-like receptor 3 on human primary and metastatic cancer cells. Scand J Immunol 70:18–24
58. Jimeno A, Kulesza P, Wheelhouse J, Chan A, Zhang X et al (2007) Dual EGFR and mTOR targeting in squamous cell carcinoma models, and development of early markers of efficacy. British J Cancer 96:952–959
59. Patel V, Marsh CA, Dorsam RT, Mikelis CM, Masedunskas A et al (2011) Decreased lymphangiogenesis and lymph node metastasis by mTOR inhibition in head and neck cancer. Cancer Res 71:7103–7112
60. O'Malley BW Jr., Cope KA, Johnson CS, Schwartz MR (1997) A new immunocompetent murine model for oral cancer. Arch Otolaryngol Head Neck Surg 123:20–24

61. Cui N, Nomura T, Noma H, Yokoo K, Takagi R et al (2005) Effect of YM529 on a model of mandibular invasion by oral squamous cell carcinoma in mice. Clin Cancer Res 11:2713–2719
62. Behren A, Kamenisch Y, Muehlen S, Flechtenmacher C, Haberkorn U et al (2010) Development of an oral cancer recurrence mouse model after surgical resection. Int J Oncol 36:849–855
63. Yu Z, Li S, Huang YY, Lin SF, Fong Y et al (2008) Sensitivity of squamous cell carcinoma lymph node metastases to herpes oncolytic therapy. Clin Cancer Res 14:1897–1904
64. Matsumoto G, Yajima N, Saito H, Nakagami H, Omi Y et al (2010) Cold shock domain protein A (CSDA) overexpression inhibits tumor growth and lymph node metastasis in a mouse model of squamous cell carcinoma. Clin Exp Metastasis 27:539–547
65. Judd NP, Winkler AE, Murillo-Sauca O, Brotman JJ, Law JH et al (2012) ERK1/2 Regulation of CD44 Modulates Oral Cancer Aggressiveness. Cancer Res 72:365–374
66. Caulin C, Nguyen T, Longley MA, Zhou Z, Wang XJ et al (2004) Inducible activation of oncogenic K-ras results in tumor formation in the oral cavity. Cancer Res 64:5054–5058
67. Vitale-Cross L, Amornphimoltham P, Fisher G, Molinolo AA, Gutkind JS (2004) Conditional expression of K-ras in an epithelial compartment that includes the stem cells is sufficient to promote squamous cell carcinogenesis. Cancer Res 64:8804–8807
68. Raimondi AR, Molinolo A, Gutkind JS (2009) Rapamycin prevents early onset of tumorigenesis in an oral-specific K-ras and p53 two-hit carcinogenesis model. Cancer Res 69:4159–4166
69. Moral M, Segrelles C, Lara MF, Martinez-Cruz AB, Lorz C et al (2009) Akt activation synergizes with Trp53 loss in oral epithelium to produce a novel mouse model for head and neck squamous cell carcinoma. Cancer Res 69:1099–1108
70. Saranath D, Chang SE, Bhoite LT, Panchal RG, Kerr IB et al (1991) High frequency mutation in codons 12 and 61 of H-ras oncogene in chewing tobacco-related human oral carcinoma in India. Br J Cancer 63:573–578
71. Munirajan AK, Mohanprasad BK, Shanmugam G, Tsuchida N (1998) Detection of a rare point mutation at codon 59 and relatively high incidence of H-ras mutation in Indian oral cancer. Int J Oncol 13:971–974
72. Kuriakose MA, Trivedi NP (2009) Sentinel node biopsy in head and neck squamous cell carcinoma. Curr Opin Otolaryngol Head Neck Surg 17:100–110
73. Stoeckli SJ, Alkureishi LW, Ross GL (2009) Sentinel node biopsy for early oral and oropharyngeal squamous cell carcinoma. Eur Arch Otorhinolaryngol 266:787–793
74. Jefferson GD, Sollaccio D, Gomez-Fernandez CR, Civantos F Jr. (2011) Evaluation of immunohistochemical fine sectioning for sentinel lymph node biopsy in oral squamous cell carcinoma. Otolaryngol Head Neck Surg 144:216–219
75. Coughlin A, Resto VA (2010) Oral cavity squamous cell carcinoma and the clinically n0 neck: the past, present, and future of sentinel lymph node biopsy. Current oncology reports 12:129–135
76. Alkureishi LW, Ross GL, Shoaib T, Soutar DS, Robertson AG et al (2010) Sentinel node biopsy in head and neck squamous cell cancer: 5-year follow-up of a European multicenter trial. Ann Surg Oncol 17:2459–2464
77. Harrell MI, Iritani BM, Ruddell A (2008) Lymph node mapping in the mouse. J Immunol Methods 332:170–174
78. Alitalo A, Detmar M (2011) Interaction of tumor cells and lymphatic vessels in cancer progression. Oncogene 31(42):4499–4508
79. Bredell MG (2010) Sentinel lymph node mapping by indocyanin green fluorescence imaging in oropharyngeal cancer—preliminary experience. Head Neck Oncol 2:31
80. Mathelin C, Croce S, Brasse D, Gairard B, Gharbi M et al (2009) Methylene blue dye, an accurate dye for sentinel lymph node identification in early breast cancer. Anticancer Res 29:4119–4125
81. Wong JH, Cagle LA, Morton DL (1991) Lymphatic drainage of skin to a sentinel lymph node in a feline model. Ann Surg 214:637–641
82. Rebhun RB, Lazar AJ, Fidler IJ, Gershenwald JE (2008) Impact of sentinel lymphadenectomy on survival in a murine model of melanoma. Clin Exp Metastasis 25:191–199
83. Hoshida T, Isaka N, Hagendoorn J, di Tomaso E, Chen YL et al (2006) Imaging steps of lymphatic metastasis reveals that vascular endothelial growth factor-C increases metastasis

by increasing delivery of cancer cells to lymph nodes: therapeutic implications. Cancer Res 66:8065–8075
84. Nagy JA, Vasile E, Feng D, Sundberg C, Brown LF et al (2002) Vascular permeability factor/vascular endothelial growth factor induces lymphangiogenesis as well as angiogenesis. J Exp Med 196:1497–1506
85. Close DM, Xu T, Sayler GS, Ripp S (2011) In Vivo Bioluminescent Imaging (BLI): noninvasive visualization and interrogation of biological processes in living animals. Sensors (Basel) 11:180–206
86. Sano D, Fooshee DR, Zhao M, Andrews GA, Frederick MJ et al (2011) Targeted molecular therapy of head and neck squamous cell carcinoma with the tyrosine kinase inhibitor vandetanib in a mouse model. Head Neck 33:349–358
87. Sano D, Matsumoto F, Valdecanas DR, Zhao M, Molkentine DP et al (2011) Vandetanib restores head and neck squamous cell carcinoma cells' sensitivity to cisplatin and radiation in vivo and in vitro. Clin Cancer Res 17:1815–1827
88. Sano D, Choi S, Milas ZL, Zhou G, Galer CE et al (2009) The effect of combination anti-endothelial growth factor receptor and anti-vascular endothelial growth factor receptor 2 targeted therapy on lymph node metastasis: a study in an orthotopic nude mouse model of squamous cell carcinoma of the oral tongue. Arch Otolaryngol Head Neck Surg 135:411–420
89. Rosenthal EL, Kulbersh BD, King T, Chaudhuri TR, Zinn KR (2007) Use of fluorescent labeled anti-epidermal growth factor receptor antibody to image head and neck squamous cell carcinoma xenografts. Mol Cancer Ther 6:1230–1238
90. Keereweer S, Kerrebijn JD, Mol IM, Mieog JS, Van Driel PB et al (2011) Optical imaging of oral squamous cell carcinoma and cervical lymph node metastasis. Head Neck 34(7):1002–1008
91. Niu G, Li Z, Xie J, Le QT, Chen X (2009) PET of EGFR antibody distribution in head and neck squamous cell carcinoma models. J Nucl Med 50:1116–1123
92. Niu G, Sun X, Cao Q, Courter D, Koong A et al (2010) Cetuximab-based immunotherapy and radioimmunotherapy of head and neck squamous cell carcinoma. Clin Cancer Res 16:2095–2105
93. Savastano LE, Castro AE, Fitt MR, Rath MF, Romeo HE, Muñoz EM (2010) A standardized surgical technique for rat superior cervical ganglionectomy. J Neurosci Methods 192(1):22–33
94. Keereweer S, Mol IM, Vahrmeijer A, Driel PV, Baatenburg deJRJ, Kerrebijn JD, Lowik C (2011) Towards optical image-guided head and neck cancer surgery: Multi-targeted dual wavelength detection using near-infrared fluorescence probes. The fourth annual world molecular imaging congress, Scientific Session 17: Cancer Cell Detection. Presentation Number T154

Chapter 3
Breast Cancer Invasion and Metastasis

Shane Stecklein, Hanan Elsarraj, Kelli Valdez, Arindam Paul and Fariba Behbod

Abstract Breast cancer is the most common malignancy among western women, and 10–15 % of all breast cancer patients develop and ultimately succumb to metastatic disease. In breast cancer, malignant cells disseminate through lymphatic or hematogenous routes to distant organs. Over the last decades, the 5-year survival of breast cancer has increased due to early screening and advanced local and systemic treatments. Understanding the fundamental biology underlying the progression of breast cancer has fostered the identification and development of therapeutics. In this chapter, we discuss the morphologic and molecular heterogeneity of breast cancer and the relationship between breast cancer subtype and metastatic potential. Moreover, we detail different *in vitro* assays which provide simple and robust systems to study basic cellular processes that are critical to orchestrating metastatic progression of breast cancer. Lastly, we address the strengths and shortcomings of different *in vivo* models that allow integrated analysis of heterotypic signaling and tissue architecture in breast cancer progression.

Abbreviations

TDLU	terminal ductal lobular units
DCIS	ductal carcinoma in situ
DCISM	DCIS with microinvasion
ER	estrogen receptor α
PR	progesterone receptor
VEGF-A	vascular endothelial growth factor-A
PlGF	placenta growth factor
SDF-1	stromal-cell derived factor-1
FGF2	fibroblast growth factor 2
HGF	hepatocyte growth factor
IGFs	insulin-like growth factors
EMT	epithelial-mesenchymal transition
CSC	cancer stem cell
MET	mesenchymal-to-epithelial transitions
ECM	extracellular matrix

F. Behbod (✉) · S. Stecklein · H. Elsarraj · K. Valdez · A. Paul
Department of Pathology and Laboratory Medicine, The University of Kansas Medical Center, Kansas City, USA
e-mail: fbehbod@kumc.edu

A. Malek (ed.), *Experimental Metastasis: Modeling and Analysis,*
DOI 10.1007/978-94-007-7835-1_3,

MMC	mitomycin C
IR	ionizing radiation
MMPs	matrix metalloproteinases
TIMPs	tissue inhibitor of metalloproteinases
MMTV	mouse mammary tumor virus
BLG	beta-lactoglobulin
PyMT	polyoma middle T antigen
TGFβ	transforming growth factor β
MIND	mouse intraductal
SLN	sentinel lymph node

3.1 Introduction

Breast cancer is the most common malignant disease in Western women [1]. In these patients, it is not the primary tumor, but distant metastasis that is the main cause of death [1]. Recently, breast cancer mortality and metastatic rates have decreased as a result of early detection by mammographic screening and the implementation of systemic adjuvant therapy [1].

Invasive breast carcinomas are a group of malignant epithelial tumors characterized by invasion of adjacent tissues with a marked tendency to metastasize to distant sites [2]. The vast majority of these tumors are adenocarcinomas and are believed to originate from the mammary parenchymal epithelium, particularly cells of the terminal ductal lobular units (TDLU) [2]. Intraductal and intralobular hyperplastic lesions also known as ductal hyperplasia are a group of cytologically and architecturally diverse proliferations, also originating from the TDLU, but which remain confined to the mammary ductal and lobular system. Despite their localized nature, these lesions are precursors to invasive breast cancer, and their identification is associated with a risk for developing invasive cancer [2]. Ductal carcinoma *in situ* (DCIS) of the breast is a proliferation of malignant cells within the ducts and terminal lobular units of the breast that have not breached the ductal basement membrane [3]. DCIS with microinvasion (DCISM) was defined in 2003 by the American Joint Committee on Cancer as " the extension of cancer cells beyond the basement membrane into the adjacent tissues, with no single focus larger than 1 mm in greatest dimension" [3]. Breast cancer progresses through a well-defined sequence, where benign or *in situ* proliferative lesions initially form microinvasive disease, the unhindered progression of which leads to frank invasive disease, and finally, the appearance and growth of metastatic tumors at distant sites. Survival rates for breast cancer are intimately linked with disease stage, as the five-year survival rates for DCIS and metastatic disease are approximately 100% and 15%, respectively [4]. These statistics highlight the importance of early detection in reducing breast cancer-related mortality, while also reiterating the necessity to understand, at the most fundamental level, the biology underlying breast cancer progression and metastasis.

Approximately 230,480 new cases of invasive breast cancer and 39,520 breast cancer deaths are expected to occur among US women in 2011. Approximately 78% of new cases and 87% of breast cancer deaths in 2011 will occur among women aged 50 years and older. In addition to invasive breast cancers, about 57,650 new diagnoses of *in situ* breast cancer are expected among US women in 2011 [5]. Five-year relative survival has increased from 63% in the early 1960s to 90% today [6]. Despite this marked improvement in overall survival, 10–15% of today's breast cancer patients will develop and succumb to metastatic disease [7].

3.2 Classification of Breast Cancer

3.2.1 Histological Classification of Breast Cancer

Breast carcinomas exhibit a wide range of morphological phenotypes and specific histopathological types have particular prognostic and clinical characteristics. Tissue and cell morphology allows, in most cases, the distinction between benign or malignant tumors and therefore provides clinicians with essential information for determining appropriate therapy [2]. In the pathology laboratory, immunohistochemistry and molecular biology have improved the specificity of breast cancer diagnosis and have introduced new prognostic and predictive markers for tumor management [8]. The latest edition of the WHO classification, released in 2003, distinguishes 21 varieties of invasive carcinoma and 2 categories of intraepithelial neoplasia based on morphologic and immunohistochemical parameters [8] (Table 3.1). The two most common types of invasive breast cancer are invasive ductal carcinoma, no special type, and invasive lobular carcinoma.

- *Invasive ductal carcinoma, no special type (NST)* [9]. Invasive ductal carcinoma accounts for 47–70% of invasive breast cancers, with women younger than 35 years developing ductal tumors more commonly than older patients. Grossly, the tumor is moderately well defined or ill-defined, nodular or stellate, with a firm to hard cut surface. Microscopically, tumor cells form trabeculae, sheets, nests and glands. Nuclear pleomorphism and mitotic counts vary. The surrounding stroma ranges from desmoplastic to collagenous, with higher grade tumors often exhibiting necrosis. Most tumors (70–80%) are estrogen receptor α (ER) and/or progesterone receptor (PR) positive and 15–20% demonstrate overexpression of the HER2 oncogene. Overall, these tumors are associated with a 35–50% 10-year survival, depending on the status of traditional prognostic features including grade, tumor and lymph node stage and the presence of lymphovascular invasion.
- *Invasive lobular carcinoma* [9]. Invasive lobular carcinoma is the second most common form of invasive breast cancer, representing 5–15% of all invasive lesions. Lobular cancers characteristically show loss of E-cadherin expression and diffusely infiltrate the stroma, often without desmoplasia. Cells frequently line

up in single file, and may show periductal "targetoid" arrangement. They do not form ducts, but may form solid sheets, trabeculae or nests. Invasive lobular carcinomas are more often ER positive than ductal NST, although high-grade lobular cancers may lack ER or show HER2 positivity. Lobular carcinoma shows a particular pattern of metastasis with a tendency to spread to the peritoneum, retroperitoneum, ovary and uterus, leptomeninges and gastrointestinal tract. Matched for grade and stage, lobular carcinoma has a similar prognosis, in terms of disease-free and overall survival, to that of ductal, NST cancers.

3.2.2 Molecular Subtypes of Breast Cancer

Though the histological heterogeneity of breast cancer has been appreciated for many years, we have only recently gained insight into the molecular diversity of these malignancies. Pioneering studies by Charles Perou and colleagues delineated four major molecular taxonomies of breast cancer based on gene expression patterns: ER^+/luminal-like, basal-like, *ERBB2*$^+$, and normal breast-like [10]. The same group soon published another report that further divided the ER^+/luminal-like cluster into three distinct groups known as luminal-A, -B and -C, and demonstrated that these six classifications were predictive of clinical course and survival [11]. Specifically, this study noted that luminal-A tumors, which exhibit robust luminal phenotypes and express high levels of ER were indolent and both relapse-free and overall survival were high, while tumors exhibiting the basal-like and *ERBB2*$^+$ gene expression signatures were more likely to recur and were associated with an aggressive clinical course and poor long-term survival [11]. Refinements in our current classification scheme have elaborated the number of known molecular subtypes, and it is likely that as we analyze more independent samples we will identify additional distinct subtypes of breast cancer. The following is a brief overview of the currently recognized molecular classifications of breast cancer.

- Luminal-A and –B/C breast cancers. The majority of invasive ductal and lobular breast carcinomas exhibit luminal differentiation. Such tumors usually express markers consistent with a mature fate, including ER, PR and the transcription factor GATA3 and are thus amenable to therapies that target ER signaling or estrogen synthesis [10, 12]. Gene expression signatures in these tumors were found to be similar to the signature observed in normal mammary epithelial cells that were in the terminal stages of differentiation [13]. It is thus likely that the majority of human breast cancers arise from transformation of a cell that already specified a luminal terminal fate. Luminal- A tumors are the most highly differentiated and robustly express ER, while the luminal-B/C tumors express ER (though to a lesser extent than the luminal-A subtype).The luminal-C tumors is distinguished from luminal-A and luminal-B tumors by the expression of novel genes which they share with basal-like and Erbb2+ subtypes of breast cancers. Luminal-B/C tumors exhibit higher mitotic indices and histological grade, and are accordingly associated with a significantly poorer prognosis than luminal-A malignancies [11, 14].

- *ERBB2*$^{+}$*breast cancers.* The *ERBB2* gene is amplified in 20–25 % of all breast cancers, leading to overexpression of wild-type HER2 receptor tyrosine kinase at the plasma membrane. Such overexpression of HER2 induces constitutive activation of numerous signaling nodes that influence proliferation, differentiation and apoptosis [15]. Like the luminal-A and -B/C malignancies, transcriptional data suggest that *ERBB2*$^{+}$ tumors arise from a cell committed to a luminal fate [13]. Prior to the implementation of trastuzumab (Herceptin®), the first HER2-targeted therapy, HER2^{+} (*ERBB2*$^{+}$) breast cancer was associated with a grave prognosis. Though trastuzumab revolutionized the treatment of HER2^{+} breast cancer and significantly improved morbidity and mortality from this disease, HER2^{+} breast cancer continues to follow a more aggressive course than do luminal tumors without *ERBB2* amplification, are more resistant to chemotherapeutic agents, and have an increased risk of distant metastasis [11, 16, 17].
- *Basal-like breast cancers.* Basal-like breast cancers were so named because they recurrently express molecules normally confined to the basal (myoepithelial) compartment of the mammary ductal and lobular epithelium, including the basal cytokeratins 5, 6 and 14 [18]. These tumors account for roughly 15 % of all invasive breast cancers, are commonly "triple-negative" (i.e., ER-, PR- and HER2-negative), are of high histological grade and exhibit *TP53* mutations [19, 20]. Unexpectedly, it was found that the gene expression signature of basal-like malignancies was highly similar to that of the normal mammary luminal progenitor cell, refuting the assumption that these neoplasms arose from the mammary stem cell or a progenitor committed to the myoepithelial lineage [13]. Due to absence of sex hormone receptors and HER2 expression, the basal-like malignancies are not amenable to the endocrine and HER2-targeting therapies that have revolutionized treatment of the luminal and *ERBB2*$^{+}$ breast cancers. This lack of targeted therapy, coupled with specific inherent biological features of these tumors make basal-like tumors the most aggressive and lethal molecular category of breast cancer [11].
- *Normal breast-like, claudin-low and metaplastic breast cancers.* The normal breast-like tumors were originally described based on their transcriptional similarly to normal breast tissue, a signature typified by high expression of basal/myoepithelial- and adipocyte-restricted genes, and low expression of luminal-associated genes [10]. Comparison of normal breast-like malignancies with sorted populations of mammary epithelial cells revealed that these tumors were transcriptionally most similar to the mammary stem cell-enriched population, and thus likely arise from transformation of a developmentally primitive mammary epithelial cell [13]. These tumors appear to have an intermediate prognosis, with improved relapse-free and overall survival compared to the basal-like breast cancers, but a significantly poorer prognosis than the highly differentiated luminal-A tumors [11]. Though the normal breast-like classification was identified in the first report describing molecular breast cancer heterogeneity, refinements in transcriptional profiling and comparative analysis of human and murine mammary tumors illuminated a previously unappreciated distinct subtype [21]. This new entity, the claudin-low subtype, exhibits low expression of components of the tight and adherens junctions, including claudins 3, 4 and 7 and

E-cadherin, shows recurrent copy number gains at the *KRAS2* locus, and exhibits exaggerated expression of genes associated with immunological responses, cellular communication, extracellular matrix, migration and angiogenesis [21, 22]. Transcriptionally, these lesions were concordant with the signatures of both the mammary stem cell-enriched and stromal cells of the normal mammary gland, suggesting that these lesions may also stem from transformation of an undifferentiated epithelial cell [13]. Metaplastic breast cancers are a morphologically diverse group of mostly TN malignancies that exhibit mesenchymal, sarcomatoid and/or squamous metaplasia [23–26]. Transcriptional profiling of these tumors originally classified them as basal-like malignancies [26]. By refining the criteria used for classification and including the recently-identified claudin-low subtype, metaplastic lesions were shown to be molecularly heterogeneous and may cluster with the basal-like, claudin-low or normal breast-like subtypes [22, 27].

3.2.3 Genetics: Sporadic and Hereditary Breast Cancers

Approximately 90% of all breast cancers are sporadic in origin. Of the remaining 10% which appear to be associated with inheritance of dominantly-acting genes, roughly half are caused by inheriting a deleterious allele of the highly-penetrant breast cancer susceptibility genes *BRCA1* or *BRCA2*/*FANCD1* [28]. The remaining fraction of hereditary breast cancers is caused by heterogeneous inherited genetic defects, many of which remain unknown. Among those identified to be minor breast cancer susceptibility genes are *PALB2*/*FANCN*, *BRIP1*/*FANCJ* and *RAD51C*/*FANCO*, *ATM*, *TP53*, *PTEN*, *STK11/LKB1*, *CDH1*, *CHEK2*, *MLH1* and *MSH2* [28–32]. Despite the identification of these low-penetrance minor loci, we have yet to find the genetic lesions responsible for many non-*BRCA1/2* hereditary breast cancers.

BRCA1 and *BRCA2* are critical components of the Fanconi-BRCA DNA repair pathway which is responsible for repairing double strand DNA breaks and interstrand crosslinks by homologous recombination [33]. Despite the functional similarity of these two genes, *BRCA1*-associated breast cancers are strikingly different from those that arise in *BRCA2* mutation carriers. The latter are generally well-differentiated ER^+ carcinomas that have genetic, epigenetic and transcriptional signatures that are similar to those seen in sporadic cancers. Conversely, cancers arising in *BRCA1* mutation carriers are most commonly triple-negative, transcriptionally cluster with the basal-like malignancies and more commonly exhibit medullary histology [17, 34, 35]. While BRCA1 dysfunction is notably associated with inherited breast cancers, several studies have reported loss of BRCA1 expression by non-mutational means in 30–40% of sporadic malignancies [36, 37]. Sporadic breast cancers that exhibit loss of BRCA1 expression have a strong tendency to be of the basal-like phenotype, whereas those that maintain expression of functional BRCA1 are almost uniformly luminal-type cancers [20, 36, 38, 39]. Taken together, these findings suggest that loss of BRCA1 expression and/or function has a causal role in the development of the basal-like phenotype.

3.3 Breast Cancer Metastasis

3.3.1 General Aspects of Breast Cancer Metastasis

Several mechanisms mediate tumor cell dissemination, including local tissue invasion, lymphatic and hematogenous spread, and direct seeding of the body cavities [40]. In breast cancer, tumor cells often migrate to the regional lymph nodes, either draining via pre-existing afferent lymphatic vessels or through newly formed lymphatic capillaries [40]. During metastatic dissemination, a cancer cell from a primary tumor must execute the following sequence of steps: (1) invade the surrounding tissue, (2) intravasate into the microvasculature of the lymph and/or blood systems, [41], (3) survive and translocate through the bloodstream to microvessels of distant tissues, (4) extravasate from the bloodstream, (5) survive the novel microenvironment of distant tissues, and (5) adapt to the foreign microenvironment of these tissues in ways that facilitate cell proliferation and the formation of a macroscopic secondary tumor (colonization) [42].

Over the last three decades, many investigators have made valuable contributions to our understanding of breast cancer pathogenesis and metastasis. Many models for metastatic formation in general have been formulated. Besides the ‘seed and soil’ model of metastasis formation [43], the concept of a ‘premetastatic niche’ has recently been introduced by David Lyden and colleagues [44], proposing that future sites for cancer cells metastases are prepared by bone marrow-derived hematopoietic progenitors which preferentially localize in these future sites [45]. In breast cancer, supporting evidence from Gupta et al. [46] showed that ER negative breast cancer cell lines were more aggressive in the presence of estrogen, they elucidated that estrogen promoted angiogenesis and thus tumor stromal growth [46]. Another study by Karnoub et al. [47] revealed that coinjection of weakly metastatic breast cancer cells along with bone marrow derived mesenchymal stem cells increases their metastatic potency [47].

3.3.2 Lymphangitic Metastasis

The spread of tumor cells to lymph nodes is a common occurrence in breast cancer, indicating that the lymphatic vasculature is an important route of metastasis. Moreover, spread to lymph nodes is often an early event in metastatic disease and is significant for the staging of cancer [48]. Expression of lymphangiogenic growth factors in a range of animal tumor models leads to formation of lymphatic vessels either within or at the periphery of the tumors and this is accompanied by enhanced lymphatic metastasis and, in some cases, by distant organ metastasis [48]. These molecules may be potential targets for therapeutic approaches designed to restrict metastasis by blocking tumor lymphangiogenesis [48].

Five years ago, the only known lymphangiogenic growth factors were VEGF-C and VEGF-D. These proteins clearly play an important role in promoting tumor

lymphangiogenesis via VEGFR-3 signaling and may promote lymphatic metastasis in human cancer [48]. Recently, other lymphangiogenic growth factors have been identified, namely VEGF-A, PDGF-BB, angiopoietins, fibroblast growth factor 2 (FGF2), hepatocyte growth factor (HGF) and insulin-like growth factors (IGFs). Of these, only VEGF-A and PDGF-BB have been shown to promote tumor lymphangiogenesis and lymphatic metastasis in animal models [48]. It has been observed that lymphangiogenesis in cancer is not restricted to regions within or immediately adjacent to a primary tumor, but can also occur in the sentinel lymph nodes [49]. Furthermore, lymphangiogenic growth factors produced by the primary tumor appear to act at a distance by inducing lymphangiogenesis (sinusoidal hyperplasia) in the sentinel lymph node even before the arrival of the first metastatic cells [50–53]. It has been suggested that in this way, the tumor cells prepare the 'soil' in the lymph node beforehand to render it more hospitable for secondary tumor formation [54].

From a clinical point of view, the extent of lymph node (N) metastasis is the major factor influencing staging and prognosis of most malignancies and often determines therapeutic decision. Sentinel lymph node (SLN) biopsy was developed for the axillary staging of breast cancer. If the SLN does not contain metastasis, then surgeons can avoid axillary-lymph-node dissection (ALND), with a favorable effect on patients' quality of life [55].

The relationship between isolated tumor cells or micrometastases in the regional lymph nodes and clinical outcome has been studied, both in patients who had undergone a SLN procedure, and who did or did not receive systemic adjuvant therapy. The results showed a reduction in the 5-year rate of disease-free survival among women with favorable early-stage breast cancer who did not receive adjuvant therapy, while in the other group who received adjuvant therapy, disease-free survival was improved [56]. This indicates that size of the tumor deposit may not be an influence on the clinical outcome.

Recent studies have aimed to identify diagnostic biomarkers for lymph node metastasis by studying protein expression changes at different stages of N according to TNM staging systems. These studies illuminated potential biomarkers for each N stage, with HSP70 for N0, protein H precursor and PDI for N1 stage, while glucose-regulated protein was found useful for N2 stage. In addition, significant up-regulation of PDI A3 was detected only in metastasized breast cancer [57].

3.4 Modeling Breast Cancer Invasion and Metastasis

Much of the fundamental biology underlying the progression of breast cancer has been elucidated using *in vitro* cell systems. Though these models lack the heterotypic signaling and tissue architecture that are afforded by *in vivo* models, they provide simple and robust systems for examining elementary cellular processes that are critical to orchestrating metastatic progression of breast cancer. Acquisition of motility, secretion of matrix-degrading enzymes and resistance to detachment-induced apoptosis are examples of fundamental cellular processes that must precede frank

metastasis. These and other cellular phenotypes are imbued through an elaborate transcriptional and epigenetic reprogramming event known as the epithelial-mesenchymal transition (EMT).

Epithelial cells are typified by robust adhesion with neighboring cells and/or with basement membrane. During the invasive progression of epithelial cancers, these adhesion complexes must be dismantled and cells must gain the ability to degrade extracellular matrix components and migrate. It is this initial invasion through the basement membrane that presages metastatic dissemination of epithelial malignancies. Striking similarities at both the molecular and morphological levels have been noted between invasive cancer cells and migratory cells that arise during both development and physiological wound healing through EMT. In all of these contexts, these developmental programs allow polarized epithelial cells to assume a mesenchymal-like phenotype, gain migratory and invasive capacity, and resist anoikis (i.e., apoptosis resulting from loss of adhesion). EMT is critical in numerous early developmental processes, as embryo implantation, placentation, specification of the mesendoderm from the primitive streak and formation of neural crest cells from the neuroectoderm all require such a transition. Moreover, in both physiologic wound healing as well as pathologic fibrosis, inflammation-associated signaling induces epithelial cell changes that facilitate wound closure and deposition of extracellular matrix components [58].

In malignant disease, EMT has been implicated in conferring two of the most insidious properties of cancer: the ability of epithelial cancer cells to invade and migrate away from the primary site, and the ability to resist cytotoxic chemotherapy and ionizing radiation. Both properties are the result of complex transcriptional and epigenetic programs that are likely activated by heterotypic signals derived from the tumor itself and the tumor-associated stroma. Though numerous soluble and cell contact-dependent morphogens and growth factors have been implicated in EMT, TGFβ, PDFG, HGF (scatter factor) and EGF are the most notable. These factors induce or activate a complement of transcription factors, including Snail, Slug, Twist, FOXC2, GSC and ZEB1, which cooperate with other signaling nodes to orchestrate cytoskeletal rearrangement, extracellular matrix remodeling, and acquisition of both invasive potential and cancer stem cell (CSC)-like phenotype [58]. Indeed, several studies have demonstrated that forced induction of EMT in mammary epithelial cells by expression of mesenchyme-associated transcription factors or TGFβ increased expression of CSC-associated genes, caused dramatic expansion of the $CD44^{Hi}/CD24^{-/Low}$ CSC population, increased mammosphere-forming capacity and improved outgrowth potential in xenotransplant assays [59, 60]. There is emerging evidence of at least two distinct forms of cellular motility, collective and single, and that these modes of migration are determined by heterotypic signaling within the tumor. TGFβ, a well-characterized inducer of EMT, has been shown in several *in vivo* models of breast cancer to promote single cell motility [61]. Since TGFβ can also be strongly growth suppressive, incipient metastatic cancer cells must be able to activate TGFβ signaling transiently to allow migration and dissemination, but then to strongly suppress this signaling node in order to allow proliferation at distantly colonized sites [61]. Interestingly, it has also been noted that TGFβ signaling,

and thus single cell migration, is required for hematogenous, but not for lymphatic metastasis of breast cancer [61]. This could be explained by the fact that lymphatic capillaries lack smooth muscle and/or pericyte sheaths and basement membranes and also do not exhibit tight intercellular junctions exhibitied by vascular endothelial cells [62]. Thus, TGFβ-independent cohesive movement may still allow invasion into "leaky" lymphatic vessels, whereas only TGFβ-induced single-cell movement is compatible with diapedesis into the bloodstream. Cunningham and colleagues demonstrated that expression of the CCR7 chemokine receptor strongly influenced metastatic route in a PyVmT model of breast cancer, with $CCR7^-$ negative cells exhibiting pulmonary metastasis in the absence of lymphatic involvement, whereas CCL19 and CCL21-dependent activation of $CCR7^+$ mammary tumors led to a significant increase in lymphatic involvement and a corresponding decrease in pulmonary metastases [63]. Additionally, co-expression of α9β1 integrin and the lymphangiogenic growth factor VEGF-D have also been shown to promote lymphatic metastasis of breast cancer in a xenograft model of human breast cancer metastasis [64, 65].

Though EMT is critical for incipient metastatic cells to leave their site of origin, an equally profound but opposite transition appears to be critical in facilitating colonization of distant sites. This duality in plasticity has been inferred from observations that, despite the mesenchymal morphology and biochemical characteristics of migratory cancer cells, distant metastatic colonies closely resemble the primary malignancy from which they arose. Like the EMT that initially fostered invasive progression, these mesenchymal-to-epithelial transitions (MET) in metastatic niches likely stem from heterotypic signaling (or lack thereof) in the tissue being colonized. This is again reflected by studies showing that while cells constitutively overexpressing TGFβ are increasingly able to seed metastatic sites, perpetual activation of these EMT-inducing soluble signals impairs proliferation at distant sites [61]. Though our understanding of the molecular events that incite or elaborate cancer progression remains incomplete, it is clear that epithelial-mesenchymal plasticity is a critical element in both the invasion and colonization phases of metastasis.

3.4.1 In Vitro Models

Because entry into and completion of an EMT is thought to be required for the early invasive progression of breast cancer, diverse assays have been developed to model specific elements of this process *in vitro*. Taken together, these assays can rigorously assess migration, invasion, secretion of active matrix-remodeling enzymes, resistance to anoikis and acquisition of a CSC-like phenotype. These assays are rapid, cost-effective and are particularly useful for mechanistic studies prior to modeling in animal systems. Moreover, many of these assays can be modified in ways that are amenable to high-throughput screening, enabling evaluation of target identification libraries and/or pharmacologic or genetic interventions.

3.4.1.1 Wound-Healing ("Scratch") Assay (Fig. 3.1b)

Disruption of a confluent epithelial monolayer, such as that which occurs in a cutaneous wound, incites polarized movement of epithelial cells and substantial remodeling of the extracellular matrix (ECM). Creation of an artificial wound in a confluent monolayer of cultured cells will provoke a similar reaction, causing cells at the edge of the wound to undergo polarized cell migration medially until new cell-cell contacts are established. This assay has been widely used for decades as it is economical, is technically simple to perform without requiring specialized instrumentation, can be modified to examine the role of specific extracellular matrix components, and enables qualitative and quantitative assessment of both cohesive and individual cell migration. The following is a basic protocol for conducting a wound-healing assay:

- *Coating cell culture dishes (optional).* Coat 60 mm dishes with desired ECM component (e.g., fibronectin, collagen, laminin, poly-*L*-lysine, etc. overnight at 4 °C or for 1–2 h at 37 °C. Remove unbound ECM and block with 2 mg/mL BSA for 1 h at 37 °C. Wash the plates three times with PBS, and then add serum-free media until ready to plate cells.
- *Plate cells.* Trypsinize and count a sub-confluent culture of the cell line to be assayed and plate into the prepared 60 mm dishes (with complete medium) such that a confluent monolayer is reached within 24 h. The number of cells required will differ based on cell type, and must be determined empirically.
- *Starvation (optional).* Serum starvation can increase the expression and availability of growth factor and morphogen receptors at the cell membrane, increasing the responsiveness of cells to soluble factors which induce migration. After cells reach confluence, wash the monolayer three times with PBS and replace with serum-free medium. Starve cells for 12–24 h before beginning the wound assay.
- *Mitomycin C treatment or irradiation (optional).* Closure of a wound can occur by two non- exclusive processes: (1) proliferation into the wound, and (2) directional migration of cells into the wound. These processes can occur simultaneously and both are stimulated by growth factors present in serum. Extensive proliferation may be problematic, as it can complicate one's ability to assess the precise contribution of directional migration in wound closure. Treatment with the DNA crosslinker mitomycin C (MMC) or exposure to ionizing radiation (IR) can render cells unable to divide, and thus can eliminate proliferation as a confounding element in wound closure assays. A 30 min treatment with mitomycin C (5–25 μg mL^{-1}) or exposure to 10–50 Gy γ radiation immediately before wounding is sufficient to render cells incapable of proliferation.
- *Wounding.* Using a p200 pipette tip, apply even pressure to create a straight scratch in the cell monolayer. Remove debris by washing once with growth medium. Add media with serum or specific growth factor(s) being assayed at empirically determined concentrations. Note that if cells are not treated with MMC or IR, high concentrations of serum and certain growth factors will induce proliferation that may confound interpretation of migration. To ensure imaging the

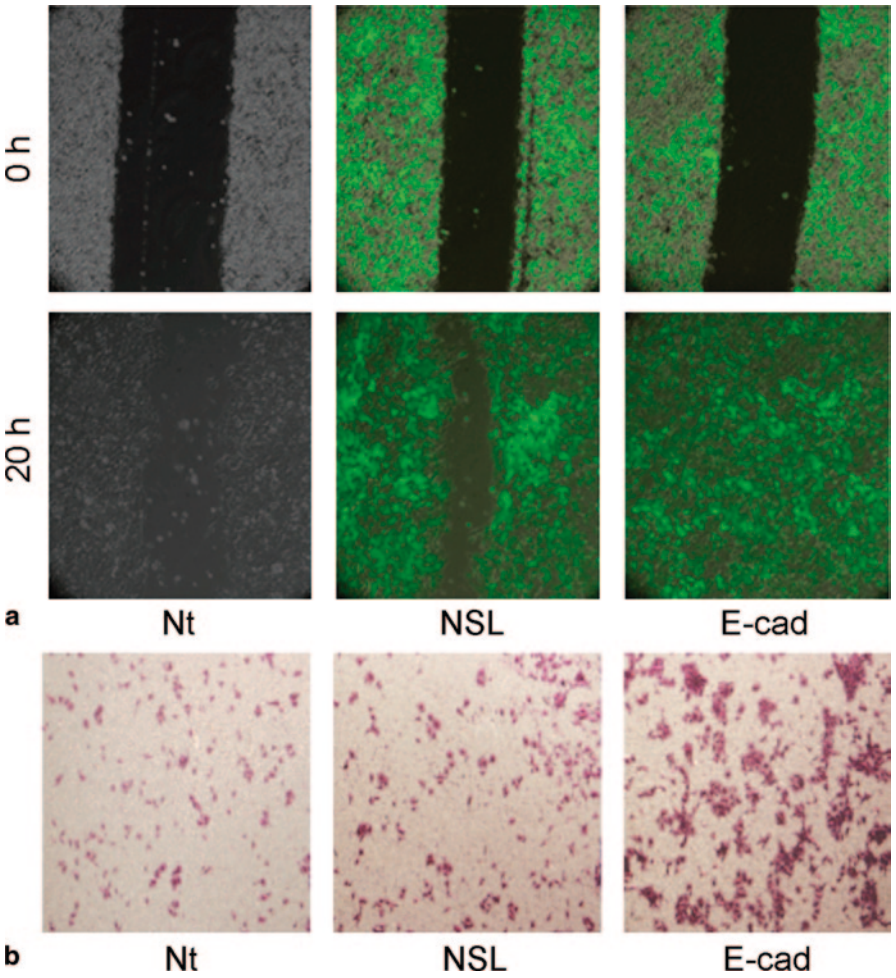

Fig. 3.1 In vitro migration assays. DCIS.COM cells were transduced with no virus (Nt), virus containing scrambled shRNA (NSL), and shRNA against E-cadherin (E-cad). Knockdown of E-cadherin showed invasion in both wound healing **a** and transwell **b** assays compared to controls

same area at each time interval, it is helpful to make markings on the plate using either an ultrafine tip marker or a razor blade.

- *Imaging and analysis*. At empirically determined intervals (typically every 6–8 h), image the wound on a phase-contrast microscope, using the marker or razor landmarks to ensure the same area is imaged at each time point. The last interval should correspond to the point at which the fastest migrating population just achieves complete wound closure. Wound closure can be quantitated in several ways, including measuring the distance between the edges of the wound over time or counting cells that cross into the wound area. Both of these can be accomplished using various software platforms (e.g., Adobe® Photoshop or ImageJ (NIH)).

3.4.1.2 Trans-well (Boyden Chamber) Migration/Invasion Assay(Fig. 3.1b)

Another widely used assay for cell migration entails measurement of chemotaxis through a microporous membrane. This assay, originally developed by Stephen Boyden to measure leukocyte chemotaxis [66], enables quantitative measurement of both migration and, when modified, invasion in response to soluble factors. Unlike the wound-healing assay, which does not require disruption of the monolayer, the trans-well assay measures migration and/or invasion of cells that begin as a single-cell suspension. Moreover, the trans-well assay enables assessment of directional migration towards a chemotactic stimulus.

This assay is based on two medium-filled compartments, separated by a microporous membrane. The cells to be assayed are placed in the upper chamber in serum-free medium, while the bottom chamber contains chemotactic factors. This concentration gradient incites directional migration of cells in the upper chamber towards and ultimately through the membrane. After incubation, the microporous membrane is fixed and stained, and the number of cells that have successfully migrated to the lower side of the chamber are quantified. Though migration and invasion are related, they are biologically distinct processes in that migration is necessary but not sufficient for invasion. The trans-well assay can be easily modified to allow discrete quantitation of both migration and invasion. When examining the migration alone, the microporous membrane is often coated with an ECM component like fibronectin to allow cells to adhere to the bottom side of the membrane. Invasion can be assessed by generating a basement membrane-like layer (using Matrigel™, BD Biosciences) on the microporous membrane. This variation of the assay requires cells to secrete matrix-modifying enzymes prior to migration through the micropores. The following is a basic assay for measuring migration or invasion using a 24-well trans-well assay (e.g., Costar® #3422, Corning, Inc.):

- *Starve cells.* Wash a sub-confluent culture of cells three times with PBS and replace with serum-free medium. Starve for 12–24 h.
- *Coat trans-well membranes.* To assess migration, dilute fibronectin to 50 μg mL^{-1} in PBS with 0.1% gelatin. To assess invasion, dilute growth-factor reduced Matrigel™ to 1 mg mL^{-1} in serum-free medium. For both assays, add 100 μL of the diluted ECM component to the top side of each trans-well membrane and 400 μL to the bottom chamber. Incubate the plate for one hour at room temperature (fibronectin) or for one hour at 37 °C (Matrigel™). Remove excess ECM component by aspiration, and wash the top and bottom chambers three times with serum-free medium.
- *Plate cells.* Trypsinize starved cells into a single cell suspension, count, and dilute to 2.5×10^5 cells/mL in serum-free (or low serum) medium. Note that cells should be washed with serum-free medium or PBS after neutralization of trypsin (with complete medium) to remove growth factors. Add 100 μL of cell suspensions (2.5×10^4 cells) to the upper chamber and 600 μL of media with serum or defined growth factor(s) to the lower chamber.
- *Fix and stain cells.* At empirically determined time points (typically 8–48 h), gently aspirate media from both the upper and lower chambers and fix cells for

20 min at room temperature in 10% neutral-buffered formalin. Aspirate fixative and stain cells with 0.1% crystal violet in PBS for 10 min at room temperature. Aspirate stain and wash membranes with PBS or deionized H_2O three times. Remove cells from the upper chamber using a cotton swab, and allow membranes to air dry.

- *Imaging and analysis.* Invert trans-well inserts under a dissecting microscope and count the number of invasive cells in 3–5 random high-magnification fields per insert.

3.4.1.3 Zymography Assays

Active secretion of matrix-modifying enzymes, namely the matrix metalloproteinases (MMPs), is necessary for cancer cell invasion. To date, more than 20 MMPs have been identified, and they are classified into six groups based on structural domains, sequence similarity and substrate specificity. Most MMPs are secreted, though six exist as membrane-bound forms. All MMPs exist initially in an inactive form and require both intramolecular activation and proteolytic processing to gain full catalytic activity. Another class of molecules known as TIMPs (tissue inhibitor of metalloproteinases) bind to MMPs in a 1:1 stoichiometric ratio and block access of substrates to the catalytic domain of MMPs. In almost all human cancers, overexpression and/or hyperactivity of MMPs have been noted. In breast cancer, the expression and/or activity of many MMPs and TIMPs has been investigated, especially MMP-1, -2, -9, -11, and -14, and TIMP-1 and -2. Levels of these and other MMPs and TIMPs, measured in breast tumors, their surrounding stroma, or in the blood or urine of breast cancer patients have revealed that these molecules may be informative biomarkers of disease status and prognosis [67]. Functional evaluation of MMPs and TIMPs can be accomplished *in vitro* or in non-fixed tissue specimens. For a comprehensive treatment of zymographic techniques, we refer readers to a review by Snoek-van Beurden and Von den Hoff [68].

3.4.1.4 Detachment-Induced Apoptosis (Anoikis) Assay

Epithelial cells require appropriate engagement with their extracellular matrix and/or neighboring cells to survive. Improper or absent contact induces cell death; though physiologically identical to apoptosis, induced cell death in this context is termed anoikis (Greek for ‘homelessness’). Early studies documented that various cell types exhibit different sensitivity to anoikis, with epithelial and endothelial cells being more sensitive to detachment than fibroblasts. Moreover, expression of oncogenes or treatment with certain soluble factors could promote resistance to anoikis and often also induce migration. We now understand that intracellular signaling scaffolds are assembled at sites of attachment to the ECM and that, through a number of pathways, these complexes promote survival signaling [69]. Since metastasis requires that cells lose their attachment to the basement membrane, an

implicit requirement of the metastatic cascade is that cells be able to suppress anoikis. Simple *in vitro* methods have been developed to qualitatively and quantitatively assess detachment-induced apoptosis. The use of a hydrophilic hydrogel known as polyHEMA can prevent cellular adhesion and spreading, and has found extensive use as a biopolymer in both research and in medical and dental applications [70]. The following is a basic assay for assessing anoikis using polyHEMA:

- *Coating cell culture dishes*. Prepare a 12 mg/mL stock solution of poly-(2-hydroxyethyl methacyrylate) (polyHEMA) in 95 % ethanol and add 200 μL to each well of a 12-well tissue culture plate. Incubate overnight at 37 °C to allow evaporation.
- *Plate cells.* Trypsinize cells into a single cell suspension, count, and dilute to 1×10^5 cells/mL in complete medium. Plate 1–2 mL of the cell suspension ($1–2 \times 10^5$ cells) into each well and return plate to incubator.
- *Analysis.* Various methods of assessing cell viability and apoptosis can be used, including MTT assay, annexin V staining, TUNEL, etc. Most cells that are susceptible to anoikis will exhibit features of apoptosis within 12–24 h, though later time points may be informative for certain cells.

3.4.1.5 Mammosphere Culture (Fig. 3.2)

Stem cells are defined by their ability to self-renew (i.e., symmetrically divide to produce another stem cell) and to undergo lineage restriction to form differentiated progeny through asymmetric division. It is now appreciated that induction of EMT in a number of cell types, including mammary epithelial cells, promotes self-renewal and expansion of a population of cells with stem-cell like properties. The gold standard for measuring self-renewal capacity in mammary gland biology is via serial transplantation of cells into cleared fat pads. This technique is technically involved and requires months to perform. A major advance in studying mammary gland stem cells came from adapting a technique that had proven invaluable in enriching and propagating neural stem cells, the 'neurosphere' culture system. This technique entailed growing neural cells in suspension, where it was found that a small percentage of cells were able to form sphere-like structures that contained 4–20 % stem cells that were capable of multilineage differentiation [71, 72]. Max Wicha and colleagues adapted this protocol to permit propagation of undifferentiated mammary epithelial cells that retained the capacity to undergo luminal, myoepithelial and alveolar differentiation [73]. This culture system has been widely used as a surrogate assay for self-renewal as it is technically simple and can be performed in a matter of weeks. The following is basic protocol for analyzing self-renewal using the mammosphere culture with commercially available low-attachment plates or dishes:

- *Prepare mammosphere culture medium.* The mammosphere culture system employs a defined serum-free medium. Several sources are available, but we routinely use modified mammary epithelial growth medium (MEGM, Lonza).

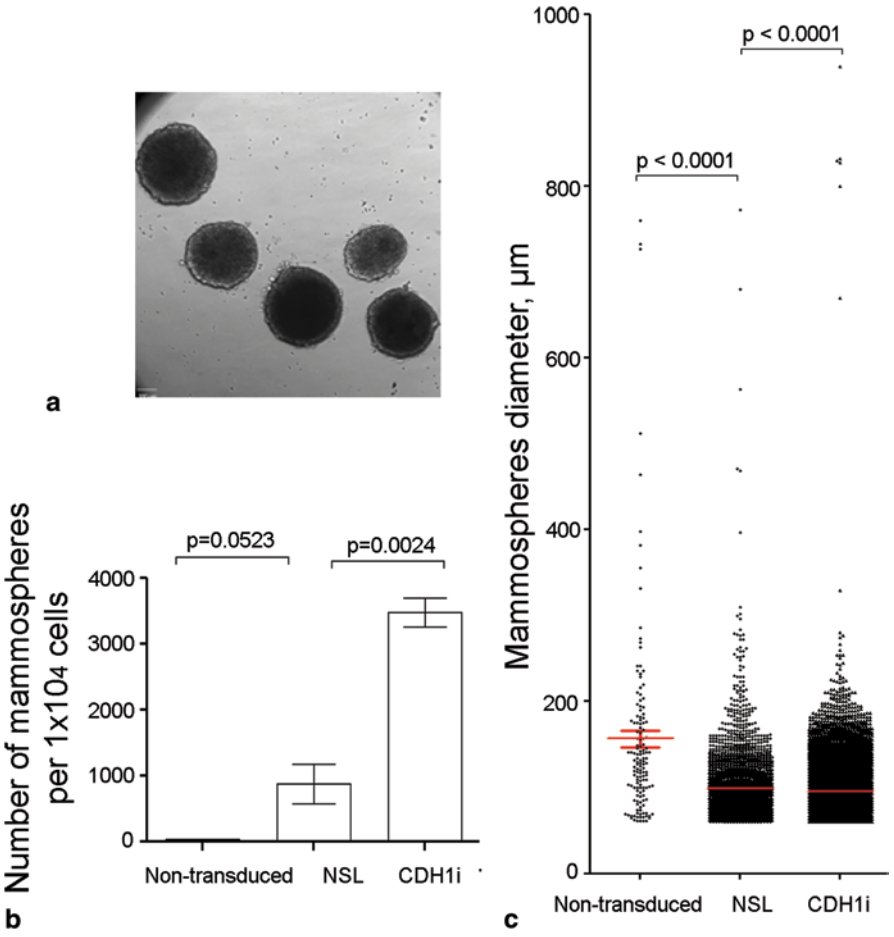

Fig. 3.2 Mammosphere Assay. **a** An example of human primary DCIS cells forming second generation mammospheres in non-adherent tissue culture plates. The number **b** and size **c** of mammospheres formed by SUM-225 (A DCIS cell line) non-transduced, transduced with a control shRNA lentiviral construct (NSL) and an shRNA to E-cadherin (CDH1i)

MEGM can be purchased as a BulletKit® that contains growth factors and supplements (rhEGF, hydrocortisone, insulin, bovine pituitary extract, and gentamycin/amphotericin). To make the modified formulation of MEGM that is suitable for mammosphere culture:

To 500 mL MEGM, add:
All growth factors and supplements that come with the BulletKit®, with the exception of the bovine pituitary extract.
10 µg bFGF (Invitrogen), to make a final concentration of 20 ng/mL.
10 mL B-27 Supplement (Invitrogen).
Heparin calcium to a final concentration of 4 µg/mL.

- *Plate cells.* Trypsinize cells to obtain a single cell suspension. It is useful to pass cells through a 40 μm strainer to ensure that aggregated cells are removed prior to plating. Cells should be plated at relatively low density (e.g., 1×10^4– 2.5×10^4 cells/mL) in a 6- or 24-well ultra-low attachment plate (Corning) in mammosphere medium. Return cells to incubator for 7–10 days, adding additional mammosphere medium every 3–4 days.
- *Analysis.* Spheres can be counted manually or using automated imaging devices (e.g., Celigo, Cyntellect). The number of spheres formed indicates the number of 'stem cells' that were plated into the initial culture, and can be expressed as number of cells per cells plated, or more generically as a percentage corresponding to 'sphere forming efficiency.' Automated imaging instruments can also provide objective information about sphere size. While sphere number corresponds to the percentage of stem cells, the size parameter is thought to indicate the proliferative potential of progenitor cells that arise from asymmetric division of stem cells.
- *Serial passaging.* Mammospheres can be serially passaged, and the ability of these cultures to form spheres over multiple generations can be informative of long-term self-renewal potential. To serially passage these structures, collect mammospheres by passing the suspension culture through a 40 μm strainer, and then inverting the filter and flushing them into a conical tube with PBS. After centrifugation, trypsinize the structures until a single cell suspension is obtained. Pass the single cell suspension through a clean 40 μm filter and then proceed with plating as described above.

3.4.2 In Vivo Transgenic Models

Although *in vitro* culture of established breast cancer cell lines is probably the most widely used model for preclinical evaluation, these *in vitro* systems are limited in so far as they contain no stromal cells and, as generally used, lack three-dimensional structure. These limitations make them poorly representative of real cancers. Animal models in which stroma and structure are present should, if they are to be useful, possess genetic and other biomarker abnormalities similar, if not identical, to their human counterparts [74]. In this section we discuss different *in vivo* models which are used to study different breast cancer stages ranging from early progression of pre-neoplastic breast lesions (DCIS) towards invasive and metastatic tumors.

The procedure of homologous recombination in mouse embryonic stem cells allows researchers to remove a gene (knock out), or replace it (knock in), or perform a variety of other alterations of mouse DNA to recreate discrete genetic aberrations or mutations that the research community has found to be associated with human tumors. The application of transgenic technology in mice to study the progression of mammary cancer has proven extremely informative in understanding important principles of tumorigenesis and evaluating response to therapy [75]. In these transgenic mouse models, researchers have developed approaches that enable targeted gene expression or loss specifically to the mammary epithelium, in many cases by

placing the transgene expression under the control of the mouse mammary tumor virus (MMTV) promoter [75]. Efficient expression of MMTV occurs predominantly in the mammary alveolar and ductal epithelial cells. Consequently, MMTV induces premalignant lesions and malignant tumors of the mammary gland by acting as an insertional mutagen or by activating transcription of nearby oncogenes [76]. In addition to the MMTV-LTR, whey acidic protein (*WAP*) [32] and beta-lactoglobulin (*BLG*) promoters have also been extensively used to create transgenic mouse models of breast cancer [77]. The MMTV-LTR has most frequently been used to express a gene of interest in the mammary epithelium since this promoter is active in both non-lactating and lactating females [76].

More than 50 transgenic mouse models of breast cancer have been generated. These include MMTV-*neu/ErbB2*, *cyclin D1*, *cyclin E*, *Ras*, *Myc*, *int-1/Wnt1* and c-*rel* models which are relevant to human breast cancer research [76]. Mouse models in which the oncogenes *ErbB2* and polyoma middle T antigen (PyMT) have been expressed under the control of MMTV (MMTV–PyMT and MMTV–*ErbB2*) are models of breast cancer do develop spontaneous metastatic disease (for example, to the lungs and other organs) [78].

PyMT Mice [75] In this model, oncogenesis is induced by expression of PyMT oncoprotein (PyMT mice) [75]. The expression of the PyMT oncoprotein is under the control of the MMTV-LTR and is therefore restricted to the mammary epithelium. Previous studies used this model to study the effect of the mononuclear phagocyte growth factor colony-stimulating growth factor-1 (CSF-1) in mammary tumor progression [79]. It was found that it selectively promotes the development of malignancy and enhances metastatic potential by regulating the infiltration and function of tumor-associated macrophages as, at the tumor site, CSF1R expression was restricted to macrophages [79]. Furthermore, subsequent studies indicated that the PyMT model recapitulates many processes found in human breast cancer progression not only morphologically but also in the pattern of expression of biomarkers associated with human breast cancer, with poor prognostic features including loss of ERs and PRs and overexpression of ErbB2/Neu and cyclin D1 [75]. Therefore, this mouse model of mammary carcinogenesis is a powerful system to study the causal events associated with malignant progression and metastasis [75].

Her2/Neu models (over expression) Increased expression of ERBB2 has been observed in a large proportion of sporadic human breast cancers and their derived cell lines [80]. This required the generation of transgenic mouse models that overexpressed human ERBB2 or rat NEU, specifically in the mammary gland. Transgenic studies using the MMTV-based NEU mouse models have led to our understanding of signaling pathways that function downstream of, or in concert with this receptor to control the metastatic process. The generation of bigenic mice that overexpress constitutively active type I or dominant-negative type II transforming growth factor β (TGFβ) family receptors have conclusively shown that the activation of the TGFβ pathway promotes the formation of lung metastases in NEU transformed breast cancer cells [80].

These genes can be used both as new diagnostic tools and for the development of new adjuvant therapeutics to better combat breast cancer and increase patient

survival. Despite this fact, one major limitation of the current mouse models is their inability to accurately recapitulate all of the metastatic sites associated with human breast cancer, including brain, lung, liver and bone. The development of new mouse models that metastasize to these organs will increase our understanding of the aggressive nature of ERRB2-positive breast cancer [80].

Conditional Models Global perturbations in proto-oncogenes or tumor suppressor genes during embryogenesis often have devastating consequences for development. Conditional models, in which manipulation of the gene can be induced in specific contexts or at defined spatiotemporal points, allows the mechanistic interrogation of the functions of alleles that are normally associated with embryonic lethality. Importantly, these models can also be used to target mammary epithelial subpopulations (stem cell, differentiated cell, etc) to examine the relationship between cell phenotype and tumor phenotype [81].

A recent model has been developed where mammary-specific inactivation of conditional E-cadherin and p53, the results revealed that this dual loss of function impairs alveolo-lobular development during pregnancy. Furthermore, these models developed highly invasive tumors that metastasize to the gastrointestinal tract, peritoneum, lung, lymph nodes and bone with lymphangiogenic potential [82].

3.4.3 In Vivo Transplantation Models

To be truly representative of spontaneous metastasis, tumor cells must be implanted orthotopically and allowed to complete the entire sequence of events in the metastatic cascade [83]. For breast cancer studies, this requires implantation of tumor cells into the mammary fat pads of female mice, such that it will simulate the normal progression of preneoplastic breast lesions into invasive and metastatic breast cancers. Transplantation of mammary tissue fragments from transgenic or knockout mice into cleared fat pads of wild-type mice has been used when the genetic manipulation resulted in a sterile animal or embryonic lethal phenotype [84]. There are many human xenograft models available for use in breast cancer research, most derived from established cancer cell lines and spontaneously or genetically immortalized normal breast epithelial cells [74]. Recent reports have also demonstrated primary human breast lesions and cancers that been successfully grown in mice mammary glands [85, 86]. Two common transplantation models are used to study breast cancer progression and metastasis: the cleared fat pad transplantation model and the mouse intraductal (MIND) model.

3.4.3.1 Cleared Fat Pad Transplantation Model (Fig. 3.3)

Although the technique of mammary gland clearing and transplantation was developed in the late 1950s, it is still most useful to answer many modern experimental questions [84]. This assay is possible because of the peculiar nature of mammary development, in which most of the epithelial growth takes place after birth. In the

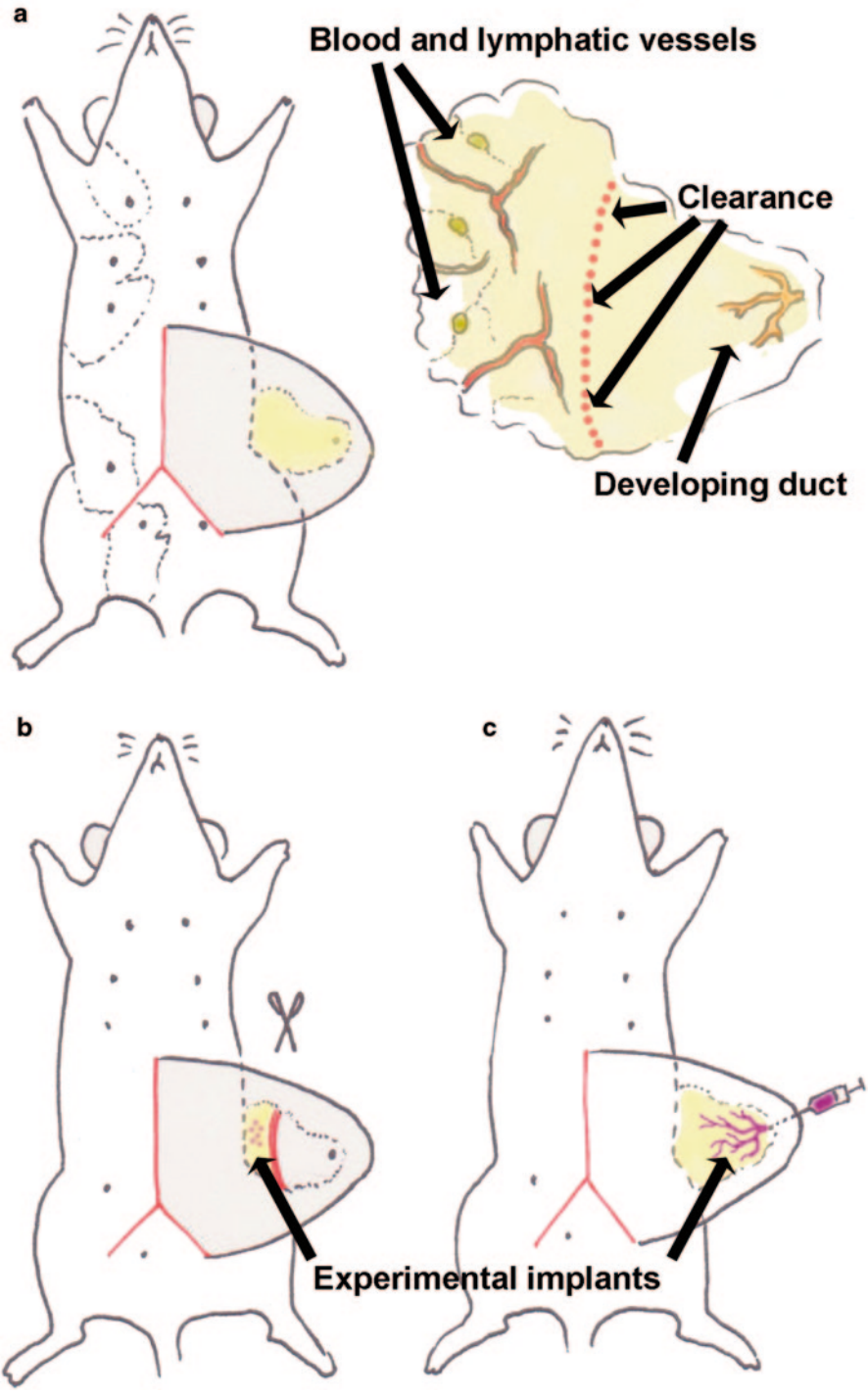

Fig. 3.3 Techniques of in vivo modeling **a** Schematic anatomy of mice mammary glands. **b** Cleared fat pad transplantation. In the 3-week old mouse, the mammary epithelium is still concentrated in the nipple area and has not yet grown out beyond the mammary lymph node and penetrated

fourth (abdominal) mammary fat pad (of which there are five pairs in the mouse) of the 3-week old mouse, the mammary epithelium is still concentrated in the nipple area and has not yet grown out beyond the mammary lymph node and penetrated the bulk of the fat pad. This provides an anatomical fixed point that enables the fat pad from the nipple to the lymph node to be cut away ('cleared'), leaving the bulk of the fat pad free of epithelium and ready to receive cells. The clearing of the endogenous epithelium is required, as otherwise the endogenous tree would rapidly overgrow the transplanted cells before they have had time to generate their own outgrowth [87]. The following procedure represents the standard surgical technique for clearing fat pads:

- *Anesthesia and surgical incision.* Three week weaning female mice are anesthetized, under aseptic technique, the surgical site is cleaned, and a Y-shaped incision is made on the abdominal skin.
- *Exposing the mammary glands.* The skin flaps are pulled back to expose the inguinal mammary fat pads, which lie on the subcutaneous surface of the skin.
- *Cauterization and dissection.* The blood vessels leading to the inguinal and axillary fat pads are cauterized with a pencil-type cautery, and the fat pad between the nipple and inguinal lymph node is dissected free from the skin.
- *Transplantation.* About 80% of the fat pad remains after dissection, which is clear from mammary epithelium, this portion is used for transplantation of the cells.
- *Wound closure.* After transplantation the skin is clipped with stainless steel wound clips.

A video detailing this procedure can be found at: http://www.kumc.edu/school-of-medicine/pathology/behbod-lab/protocols.html

To investigate the growth and metastasis of human breast cancer cell lines *in vivo*, xenograft transplantation experiments are performed in immunocompromised mice. Human breast cancer cells can be injected subcutaneously, intravenously, intracardially, or orthotopically into the fat pad of mice. For example, MDA-MB-231 cells, an estrogen-independent breast cancer cell line derived from the pleural effusion of a cancer patient, is able to colonize bone, liver, lung, adrenal glands, ovary, and brain after intravenous injection [88]. However, there are clear limitations to xenograft models. First, immune responses, which have a key role during tumor development, are severely impaired or completely compromised in immunocompromised mice. Second, stromal components are not of tumor origin. For example, carcinoma-associated fibroblasts derived from a breast cancer patient

---

the bulk of the fat pad. This provides an anatomical fixed point that enables the fat pad from the nipple to the lymph node to be cut away ('cleared'), leaving the bulk of the fat pad free of epithelium and ready to receive cells. **c** MIND transplantation. A Y-incision is made on the abdomen of an 8–12 week old mouse to allow the skin covering the inguinal mammary fat pads to be peeled back, exposing the inguinal gland. The nipple is snipped so that the needle can be directly inserted through into the primary duct. A 30-gauge Hamilton syringe, with a blunt-ended needle, is used to inject cell suspension

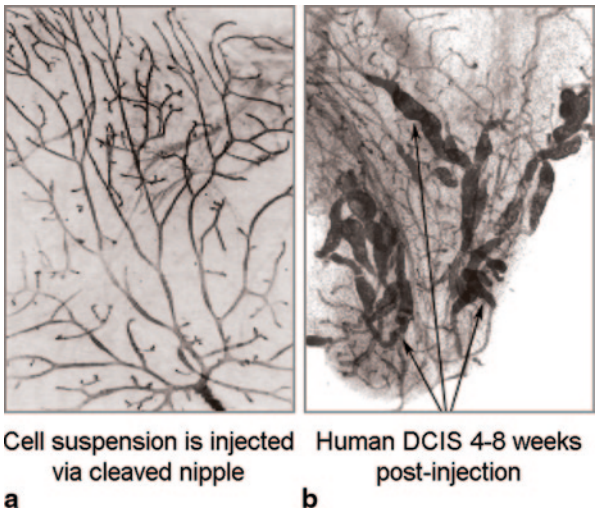

Fig. 3.4 MIND transplantation. **a** Injected liquid (2 µl of PBS containing cells and colored with 0.1 % trypan blue) can be visually detected in the duct. **b** Progressive growth of transplanted cells can be observed several weeks after injection.

support the growth of a breast carcinoma cell line better than the normal tissue in a xenograft mouse co-implantation model [88].

As we mentioned above, one criticism of transplantable tumor models, especially with human tumor xenografts, is the lack of stromal elements from the tumor microenvironment derived from the appropriate tissue [89], so tissue-recombinant xenograft models have been developed. In these models, the mouse mammary fat pads are "humanized" by introducing human breast fibroblast into cleared mouse glands, and at a later time point engrafting human breast epithelial and stromal cells into humanized fat pads [90]. The addition of the stromal cells and matrix proteins may stimulate the local release of cytokines and factors that contribute to improved vascularity, and hence improved growth of the tumors [91].

3.4.3.2 Mouse Intraductal (MIND) Model (Figs. 3.3, 3.4, 3.5)

MIND is a form of mammary transplantation technique that models early processes of breast cancer non-invasive to invasive progression. The unique feature of this approach is that the cancer cells are introduced directly into the primary mammary ducts of immunocompromised mice, thus mimicking DCIS in its normal environment inside the ducts [92]. The model allows one to follow the natural progression of human breast cancers i.e., their initial growth as carcinoma *in situ* inside the ducts, sometimes followed by invasion into the stroma by overcoming the barriers of an intact myoepithelial cell layer and a basement membrane [92]. The intraductal models have been established by injection of human DCIS cell lines (DCIS.COM and SUM-225), as well as cells derived from primary human DCIS, directly into the primary mouse mammary ducts via cleaved nipple. Depending on

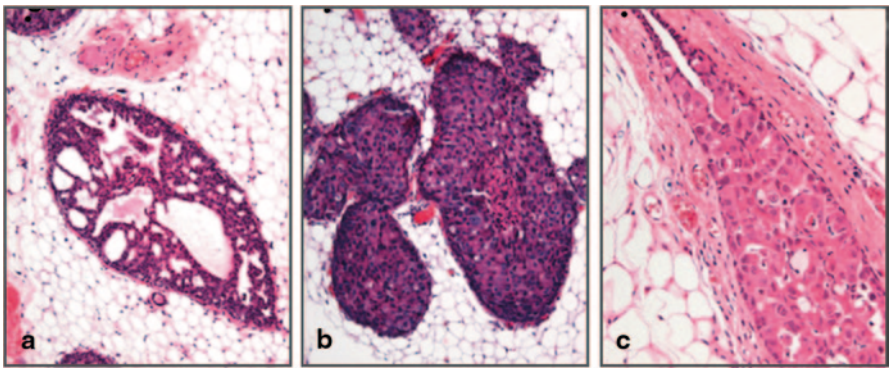

Fig. 3.5. The technique of MIND transplantation had been successful with both cell lines (DCIS.COM and SUM225) and primary human DCIS cells. Representative H&E images of MIND xenografts of DCIS.COM **a** and SUM225 cell lines **b**, and primary human DCIS cells **c** are shown

the study, weeks to months after injections, whole-mount, hematoxylin and eosin, and immunofluorescence staining can be performed to evaluate the type and extent of growth and more importantly the invasive potential of the injected cancer cells [92]. By utilizing the MIND model, the xenografted DCIS lesions derived from primary human DCIS recapitulated the same pathology and heterogeneity of human disease. Therefore, MIND may be utilized to characterize the distinct cellular and molecular basis of inter- and intra-tumoural heterogeneity and the processes of DCIS to early invasive breast cancer progression [93]. The following technique had been successful with both cell lines (DCIS.COM and SUM225) and primary human DCIS cells:

Cell suspensions are prepared fresh before injections.

- *Aesthesia and surgical incision:* The 8–12 week old mouse is anesthetized, placed on an impervious board, a Y-incision is made on the abdomen to allow the skin covering the inguinal mammary fat pads to be peeled back, exposing the inguinal gland.
- *Intraductal injection:* The nipple is snipped so that the needle can be directly inserted through into the primary duct. A 30-gauge Hamilton syringe, with a blunt-ended needle, is used to deliver 2 µl of PBS (with 0.1 % trypan blue) containing cells (10,000–40,000); the injected liquid can be visually detected in the duct.
- *Wound closure:* The skin flaps are re-positioned normally and held together with wound clips.

A video detailing this procedure can be found at: http://www.kumc.edu/school-of-medicine/pathology/behbod-lab/protocols.html

3.5 Application of Previous Models to Lymphangitic Metastasis

The mouse xenograft model has been widely used to assess breast cancer lymphangiogenesis and lymph node metastasis. In recent studies, genetically fluorescent MDA-MB-435/green fluorescent protein (GFP) and MCF7 human breast cancer cells were transfected to over-express VEGF-C and injected orthotopically into the nude mouse model of spontaneous breast cancer metastasis [94]. The results demonstrated the occurrence of intratumoral lymphangiogenesis in breast cancer and identified VEGF-C as a potent enhancer of tumor lymphangiogenesis, leading to increased metastatic spread of breast cancer cells to lymph nodes and lungs [94, 95]. To visualize tumor-associated lymphatic vessels, tissue staining was performed with antibodies specific for the mouse LYVE-1 hyaluronan receptor, which, like its human orthologue, is a highly specific marker of lymphatic vessels in a variety of different mouse tissues and in mouse lymphangiomas [94]. Furthermore, the role of regulatory factors have been elucidated using these models, in a recent study, a CCR7-expressing mouse xenograft model of breast cancer metastasis has been developed, and it showed that CCR7 induces cell spread and direct both human and murine breast cancers cells to the lymph nodes in vivo by functioning through β_1-integrins [63], another study used PDGFDD-expressing xenografts, and showed that PDGFDD increases lymph node metastasis through CXCR4 [96]. Netrin-4 is a laminin-related secreted protein, and it was shown to be a lymphangiogenic factor by using a subcutaneous xenograft of poorly invasive human breast carcinoma MCF-7 cells; and an orthotopic transplant of metastatic murine mammary carcinoma 66c14 cells. Netrin-4 overexpression induced tumor lymphangiogenesis, and lymphatic vessels with wider lumens containing cancer cells were observed in Netrin-4 tumors and were correlated with increased tumor metastasis to axillary lymph nodes [97]. The importance of other lymphangiogenic growth factors in breast cancer are not yet clear and development of animal models for many of these lymphangiogenic factors has not been reported so far [48].

3.6 Quantification of Metastasis In Vivo

Various methods have been established to allow a quantitative assessment of metastasis to be made using *in vivo* models. Early studies relied heavily on measurements of target organ weight and visual observation of metastatic lesions [63, 98, 99]. While visual assessment is still commonly used to assign a metastatic index, recent developments in methodology have enhanced our abilities to detect, and even monitor over time, breast cancer metastasis. Molecular techniques such as qPCR have increased the precision and accuracy of metastasis quantitation. Live *in vivo* imaging using labeled cells or biomarkers of cancer cells allowed the continuous monitoring of the metastatic process over time.

Histological examination To establish a metastatic index based on visual counting of lesions in the target organ, the excised tissue is fixed, embedded in paraffin, sectioned, and stained with hemotoxylin–eosin. Metastasis is quantified by determining the total tissue area per section (D1) and metastasis present in the same area (D2) using a reference grid. The metastatic index is calculated by the ratio D2/D1 [98]. To quantify lung metastasis in a highly metastatic transgene-induced mammary tumor model, Lancaster et al. examined three coronal nonadjacent sections of both lungs, each separated by 100 μm, from each animal. Under 12X magnification three fields were scored for each slide, for a total of 9 fields per animal. Pulmonary metastatic density was determined using a Leica Q500MC Image Analysis System. The metastasis index was measured as the number of metastatic lesions observed per square micron of lung tissue. Additionally, average metastasis size was calculated based on the total area of metastatic tissue on the slide divided by the number of metastases observed [100].

Intravital assessment of breast cancer metastases While both visual counting of metastatic foci and qPCR allow for sensitive quantification of metastasis burden, they only allow examination at one time point, e.g. upon excision of the target organ. As reviewed by Winnard et al., *in vivo* techniques utilizing magnetic resonance imaging (MRI), positron emission tomography (PET), bioluminescence, and fluorescence have recently facilitated molecular imaging of metastatic potential across a time course [101]. Numerous studies tracking the fate of labeled metastatic breast cancer cells have been performed in recent years [101–105]. Depending on the imaging system used, the luminescent- or fluorescent-forming units are typically calculated by the imaging system software. Jenkins et al. used human breast cancer MDA-MB-231 cells that stably expressed firefly luciferase to follow metastasis in an *in vivo* mouse model [102]. Spontaneous metastases to lymph nodes were quantified as total photon counts or photons/s using Living Image® software (Xenogen).

3.7 Closing Remarks

More than 90% of breast cancer-related deaths occur because of metastasis. This insidious process begins early in the natural course of the disease as cells bypass their normal anatomical boundaries and progress to regional lymph nodes and the vasculature. From here, cells gain access to the systemic circulation and a small minority will acquire all of the properties necessary to colonize a distant site. If we are to truly mpact survival from breast cancer, we must concentrate on understanding, at the most fundamental level, the processes by which pre-neoplastic cells acquire the capacity to invade and migrate beyond the breast. Decades of *in vitro* research have shed light upon rudimentary cellular processes that reprogram incipient metastatic cells to complete this sinister mission, and more recently, advanced genetic models have allowed *in vivo* modeling of this process in its entirety. Despite these

advances, current models are limited by their inability to faithfully recapitulate the spectrum of metastatic disease seen in human patients, and inadequacies in mimicking the complex interplay between the immune system and neoplastic cells in xenotransplantation assays. Additional models that address these concerns and enable the interrogation of the complex genetic, cellular, endocrine and humoral landscape of tumor progression are sorely needed.

References

1. Weigelt B, Peterse JL, van 't Veer LJ (2005) Breast cancer metastasis: markers and models. Nat Rev Cancer 5:591–602
2. Fattenah A. Tavassoli PD (ed) (2003) Pathology and genetics of tumours of the breast and female genital organs, 3rd edn. Lyon: IARC Press
3. Leonard GD, Swain SM (2004) Ductal carcinoma in situ, complexities and challenges. J Natl Cancer Inst 96:906–920
4. Howlader N, Noone AM, Krapcho M, Neyman N, Aminou R et al (2011) SEER Cancer Statistics Review, 1975–2008
5. Desantis C, Siegel R, Bandi P, Jemal A (2011) Breast cancer statistics, 2011. CA Cancer J Clin 61(6):409–418
6. American Cancer Society (2011) Cancer facts & figs. 2011
7. Harris JR (2004) Diseases of the breast. Philadelphia: Lippincott Williams & Wilkins. xvii, (1563 p. 1516 plates p)
8. Fabbri A, Carcangiu ML, Carbone A (2008) Histological Classification of Breast Cancer. In: Bombardieri E, Gianni L, Bonadonna G (eds) Springer Berlin Heidelberg. pp. 3–14
9. Hoda SA, Hoda RS (2004) Rubin's pathology: clinicopathologic foundations of medicine. JAMA: J Am Med Assoc 292:1376–1377
10. Perou CM, Sorlie T, Eisen MB, van de Rijn M, Jeffrey SS et al (2000) Molecular portraits of human breast tumours. Nature 406:747–752
11. Sorlie T, Perou CM, Tibshirani R, Aas T, Geisler S et al (2001) Gene expression patterns of breast carcinomas distinguish tumor subclasses with clinical implications. Proc Natl Acad Sci USA 98:10869–10874
12. Asselin-Labat ML, Sutherland KD, Barker H, Thomas R, Shackleton M et al (2007) Gata-3 is an essential regulator of mammary-gland morphogenesis and luminal-cell differentiation. Nat Cell Biol 9:201–209
13. Lim E, Vaillant F, Wu D, Forrest NC, Pal B et al (2009) Aberrant luminal progenitors as the candidate target population for basal tumor development in BRCA1 mutation carriers. Nat Med 15:907–913
14. Tamimi RM, Baer HJ, Marotti J, Galan M, Galaburda L et al (2008) Comparison of molecular phenotypes of ductal carcinoma in situ and invasive breast cancer. Breast Cancer Res 10:R67
15. Casalini P, Iorio MV, Galmozzi E, Menard S (2004) Role of HER receptors family in development and differentiation. J Cell Physiol 200:343–350
16. Rodriguez-Pinilla SM, Sarrio D, Honrado E, Hardisson D, Calero F et al (2006) Prognostic significance of basal-like phenotype and fascin expression in node-negative invasive breast carcinomas. Clin Cancer Res 12:1533–1539
17. Sorlie T, Tibshirani R, Parker J, Hastie T, Marron JS et al (2003) Repeated observation of breast tumor subtypes in independent gene expression data sets. Proc Natl Acad Sci USA 100:8418–8423
18. Gusterson BA, Ross DT, Heath VJ, Stein T (2005) Basal cytokeratins and their relationship to the cellular origin and functional classification of breast cancer. Breast Cancer Res 7:143–148

19. Turner NC, Reis-Filho JS (2006) Basal-like breast cancer and the BRCA1 phenotype. Oncogene 25:5846–5853
20. Turner NC, Reis-Filho JS, Russell AM, Springall RJ, Ryder K et al (2007) BRCA1 dysfunction in sporadic basal-like breast cancer. Oncogene 26:2126–2132
21. Herschkowitz JI, Simin K, Weigman VJ, Mikaelian I, Usary J et al (2007) Identification of conserved gene expression features between murine mammary carcinoma models and human breast tumors. Genome Biol 8:R76
22. Prat A, Parker JS, Karginova O, Fan C, Livasy C et al Phenotypic and molecular characterization of the claudin-low intrinsic subtype of breast cancer. Breast Cancer Res 12:R68
23. Gutman H, Pollock RE, Janjan NA, Johnston DA (1995) Biologic distinctions and therapeutic implications of sarcomatoid metaplasia of epithelial carcinoma of the breast. J Am Coll Surg 180:193–199
24. Hennessy BT, Giordano S, Broglio K, Duan Z, Trent J et al (2006) Biphasic metaplastic sarcomatoid carcinoma of the breast. Ann Oncol 17:605–613
25. Hennessy BT, Krishnamurthy S, Giordano S, Buchholz TA, Kau SW et al (2005) Squamous cell carcinoma of the breast. J Clin Oncol 23:7827–7835
26. Reis-Filho JS, Milanezi F, Steele D, Savage K, Simpson PT et al (2006) Metaplastic breast carcinomas are basal-like tumours. Histopathology 49:10–21
27. Hennessy BT, Gonzalez-Angulo AM, Stemke-Hale K, Gilcrease MZ, Krishnamurthy S et al (2009) Characterization of a naturally occurring breast cancer subset enriched in epithelial-to-mesenchymal transition and stem cell characteristics. Cancer Res 69:4116–4124
28. Campeau PM, Foulkes WD, Tischkowitz MD (2008) Hereditary breast cancer: new genetic developments, new therapeutic avenues. Hum Genet 124:31–42
29. Walsh T, Casadei S, Coats KH, Swisher E, Stray SM et al (2006) Spectrum of mutations in BRCA1, BRCA2, CHEK2, and TP53 in families at high risk of breast cancer. JAMA 295:1379–1388
30. Southey MC, Teo ZL, Dowty JG, Odefrey FA, Park DJ et al (2010) A PALB2 mutation associated with high risk of breast cancer. Breast Cancer Res 12:R109
31. Byrnes GB, Southey MC, Hopper JL (2008) Are the so-called low penetrance breast cancer genes, ATM, BRIP1, PALB2 and CHEK2, high risk for women with strong family histories? Breast Cancer Res 10:208
32. Meindl A, Hellebrand H, Wiek C, Erven V, Wappenschmidt B et al (2010) Germline mutations in breast and ovarian cancer pedigrees establish RAD51C as a human cancer susceptibility gene. Nat Genet 42:410–414
33. Huen MS, Sy SM, Chen J (2010) BRCA1 and its toolbox for the maintenance of genome integrity. Nat Rev Mol Cell Biol 11:138–148
34. Foulkes WD, Stefansson IM, Chappuis PO, Begin LR, Goffin JR et al (2003) Germline BRCA1 mutations and a basal epithelial phenotype in breast cancer. J Natl Cancer Inst 95:1482–1485
35. Lakhani SR, Reis-Filho JS, Fulford L, Penault-Llorca F, van der Vijver M et al (2005) Prediction of BRCA1 status in patients with breast cancer using estrogen receptor and basal phenotype. Clin Cancer Res 11:5175–5180
36. Thompson ME, Jensen RA, Obermiller PS, Page DL, Holt JT (1995) Decreased expression of BRCA1 accelerates growth and is often present during sporadic breast cancer progression. Nat Genet 9:444–450
37. Sourvinos G, Spandidos DA (1998) Decreased BRCA1 expression levels may arrest the cell cycle through activation of p53 checkpoint in human sporadic breast tumors. Biochem Biophys Res Commun 245:75–80
38. Catteau A, Harris WH, Xu CF, Solomon E (1999) Methylation of the BRCA1 promoter region in sporadic breast and ovarian cancer: correlation with disease characteristics. Oncogene 18:1957–1965
39. Yang Q, Sakurai T, Mori I, Yoshimura G, Nakamura M et al (2001) Prognostic significance of BRCA1 expression in Japanese sporadic breast carcinomas. Cancer 92:54–60
40. Mansel RE, Fodstad O, Jiang WG (2007) Metastasis of breast cancer: an introduction Metastasis of Breast Cancer. In: Mansel RE, Fodstad O, Jiang WG, eds. Springer Netherlands. pp. 1–5

41. Willert K, Brown JD, Danenberg E, Duncan AW, Weissman IL et al (2003) Wnt proteins are lipid-modified and can act as stem cell growth factors. Nature 423:448–452
42. Chaffer CL, Weinberg RA (2011) A perspective on cancer cell metastasis. Science 331:1559–1564
43. Fidler IJ (2003) The pathogenesis of cancer metastasis: the 'seed and soil' hypothesis revisited. Nat Rev Cancer 3:453–458
44. Psaila B, Lyden D (2009) The metastatic niche: adapting the foreign soil. Nat Rev Cancer 9:285–293
45. Polyak K, Kalluri R (2010) The role of the microenvironment in mammary gland development and cancer. Cold Spring Harb Perspect Biol 2:a003244
46. Gupta PB, Proia D, Cingoz O, Weremowicz J, Naber SP et al (2007) Systemic stromal effects of estrogen promote the growth of estrogen receptor-negative cancers. Cancer Res 67:2062–2071
47. Karnoub AE, Dash AB, Vo AP, Sullivan A, Brooks MW et al (2007) Mesenchymal stem cells within tumour stroma promote breast cancer metastasis. Nature 449:557–563
48. Achen MG, Stacker SA (2006) Tumor lymphangiogenesis and metastatic spread-new players begin to emerge. Int J Cancer 119:1755–1760
49. Achen MG, Stacker SA (2008) Molecular control of lymphatic metastasis. Ann N Y Acad Sci 1131:225–234
50. Harrell MI, Iritani BM, Ruddell A (2007) Tumor-induced sentinel lymph node lymphangiogenesis and increased lymph flow precede melanoma metastasis. Am J Pathol 170:774–786
51. Hirakawa S, Kodama S, Kunstfeld R, Kajiya K, Brown LF et al (2005) VEGF-A induces tumor and sentinel lymph node lymphangiogenesis and promotes lymphatic metastasis. J Exp Med 201:1089–1099
52. Hirakawa S, Brown LF, Kodama S, Paavonen K, Alitalo K et al (2007) VEGF-C-induced lymphangiogenesis in sentinel lymph nodes promotes tumor metastasis to distant sites. Blood 109:1010–1017
53. Kozlowski H, Hrabowska M (1975) Types of reaction in the regional lymph nodes in non-metastatic and minute-metastatic carcinoma of the uterine cervix. Arch Geschwulstforsch 45:658–659
54. Tobler NE, Detmar M (2006) Tumor and lymph node lymphangiogenesis–impact on cancer metastasis. J Leukoc Biol 80:691–696
55. Veronesi U, Paganelli G, Viale G, Luini A, Zurrida S et al (2006) Sentinel-lymph-node biopsy as a staging procedure in breast cancer: update of a randomised controlled study. Lancet Oncol 7:983–990
56. de Boer M, van Deurzen CH, van Dijck JA, Borm GF, van Diest PJ et al (2009) Micrometastases or isolated tumor cells and the outcome of breast cancer. N Engl J Med 361:653–663
57. Lee HH, Lim CA, Cheong YT, Singh M, Gam LH (2012) Comparison of protein expression profiles of different stages of lymph nodes metastasis in breast cancer. Int J Biol Sci 8:353–362
58. Kalluri R, Weinberg RA (2009) The basics of epithelial-mesenchymal transition. J Clin Invest 119:1420–1428
59. Mani SA, Guo W, Liao MJ, Eaton EN, Ayyanan A et al (2008) The epithelial-mesenchymal transition generates cells with properties of stem cells. Cell 133:704–715
60. Morel AP, Lievre M, Thomas C, Hinkal G, Ansieau S et al (2008) Generation of breast cancer stem cells through epithelial-mesenchymal transition. PLoS ONE 3:e2888
61. Giampieri S, Manning C, Hooper S, Jones L, Hill CS et al (2009) Localized and reversible TGFbeta signalling switches breast cancer cells from cohesive to single cell motility. Nat Cell Biol 11:1287–1296
62. Alitalo K, Carmeliet P (2002) Molecular mechanisms of lymphangiogenesis in health and disease. Cancer Cell 1:219–227
63. Cunningham HD, Shannon LA, Calloway PA, Fassold BC, Dunwiddie I et al (2010) Expression of the C-C chemokine receptor 7 mediates metastasis of breast cancer to the lymph nodes in mice. Transl Oncol 3:354–361

64. Majumder M, Tutunea-Fatan E, Xin X, Rodriguez-Torres M, Torres-Garcia J et al (2012) Co-Expression of alpha9beta1 Integrin and VEGF-D Confers Lymphatic Metastatic Ability to a Human Breast Cancer Cell Line MDA-MB-468LN. PLoS ONE 7:e35094
65. Stacker SA, Caesar C, Baldwin ME, Thornton GE, Williams RA et al (2001) VEGF-D promotes the metastatic spread of tumor cells via the lymphatics. Nat Med 7:186–191
66. Boyden S (1962) The chemotactic effect of mixtures of antibody and antigen on polymorphonuclear leucocytes. J Exp Med 115:453–466
67. Chabottaux V, Noel A (2007) Breast cancer progression: insights into multifaceted matrix metalloproteinases. Clin Exp Metastasis 24:647–656
68. Snoek-van Beurden PA, Von den Hoff JW (2005) Zymographic techniques for the analysis of matrix metalloproteinases and their inhibitors. Biotechniques 38:73–83
69. Gilmore AP (2005) Anoikis. Cell Death Differ 12(Suppl 2):1473–1477
70. Lombello CB, Malmonge SM, Wada ML (2000) PolyHEMA and polyHEMA-poly(MMA-co-AA) as substrates for culturing Vero cells. J Mater Sci Mater Med 11:541–546
71. Weiss S, Reynolds BA, Vescovi AL, Morshead C, Craig CG et al (1996) Is there a neural stem cell in the mammalian forebrain? Trends Neurosci 19:387–393
72. Reynolds BA, Weiss S (1996) Clonal and population analyses demonstrate that an EGF-responsive mammalian embryonic CNS precursor is a stem cell. Dev Biol 175:1–13
73. Dontu G, Abdallah WM, Foley JM, Jackson KW, Clarke MF et al (2003) In vitro propagation and transcriptional profiling of human mammary stem/progenitor cells. Genes Dev 17:1253–1270
74. Kim JB, O'Hare MJ, Stein R (2004) Models of breast cancer: is merging human and animal models the future? Breast Cancer Res 6:22–30
75. Lin EY, Jones JG, Li P, Zhu L, Whitney KD et al (2003) Progression to malignancy in the polyoma middle T oncoprotein mouse breast cancer model provides a reliable model for human diseases. Am J Pathol 163:2113–2126
76. Taneja P, Frazier DP, Kendig RD, Maglic D, Sugiyama T et al (2009) MMTV mouse models and the diagnostic values of MMTV-like sequences in human breast cancer. Expert Rev Mol Diagn 9:423–440
77. Hennighausen L (2000) Mouse models for breast cancer. Breast Cancer Res 2:2–7
78. Francia G, Cruz-Munoz W, Man S, Xu P, Kerbel RS (2011) Mouse models of advanced spontaneous metastasis for experimental therapeutics. Nat Rev Cancer 11:135–141
79. Lin EY, Nguyen AV, Russell RG, Pollard JW (2001) Colony-stimulating factor 1 promotes progression of mammary tumors to malignancy. J Exp Med 193:727–740
80. Ursini-Siegel J, Schade B, Cardiff RD, Muller WJ (2007) Insights from transgenic mouse models of ERBB2-induced breast cancer. Nat Rev Cancer 7:389–397
81. Allred DC, Medina D (2008) The relevance of mouse models to understanding the development and progression of human breast cancer. J Mammary Gland Biol Neoplasia 13:279–288
82. Derksen PW, Braumuller TM, van der Burg E, Hornsveld M, Mesman E, et al (2011) Mammary-specific inactivation of E-cadherin and p53 impairs functional gland development and leads to pleomorphic invasive lobular carcinoma in mice. Dis Model Mech 4:347–358
83. Fidler IJ (2006) Models for spontaneous metastasis. Cancer Res 66:9787
84. Brill B, Boecher N, Groner B, Shemanko CS (2008) A sparing procedure to clear the mouse mammary fat pad of epithelial components for transplantation analysis. Lab Anim 42:104–110
85. Derose YS, Wang G, Lin YC, Bernard PS, Buys SS et al (2011) Tumor grafts derived from women with breast cancer authentically reflect tumor pathology, growth, metastasis and disease outcomes. Nat Med 17:1514–1520
86. Valdez KE, Fan F, Smith W, Allred DC, Medina D et al (2011) Human primary ductal carcinoma in situ (DCIS) subtype-specific pathology is preserved in a mouse intraductal (MIND) xenograft model. J Pathol 225:565–573
87. Smalley M, Ashworth A (2003) Stem cells and breast cancer: a field in transit. Nat Rev Cancer 3:832–844
88. Fantozzi A, Christofori G (2006) Mouse models of breast cancer metastasis. Breast Cancer Res 8:212

89. Frese KK, Tuveson DA (2007) Maximizing mouse cancer models. Nat Rev Cancer 7:645–658
90. Kuperwasser C, Chavarria T, Wu M, Magrane G, Gray JW et al (2004) Reconstruction of functionally normal and malignant human breast tissues in mice. Proc Natl Acad Sci USA 101:4966–4971
91. Tlsty TD, Coussens LM (2006) Tumor stroma and regulation of cancer development. Annu Rev Pathol 1:119–150
92. Behbod F, Kittrell FS, LaMarca H, Edwards D, Kerbawy S et al (2009) An intraductal human-in-mouse transplantation model mimics the subtypes of ductal carcinoma in situ. Breast Cancer Res 11:R66
93. Valdez KE, Fan F, Smith W, Allred DC, Medina D, Behbod F (2011) Human Primary Ductal Carcinoma in situ (DCIS) subtype-specific pathology is preserved in a mouse intraductal (MIND) xenograft model. J Pathol 225(4):565–573
94. Skobe M, Hawighorst T, Jackson DG, Prevo R, Janes L et al (2001) Induction of tumor lymphangiogenesis by VEGF-C promotes breast cancer metastasis. Nat Med 7:192–198
95. Karpanen T, Egeblad M, Karkkainen MJ, Kubo H, Yla-Herttuala S et al (2001) Vascular endothelial growth factor C promotes tumor lymphangiogenesis and intralymphatic tumor growth. Cancer Res 61:1786–1790
96. Liu J, Liao S, Huang Y, Samuel R, Shi T et al (2011) PDGF-D improves drug delivery and efficacy via vascular normalization, but promotes lymphatic metastasis by activating CXCR4 in breast cancer. Clin Cancer Res 17:3638–3648
97. Larrieu-Lahargue F, Welm AL, Thomas KR, Li DY (2010) Netrin-4 induces lymphangiogenesis in vivo. Blood 115:5418–5426
98. Muller A, Homey B, Soto H, Ge N, Catron D et al (2001) Involvement of chemokine receptors in breast cancer metastasis. Nature 410:50–56
99. Nielsen BS, Lund LR, Christensen IJ, Johnsen M, Usher PA et al (2001) A precise and efficient stereological method for determining murine lung metastasis volumes. Am J Pathol 158:1997–2003
100. Lancaster M, Rouse J, Hunter KW (2005) Modifiers of mammary tumor progression and metastasis on mouse chromosomes 7, 9, and 17. Mamm Genome 16:120–126
101. Winnard PT Jr., Pathak AP, Dhara S, Cho SY, Raman V et al (2008) Molecular imaging of metastatic potential. J Nucl Med 49(Suppl 2):96S–112S
102. Jenkins DE, Hornig YS, Oei Y, Dusich J, Purchio T (2005) Bioluminescent human breast cancer cell lines that permit rapid and sensitive in vivo detection of mammary tumors and multiple metastases in immune deficient mice. Breast Cancer Res 7:R444–R454
103. Crnic I, Christofori G (2004) Novel technologies and recent advances in metastasis research. Int J Dev Biol 48:573–581
104. Mendoza A, Hong SH, Osborne T, Khan MA, Campbell K et al (2010) Modeling metastasis biology and therapy in real time in the mouse lung. J Clin Invest 120:2979–2988
105. Cossigny D, Quan GM In vivo animal models of spinal metastasis. Cancer Metastasis Rev 31(1–2):99–108

Chapter 4
Mouse Models of Pancreatic Cancer

Katherine T. Ostapoff, Michael T. Dellinger, Niranjan Awasthi, Rolf A. Brekken and Roderich E. Schwarz

Abstract Pancreatic ductal adenocarcinoma (PDAC) is a disease characterized by aggressive tumor biology, desmoplasia and chemoresistance. Given the insidious nature of its onset, multiple models have been developed to study progression from in situ lesions (PanIN) to PDAC in transgenic mouse models. These have been developed using known mutations that are present in human tumors including *K-ras*, *p53*, *DPC4*, *CDNK2a*, *p16* and *Brca2*. The metastatic character of each of these models is variable and described here. Metastasis to the lymph nodes, liver and peritoneum are also prominent features of PDAC. Syngeneic models and xenograft models (i.e. orthotopic, direct xenograft and metastatic models) are also used to study primary tumor development and metastatic disease and are described.This chapter seeks to describe murine models of experimental PDAC that are currently used to investigate mechanisms of carcinogenesis and metastatic progression, individual risk factors, tumor biology aspects, mechanisms of in vivo chemoresistance, analysis of therapeutic targets and experimental therapies.

R. E. Schwarz (✉)
IU Health Goshen Center for Cancer Care,
Indiana University School of Medicine, Goshen, USA
e-mail: RSchwarz@iuhealth.org

K. T. Ostapoff · N. Awasthi · R. A. Brekken
Department of Surgery, Division of Surgical Oncology,
Hamon Center for Therapeutic Oncology Research, University of Texas,
Southwestern, Dallas, USA

M. T. Dellinger
Hamon Center for Therapeutic Oncology Research,
University of Texas, Southwestern, Dallas, USA

R. A. Brekken
Department of Pharmacology, Simmons Comprehensive Cancer Center,
University of Texas, Southwestern, Dallas, USA

A. Malek (ed.), *Experimental Metastasis: Modeling and Analysis,*
DOI 10.1007/978-94-007-7835-1_4,

Abbreviations

CEA	Carcinoembryonic antigen
CK-19	Cytokeratin 19
DDRs	Discoid domain receptors
EGFR	Epidermal growth factor receptor
EL	Elastase
Fbln5	Fibulin 5
GEMM	Genetically engineered mouse model
GFP	Green floursecent protein
HCC	Hepatocellular cancer
IPMN	Intraductal papillary mucinous neoplasm
KPC	$Kras^{G12D}Trp53^{R172H}Pdx1^{Cre}$
MRI	Magnetic resonance imaging
PanIN	Pancreatic intraepithelial neoplasm
PAS	Periodic acid-Schiff
PDAC	Pancreatic ductal adenocarcinoma
PET/CT	Positron emission tomograph/computed tomography
RFP	Red flouresecent protein
RTKi	Receptor tyrosine kinase inhibitor
SCID/NOD	Severe combined immunodeficiency/non-obese diabetic mice
Shh	Sonic hedgehog
shRNA	Short hairpin RNA
SPARC	Secreted protein acidic and rich in cysteine
TGF-α, TGF-β	Transforming growth factor -alpha, -beta
VEGF-C, VEGF-D	Vascular endothelial growth factor -C, -D
VEGFR-3	Vascular endothelial growth factor receptor 3

4.1 Introduction

Pancreatic adenocarcinoma is the fourth leading cause of cancer death in the United States with a five year survival that remains at less than 5% [1]. While surgical resection remains the only option for cure, the majority of patients present with advanced metastatic disease unsuitable for surgical resection, and the majority of resected patients experience subsequent recurrence and death. The current standard of care in terms of systemic therapies includes gemcitabine, or for patients with high performance status FOLFIRINOX (5-Fluorouracil, Irinotecan and Oxaliplatinin) [2]. Radiotherapy is usually considered for non-resection candidates, and may be applied in an adjuvant setting. Despite these options, few patients have tumors that are sensitive to gemcitabine (26%) [3] or are able to tolerate the high side effect profile of FOLFIRINOX [2].

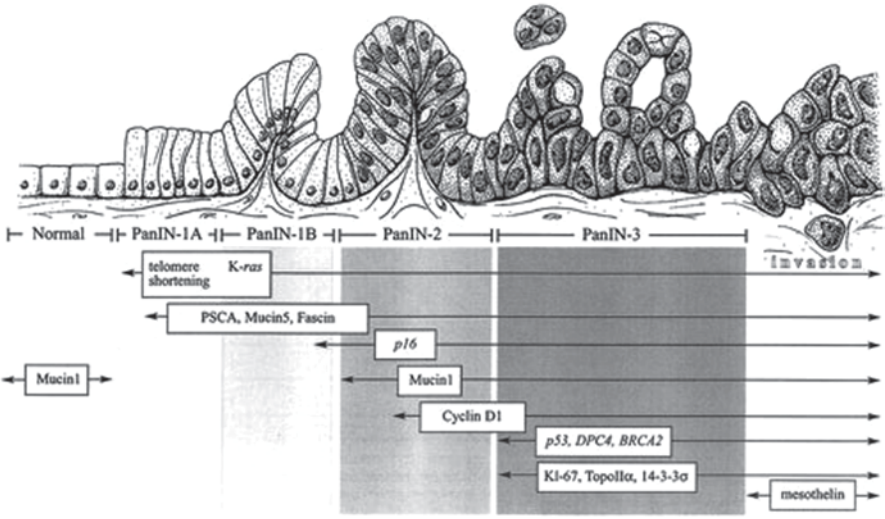

Fig. 4.1 Multiple mutations are required for the development of PDAC. Activating mutations in KRAS have been implicated as an early driver of neoplasia, which progresses through pre-neoplastic stages including pancreatic intraepithelial neoplasia (PanIN) lesions illustrated above. Subsequent mutations in CDKN2A, Mucin1, and Cyclin D1 drive additional changes in ductal epithelia. Additional mutations in p53, DPC4 and BRCA2 and others foster progression towards fully developed PDAC. Adapted with permission from Maitra A et al., Mod Pathology 2003 [137]

Pancreatic ductal adenocarcinoma (PDAC) accounts for over 90 % of pancreatic malignancies, with the remaining 10 % consisting primarily of acinar carcinomas, papillary or cystic mucinous adenocarcinomas (including intraductal papillary mucinous neoplasms, IPMNs) and malignant neuroendocrine tumors. The remarkably poor survival characteristic of PDAC is multifactorial due to advanced stage upon presentation, rapid tumor progression with early metastatic mechanisms, and biologic factors that lead to poor treatment susceptibility. PDAC often has an insidious onset with patients generally remaining asymptomatic until they have near total ductal obstruction (jaundice, exocrine insufficiency), pain (through neural invasion mechanisms) or impairment of endocrine function (diabetes) through peripheral insulin resistance. Risk factors include diabetes [4], chronic pancreatitis, family history, smoking [5, 6] and obesity [7]. Given the increasing prevalence of these conditions and the persisting challenges regarding early diagnosis and effective therapy, the study of carcinogenesis and the progression spectrum of PDAC carry great clinical relevance.

Mutations that are known to frequently contribute to PDAC development include KRAS, DPC4, p53 and CDKN2A (p16) in 90, 60, 75 and 95 % of cases respectively (Fig. 4.1) [8]. In addition, BRCA2 is mutated in 10 % of sporadic cases and 19 % of familial PDAC. Patient survival correlates with these mutations, as a worse prognosis is linked to mutations in Kras [9], or functional deletions of SMAD4 (encoded by DPC4) [10, 11], p53 [12] or p16 [13]. The identification of these mutations and

their inverse correlation with survival provide a potential opportunity for the individualization of treatment based on mutation analysis [14], although currently this remains an area of research without established clinical applications.

Clinical progression of PDAC frequently appears rapid but its development is thought to occur over many years [15]. In fact, it has been shown in patient samples that the development of distant metastasis due to mutations arising in the primary lesion can take up to ten years to develop [16]. Genetic mutations that occur early in carcinogenesis and the prolonged nature of tumor development are consistent with the PanIN model [17]. Furthermore, the high incidence of metastasis at disease diagnosis emphasizes the importance of studying carcinogenesis and metastatic mechanisms, including the progression from micro- to macrometastasis. It has been hypothesized that the desmoplasia of the tumor microenvironment contributes to intrinsic tumor cell resistance to current cytotoxic chemotherapy regimens that typically accompanies PDAC. Understanding the contribution of tumor cell autonomous and non-autonomous factors in the response of PDAC to therapy remains a key challenge to developing therapeutic strategies to treat localized and metastatic disease.

This chapter seeks to describe murine models of experimental PDAC that are currently used to investigate mechanisms of carcinogenesis and metastatic progression, individual risk factors, tumor biology aspects, mechanisms of in vivo chemoresistance, analysis of therapeutic targets and experimental therapies.

4.2 Genetically Engineered/Transgenic Models

Multiple research groups have targeted known mutations in human PDAC tumors for the development of mouse models to study early and late carcinogenesis [18] as well as therapeutics [19]. The spectrum of available models ranges from those that identified molecular mechanisms for pre-invasive lesions for the study of chemoprevention to those utilizing the introduction of specific mutations to follow tumor development from in situ lesions (PanIN 1-3) to invasive PDAC and subsequent metastasis. Herein we describe several of the more commonly utilized models of pancreatic adenocarcinoma and focus on their in vivo disease characteristics as summarized in Table 4.1. The earliest models failed to consistently achieve the development of PDAC as in those employing TGF-α and Pdx-1Cre $Kras^{G12D}$, which has limited the utility of these models.

4.2.1 TGF-a

Early transgenic models failed to develop PDAC but provided important information with respect to other subtypes of pancreatic cancer. Discovered in the 1990s, *TGF-α* has been used as a driver of tumorigenesis when combined with various promoters (Elastase, Simian Virus 40 T antigen or c-myc oncogene) to form acinar carcinoma. These mice have a median survival of less than 15 weeks [20]. Large

Table 4.1 Transgenic models of pancreatic adenocarcinoma development

Model	Median survival (mo)	PDAC	Predominant histology	Metastasis(y/n)	Liver	Ascites	Extra pancreatic malignancy	Reference
EL-TGFα	15	Yes	Acinar	Not described			Primary hepatic tumors	Sandgren EP et al. 1993 [20]
EL-TGFα $P53^{-/-}$	3–8	Yes	Acinar	Yes	Yes	No	Thymic lymphoma	Wagner M et al. 2001 [21]
p48-Cre $Kras^{G12D}$		Rare (2/29)		No (in 2/29 that developed PDAC)	No	No	No	Hingorani SR et al. 2003 [25]
p48 Cre $Kras^{G12D}$ $Cdnk2^{lox/lox}$	2.5	Yes	Sarcomatoid	Yes, rarely	Yes	Yes	CNS tumors	Aguirre AJ et al. 2003 [26], Hingorani SR et al. 2003 [25]
$Kras^{G12D}$ Pdx1-Cre $Smad^{lox/lox}$	8	Yes	Mucinous	Rare	Rare	No	Pdx1 cre-gastric tumors	Bardeesy N et al. 2006 [27], Kojima K et al. 2007 [28]
$Kras^{G12D}$ p48Cre $Smad4^{lox/lox}$	8	Yes	Invasive and mucinous	Yes 53% Micro > Macro	Yes	Yes	MCN	Izeradjene K et al. 2007 [29]
$Kras^{G12D}$ p48Cre Smad4 $^{lox/wt}$	15	Yes	Invasive and mucinous	Yes 35% Micro > Macro	Yes	Yes	MCN	Izeradjene K el al. 2007 [29]
Mist1$Kras^{G12D}$	10.8	Yes	Acinar	Occasional gross	Rare	Yes	HCC	Tuveson DA et al. 2006 [30]
Mist1$Kras^{G12D}$ $Trp53^{R12D}$	6.4	Yes	Pleomorphic	Yes	Yes	Yes	HCC 1/12 mice	Tuveson DA et al. 2006 [30]
$Kras^{G12D}$ p48Cre $Trp53^{R12D}$	5	Yes	Glandular	Yes	Yes	Yes	Rare thymic lymphomas or teratocaricinomas	Hingorani SR et al. 2005 [31]
$Kras^{G12D}$ p48Cre Trp53 $Brca2^{Tr/\Delta 11}$	2.8	Yes	Tubular 100%, sarcomatoid (50%)acinar 18%	Yes, liver and lymph node	Yes	Unk	1 report of neuroendocrine tumor	Skoulidis F et al. 2010 [32]
Pdx1-Cre $Trp53^{R12D}$ $Brca2^{f/f}$	12.3	Yes	Glandular and sarcomatoid	Yes (rare), in longer survivors	Yes	No	Early deaths without tumors	Feldman G et al. 2011 [33]

All transgenic models listed above develop PanIN lesions

h head, *t* tail, *b* body predominant location of tumor, *CNS* central nervous system tumors, *MCN* mucinous cystic neoplasms, *HCC* hepatocellular carcinoma

(>2 cm) hepatic tumors (hepatocellular and cholangiocarcinomas) were found in over 50% of the mice [20].

Subsequent work resulted in *EL-TGF-α/ p53*$^{-/+}$ and *EL-TGF-α/ p53*$^{-/-}$ mice [21]. In the heterozygotes (p53$^{+/-}$) 3% of mice developed epithelial tumors or sarcomas. Mice in each group (*EL-TGF-α/ p53*$^{-/+}$ and *EL-TGF-α/ p53*$^{-/-}$) however developed pancreatic tumors after extended periods of time that expressed multiple epithelial markers and had limited fibrosis [22]. Unique to this model, additional mutations were acquired during tumor development. Although they did not occur in 100% of tumor bearing mice, new loss of heterozygosity occurring in the *Ink4a/Arf (Cdkn2a)*, *Rb* and *Smad4* loci were identified [21]. These have since been attributed to mutations on chromosome 11 and 15 [23]. Furthermore, a tumor specific immune response was identified in this model showing increased intratumoral levels of TNF-α, IFN-γ, IL-6, and MCP-1 [24].

Although mice with TGF-α mutations do not uniformly develop PDAC, this early model provided evidence that fibrosis is a key feature in PDAC development. This model continues to be used to study tumor immunology [24]. With the development of new mutations during tumor development, this model also has the potential to be used for studying the mechanisms of acquired mutations in metastasis.

4.2.2 *Kras^{G12D} p48-Cre*

This model relies on expression of an activating *Kras* mutation predominately in the pancreas. Identified by Kawaguchi et al., p48/Pft-1 is a transcription factor during embryological development expressed by pancreatic precursor cells both of endocrine and exocrine lineages [25]. Under the effect of this pancreas-specific promoter, cells within the pancreas under model conditions express mutations in Kras^{G12D} and subsequently generate a more nodular pancreas [26]. These mice were found to have predominantly normal pancreata at 9 weeks, but subsequently developed PanIN 1-3 lesions by 9 months, with only few mice developing invasive PDAC [26]. In 29 mice, only 3 developed invasive PDAC with hallmark features of hemorrhagic ascites and liver metastasis [26]. Other groups using this model also found minimal development of invasive PDAC, with significant PanIN lesions seen within 30 weeks [27]. Despite the lower incidence of invasive lesions, a proteomic signature was developed that identified preinvasive lesions with a sensitivity of 90.5% and specificity of 97.7%. Further work with this model has shown that TGF-β and BMP4 are highly expressed; this has propelled further investigations on the contribution of TGF-β to tumor progression and metastasis [28].

4.2.3 *LSL-Kras^{G12D}; Cdkn2a$^{lox/lox}$; Pdx1^{Cre}*

Given the slow disease progression of animals engineered to express *Kras^{G12D}* in the pancreas, additional mutations have been added to force more consistent PDAC

disease promotion. Mutations in p16/p19 are commonly identified in clinical specimens. These mutations result in the deletion of the *Cdkn2a* (Ink4a/Arf) locus product [29] and in concert with activated Kras promote PDAC tumorigenesis [30]. By combining an activating mutation in Kras (*LSL-Kras^{G12D}*) and deletion of Cdkn2a (*Cdkn2a$^{lox/lox}$*) with pancreas-specific Cre expression (*Pdx1^{Cre}* or *p48^{Cre}*) mice developed solid lesions that can progress rather rapidly; animals can become moribund with evidence of ascites, weight loss or jaundice between 7 and 11 weeks [27]. These mice at early time points (as early as 3 weeks) were shown to have precursor PanIN lesions and early stage invasive PDAC (as early as 4 weeks).

On necropsy, mice in general did not show grossly evident liver metastases but showed histologic evidence of lymph node metastasis and liver micrometastasis. Development of jaundice due to bile duct obstruction aside from ascites in end stage disease is common. In one survival experiment, 23 of 24 mice had local invasion into adjacent organs by the primary tumor [27]. Primary tumors had glandular features with abundant stroma with strong collagen (trichrome) staining and abundant mucin (PAS positive).

These mice have been shown to retain p53 function throughout tumor progression, a deviation from the common clinical tumor characteristics [31]. However, these models retain a dense stromal component, which is consistent with the human disease. This model has been used to evaluate therapeutic efficacy using a variety of strategies including sonic hedgehog inhibition [32], and combination of a smac mimetic and cytotoxic chemotherapy [33]. *Kras^{G12D} Cdkn2a* tumors are sensitive to gemcitabine in vivo as well, rendering the model a tool for the examination of combination therapy approaches.

4.2.4 Kras^{G12D} Pdx1-Cre Trp53^{R172H} (KPC mice)

The relatively low incidence of gross metastasis in murine models utilizing active Kras and loss of Cdkn2a promoted further work directed towards identifying a highly metastatic murine PDAC model. Trp53^{R172H} was originally identified as a driver of Li-Fraumeni Syndrome [34]. Hingorani et al. discovered that heterozygous mutation of p53(*Trp53^{R172H}*) combined with Pdx1-Cre Kras^{G12D} (KPC) resulted in an aggressive PDAC model with a median survival of 5 months and 100% mortality by 1 year [35]. These animals typically present with pancreatic head lesions with biliary obstruction. Furthermore, this model of PDAC generally progresses with tumor sequelae that are consistent with the human disease, including ascites and macroscopically identifiable liver, peritoneal and lung metastases (Fig. 4.2).

In this model lesions expressed high levels of ductal markers, including CK-19 and mucin, in well differentiated areas. Across tumor samples, investigators found heterogeneity of EGFR and Her2 expression between PanIN and PDAC lesions. However, uniform expression of Shh was found to be elevated in preinvasive and invasive lesions throughout the pancreas. Interestingly, during the course of disease progression, mice were found to develop homozygous loss of p53 in all primary

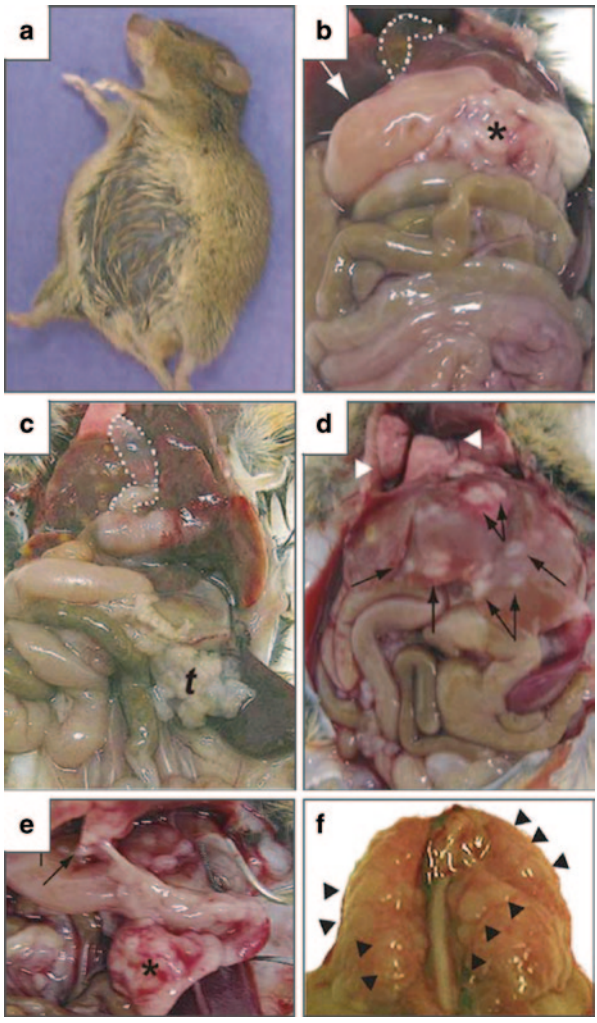

Fig. 4.2 KPC mice develop significant metastatic burden. Once moribund, mice develop significant ascites **a**. Primary tumors are typically in the pancreas head location (*) and cause biliary and duodenal obstruction (*white arrow*, **b** and gallbladder distension **c**. Multiple liver **d**, diaphragm **e** and lung metastases (*black arrows*) are seen **f**. (Adapted with permission from [35])

tumors and metastases. In addition, cells lines from tumors at different time points were found to display chromosome instability. Throughout tumor progression, pancreatic lesions were found to maintain p16Ink4a, Smad4, Rb, Akt and Myc protein expression without development of mutations or other alterations [35].

This model has been also used to evaluate various therapeutic strategies. For instance, the use of a Shh inhibitor enhanced delivery of chemotherapy and improved tumor control in KPC mice [36]. Additionally, dasatinib, a receptor tyrosine kinase inhibitor (RTKi) that inhibits Src, BCR-Abl, and DDRs among others, was found to inhibit metastasis but not primary tumor growth, within this model [37]. This model has also been used for evaluating chemoprevention. Use of enalapril and aspirin resulted in decreased development of invasive PDAC lesions compared to untreated

mice (17 vs. 60%) [38]. Synthetic triterpenoids also prolonged survival when added to the chow of these mice [39].

The KPC model is useful to study tumor biology as well as for therapeutic investigation. With a prolonged time course and high metastatic incidence, it represents human PDAC disease characteristics well. This model does not acquire new mutations during development, making it a good choice for examining the biology of metastasis without the spontaneous development and impact of new mutations. Although many transgenic mouse models lead to development of liver metastases, this model generates frequent lung metastases. KPC mice are also good for studying chemoprevention given the slower time course of disease development. Perhaps one of the most desirable features of this model is that KPC tumors are resistant to gemcitabine as a single agent in vivo, similar to the relative insensitivity of patients to gemcitabine.

4.2.5 *Kras^{G12D} Smad4$^{lox/lox}$*

Dpc4 is the gene that encodes Smad4, the signaling intermediate critical for canonical TGF-β signaling. Its activation drives transcription of genes that counteract or prevent mechanisms of tumor proliferation, migration, survival and epithelial to mesenchymal transition. As a major regulator of TGF-β, Smad4 has been shown to be mutated in aggressive tumor phenotypes. Furthermore, patients with PDAC mutations in Smad4 have a decreased survival [11]. The role of this mutation has been studied in many transgenic models. Although loss of Smad4 alone was insufficient for tumor formation, homozygous loss of *Smad4* combined with *Pdx1* or *p48* driven *Kras^{G12D}* activation resulted in tumor formation at 7-12 weeks of age and a median survival of 8 months [28]. In addition to invasive PDAC, *Kras^{G12D} Smad4$^{lox/lox}$ Pdx1-Cre* animals also developed IMPNs and squamous and adenosquamous gastric cancers. PDAC tumors in this model showed elevated stromal components [28], although metastasis was infrequent and mostly associated with a sarcomatoid histology compared to *Kras^{G12D} Pdx1-Cre* mice [40]. Additionally, these tumors had areas of inflammatory cells and evidence of chronic pancreatitis in 6 of 16 mice [40].

Median survival for *Kras^{G12D} Smad4$^{lox/wt}$ p48Cre* (haploinsufficiency) mice was 15 months with low grade PanIN lesions seen at 7-8 months [41]. Tumors were identified in major and minor ducts, a feature not represented in the majority of genetic models of PDAC [41]. Tumors from these animals were found to have elevated EGFR, ErbB2, Hedgehog and Hes1 expression [41].

Although this model has not been used for therapy studies to date, its prolonged time course and modeling of an important mutation in PDAC make it a valuable model to study early therapeutic strategies. An unusual but important feature of *Kras^{G12D} Smad4$^{lox/lox}$ p48Cre* mice is that they develop both PanIN and IPMN lesions. By having both types of precursor lesions, the mechanisms of invasive tumor development and metastasis from these convergent pathways can be studied.

4.2.6 *Mist1-Kras^{G12D}*

Mist1 is a protein that is expressed highly in mature pancreatic acinar cells and is required for normal acinar architecture [42]. The Tuveson group proposed that mutations in *Mist1* may participate in PDAC development. Unlike previous models described, in *Mist1Kras^{G12D}* mice a mutation in *Kras^{G12D}* is knocked into the *Mist1* locus. *Mist1Kras^{G12D}* mice have a median survival of 10.8 months and typically develop ascites when 3 months old. Addition of a targeted p53 mutation *(LSL-p53^{R172H})* reduced median survival to 6.8 months [43]. Mice without p53 mutations had cystic and papillary features with few cases of glandular differentiation. A minority of *Mist1Kras^{G12D}* mice developed liver metastasis but 25 of 44 mice developed hepatocellular cancer. Conversely, in *Mist1Kras^{G12D} Trp53^{R172H}* animals, liver metastasis occurred in roughly 50% of mice, and rare (1 of 12) hepatocellular cancers were noted. These mice had pleomorphic carcinomas. *Mist1Kras^{G12D}* mice were found to have increased protein expression of Akt and Ras and mRNA expression of *Hes1, Hey1* and *Hey2* but decreased levels of *Mist1* [43]. When comparing an elastase inducible *Pdx1-Cre Kras^{G12D}* to *Mist1Kras^{G12D}* mice, Habbe et al., found similar patterns of PanIN lesions between the models [44].

This model provides important additional evidence for the mechanisms of pancreato-hepatobiliary carcinoma. The high incidence of other hepatobiliary tumors (HCC and cholangiocarcinomas) make this a difficult model to use for PDAC therapy studies, but there is the potential to provide insight into the common causes of chemoresistance and metastasis between these tumor types.

4.2.7 *Models of Familial Pancreatic Cancer with Brca2 mutations*

Familial pancreatic cancer represents a small percentage of patients who develop PDAC. The most common mutations found in familial cases are BRCA2 [45, 46] and PALB2 [47]. Skoulidis et al describe *Kras^{G12D} Brca2$^{flox/wt}$* animals in which a heterozygosity for *Brca2* results in murine PDAC [48]. They also found that homozygous deletion of *Brca2* in the *KPC* model resulted in a high penetrance of adenocarcinoma and reduced median survival (86 vs. 168 days) compared to *KPC* mice. Interestingly, heterozygous loss of *Brca2* also resulted in decreased median survival of 143 days. These mice frequently developed liver and lymph node metastases. In mice with wild-type p53, i.e. *Pdx1-Cre Kras^{G12D} Brca2$^{flox/wt}$*, the mice frequently developed pancreatic insufficiency. This suggests that mutation of one copy of *Brca2* is not sufficient, even in the context of *Kras* activation, to drive tumor formation and highlights the redundancy of DNA repair mechanisms. The predominant histology of the *Kras^{G12D} Pdx1-Cre Trp53^{R172H} Brca2$^{lox/wt}$* model includes tubular (~100% of mice), sarcomatoid (~50%) and acinar cell histology, which mirrors those found in patients with familial *BRCA2^{999del5}* PDAC. In the het-

erozygous model, all of the mice were found to retain one copy of wild type *BRCA2* expression within their tumors.

An additional Brca2-based model has been developed to mimic familial PDAC. This author group found that pancreas-specific homozygous mutations of *BRCA2* with or without *p53* mutations also results in PDAC development. In *Pdx1-Cre* $Brca2^{lox/lox}$ and *Pdx1-Cre* $Trp53^{R172H}$ $Brca2^{flox/flox}$ mice, median survival is 454 and 375 days respectively [49]. In the cohort of mice that died early, histological analysis revealed pancreata replaced with adipose tissue and depletion of acinar cells. In mice that lived > 1 year, preinvasive lesions were identified. Tumor histology was sarcomatoid and glandular. Mutations in *p53* resulted in increased frequency of invasive lesions and metastatic disease at 15-17 months. In mice with only *Brca2* mutations, metastatic events were infrequent. There were no acquired mutations in *Kras* found in either tumor type. Increased expression of *Shh* was found only in neoplastic glands and not in non-neoplastic cystic epithelium [49].

Despite the low incidence of familial PDAC, these models provide evidence for an alternative mechanism for tumor development in susceptible individuals. With these models, (particularly the *KPC* $Brca2^{lox/lox}$ mice) the potential to study chemoprevention aimed at this population is apparent. Other known genetic alterations linked to familial PDAC have not been modeled in animals, such as the mutation and overexpression of the actin associate palladin [50]. Interestingly, isoform overexpression of palladin in murine PDAC tumors has been identified primarily within fibroblasts but not epithelial cells indicating scenarios of specific mechanisms of tumor invasion and metastasis that deserve recognition for future disease modeling efforts [51].

4.2.8 Additional Models

Additional genes have been targeted in an attempt to develop PDAC models that mirror human disease. Although $Kras^{G12D}$*-Nestin* lesions developed PanIN lesions and did not progress to PDAC, evidence suggests *Nestin* positive cells are progenitors to PDAC [52]. *CK-19* driven $Kras^{V12}$, resulted in mice that developed ductal hyperplasia in the pancreas and stomach but no PanIN lesions [53].

Genetically engineered mouse models (GEMM) certainly have many advantages for studying carcinogenesis and early metastasis. They recapitulate many of the progressive genetic events that are believed to account for the development of pancreatic cancer. Depending on the model, they have various time courses with median survivals ranging from 2 months to > 1 year [27, 41]. An additional benefit of these mice is that they are bred on immunocompetent backgrounds and allow for the evaluation of innate and adaptive immunity in tumor biology.

Conversely, disadvantages include the lengthy time period for development of new models or use of existing models. Regardless of the model, all mice that are competent to develop PDAC will eventually develop tumors throughout the entire pancreas and various stages in a manner often unlike the course of disease in human

patients. As areas within the pancreas develop tumors at different rates, it can be challenging to conduct efficient therapeutic experiments, or to study targeted pathways such as TGF-β, which can inhibit tumor progression early and drive progression at later stages. The genetic background of the model is also a critical feature that can be altered by crossing different strains of mice; naturally, the comparison of median survival across strains is challenging. Furthermore, genetically engineered mouse models are costly and require significant resources to maintain. However, despite these challenges, they are a valuable resource for understanding tumor progression and metastasis in a heterogeneous tumor cell population.

4.3 Syngeneic Models

Although the isolation of cell lines from transgenic mice is occurring more frequently [35], this is rather labor intensive, and not all cell lines isolated will form tumors once implanted in vivo [24]. As the role of the immune system is important in tumor progression and metastasis, specific models are needed in immunocompetent systems. These models are useful for studying potential immunotherapy and vaccine therapy in PDAC [54].

Currently two cell lines are commercially available that can be grown in immunocompetent C57BL/6 mice. These cell lines, Pan02 (Panc02) and Pan03 (Panc03), (DTP, NCI) were isolated from C57Bl/6 mice that developed a chemically induced pancreatic adenocarcinoma. To establish these cell lines, a suture impregnated with the carcinogen 3-methyl-cholanthrene (3-MCA) was sutured into the pancreas of a C57BL/6 mouse [55]. Two of the 13 PDAC tumors established survived explant culture and re-passage (Pan02 and Pan03). Pan02 was found to be high grade (grade 3 but became undifferentiated with additional passages) and highly metastatic with 80% of mice developing lung metastasis in the original report of its use [55]. Availability of murine syngeneic pancreatic cancer cell lines has facilitated investigation of function and contribution of the innate and adaptive immune system in pancreatic cancer progression and metastasis [56, 57]. Additionally, the function of T cells in pancreatic tumors has been studied in Pan02 tumors [58]. Pan02 tumors have high levels of T regulatory cells and macrophages. Inhibition of TGF-β mediated T cell differentiation into T regulatory cells can result in a reduction in tumor growth and metastasis [59]; induction of Th17 cells results in prolonged survival [60]. Further description of this model with respect to metastatic incidence (Table 4.2) and lymphatic metastasis are discussed in later sections of this chapter.

The availability of C57BL/6 animals with genetic ablation of target genes has enabled the evaluation of the function of target proteins in the development and progression of Pan02 tumors. For example, orthotopic Pan02 implantation in *fibulin* $5^{-/-}$ mice, resulted in smaller and less invasive tumors than tumors grown in *wild-type* animals. *Fibulin-5* (*Fbln5*) is a matricellular protein implicated in regulation of angiogenesis [61] and elastic fiber formation [62]. Importantly, Pan02 tumors grown in the absence of *Fbln5* displayed reduced microvessel density. Investiga-

Table 4.2 Orthotopic tumor establishment and metastatic potential of cell lines

Cell line	Number cells injected	Time length of experiment	Location of metastasis	Reference
AsPC-1	1×10^6	6 weeks	Peritoneum, Liver	Fujioka SF et al. 2003 [78]
BxPC-3	2 mm^3 sc tumor	8 weeks	LN, minimal metastasis noted	Matsuo Y et al. 2009 [79]
Capan-1	1 mm^3 sc tumor	14 weeks	Liver, LN	Bhargava S et al. 2007 [80]
Capan-2	1×10^6	12 weeks	LN 60%, Liver 50% Spleen, GI	Bailey JM et al. 2009 [81]
CFPAC-1	1×10^6	8 weeks	Not described	Yao J et al. 2010 [82]
Colo357 (L3.6pl)	1×10^6	5 weeks	Liver, LN, occasional peritoneal	Bondar VM et al. 2002 [83]
HPAC	1×10^6	3-4 weeks	None	Mohammed RM et al. 1998 [77]
HPAF-II	2×10^6	5 weeks	LN only	Fujisawa T et al. 2009 [84]
Hs766T	2×10^6	5 weeks	LN and 50% Liver	Fujisawa T et al. 2009 [84]
MiaPaca-2	1×10^6	8-10 weeks	Liver	Dineen SP et al. 2010 [39]
MPanc-96	1×10^6	Not described	Lung 100% Liver100%	Ramachandran V et al. 2008 [85]
Panc-1	1×10^6	12 weeks	Minimal	Awasthi N et al. 2011 [86]
SW1990	1 mm^3 sc tumor	8 weeks	80–100% Metastasis, Liver	Jia L et al. 2005 [87]
Pan02*	5×10^5	7 weeks	Liver, peritoneum, LN	Dineen SP et al. 2008 [88]

The following lines have only been done in subcutaneous models: Panc03.27, Su 86.86, PL45, Panc 10.05. According to literature search the following ATCC lines have not be performed in vivo models: Panc 08.13, Panc02.03, Panc02.13, Panc04.03, Panc05.04

sc primary tumor implanted from subcutaneous tumor, *LN* lymph node metastasis, *GI* gastrointestinal metastasis

*denotes mouse cell line

tion of the mechanisms underlying reduced tumor growth in the absence of Fbln5 resulted in the identification of a new function for this protein. It was discovered that Fbln5 competes with fibronectin for binding to integrin α5β1. Elevated ligation of the integrin resulted in increased production of reactive oxygen species, which resulted in endothelial cell apoptosis, reduced angiogenesis and poor tumor growth [63]. Similarly, studies of Pan02 tumor growth in the absence of the matricellular protein "secreted protein acidic and rich in cysteine" (SPARC) documented that SPARC is critical for the appropriate stromal response to pancreatic cancer formation [64]. A defining feature of tumors grown in *SPARC*$^{-/-}$ animals was reduced collagen deposition and an increase in vascular perfusion [65]. These features resulted in an increase in local invasion and distant metastases, an effect that was dependent in part on TGFβ activity [66].

Recently, groups that work with the KPC transgenic model have developed clones from primary tumors that they have implanted either subcutaneously or orthotopically [67]. These tumor cell lines are implanted in histocompatible synegenic mice depending on the background of the mouse from which the original cell line was derived. Differences between the parental cell lines vs. subcutaneous tumors vs. orthotopic tumors were however noted on CGH array.

The syngeneic model provides a tumor microenvironment with innate and adaptive immunity, but it also has some limitations. Limited variability in in vivo modeling can be achieved given that there are only two cell lines available. Furthermore, these two cell lines have not been fully characterized beyond reports of Pan02 cells expressing wild type Kras [68] and a Smad4 mutation (Arnold SA, unpublished data) and mutation in p16 (Ostapoff KT, unpublished data). Finally, Pan02 cells express a highly mesenchymal phenotype. Although this makes them highly metastatic, their lack of epithelial marker expression in vitro and in vivo may limit their utilization for some experiments.

4.4 Xenograft Models

Despite the increasing utilization of genetic models of PDAC, xenograft modeling has been and remains the mainstay of in vivo pancreatic cancer research. A finite number of PDAC cell lines have been widely used for in vivo experimentation throughout the years. An early such effort resulted in the development of Panc-1 cells that Lieber et al. found to be a stable cell line after 2 years in culture [69]. Subsequently, multiple cell lines have been developed from human primary tumors at all stages of disease, including isolates from primary tumors, lymph node metastases, liver metastases and malignant ascites. Currently, the ATCC (American Type Culture Collection) has 21 human pancreatic cancer cell lines available for purchase. Additionally, groups at MD Anderson and Johns Hopkins University have continued to develop cell lines from patients before and after preoperative chemotherapy. Baseline information on mutational status of many of these cell lines have been established and can be used as a guide for experimental testing (Table 4.3).

The development of cell lines has allowed the investigation of a variety of aspects of PDAC biology in vitro as well as in vivo, which has encompassed subcutaneous, orthotopic and intraperitoneal injection models.

4.4.1 Subcutaneous Models

In immunodeficient mice, tumors are established on the flank after subcutaneous injection of tumor cells. Tumor growth is easily followed with calipers allowing for rapid real time responses to drug treatments. Direct effects of therapeutic

Table 4.3 Genetic alterations in human pancreatic cancer cell lines

Cell line	Origin	Kras	p53	CDKN2A/p16	DPC4
AsPC-1	Ascites	12 Asp mutation	Frameshift mutation, 135 Δ1 bp, Intro 4 Δ200 bp splice site, HD exon 5	Δ2 bp frameshift mutation, HD, wild type	Wild type
CFPAC-1	Liver metastasis	12 Val mutation	242 Arg mutation	Methylated, deletion, wild type	HD mutation
HPAF-II	Ascites	12 Val mutation	151 Ser mutation	29–34 in frame deletion	Wild type
MDAPanc-3	Liver Metastasis	12 Ala mutation	273 Cys mutation	−36 to (+5) C deletion	Wild type
MiaPaca-2	Liver metastasis	12 Cys mutation	248 Trp mutation	HD mutation	Wild type
Panc-1	Primary tumor	12 Asp mutation	273 His , 273 Cys mutation	HD mutation	wild type
PancTu-I	Primary tumor	12 Val mutation	176 Ser mutation	Methylated, deletion	Wild type
Suit-2	Liver metastasis	12 Asp mutation	273 His mutation	69 Glu to Stop mutation	Wild type
Capan-1	Liver metastasis	12 Val mutation	153 Val mutation	HD mutation	577 Leu, 343 STOP mutation
Hs 766T	Lymph node metastasis	Wild type	225-282 deletion, Δexons 2-4 mutation, wild type	Intron 2 splice site mutation, , wild type	HD mutation
BxPC-3	Primary tumor	Wild type	220 Cys Mutation	HD mutation, wild type	Wild type
Capan-2	Primary tumor	12 Val mutation	wild type,Intro 4 Δ200 bp splice site	6 bp ins, 7 bp ins mutations, wild type	Low protein expression, wild type
Colo357	Lymph node metastasis	12 Asp mutation	Wild type	HD mutation, wild type,	HD mutation or wild type
SU86.86	Liver metastasis	12 Asp mutation	245 Ser mutation	HD mutation	Wild type

Modified and Adapted from Moore PS et al., Virch Arch 2001 [68], Deer EL et al., Pancreas 2010 [69] and Sipos B et al., Virch Arch 2003 [70]
HD homozygous deletion, Δ- deletion, *ins*- insertion, *bp*-base pair

interventions can be followed and regressions are in fact best seen with this model. Typically, analysis of these subcutaneous tumors allows for evaluation of tumor vasculature [70], drug delivery, apoptosis and proliferation [71]. For instance, this model has frequently been used in shRNA experiments to demonstrate the impact of specific targets on tumor growth. It is also useful for injecting a mixed cell popula-

tions. For example, the contribution of fibroblasts to the tumor microenvironment has been studied in this model by injecting mice with genetically modified fibroblasts with tumor cells [72] and by injecting tumor cells with pre-treated fibroblasts [73].

The ease and accessibility of the tumor cell injection site has made subcutaneous models the most frequently used. The model is suitable for investigation of therapeutic efficacy and tumor biology. However, primary subcutaneous pancreatic tumors typically do not metastasize and often incorporate less stroma than transgenic tumors or tumors grown in the orthotopic setting. Other possible putative differences between pancreas-based spontaneous and skin-based injected tumors are not proven, but may exist.

Subcutaneous models are certainly not ideal for analysis of metastatic parameters. Furthermore, given that these experiments are performed in immunodeficient animals, there is also a limited ability to study the role of innate immunity in tumor progression. Despite these shortcomings, advocates of this model emphasize its ease of use and application, aside from the limited training needed for performing these experiments in a quick and reliable fashion. In addition, multiple different, well-characterized cell lines can be assessed in vivo in this fashion.

4.4.2 Orthotopic Model

More recently orthotopic modeling gained more popularity since the subcutaneous model is critiqued for its altered tumor architecture and its presence of a distinct capsule. Tumor vasculature is derived from skin which may be different from the network that is provided by the pancreas. Most importantly, the subcutaneous model does not metastasize, a distinction from a common and important clinical feature of PDAC.

The orthotopic model approach attempts to recapitulate the tumor microenvironment by directly implanting human tumor cells into the pancreas of immunodeficient mice. Such developing tumors are infiltrated with murine stromal components that resemble the stroma of PDAC from patients. Critical factors that influence growth of tumors in the orthotopic site are: (1) cell line selected for implantation; (2) volume and number of cells injected; and (3) the operative technique used for tumor cell injection (Table 4.2).

Tumor cell implantation occurs at either the head or tail equivalent of the pancreas. Mice with tumors in the pancreatic head often succumb to local invasion and develop biliary obstruction prior to extensive liver metastasis. Although these may develop fewer metastases, this clinical presentation is consistent with human disease. Alternatively, tumor injection can occur at the tail of the pancreas. Tumors in the tail are able to grow for longer periods of time, typically develop more frequent metastases and provide more tissue for mechanistic analysis. Various experiences with orthotopic injection, cell numbers and metastatic incidences are included in Table 4.2. Several techniques have been developed to establish orthotopic tumors.

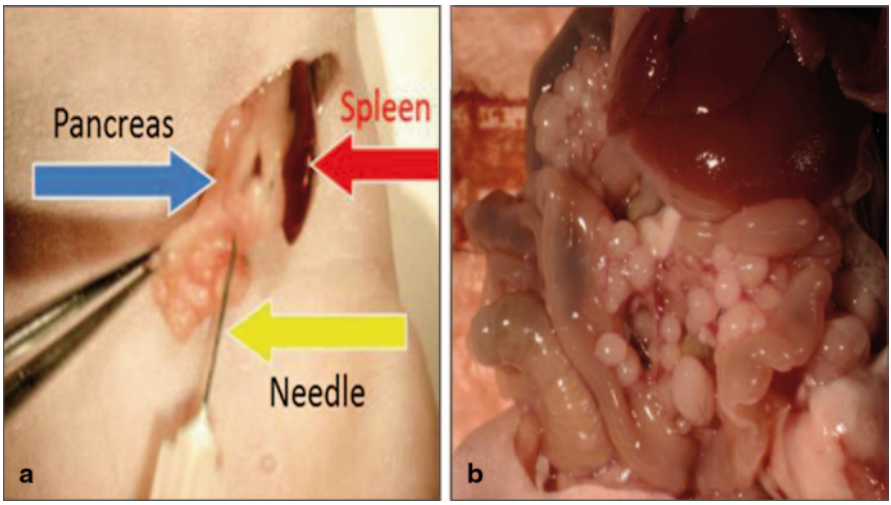

Fig. 4.3 Orthotopic injection of pancreatic cells

This includes the initial placement of subcutaneous tumor. Once established, subcutaneous tumors are harvested and cut into 1–2 mm^3 pieces and implanted with suture fixation into the pancreas [74]. Alternatively, subcutaneous tumors are minced, processed into a cell suspension [75], injected into the pancreas and followed for tumor growth [76]. Cells can also be directly injected into the pancreas from cell culture (Fig. 4.3). Prior to injection, cells are grown in culture, counted and suspended in sterile PBS or serum free medium in a desired cell concentration. After anesthetizing the recipient mouse, a left upper quadrant incision is made and the distal pancreas is introduced into the wound. Tumor cells are injected under sterile conditions into the pancreas, and the incision is closed. These two methods have been compared in several cell lines, including MiaPaca-2, Capan-1, AsPC-1 and HPAF-II. Tumors established by tumor piece implantation had an increased overall survival but decreased metastatic incidence compared to tumors established by direct tumor cell inoculation from culture [74]. Given the increased incidence of metastasis in the injection model, we use this method for orthotopic implantation. The difference in metastatic rates between these two methods is intriguing and warrants further study to further characterize the mechanisms of metastasis involved.

After anesthesia induction, a left lateral incision is made and the spleen and distal pancreas are externalized. A subcapsular injection is made forming a bubble as shown and then returned to abdomen and skin is closed. Tumor growth is then monitored (Fig. 4.3a). Many cells ultimately metastasize. Three months after MiaPaca-2 tumor cell injection, gastrointestinal, liver and lymph node metastasis are seen throughout the abdomen of the mouse (Fig. 4.3b)

The orthotopic model has been widely represented in the literature. Although gemcitabine has been used frequently as the standard of care in in vivo experiments, the dose and frequency of administration have not been similar between

Table 4.4 Gemcitabine sensitivity in vivo

Cell line	Tumor location	Gemcitabine dose	Sensitivity in vivo	Reference
AsPC-1	Subcutaneous	100 mg/kg twice weekly	Yes	Awasthi A et al. 2011 [96]
BxPC-3	Orthotopic	300 mg/kg weekly 150 mg/kg weekly	Yes 48 %No 51.8 %	Sun FX et al. 2003 [97]
Capan-1	Subcutaneous	100 mg/kg twice weekly	Yes T/C=~20 %	Kimura K et al. 2006 [98]
CFPAC-1	Subcutaneous	150 mg/kg every 3 days	Yes T/C = 5.6	Mercalli A et al. 2007 [99]
L3.6pl (Colo357)	Orthotopic subcutaneous	250 mg/kg twice weekly 62.5 mg/kg twice weekly	Yes T/C 28 % No T/C=68.9	Bruns CJ et al. 1999 [100] Bondar VM et al. 2002 [83]
HPAC	Orthotopic	2.5 mg/kg daily	No T/C=63 %	Mohammad RM et al. 1998 [77]
HPAF-II	Orthotopic	120 mg/kg	Yes T/C=25 %	Hotz B et al. 2010 [101]
MiaPaca-2	Orthotopic	25 mg/kg twice weekly	Yes T/C= 50 %	Dineen SP et al 2010 [39]
MPanc-96	Orthotopic	50 mg/kg100 mg/kg weekly	No No T/C >100 %	Pan X et al. 2008 [102] Ramachandran et al. 2008 [85]
Panc-1	Orthotopic subcutaneous	25 mg/kg twice weekly100 mg/kg	No T/C=77 % Yes T/C ~25 %	Awasthi N et al 2010 [86] Du JH et al. 2010 [103]
SU 86.86	Subcutaneous	100 mg/kg every 3 days	Yes T/C= 31%	Feng N et al. 2003 [104]
SW1990	Orthotopic subcutaneous	100 mg/kg weekly 50 mg/kg weekly 50 mg/kg every 3 days	Yes T/C =30 %, No T/C= 77 % No T/C 93 %	Jia L et al. 2005 [87] Xie Q et al. 2009 [105]
Pan02*	Orthotopic	3.5 mg/animal weekly	Yes T/C =40 %	Dineen SP et al. 2008 [88]

*murine pancreatic adenocarcinoma cell line T/C ratio is the weight of the gemcitabine treated tumor/ weight of the control treated tumor. Cell lines are considered sensitive to gemcitabine if tumor growth is reduced by 50 % or less compared to control tumor weights. T/C ratio as reported by reference or approximated from representative figures.

Literature search reveals no in vivo sensitivity results for the following ATCC lines: Capan-2, PL45 & Panc 10.05 (derived from same human tumor), Panc03.27, Panc 08.13, Panc02.03, Panc02.13, Panc04.03 and Panc05.04

experiments. Table 4.4 provides a summary of in vivo models using human PDAC cell lines and the gemcitabine dose used and the tumor response (gem tumor weight/ control tumor weight = T/C ratio). It is important to note that despite being gemcitabine-resistant in vitro, many of the human cell lines are somewhat gemcitabine-sensitive in vivo such as Panc-1 and HPAF-II (KT Ostapoff, unpublished observations). Interestingly, the converse is also true. MiaPaca-2 cells are sensitive to

Gemcitabine in vitro but are relatively resistant in vivo (KT Ostapoff unpublished observations). The role of gemcitabine effects on metastasis has not been fully characterized in these models.

4.4.3 Direct Xenografting

Direct xenografts are the newest method for studying tumor growth and metastasis in vivo. This technique uses patient samples to establish tumors. The exact method of placement varies. Small**,** usually 1 mm^3 pieces from fresh surgical specimens can be isolated and then directly implanted with suture onto the head/portal area of the pancreas [77], middle [78] or tail [79]. For tumor samples that are too small to immediately implant, tumor pieces are implanted subcutaneously and later harvested in a manner similar to that described for the orthotopic model [80]. Tumors can alternatively be isolated into single cell suspensions and then directly injected orthotopically or maintained in culture prior to injection. Groups that routinely perform these types of injections find that tumor growth improves when implantation occurs within 1 h of resection [81]. Tumors typically establish at faster rates with each additional passage.

There are several advantages to the direct xenograft model. Tumor specimens contain stromal elements from the primary tumor. Although these elements may not persist with additional passages, they contribute to the tumor microenvironment and metastasis. These stromal elements may hold a key to the increased rate of metastasis compared to cell suspensions in other models [80]. Early reports have suggested that metastasis isolated from these tumors develop mutations after transplantation in the mouse [79]. The cause of these new mutations has not been identified as of yet. It is unclear whether these new mutations are caused by interactions with mouse cells in the tumor microenvironment or if they reflect the natural progression of these cells as they find the metastatic niche (i.e. these same mutations are present in metastasis subsequently found in the patient).

A significant advantage to this approach is the potential to improve drug selection and identify individual tumor susceptibility in patients. Analysis of patient samples in vivo, have allowed researchers to study potential mutations in surgical specimens that may predict response to therapy [82]. Additionally, tumors isolated from patients after preoperative chemotherapy have been used to study drug resistance within the viable tumor and/or used to identify additional drug sensitivity of remaining tumor cells post-operatively [81].

Several disadvantages also exist for this model. Not all tumor specimens contain viable tumor for implantation. The tumor take rate (or establishment rate) is not consistent between different samples, and may in fact be problematically low (i.e. around 20%). The same sample placed in different locations (i.e. liver, pancreas or colon) within the mouse interacts differently with its host environment [83]. This method also requires specialized training and a well-organized system in place to assure rapid delivery of tumor from operating room to bench and implantation. Dif-

ferent samples reflect the clinical heterogeneity of tumors, rendering generalizable investigations more difficult due to the absence of detailed knowledge of molecular and biologic alterations involved. Regardless of these potential caveats, this model has great potential for improving patient care and chemotherapeutic agent delivery, as samples used are as much reflective of clinical tumor specimens as feasible. It also has the potential to allow researchers to study mechanisms of chemo- and radiation resistance within previously treated tumors. It provides a platform for studying the additional genetic events that occur when tumor cells develop metastases.

Xenograft models have provided excellent advances in the knowledge of disease progression and metastasis. Most cell lines invade into local tissues and metastasize to lymph nodes and liver in an orthotopic model. This allows for the study of molecular pathways of invasion, tumor to stromal interactions and metastasis as well as the study of targets in these pathways [84]. Many of these cell lines have been fully characterized in terms of their known mutations (Table 4.3) and may allow for studying specific responses to targeted therapy.

4.4.4 Monitoring Growth in PDAC Models

Several methods aid in the understanding of mechanisms of PDAC progression and metastasis that can be used both in vivo and ex vivo. Subcutaneous tumor growth is easily measured with calipers. Orthotopic models, however, present a unique challenge given intraperitoneal tumor location. Several methods have been developed for noninvasive imaging of orthotopic tumors, allowing for size monitoring in the same animal over time. If cell lines are labeled with a non-invasive probe (e.g. fluorescent protein), primary tumors and metastases can be visualized using fluorescence stereo microscopes [85]. Visualization for this technique is optimized by creating a skin flap over the primary tumor which improves sensitivity of detection of fluorescence (Fig. 4.4) [86]. Furthermore, Bouvet et al., have shown that there is strong correlation between metastatic disease using GFP or RFP labeled cells by imaging between fluorescence optical imaging (FLU), magnetic resonance imaging (MRI) and ultrasound without the use of additional contrast agents [87]. Recently, this group has shown using GFP and RFP labeled cells that micrometastasis can be identified using in vivo laparoscopy in mice [88]. In fact, using fluorescently labeled CEA (carcinoembryonic antigen), this group was also able to identify micrometastasis throughout the peritoneum after orthotopic tumor establishment with laparoscopy [89].

Bioluminescent imaging (BLI) can be used for luciferase labeled cells. Mice are injected with a luciferase substrate, anesthetized and subsequently imaged (Fig. 4.5) [90].

This technique can adequately demonstrate the development of metastatic disease during tumor progression and can be quantified. However, in our experience, luciferase labeled cells grow slower in vivo than their parental cell line and often inconsistently develop metastases; however disseminated lesions that do develop

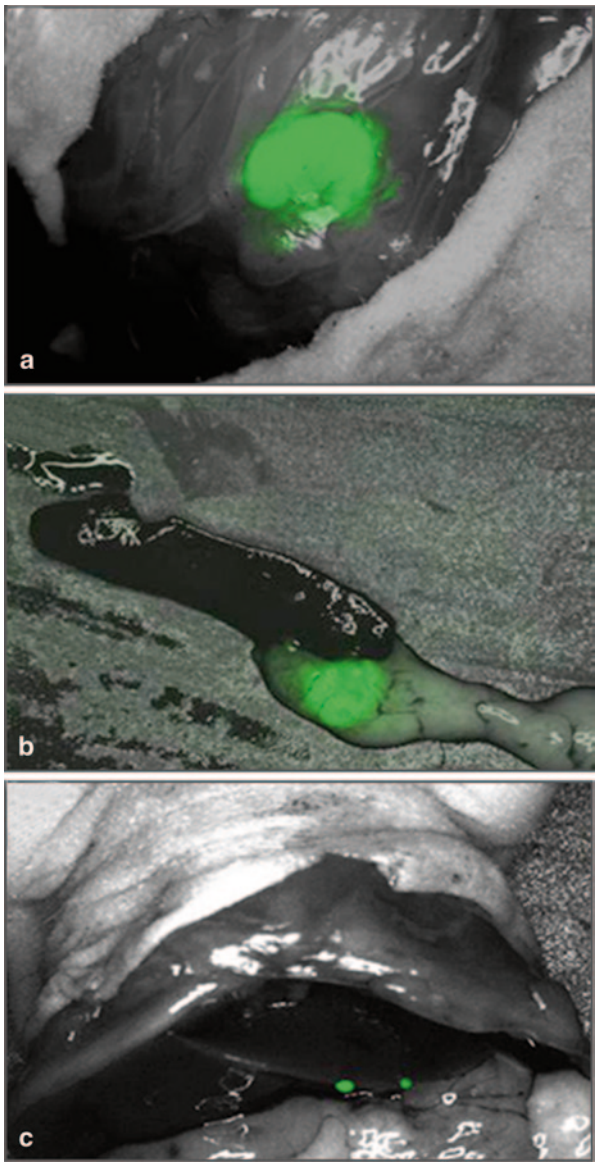

Fig. 4.4 Panc-1-GFP cell lines metastasize. After injection of GFP-Panc-1 cells orthotopically in the pancreas, primary tumors are established as shown **a** in vivo and **b** ex vivo. Liver metastases are established on liver as shown by green areas **c**

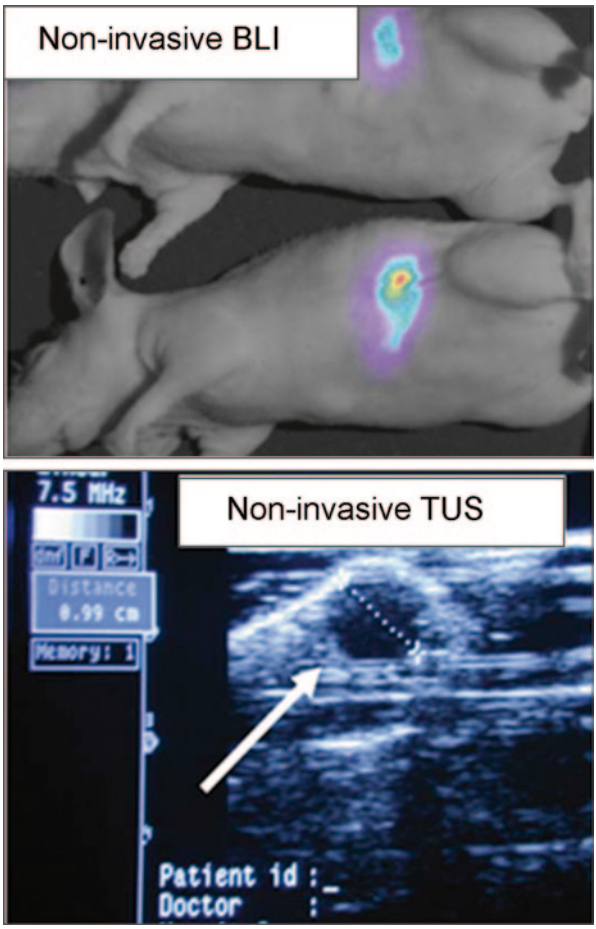

Fig. 4.5 Noninvasive imaging of tumor and metastatic growth. Using luciferase labeled cells; tumor growth after orthotopic implantation can be followed using BLI (*upper panel*). The tumor intensity is measured and can be followed over time. Without labeled cells, simple ultrasound imaging can provide evidence of tumor growth that is measureable (*lower panel*, *dotted line* is tumor measurement)

can be followed easily. Additionally, several options also exist for monitoring unlabeled cells including ultrasound with or without microbubbles [91], MRI [92] and PET/CT [93](Fig. 4.5).

4.5 Modeling Metastatic Disease

Orthotopic models facilitate studying tumor to stromal interactions and some other mechanisms of tumor progression. However, direct metastatic models are beneficial for the evaluation of the ability of tumor cells to colonize and grow at distant sites. Not all circulating tumor cells result in metastasis, and the processes under which some arrive in the metastatic niche and go on to form demonstrable metastases are complex. Specific models to disrupt or study these mechanisms are required to un-

derstand this complex relationship. It has also been suggested that specific human cell lines have predilections for metastasis from an intrapancreatic location to specific target sites (i.e. BxPC-3 tends metastasizes to lymph nodes while MiaPaca-2 tends to metastasize to the liver) [94]. This may be due to mechanisms inherent to the cell line, or due to specific evolution of tumor to stromal interactions. Several methods of developing metastatic only models allow one to study the development of micro- to macrometastasis and invasion from the vasculature into the site of metastasis.

In addition, for patients who are able to undergo pancreatic resection, survival is governed by the pre-therapeutic development of metastasis. Murine models that allow evaluation of strategies to inhibit circulating tumor cells within the metastatic niche in order to prevent subsequent metastasis would therefore have important clinical implications. This section will describe models of perineural invasion, lymphatic metastasis, liver metastasis and peritoneal spread of pancreatic cancer.

4.5.1 Perineural Invasion Models

Perineural invasion is a significant feature of human PDAC which is associated with a worse survival and an increased risk of metastasis. It also correlates with an increased risk of local recurrence after resection. The specific mechanism and its role in the evolution of metastasis remains incompletely understood.

Early reports indicated a lack of perineural invasion in orthotopic models [77, 95]. Recently however, perineural invasion has been documented in an orthotopic model. MiaPaca-2 and Capan-2 orthotopic tumors were established and then resected at 4, 6 and 8 weeks. After resection, mice with MiaPaca-2 tumors that were 6 weeks or older developed tumor recurrence that showed extensive retroperitoneal perineural invasion on histological analysis [96]. There are also two models which use nerve grafts to establish perineural invasion. In the human model, celiac or superior mesenteric artery nerve plexus were taken from recent human autopsy specimens and implanted subcutaneously in SCID/NOD mice. After 4 weeks of nerve engraftment, human cell lines were then injected in an adjacent area subcutaneously and allowed to grow [97]. Although all cell lines used (Capan-1, Capan-2, CFPAC and MPanc96) had some perineural invasion, they frequently did not invade the nerve itself. Alternatively, human pancreatic cancer cell lines were injected subcutaneously on the midline of the mouse back and allowed to grow towards the spine. Both Capan-1 and Capan2 had significant perineural invasion (in 55% and 69% of mice respectively) compared to none in HPAF-II, AsPC-1 and Panc-1 cell lines used. All lines had epineural invasion and nerve involvement [97]. Additionally, use of the mouse perineural model has been used to analyze potential transcription factors that contribute to perineural invasion and metastasis [98, 99].

With the additions of both of these animal models of perineural invasion, in vivo models are available to study mechanisms of perineural invasion that can lead to local recurrence and metastasis after a successful pancreatic resection.

In order to investigate the mechanism of perineural tumor invasion, Gil et al. used dorsal root ganglia extracted from 2–4 week old Balb/c mice and allowed MiaPaca-2 and Panc-1 tumor cells to migrate through a matrigel [100]. They found that some cell lines were able to grow towards neural cells and in fact those that did formed a spindle-shape morphology. Tumor cells also migrated towards neural cells in Boyden chambers and this was blocked by anti-GDNF antibodies[100]. The use of myenteric plexus cells isolated from Sprague-Dawley rats, plated with T3M4 pancreatic cancer cells, also demonstrates a proclivity of tumor cells to migrate towards nerve cells and change their morphology [101].

4.5.2 Lymphangitic Metastasis Models

PDAC cells exhibit a predilection to colonize regional lymph nodes. This clinical observation suggests that lymphatic vessels carry an integral function in the metastatic process of PDAC; in fact, expression of the primary lymphatic growth factor vascular endothelial growth factor-C (VEGF-C) tends to correlate with lymph node metastasis in patient specimens [102–105]. The presence of VEGF-C expression in cancer cells is associated with increased incidence of lymph node metastasis but does not correlate with decreased patient survival [102, 106]. It has also been shown that the density of lymphatic vessels is lower in intratumoral regions than normal regions of the pancreas, and intratumoral lymphatic vessels are collapsed whereas peritumoral lymphatics are enlarged in human PDAC specimens [106]. Analysis of human PDAC cell lines shows that T3M4, MiaPaca-2, Panc-1, Colo357 and BxPC-3 all express VEGF-C but do not express VEGFR-3 (vascular endothelial growth factor receptor-3) [106].

VEGF-D also plays an important role in lymph node metastasis. VEGF-D null mice after orthotopic implantation with Pan02 cells have significantly increased mesenteric lymph node metastasis and a reduction in lymph vessel diameter compared to control mice [107]. However, there is no discernable difference in primary tumor weight. As a result, this provides evidence that lymphatic vascular function is specifically and abnormally regulated in the PDAC environment. As lymphatic metastasis may play a critical role in PDAC progression, specific models may aid in understanding and studying this relationship.

The first study of the normal pancreatic lymphatic network dates back to 1881, with the work of Hoggan and Hoggan [108]. Since that time, injection methods, basic histological staining, and electron microscopy have been employed to characterize the lymphatic network of the pancreas [109]. Tumor lymphangiogenesis is seen in both subcutaneous and orthotopic tumors. Lymph node metastases are common in orthotopically implanted MiaPaca-2, BxPC-3, HPAF-II, PancTu-1, aPt45P1 and Colo357 [110–112]. Using these models, the mechanisms of lymphatic metastasis have been studied. Inhibition of TGFβRI enhances intratumoral lymphatics in subcutaneous MiaPaca-2 and BxPC-3 tumors [113]. Using MiaPaca-2 orthotopic tumors, Schultz et al. found that induction of p16 expression in tumors resulted in

an inhibition of lymph node metastasis and reduced the tumor burden in the rare affected lymph nodes [114]. Furthermore, overexpression of αVβ3 that results in c-Src activation in FG cells (a clonal line from parental Colo357 cells) was found to promote lymphatic metastasis specifically to the bowel mesentery and hepatic hilar lymph nodes [115]. This was further confirmed with the use of dasatinib (a Src inhibitor) which resulted in reduced lymph node metastasis, overall LN mass and tumor burden within the lymph node [115].

For certain lymphatic intervention approaches such as nanoparticle delivery a lymphatic metastasis model can be used, in which the mouse hindfoot is injected with tumor cells known to metastasize to lymph nodes (BxPC-3) [116]. After several weeks, lymph nodes from the popliteal, inguinal and iliac regions are harvested for analysis.

One of the limitations of xenograft models is the lack of a fully functioning immune system which quite possibly impacts the biology of lymphatic metastasis. In contrast, Pan02 cells are injected into immunocompetent mice. Furthermore, orthotopic Pan02 tumors are highly metastatic towards mesenteric lymph nodes, even though they do not exhibit profound intratumoral lymphatic vessels [117]. Lymph node metastasis can be easily calculated in this model with control mice often having 20–30 lymph node metastases. Due to this observation, multiple studies have used this model to look at effects of different therapies on lymphatic metastasis [111]. Using the Pan02 model, macrophages have been shown to play an important role in regulating peritumoral lymphangiogenesis and lymph node metastasis [117]. Furthermore, lymphatic vessel density is decreased in the presence of macrophage depletion with clodrolip or with the use of anti-PlGF (placental like growth factor) in vivo [117]. In the pancreas, there is growing evidence that lymphatic vessels facilitate the lymphatic spread of PDAC. However, the underlying mechanisms remain poorly defined. Future *in vitro* and *in vivo* studies will shed light on the pathways controlling the lymphovascular regulation and the resulting lymphatic spread of PDAC. This may help elicit novel biomarkers to identify patients at risk for disease recurrence and also identify potential therapeutic targets.

4.5.3 Liver Metastasis Models (discussed in Chapter 7 in detail)

The most common site of metastasis for PDAC is in the liver. The two most common models used to establish metastasis are portal vein injection and splenic injection models (Fig. 7.2).

4.5.3.1 Portal Vein Injection Model

In the portal vein injection model, cells are injected directly into the portal vein and subsequently form liver lesions with high frequency. Initial studies used India ink to stain tumor cells within the liver, and confirmed that cells left untreated after portal

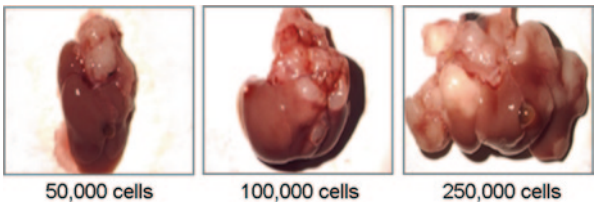

Fig. 4.6 Splenic injection results in large metastasis

injection can reliably form hepatic parenchymal metastases [118]. As early as 72 h post injection, I^{125}labeled tumors cells can be identified within the liver in the form of micrometastases [119]. In one study portal vein injection resulted in higher incidence of metastasis (71% vs. 51%) compared to orthotopic implantation of the same cell line [120]. Portal vein injection is technically challenging and bypasses many hurdles that metastatic tumor cells must overcome to establish lesions in the liver. It should however be noted that tumor cells injected into the portal vein do reach the systemic circulation and can form metastases in other organs, too (e.g., lung).

4.5.3.2 Splenic Injection Model

In addition to portal vein injection, the splenic injection method offers a reliable route to establish liver metastases. In this method, tumor cells are injected into the lower pole of the spleen and then pass through the splenic vein to the liver and systemically. Investigators using this method will often remove the spleen shortly after injection prior to closing the incision [121], although some allow the spleen to remain in place, especially if an immunotherapeutic component may be affected by a splenectomy [122]. An approach of hemisplenectomy with spleen splitting, removal of the hemispleen through which tumor cells had been injected, and preservation of the unaffected hemispleen has been described [123–125]. Tumor burden can be measured by liver weights or by gross inspection. This model typically leads to micrometastases as early as 7–14 days after injection, and may lead to near complete liver replacement with tumor typically between 5–8 weeks (Fig. 4.6).

Pan02 cells were injected into the spleen of C57bl/6 mice. After 5 weeks mice were sacrificed and evaluated for metastatic deposits. Representative livers are shown above. Metastatic burden can grossly be appreciated between different cell numbers injected.

One group comparing different cell lines found that while some lines did not form metastases even when injecting 10^6 cells (Capan-2 and PL45), other more aggressive lines could form metastases after injection with less than 10^4 cells (MiaPaca-2, AsPC-1, Panc1, Capan-1 and BxPC-3 in NOD/SCID or NOG/SCID mice [126]. This method has been effective for studying some mechanistic aspects of metastatic tumor implantation, such as by either pretreating cells prior to implantation or by treating mice after tumor cell injection with specific inhibitors of the TGF-β pathway [121].

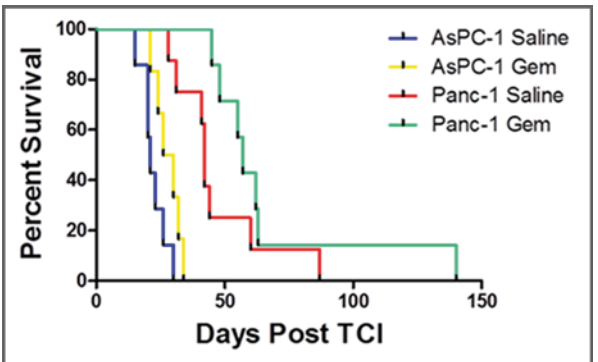

	Median Survival (Days)
AsPC-1 Saline	21
AsPC-1 Gemcitabine	28
Panc-1 Saline	42
Panc-1 Gemcitabine	57

Fig. 4.7 Survival outcomes after intraperitoneal PDAC cell injection, and potential for therapeutic testing. Control mice in both AsPC-1 and Panc-1 groups have short survival (21 and 42 days respectively). Addition of standard chemotherapy in form of gemcitabine extends survival minimally for ASPC-1 cells (gemcitabine resistant in vitro), and moderately for Panc-1 cells (gemcitabine sensitive in vitro)

The splenic injection model may still not prevent cells from circulating systemically and ultimately forming extrahepatic tumors. In our experience, after intrasplenic injection of Pan02 cells in C57bl/6 mice, the animals do not develop lung metastases (KT Ostapoff, unpublished observations). The hepatic metastases that form in this model are sufficiently large (as demonstrated in Fig. 4.6) to retrieve tissue for immunohistochemistry, protein isolates for Western blots or proteomic studies, and RNA or DNA samples for genomic arrays.

4.5.4 Intraperitoneal Injection Model

While liver metastases are common in patients, peritoneal spread of disease is also a hallmark feature of PDAC. Mechanisms of intraperitoneal recurrence and the development of intraperitoneal disease are important to understand the progression to end stage disease. Models that address the spontaneous intraperitoneal progression of PDAC have not been described. However, disease progression after intraperitoneal injection can be followed for various cell lines in xenograft or syngeneic injection models. Mice are injected with cells directly into the peritoneal cavity and develop peritoneal implants as soon as 48 h after injection. In cases of injection of AsPC-1 and Panc-1 cell lines into SCID or nude mice, spontaneous homing of the cells to the pancreas occurs [127]. After establishment of tumors, very few animals

develop ascites, but obstructive jaundice, lymph node metastases and liver metastases are common; animals must be sacrificed due to tumor associated morbidity soon after [71, 127, 128]. This model therefore can serve as a simple, reproducible and reliable survival model for experimental therapy approaches.

It has been shown to be highly replicable with respect to median survival of control and gemcitabine treated animals in both Panc-1 and AsPC-1 models and used in studying therapeutic interventions (Fig. 4.7) [71, 127–131].

Using overall survival as its primary endpoint, the intraperitoneal model is analogous to a human clinical trial. Multiple agents in combination can be tested at once, with toxicities to certain combinations identified early in the in vivo evaluation. A downside to this approach is that model outcomes will depend on the specific cell line characteristics, and therefore carry some shortcomings compared to the complexity and heterogeneity of spontaneous human PDAC tumors.

4.6 Conclusions

Due to the complexity of PDAC biology, no single animal model will provide complete understanding of the mechanisms of this disease. In fact, we can comfortably go as far as to assume that no model will completely be able to represent this disease complexity. However, we now can resort to numerous in vivo models that are able to address specific factors with relevance to PDAC development and therapy.

Genetically engineered mouse models provide improved understanding of carcinogenesis and tumor initiation; they are likely continuing to evolve through the introduction of new mutations into existing transgenic mice. Syngeneic (and transgenic) models provide an opportunity to investigate the importance of immune cells for the regulation of tumor progression, and to evaluate immunotherapy approaches in vivo. Work with established human cell lines has multiple benefits of evaluating drug response and tumor to stromal interactions. More recently, direct human-derived xenografts provide some opportunity to study chemoresistance and sensitivity in human samples as well as potentially direct therapy.

Despite the assets of these known models, multiple challenges face the field as we move towards better understanding the mechanisms of metastasis. The role of pancreatic stem cells, while still controversial, opens a new opportunity of research. Recent work suggests that cells from the pancreas and bone marrow work in conjunction in a carcinogen-induced model of pancreatic cancer [132]. There is also evidence that pancreatic stellate cells, which are known to participate in the desmoplastic reaction within the primary tumor also facilitate metastasis [133, 134]. Similarly work with mesenchymal stem cells shows promise to understand the function of host-stroma interactions and has been proposed as a potential target for treatment [135, 136].

In the era of emerging individualized care, multiple in vivo models give testament to the fact that progress is being made in the study of this challenging disease. Future work will need to address the added complexities of both the tumor microenvironment and pluripotent nature of PDAC cells. We therefore

anticipate that additional PDAC models will aid the process of ever improving insight into the molecular and genetic mechanisms and therapeutic strategies for pancreatic cancer.

References

1. Jemal A, Murray T, Ward E, Samuels A, Tiwari RC et al (2005) Cancer statistics. CA Cancer J Clin 55:10–30
2. Conroy T, Desseigne F, Ychou M, Bouche O, Guimbaud R et al (2011) FOLFIRINOX versus gemcitabine for metastatic pancreatic cancer. N Engl J Med 364:1817–1825
3. Burris HA, 3rd, Moore MJ, Andersen J, Green MR, Rothenberg ML et al (1997) Improvements in survival and clinical benefit with gemcitabine as first-line therapy for patients with advanced pancreas cancer: a randomized trial. J Clin Oncol 15:2403–2413
4. Grote VA, Rohrmann S, Nieters A, Dossus L, Tjonneland A et al (2011) Diabetes mellitus, glycated haemoglobin and C-peptide levels in relation to pancreatic cancer risk: a study within the European rospective nvestigation into Cancer and Nutrition (EPIC) cohort. Diabetologia 54(12):3037–3046
5. Lo AC, Soliman AS, El-Ghawalby N, Abdel-Wahab M, Fathy O et al (2007) Lifestyle, occupational, and reproductive factors in relation to pancreatic cancer risk. Pancreas 35:120–129
6. Blackford A, Parmigiani G, Kensler TW, Wolfgang C, Jones S et al (2009) Genetic mutations associated with cigarette smoking in pancreatic cancer. Cancer Res 69:3681–3688
7. Aune D, Greenwood DC, Chan DS, Vieira R, Vieira AR et al (2011) Body mass index, abdominal fatness and pancreatic cancer risk: a systematic review and non-linear dose-response meta-analysis of prospective studies. Ann Oncol 23(4):843–852
8. Immervoll H, Hoem D, Kugarajh K, Steine SJ, Molven A (2006) Molecular analysis of the EGFR-RAS-RAF pathway in pancreatic ductal adenocarcinomas: lack of mutations in the BRAF and EGFR genes. Virchows Arch 448:788–796
9. Lee J, Jang KT, Ki CS, Lim T, Park YS et al (2007) Impact of epidermal growth factor receptor (EGFR) kinase mutations, EGFR gene amplifications, and KRAS mutations on survival of pancreatic adenocarcinoma. Cancer 109:1561–1569
10. Tascilar M, Skinner HG, Rosty C, Sohn T, Wilentz RE et al (2001) The SMAD4 protein and prognosis of pancreatic ductal adenocarcinoma. Clin Cancer Res 7:4115–4121
11. Blackford A, Serrano OK, Wolfgang CL, Parmigiani G, Jones S et al (2009) SMAD4 gene mutations are associated with poor prognosis in pancreatic cancer. Clin Cancer Res 15:4674–4679
12. Gazzaniga GM, Papadia FS, Dezzana M, Cappato S, Filauro M et al (2001) Role of p53 mutations on survival after pancreatoduodenectomy for ductal adenocarcinoma of the pancreatic head. Hepatogastroenterology 48:1743–1745.
13. Ohtsubo K, Watanabe H, Yamaguchi Y, Hu YX, Motoo Y et al (2003) Abnormalities of tumor suppressor gene p16 in pancreatic carcinoma: immunohistochemical and genetic findings compared with clinicopathological parameters. J Gastroenterol 38:663–671
14. Mansour JC, Schwarz RE (2008) Molecular mechanisms for individualized cancer care. J Am Coll Surg 207:250–258
15. Mazur PK, Einwachter H, Lee M, Sipos B, Nakhai H et al (2010) Notch2 is required for progression of pancreatic intraepithelial neoplasia and development of pancreatic ductal adenocarcinoma. Proc Natl Acad Sci USA 107:13438–13443
16. Yachida S, Jones S, Bozic I, Antal T, Leary R et al (2010) Distant metastasis occurs late during the genetic evolution of pancreatic cancer. Nature 467:1114–1117.
17. Campbell PJ, Yachida S, Mudie LJ, Stephens PJ, Pleasance ED et al (2010) The patterns and dynamics of genomic instability in metastatic pancreatic cancer. Nature 467:1109–1113

18. Grippo PJ, Tuveson DA (2010) Deploying mouse models of pancreatic cancer for chemoprevention studies. Cancer Prev Res (Phila) 3:1382–1387
19. Olive KP, Tuveson DA (2006) The use of targeted mouse models for preclinical testing of novel cancer therapeutics. Clin Cancer Res 12:5277–5287
20. Sandgren EP, Luetteke NC, Qiu TH, Palmiter RD, Brinster RL et al (1993) Transforming growth factor alpha dramatically enhances oncogene-induced carcinogenesis in transgenic mouse pancreas and liver. Mol Cell Biol 13:320–330
21. Wagner M, Greten FR, Weber CK, Koschnick S, Mattfeldt T et al (2001) A murine tumor progression model for pancreatic cancer recapitulating the genetic alterations of the human disease. Genes Dev 15:286–293
22. Greten FR, Wagner M, Weber CK, Zechner U, Adler G et al (2001) TGF alpha transgenic mice. A model of pancreatic cancer development. Pancreatology 1:363–368
23. Schreiner B, Baur DM, Fingerle AA, Zechner U, Greten FR et al (2003) Pattern of secondary genomic changes in pancreatic tumors of Tgf alpha/Trp53+/– transgenic mice. Genes Chromosomes Cancer 38:240–248
24. Garbe AI, Vermeer B, Gamrekelashvili J, von Wasielewski R, Greten FR et al (2006) Genetically induced pancreatic adenocarcinoma is highly immunogenic and causes spontaneous tumor-specific immune responses. Cancer Res 66:508–516
25. Kawaguchi Y, Cooper B, Gannon M, Ray M, MacDonald RJ et al (2002) The role of the transcriptional regulator Ptf1a in converting intestinal to pancreatic progenitors. Nat Genet 32:128–134
26. Hingorani SR, Petricoin EF, Maitra A, Rajapakse V, King C et al (2003) Preinvasive and invasive ductal pancreatic cancer and its early detection in the mouse. Cancer Cell 4:437–450
27. Aguirre AJ, Bardeesy N, Sinha M, Lopez L, Tuveson DA et al (2003) Activated Kras and Ink4a/Arf deficiency cooperate to produce metastatic pancreatic ductal adenocarcinoma. Genes Dev 17:3112–3126
28. Bardeesy N, Cheng KH, Berger JH, Chu GC, Pahler J et al (2006) Smad4 is dispensable for normal pancreas development yet critical in progression and tumor biology of pancreas cancer. Genes Dev 20:3130–3146
29. Kamijo T, Zindy F, Roussel MF, Quelle DE, Downing JR et al (1997) Tumor suppression at the mouse INK4a locus mediated by the alternative reading frame product p19ARF. Cell 91:649–659
30. Sharpless NE, Bardeesy N, Lee KH, Carrasco D, Castrillon DH et al (2001) Loss of p16Ink4a with retention of p19Arf predisposes mice to tumorigenesis. Nature 413:86–91.
31. Bardeesy N, Aguirre AJ, Chu GC, Cheng KH, Lopez LV et al (2006) Both p16(Ink4a) and the p19(Arf)-p53 pathway constrain progression of pancreatic adenocarcinoma in the mouse. Proc Natl Acad Sci USA 103:5947–5952
32. Feldmann G, Habbe N, Dhara S, Bisht S, Alvarez H et al (2008) Hedgehog inhibition prolongs survival in a genetically engineered mouse model of pancreatic cancer. Gut 57:1420–1430
33. Dineen SP, Roland CL, Greer R, Carbon JG, Toombs JE et al (2010) Smac mimetic increases chemotherapy response and improves survival in mice with pancreatic cancer. Cancer Res 70:2852–2861
34. Olive KP, Tuveson DA, Ruhe ZC, Yin B, Willis NA et al (2004) Mutant p53 gain of function in two mouse models of Li-Fraumeni syndrome. Cell 119:847–860
35. Hingorani SR, Wang L, Multani AS, Combs C, Deramaudt TB et al (2005) Trp53R172H and KrasG12D cooperate to promote chromosomal instability and widely metastatic pancreatic ductal adenocarcinoma in mice. Cancer Cell 7:469–483
36. Olive KP, Jacobetz MA, Davidson CJ, Gopinathan A, McIntyre D et al (2009) Inhibition of Hedgehog signaling enhances delivery of chemotherapy in a mouse model of pancreatic cancer. Science 324:1457–1461
37. Morton JP, Karim SA, Graham K, Timpson P, Jamieson N et al (2010) Dasatinib inhibits the development of metastases in a mouse model of pancreatic ductal adenocarcinoma. Gastroenterology 139:292–303
38. Fendrich V, Chen NM, Neef M, Waldmann J, Buchholz M et al (2010) The angiotensin-I-converting enzyme inhibitor enalapril and aspirin delay progression of pancreatic intraepithelial

neoplasia and cancer formation in a genetically engineered mouse model of pancreatic cancer. Gut 59:630–637.
39. Liby KT, Royce DB, Risingsong R, Williams CR, Maitra A et al (2010) Synthetic triterpenoids prolong survival in a transgenic mouse model of pancreatic cancer. Cancer Prev Res (Phila) 3:1427–1434
40. Kojima K, Vickers SM, Adsay NV, Jhala NC, Kim HG et al (2007) Inactivation of Smad4 accelerates Kras(G12D)-mediated pancreatic neoplasia. Cancer Res 67:8121–8130
41. Izeradjene K, Combs C, Best M, Gopinathan A, Wagner A et al (2007) Kras(G12D) and Smad4/Dpc4 haploinsufficiency cooperate to induce mucinous cystic neoplasms and invasive adenocarcinoma of the pancreas. Cancer Cell 11:229–243
42. Pin CL, Rukstalis JM, Johnson C, Konieczny SF (2001) The bHLH transcription factor Mist1 is required to maintain exocrine pancreas cell organization and acinar cell identity. J Cell Biol 155:519–530
43. Tuveson DA, Zhu L, Gopinathan A, Willis NA, Kachatrian L et al (2006) Mist1-KrasG12D knock-in mice develop mixed differentiation metastatic exocrine pancreatic carcinoma and hepatocellular carcinoma. Cancer Res 66:242–247
44. Habbe N, Shi G, Meguid RA, Fendrich V, Esni F et al (2008) Spontaneous induction of murine pancreatic intraepithelial neoplasia (mPanIN) by acinar cell targeting of oncogenic Kras in adult mice. Proc Natl Acad Sci USA 105:18913–18918
45. Slater EP, Langer P, Fendrich V, Habbe N, Chaloupka B et al (2010) Prevalence of BRCA2 and CDKN2a mutations in German familial pancreatic cancer families. Fam Cancer 9:335–343
46. Hahn SA, Greenhalf B, Ellis I, Sina-Frey M, Rieder H et al (2003) BRCA2 germline mutations in familial pancreatic carcinoma. J Natl Cancer Inst 95:214–221
47. Jones S, Hruban RH, Kamiyama M, Borges M, Zhang X et al (2009) Exomic sequencing identifies PALB2 as a pancreatic cancer susceptibility gene. Science 324:217
48. Skoulidis F, Cassidy LD, Pisupati V, Jonasson JG, Bjarnason H et al (2010) Germline Brca2 heterozygosity promotes Kras(G12D)-driven carcinogenesis in a murine model of familial pancreatic cancer. Cancer Cell 18:499–509
49. Feldmann G, Karikari C, dal Molin M, Duringer S, Volkmann P et al (2011) Inactivation of Brca2 cooperates with Trp53(R172H) to induce invasive pancreatic ductal adenocarcinomas in mice:a mouse model of familial pancreatic cancer. Cancer Biol Ther 11:959–968
50. Pogue-Geile KL, Chen R, Bronner MP, Crnogorac-Jurcevic T, Moyes KW et al (2006) Palladin mutation causes familial pancreatic cancer and suggests a new cancer mechanism. PLoS Med 3:e516
51. Goicoechea SM, Bednarski B, Stack C, Cowan DW, Volmar K et al (2010) Isoform-specific upregulation of palladin in human and murine pancreas tumors. PLoS One 5:e10347
52. Carriere C, Seeley ES, Goetze T, Longnecker DS, Korc M (2007) The Nestin progenitor lineage is the compartment of origin for pancreatic intraepithelial neoplasia. Proc Natl Acad Sci USA 104:4437–4442
53. Brembeck FH, Schreiber FS, Deramaudt TB, Craig L, Rhoades B et al (2003) The mutant K-ras oncogene causes pancreatic periductal lymphocytic infiltration and gastric mucous neck cell hyperplasia in transgenic mice. Cancer Res 63:2005–2009
54. Ishizaki H, Manuel ER, Song GY, Srivastava T, Sun S et al (2011) Modified vaccinia Ankara expressing survivin combined with gemcitabine generates specific antitumor effects in a murine pancreatic carcinoma model. Cancer Immunol Immunother 60:99–109
55. Corbett TH, Roberts BJ, Leopold WR, Peckham JC, Wilkoff LJ et al (1984) Induction and chemotherapeutic response of two transplantable ductal adenocarcinomas of the pancreas in C57BL/6 mice. Cancer Res 44:717–726
56. Zaharoff DA, Hance KW, Rogers CJ, Schlom J, Greiner JW (2010) Intratumoral immunotherapy of established solid tumors with chitosan/IL-12. J Immunother 33:697–705
57. Jacobs C, Duewell P, Heckelsmiller K, Wei J, Bauernfeind F et al (2011) An ISCOM vaccine combined with a TLR9 agonist breaks immune evasion mediated by regulatory T cells in an orthotopic model of pancreatic carcinoma. Int J Cancer 128:897–907

58. Tan MC, Goedegebuure PS, Belt BA, Flaherty B, Sankpal N et al (2009) Disruption of CCR5-dependent homing of regulatory T cells inhibits tumor growth in a murine model of pancreatic cancer. J Immunol 182:1746–1755
59. Moo-Young TA, Larson JW, Belt BA, Tan MC, Hawkins WG et al (2009) Tumor-derived TGF-beta mediates conversion of CD4+ Foxp3+ regulatory T cells in a murine model of pancreas cancer. J Immunother 32:12–21
60. Gnerlich JL, Mitchem JB, Weir JS, Sankpal NV, Kashiwagi H et al (2010) Induction of Th17 cells in the tumor microenvironment improves survival in a murine model of pancreatic cancer. J Immunol 185:4063–4071
61. Albig AR, Schiemann WP (2004) Fibulin-5 antagonizes vascular endothelial growth factor (VEGF) signaling and angiogenic sprouting by endothelial cells. DNA Cell Biol 23:367–379
62. Yanagisawa H, Davis EC, Starcher BC, Ouchi T, Yanagisawa M et al (2002) Fibulin-5 is an elastin-binding protein essential for elastic fibre development in vivo. Nature 415:168–171
63. Schluterman MK, Chapman SL, Korpanty G, Ozumi K, Fukai T et al (2010) Loss of fibulin-5 binding to beta1 integrins inhibits tumor growth by increasing the level of ROS. Dis Model Mech 3:333–342
64. Arnold S, Mira E, Muneer S, Korpanty G, Beck AW et al (2008) Forced expression of MMP9 rescues the loss of angiogenesis and abrogates metastasis of pancreatic tumors triggered by the absence of host SPARC. Exp Biol Med (Maywood) 233:860–873
65. Arnold SA, Rivera LB, Miller AF, Carbon JG, Dineen SP et al (2010) Lack of host SPARC enhances vascular function and tumor spread in an orthotopic murine model of pancreatic carcinoma. Dis Model Mech 3:57–72
66. Arnold SA, Rivera LB, Carbon JG, Toombs JE, Chang CL et al (2012) Losartan slows pancreatic tumor progression and extends survival of SPARC-null mice by abrogating aberrant TGFbeta activation. PLoS One 7:e31384
67. Tseng WW, Winer D, Kenkel JA, Choi O, Shain AH et al (2010) Development of an orthotopic model of invasive pancreatic cancer in an immunocompetent murine host. Clin Cancer Res 163684–3695
68. Wilder PJ, Chakravarthy H, Hollingsworth MA, Rizzino A (2009) Comparison of ras-responsive gene enhancers in pancreatic tumor cells that express either wild-type or mutant K-ras. Biochem Biophys Res Commun 381:706–711
69. Lieber M, Mazzetta J, Nelson-Rees W, Kaplan M, Todaro G (1975) Establishment of a continuous tumor-cell line (panc-1) from a human carcinoma of the exocrine pancreas. Int J Cancer 15:741–747
70. Sullivan LA, Carbon JG, Roland CL, Toombs JE, Nyquist-Andersen M et al (2010) r84, a novel therapeutic antibody against mouse and human VEGF with potent anti-tumor activity and limited toxicity induction. PLoS One 5:e12031
71. Awasthi N, Schwarz MA, Schwarz RE (2011) Antitumour activity of sunitinib in combination with gemcitabine in experimental pancreatic cancer. HPB (Oxford) 13:597–604
72. Ijichi H, Chytil A, Gorska AE, Aakre ME, Bierie B et al (2011) Inhibiting Cxcr2 disrupts tumor-stromal interactions and improves survival in a mouse model of pancreatic ductal adenocarcinoma. J Clin Invest 121:4106–4117
73. Kraman M, Bambrough PJ, Arnold JN, Roberts EW, Magiera L et al (2010) Suppression of antitumor immunity by stromal cells expressing fibroblast activation protein-alpha. Science 330:827–830
74. Hotz HG, Reber HA, Hotz B, Yu T, Foitzik T et al (2003) An orthotopic nude mouse model for evaluating pathophysiology and therapy of pancreatic cancer. Pancreas 26e89–98
75. Alisauskus R, Wong GY, Gold DV (1995) Initial studies of monoclonal antibody PAM4 targeting to xenografted orthotopic pancreatic cancer. Cancer Res 55:5743s-5748s
76. Mohammad RM, Al-Katib A, Pettit GR, Vaitkevicius VK, Joshi U et al (1998) An orthotopic model of human pancreatic cancer in severe combined immunodeficient mice: potential application for preclinical studies. Clin Cancer Res 4:887–894
77. Fu X, Guadagni F, Hoffman RM (1992) A metastatic nude-mouse model of human pancreatic cancer constructed orthotopically with histologically intact patient specimens. Proc Natl Acad Sci USA 89:5645–5649

78. Furukawa T, Fu X, Kubota T, Watanabe M, Kitajima M et al (1993) Nude mouse metastatic models of human stomach cancer constructed using orthotopic implantation of histologically intact tissue. Cancer Res 53:1204–1208
79. Reyes G, Villanueva A, Garcia C, Sancho FJ, Piulats J et al (1996) Orthotopic xenografts of human pancreatic carcinomas acquire genetic aberrations during dissemination in nude mice. Cancer Res 56:5713–5719
80. Kim MP, Evans DB, Wang H, Abbruzzese JL, Fleming JB et al (2009) Generation of orthotopic and heterotopic human pancreatic cancer xenografts in immunodeficient mice. Nat Protoc 4:1670–1680
81. Kim MP, Truty MJ, Choi W, Kang Y, Chopin-Lally X et al (2011) Molecular profiling of direct xenograft tumors established from human pancreatic adenocarcinoma after neoadjuvant therapy. Ann Surg Oncol 19(Suppl 3):S395–403
82. Loukopoulos P, Kanetaka K, Takamura M, Shibata T, Sakamoto M et al (2004) Orthotopic transplantation models of pancreatic adenocarcinoma derived from cell lines and primary tumors and displaying varying metastatic activity. Pancreas 29:193–203
83. Farre L, Casanova I, Guerrero S, Trias M, Capella G et al (2002) Heterotopic implantation alters the regulation of apoptosis and the cell cycle and generates a new metastatic site in a human pancreatic tumor xenograft model. FASEB J 16:975–982
84. Manzotti C, Audisio RA, Pratesi G (1993) Importance of orthotopic implantation for human tumors as model systems: relevance to metastasis and invasion. Clin Exp Metastasis 11:5–14
85. Bouvet M, Wang J, Nardin SR, Nassirpour R, Yang M et al (2002) Real-time optical imaging of primary tumor growth and multiple metastatic events in a pancreatic cancer orthotopic model. Cancer Res 62:1534–1540
86. Yang M, Baranov E, Wang JW, Jiang P, Wang X et al (2002) Direct external imaging of nascent cancer, tumor progression, angiogenesis, and metastasis on internal organs in the fluorescent orthotopic model. Proc Natl Acad Sci USA 99:3824–3829
87. Bouvet M, Spernyak J, Katz MH, Mazurchuk RV, Takimoto S et al (2005) High correlation of whole-body red fluorescent protein imaging and magnetic resonance imaging on an orthotopic model of pancreatic cancer. Cancer Res 65:9829–9833
88. Cao HS, Kaushal S, Metildi CA, Menen RS, Lee C et al (2012) Tumor-specific fluorescence antibody imaging enables accurate staging laparoscopy in an orthotopic model of pancreatic cancer. Hepatogastroenterology 59:1994–1999
89. Metildi CA, Kaushal S, Lee C, Hardamon CR, Snyder CS et al (2012) An LED light source and novel fluorophore combinations improve fluorescence laparoscopic detection of metastatic pancreatic cancer in orthotopic mouse models. J Am Coll Surg 214(6):997–1007
90. Lee CJ, Spalding AC, Ben-Josef E, Wang L, Simeone DM (2010) In vivo bioluminescent imaging of irradiated orthotopic pancreatic cancer xenografts in nonobese diabetic-severe combined immunodeficient mice: a novel method for targeting and assaying efficacy of ionizing radiation. Transl Oncol 3:153–159
91. Korpanty G, Carbon JG, Grayburn PA, Fleming JB, Brekken RA (2007) Monitoring response to anticancer therapy by targeting microbubbles to tumor vasculature. Clin Cancer Res 13:323–330
92. Kim H, Folks KD, Guo L, Sellers JC, Fineberg NS et al (2011) Early therapy evaluation of combined cetuximab and irinotecan in orthotopic pancreatic tumor xenografts by dynamic contrast-enhanced magnetic resonance imaging. Mol Imaging 10:153–167
93. Flores LG, Bertolini S, Yeh HH, Young D, Mukhopadhyay U et al (2009) Detection of pancreatic carcinomas by imaging lactose-binding protein expression in peritumoral pancreas using [18F]fluoroethyl-deoxylactose PET/CT. PLoS One 4:e7977
94. Bouvet M, Yang M, Nardin S, Wang X, Jiang P et al (2000) Chronologically-specific metastatic targeting of human pancreatic tumors in orthotopic models. Clin Exp Metastasis 18:213–218
95. Capella G, Farre L, Villanueva A, Reyes G, Garcia C et al (1999) Orthotopic models of human pancreatic cancer. Ann N Y Acad Sci 880:103–109
96. Eibl G, Reber HA (2005) A xenograft nude mouse model for perineural invasion and recurrence in pancreatic cancer. Pancreas 31:258–262.

97. Koide N, Yamada T, Shibata R, Mori T, Fukuma M et al (2006) Establishment of perineural invasion models and analysis of gene expression revealed an invariant chain (CD74) as a possible molecule involved in perineural invasion in pancreatic cancer. Clin Cancer Res 12:2419–2426
98. Hibi T, Mori T, Fukuma M, Yamazaki K, Hashiguchi A et al (2009) Synuclein-gamma is closely involved in perineural invasion and distant metastasis in mouse models and is a novel prognostic factor in pancreatic cancer. Clin Cancer Res 15:2864–2871
99. Marchesi F, Piemonti L, Fedele G, Destro A, Roncalli M et al (2008) The chemokine receptor CX3CR1 is involved in the neural tropism and malignant behavior of pancreatic ductal adenocarcinoma. Cancer Res 68:9060–9069
100. Gil Z, Cavel O, Kelly K, Brader P, Rein A et al (2010) Paracrine regulation of pancreatic cancer cell invasion by peripheral nerves. J Natl Cancer Inst 102:107–118
101. Ceyhan GO, Demir IE, Altintas B, Rauch U, Thiel G et al (2008) Neural invasion in pancreatic cancer: a mutual tropism between neurons and cancer cells. Biochem Biophys Res Commun 374:442–447
102. Tang RF, Wang SX, Peng L, Zhang M, Li ZF et al (2006) Expression of vascular endothelial growth factors A and C in human pancreatic cancer. World J Gastroenterol 12:280–286
103. Esposito I, Menicagli M, Funel N, Bergmann F, Boggi U et al (2004) Inflammatory cells contribute to the generation of an angiogenic phenotype in pancreatic ductal adenocarcinoma. J Clin Pathol 57:630–636
104. Kurahara H, Takao S, Maemura K, Shinchi H, Natsugoe S et al (2004) Impact of vascular endothelial growth factor-C and -D expression in human pancreatic cancer: its relationship to lymph node metastasis. Clin Cancer Res 10:8413–8420
105. Tang RF, Itakura J, Aikawa T, Matsuda K, Fujii H et al (2001) Overexpression of lymphangiogenic growth factor VEGF-C in human pancreatic cancer. Pancreas 22:285–292
106. Schneider M, Buchler P, Giese N, Giese T, Wilting J et al (2006) Role of lymphangiogenesis and lymphangiogenic factors during pancreatic cancer progression and lymphatic spread. Int J Oncol 28:883–890
107. Koch M, Dettori D, Van Nuffelen A, Souffreau J, Marconcini L et al (2009) VEGF-D deficiency in mice does not affect embryonic or postnatal lymphangiogenesis but reduces lymphatic metastasis. J Pathol 219:356–364
108. Hoggan G, Hoggan FE (1881) On the lymphatics of the pancreas. J Anat Physiol 15:475–495
109. O'Morchoe CC (1997) Lymphatic system of the pancreas. Microsc Res Tech 37:456–477
110. Sipos B, Kojima M, Tiemann K, Klapper W, Kruse ML et al (2005) Lymphatic spread of ductal pancreatic adenocarcinoma is independent of lymphangiogenesis. J Pathol 207:301–312
111. Barnett CC Jr., Beck AW, Holloway SE, Kehler M, Schluterman MK et al (2010) Intravenous delivery of the plasma fraction of stored packed erythrocytes promotes pancreatic cancer growth in immunocompetent mice. Cancer 116:3862–3874
112. Taeger J, Moser C, Hellerbrand C, Mycielska ME, Glockzin G et al (2011) Targeting FGFR/PDGFR/VEGFR impairs tumor growth, angiogenesis, and metastasis by effects on tumor cells, endothelial cells, and pericytes in pancreatic cancer. Mol Cancer Ther 10:2157–2167
113. Oka M, Iwata C, Suzuki HI, Kiyono K, Morishita Y et al (2008) Inhibition of endogenous TGF-beta signaling enhances lymphangiogenesis. Blood 111:4571–4579
114. Schulz P, Scholz A, Rexin A, Hauff P, Schirner M et al (2008) Inducible re-expression of p16 in an orthotopic mouse model of pancreatic cancer inhibits lymphangiogenesis and lymphatic metastasis. Br J Cancer 99:110–117
115. Desgrosellier JS, Barnes LA, Shields DJ, Huang M, Lau SK et al (2009) An integrin alpha(v) beta(3)-c-Src oncogenic unit promotes anchorage-independence and tumor progression. Nat Med 15:1163–1169
116. Yang F, Hu J, Yang D, Long J, Luo G et al (2009) Pilot study of targeting magnetic carbon nanotubes to lymph nodes. Nanomedicine (Lond) 4:317–330
117. Fischer C, Jonckx B, Mazzone M, Zacchigna S, Loges S et al (2007) Anti-PlGF inhibits growth of VEGF(R)-inhibitor-resistant tumors without affecting healthy vessels. Cell 131:463–475

118. Lafreniere R, Rosenberg SA (1986) A novel approach to the generation and identification of experimental hepatic metastases in a murine model. J Natl Cancer Inst 76:309–322
119. Kimura Y, Kobari M, Yusa T, Sunamura M, Kimura M et al (1996) Establishment of an experimental liver metastasis model by intraportal injection of a newly derived human pancreatic cancer cell line (KLM-1). Int J Pancreatol 20:43–50
120. Marincola FM, Drucker BJ, Siao DY, Hough KL, Holder WD Jr. (1989) The nude mouse as a model for the study of human pancreatic cancer. J Surg Res 47:520–529
121. Melisi D, Ishiyama S, Sclabas GM, Fleming JB, Xia Q et al (2008) LY2109761, a novel transforming growth factor beta receptor type I and type II dual inhibitor, as a therapeutic approach to suppressing pancreatic cancer metastasis. Mol Cancer Ther 7:829–840
122. Roland CL, Harken AH, Sarr MG, Barnett CC Jr. (2007) ICAM-1 expression determines malignant potential of cancer. Surgery 141:705–707
123. Zheng L, Foley K, Huang L, Leubner A, Mo G et al (2011) Tyrosine 23 phosphorylation-dependent cell-surface localization of annexin A2 is required for invasion and metastases of pancreatic cancer. PLoS One 6:e19390
124. Jain A, Slansky JE, Matey LC, Allen HE, Pardoll DM et al (2003) Synergistic effect of a granulocyte-macrophage colony-stimulating factor-transduced tumor vaccine and systemic interleukin-2 in the treatment of murine colorectal cancer hepatic metastases. Ann Surg Oncol 10:810–820
125. Yoshimura K, Jain A, Allen HE, Laird LS, Chia CY et al (2006) Selective targeting of antitumor immune responses with engineered live-attenuated Listeria monocytogenes. Cancer Res 66:1096–1104
126. Suemizu H, Monnai M, Ohnishi Y, Ito M, Tamaoki N et al (2007) Identification of a key molecular regulator of liver metastasis in human pancreatic carcinoma using a novel quantitative model of metastasis in NOD/SCID/gammacnull (NOG) mice. Int J Oncol 31:741–751
127. Schwarz RE, McCarty TM, Peralta EA, Diamond DJ, Ellenhorn JD (1999) An orthotopic in vivo model of human pancreatic cancer. Surgery 126:562–567
128. Awasthi N, Yen PL, Schwarz MA, Schwarz RE (2011) The efficacy of a novel, dual PI3K/mTOR inhibitor NVP-BEZ235 to enhance chemotherapy and antiangiogenic response in pancreatic cancer. J Cell Biochem 113(3):784–791
129. Schulz P, Fischer C, Detjen KM, Rieke S, Hilfenhaus G et al (2011) Angiopoietin-2 drives lymphatic metastasis of pancreatic cancer. FASEB J 25:3325–3335
130. Awasthi N, Schwarz MA, Schwarz RE (2009) Proteasome inhibition enhances antitumour effects of gemcitabine in experimental pancreatic cancer. HPB (Oxford) 11:600–605
131. Konduri S, Schwarz MA, Cafasso D, Schwarz RE (2007) Androgen receptor blockade in experimental combination therapy of pancreatic cancer. J Surg Res 142:378–386
132. Scarlett CJ, Colvin EK, Pinese M, Chang DK, Morey AL et al (2011) Recruitment and activation of pancreatic stellate cells from the bone marrow in pancreatic cancer: a model of tumor-host interaction. PLoS One 6:e26088
133. Xu Z, Vonlaufen A, Phillips PA, Fiala-Beer E, Zhang X et al (2010) Role of pancreatic stellate cells in pancreatic cancer metastasis. Am J Pathol 177:2585–2596
134. Duner S, Lopatko Lindman J, Ansari D, Gundewar C, Andersson R (2010) Pancreatic cancer: the role of pancreatic stellate cells in tumor progression. Pancreatology 10:673–681
135. Ghaedi M, Soleimani M, Taghvaie NM, Sheikhfatollahi M, Azadmanesh K et al (2011) Mesenchymal stem cells as vehicles for targeted delivery of anti-angiogenic protein to solid tumors. J Gene Med 13:171–180.
136. Niess H, Bao Q, Conrad C, Zischek C, Notohamiprodjo M et al (2011) Selective targeting of genetically engineered mesenchymal stem cells to tumor stroma microenvironments using tissue-specific suicide gene expression suppresses growth of hepatocellular carcinoma. Ann Surg 254:767–775
137. Maitra A, Adsay NV, Argani P, Iacobuzio-Donahue C, De Marzo A et al (2003) Multicomponent analysis of the pancreatic adenocarcinoma progression model using a pancreatic intraepithelial neoplasia tissue microarray. Mod Pathol 16:902–912

Chapter 5
Brain Metastasis

Yvonne Kienast

Abstract Metastatic dissemination to the central nervous system (CNS) causes physical and cognitive impairments and limits the survival of cancer patients, particularly those with advanced melanoma, lung and breast cancer. As systemic therapies improve for other cancer types, relapse to the CNS is likely to rise as a sanctuary site presumably due to the inability of presently available drugs to cross the blood-brain barrier (BBB). Patients at risk would therefore benefit from the development of prevention and improved therapies. With this in mind, this chapter discusses preclinical approaches to study the biology, treatment or prevention of brain metastasis formation. Experimental imaging techniques for the study of brain metastasis formation are also reviewed. By integrating the information obtained from various modeling approaches, we hope to obtain a deeper level of understanding of the biology and molecular basis of CNS metastasis, and to uncover therapeutic vulnerabilities of this fatal disease.

Abbreviations

BBB	Blood-brain barrier
CCA	Common carotid artery
CNS	Central nervous system
EC	Endothelial cells
ECA	External carotid artery
HBMEC	Human brain microvascular endothelial cells
ICA	Internal carotid artery
MPLSM	Multi-photon laser-scanning microscopy
MRI	Magnetic resonance imaging
SRS	Stereotactic radiosurgery

Y. Kienast (✉)
Pharma Research and Early Development, Roche Diagnostics GmbH, Penzberg, Germany
e-mail: yvonne.kienast@roche.com

A. Malek (ed.), *Experimental Metastasis: Modeling and Analysis,*
DOI 10.1007/978-94-007-7835-1_5,

5.1 Introduction: The Biology of Brain Metastasis

Metastasis of various tumors to the brain is the most feared complication of systemic cancer and the most common intracranial tumor in adults, outnumbering primary brain tumors 10-fold [1]. Although the exact incidence and prevalence are unknown, brain metastasis has been reported to occur in about 10–40 % of patients with solid malignancies [2]. Common sources of central nervous system (CNS) metastasis include carcinomas of the lung, breast, and melanoma. Why metastases from these primary sites have an increased predilection for brain tissue is a matter of current research, but most likely depends on complex organotropic factors [3] as well as interactions with the brain endothelial cells and the basement membrane at the perivascular niche after vascular delivery of tumor cells [4–6]. Moreover, it is increasingly evident that, according to Paget's "seed-and soil" hypothesis postulated in 1889 [7], outgrowth of metastatic cancer cells depends on site-specific interactions with the unique microenvironment in the brain [8, 9]. In this respect, reactive astrocytes and microglia generate an altered neuroinflammatory brain microenvironment that is more permissive to tumor growth and invasion [8–10].

There are also significant differences between the tumor entities: Primary melanoma and lung tumors are more likely to produce multiple metastases, whereas solitary metastases are more commonly seen in patients with breast, colon, and renal cancer [11]. Moreover, latencies vary among different tumor types: small lung cancer patients exhibit metastatic lesions in the brain at the time of primary tumor diagnosis, for breast cancer patients brain metastases can stay dormant and occur years after diagnosis of the primary tumor. The exact molecular mechanism for this discrepancy remains elusive, though distinct tumor cell properties from different primary tumors as well as diverse growth and vascularization patterns [5] may account for this phenomenon.

Common sites of metastases are the gray-white junction and terminal watershed areas at the border zones between major intracranial arteries [2], likely due to the narrowing of blood vessels at these points. Lesions are located in the cerebrum (80–85 %), in the cerebellum (10–15 %), and in the brain stem (3–5 %). By definition, solitary brain metastases are distinguished from singular brain metastases: A solitary brain metastasis is defined as the only known metastasis of a tumor in the whole body located in the CNS, whereas a patient with a singular brain metastasis presents with additional metastases in other organ systems. In half of the cases, brain metastases are multiple at the time of diagnosis.

CNS metastases are a major cause of morbidity and mortality and are often indicated by symptoms including headache, seizure, loss of motory and sensory functions and cognitive decline largely affecting the quality of life [12]. The median survival of untreated patients is approximately 1 month [2], and a successful curative treatment of brain metastases is rare enough to be the subject of case reports [13]. More than half of patients with brain metastases die from systemic disease progression [1]. The current standard of care for brain metastases includes palliative care, whole-brain radiation therapy (WBRT), stereotactic radiosurgery (SRS),

neurosurgical resection, and systemic therapies such as chemotherapies and new approaches using biological agents (details are reviewed in [14]).

The brain is a highly vascularized organ. Interestingly, vascular density in experimental metastases is lower than in the normal brain [15, 16], with tumor vessels being highly dilated and tortuous [5, 17]. Co-option of the existing brain vasculature as an alternative mechanism of tumor vascularization and growth has been reported in several models [17, 18], and the role of neo-angiogenesis during tumor cell growth is a matter of debate [19–21]. In preclinical brain metastasis models, anti-angiogenic therapy was effective at blocking the angiogenic switch and induced prolonged dormancy; tumor cells were however able to switch to vessel co-option which may represent an alternative growth mechanism in vessel-dense organs such as the brain, resulting in sustained tumor progression despite anti-angiogenic treatments [5, 22]. As efficacy of anti-angiogenic therapies for brain metastases are already validated in clinical trials [23, 24], further translational preclinical models are needed to adequately recapitulate different vascularization mechanisms in the brain, also under the influence of therapy, in order to develop better opportunities for treatment or prevention of CNS metastasis.

The incidence of brain metastasis appears to be rising exemplified in the case of HER2-positive breast cancer patients treated with Herceptin [25–27]. Reasons may include better therapies for the systemic disease with longer survival of cancer patients and earlier and more accurate detection through modern neuro-imaging modalities [28]. In addition, it is well recognized that the brain is separated from the general circulation by the blood-brain barrier (BBB) and therefore may comprise a "sanctuary site" which is protected from therapeutic drugs such as chemotherapy and large biological agents such as therapeutic antibodies [28]. Therefore, one can expect brain metastases to become even more prevalent and clinically manifest in other cancer types as systemic therapy improves.

To meet the challenge of controlling brain metastases, novel experimental models and research tools have been developed. In this way, molecular risk factors of developing brain metastasis have been identified in the gene signature [3, 29]. In primary non-small-cell lung carcinoma, the expression levels of three genes (*CDH2*, *KIFC1*, and *FALZ*) showed prognostic value, identifying patients who may benefit from prophylactic therapy to the central nervous system [29]. Neural Cadherin (CDH2) may mediate the endurance of brain metastases through interactions with the neuronal parenchyma, and *KIFC1* is a mitotic spindle checkpoint gene [29]. Interestingly, the neuronal transcription factor *FALZ* (a chromatin remodeling protein sensing methylated H3K4 chromatin marks) was found to be a negative predictor of brain metastasis [29]. Bos et al. isolated cells that preferentially infiltrate the brain from patients with advanced disease. Gene expression analysis of these cells and of clinical samples, coupled with functional analysis, identified the cyclooxygenase COX2 (also known as PTGS2), the epidermal growth factor receptor (EGFR) ligand HBEGF, and the α-2.6-sialyltransferase ST6GALNAC5 as mediators of cancer cell passage through the blood-brain barrier [3]. Additionally, TGFβ2 [30], FOXC1 [31], LEF1 and XOXB9 [32], Stat3 [33], and activation of notch signaling [34], were identified as a molecular determinants for site-specific

tumor metastasis in the brain. Expression of the integrin $\alpha_v\beta_3$ on tumor cells was associated with increased metastatic potential to the brain and promotion of angiogenesis [6]. Another important risk factor for the development of brain metastasis is the expression of HER2 in breast cancer [35] while being estrogen receptor-negative (ER), young of age and showing lymph node-positive disease [36]. Triple negative breast cancer (ER-, PR-, HER2 unamplified) is also associated with a high rate of CNS involvement after recurrence [37]. Gene expression analysis of laser-captured epithelial cells from resected human brain metastases of breast cancer patients revealed high HK2 (Hexokinase 2) expression to be significantly associated with poor patient survival after craniotomy [38]. HK2 plays a key step in glucose metabolism and apoptosis [39]. Chemokines have been reported to contribute to breast cancer metastasis and may contribute to organ specificity [40]. A ligand of the CXCR4 chemokine receptor, SDF-1α (stromal cell-derived factor 1α, also known as CXCL12), has been reported to be expressed in the brain [41].

Despite this recent scientific progress in identifying molecular determinants mediating brain metastasis, this has not yet changed the therapy of patients. However, with an increase of advanced preclinical models of CNS metastasis, our understanding of cerebral metastasis will further expand and provide valuable targets for treatment or prevention of this difficult clinical problem.

5.2 Preclinical Brain Metastasis Models and Assay Systems

Preclinical brain metastasis models and assay systems help us to study the biology and treatment of CNS metastasis. Brain metastasis models fall into different categories: *in vitro*, *ex vivo*, and experimental or spontaneous *in vivo* models. The principle mechanism and application to therapeutic treatment regiments are further discussed.

5.2.1 In Vitro Metastasis Models

5.2.1.1 Blood-Brain Barrier Transmigration Assay

The brain tissue is protected by the blood-brain barrier (BBB) consisting of endothelial cells (EC) linked by continuous tight junctions, pericytes, a basement membrane and the feet of astrocytes. BBB traversal (the process of extravasation by transendothelial cell migration) by tumor cells can be studied *in vitro* by measuring the ability of tumor cells to invade through a monolayer of human brain microvascular endothelial cells (HBMEC) growing on 3 μm pore tissue culture transwell inserts [42] that can also be co-cultured with primary astrocytes [3, 43]. In this way, a tight barrier that expresses brain endothelial markers and lacks permeability to albumin

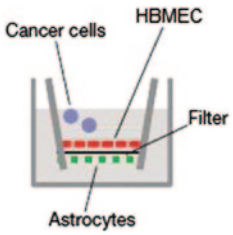

Fig. 5.1 Schematic of the in vitro blood-brain barrier transmigration assay, adapted from [3]. *In vitro* BBB transmigration activity of tumor cells can be measured by co-culturing HBMEC (human brain microvascular endothelial cells) and astrocytes on opposite sides of a polylysine-treated, gelatin-coated tissue culture transwell insert [43]. Immunostained endothelial cells and fluorescently labeled tumor cells can be visualized by microscopy

is generated. This model allows investigation of cancer cell passage through the BBB and therefore helps to gain a molecular understanding of tumor cell extravasation to the brain, genes mediating infiltration into the brain, and treatment options that can interfere with this process (Fig. 5.1). Protocol of the procedure is taken from the references [3, 43].

- To establish the culture model, astrocytes are seeded onto the underside of a gelatin-coated culture insert (1×10^5 cells/insert) with 3-µm pores (3-µm pore PET tissue culture inserts, Fisher).
- Brain microvascular endothelial cells (HBMEC) are then seeded on the upperside of the tissue culture inserts (1.6×10^4 cells/insert). Inserts are immersed in tissue culture wells containing medium M199, 10% heat-inactivated newborn calf serum, and endothelial cell growth factor. HBMEC are grown to confluence for 72 h.
- Cultures are examined microscopically to assess monolayer integrity. Tightness of the barriers is tested by permeability to serum albumin.
- For transmigration assays, cancer cells (50.000 cells, labeled with 5 µM CFMDA cell tracker green, Invitrogen) are added to the top chamber of the insert and incubated for 14–18 h.
- Inserts are washed with PBS and fixed with 4% PFA, inserted and mounted on microscope slides, immunostained and visualized by microscopy. Alternatively, cells in the bottom chamber are collected and analyzed by FACS.

5.2.1.2 Tumor-Vessel Adhesion and Interaction Assay

Since metastatic tumor cells attach closely to brain endothelial cells and can grow around pre-existing co-opted brain vessels in the perivascular niche [5], the vascular basement membrane microenvironment is thought to serve as “soil” for brain metastasis [17]. Adhesion of tumor cells on components of the vascular basement membrane (such as collagen I, collagen IV, fibronectin, laminin or vitronectin) can

be measured *in vitro* to study anchorage-dependent signaling. In this way, therapeutic manipulation of the perivascular niche can be studied with the aim to interfere with survival and proliferation abilities of the tumor cells.

- Tumor cells are plated on collagen I, collagen IV, fibronectin, laminin, vitronectin, or BSA-coated control wells (BD BioCoat) in the absence of serum.
- Cellular proliferation can be measured at 48 h by BrdU incorporation ELISA or cells lysates can be analyzed for pathway signaling (pFAK-Y397, pERK1/2) by Western Blot.
- Incubation of tumor cells with inhibitory antibodies allows to monitor interference with anchorage-dependent signaling, proliferation and survival abilities of tumor cells

5.2.1.3 Microenvironmental Interaction Assay

In soft agar colonization assays, mixed populations of glial cells, fibroblasts, astrocytes and other stromal cells composing the brain microenvironment, can be co-cultured with tumor cells to monitor anchorage-independent growth of cancer cell lines. This can be correlated with their ability to form metastases facilitated by brain microenvironmental factors *in vivo* [9].

- Ten thousand metastatic cells are plated in 2 ml of DMEM + 10 % FBS, with the addition of 0.3 % (w/v) Bactoagar, over a 2 ml layer of 0.7 % bottom agar.
- For co-culture experiments, 20.000 mixed glial cells, or 20.000 MRC5 lung fibroblast cells, are added to the 2 ml top agar.
- After 14 days in culture, colonies (> 50 μm diameter) are counted under low magnification using an inverted microscope and images are captured.

5.2.2 Ex Vivo Tumor Invasion and Vascularization Assay

In an *ex vivo* organotypic brain culture assay of vascular tumor cell invasion, tumor cells or spheroids are plated onto live, acutely isolated or slide-mounted snap frozen adult mouse brain slices at the junction between the deep cortical layers and the striatum [17, 44]. Co-optive tumor cell invasion in a finger-like fashion can be monitored using time lapse microscopy. This organotypic brain culture system can provide a valuable tool in the *ex vivo* study of co-option in the brain and offers the opportunity to monitor interference with modes of vascularization different from sprouting angiogenesis (Fig. 5.2). Protocol is taken from [44].

- Acutely isolated coronal brain slices (300 μm) are collected in chilled physiological saline with a vibratome
- 5×10^3 tumor cells (non-fluorescent tumor cells can be labeled with 5 μM CFM-DA cell tracker green, Invitrogen) are plated upon each brain slice and co-cultured at 37 °C for 2 hours before fixation in 4 % paraformaldehyde.

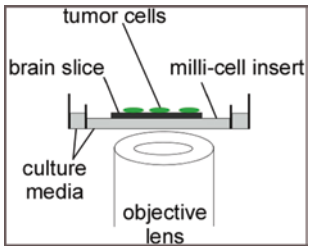

Fig. 5.2 Schematic of the ex *vivo* tumor invasion and vascularization assay. Tumor cells are plated onto live, acutely isolated adult mouse brain slices. Invasion can be monitored by time lapse microscopy

- Vessels are visualized by vital labeling with 10 µg/ml GS-IB4 isolectin conjugated to either Alexa 488 or 568 (Invitrogen) for 1 hour prior to co-culture
- Confocal recording is performed for 1–4 h in selected regions.

5.2.3 Experimental in Vivo Brain Metastasis Models

In vivo analysis of the brain metastatic process can be achieved by experimental hematogenous delivery of tumor cells. This artificial route of delivery does not allow the investigation of initial steps in the process leading to brain metastasis (such as local tissue invasion or intravasation), but can be used to effectively study the biology and treatment of early CNS lesions as well as established brain metastases [45, 46]. Tumor cell lines can be injected into the general circulation (intracardiac or intravenous injection) or directly upstream of the brain (intracarotid injection) to achieve hematogenous delivery. When cells are administered intravenously, the first bed they encounter is the pulmonary vascular bed. Lung metastases arising from this administration route hamper the specific study of brain metastases. While intracardiac injection into the left ventricle allows circumvention of the lungs, tumor cells are disseminated to other visceral sites through the arterial circulation. Cell lines with a special organotropism for the brain (see paragraph 3.2.4) offer the opportunity to selectively induce brain metastases by relative simplicity of the intracardiac injection technique.

5.2.3.1 Intracarotid Tumor Cell Delivery

Injection of tumor cells into the carotid artery is technically challenging and requires microsurgical skill and the use of a dissecting microscope. Even with extensive practice, a limitation of this technique is the number of animals that can be inoculated at one time. Furthermore, during the first days after inoculation, some animals may die of stroke. The technique involves permanent ligation of the common and external carotid arteries after tumor cell inoculation (Fig. 5.3). Collateral circulation through the circle of Willis sufficiently provides blood to the murine brain. Details of procedure are described in following protocol.

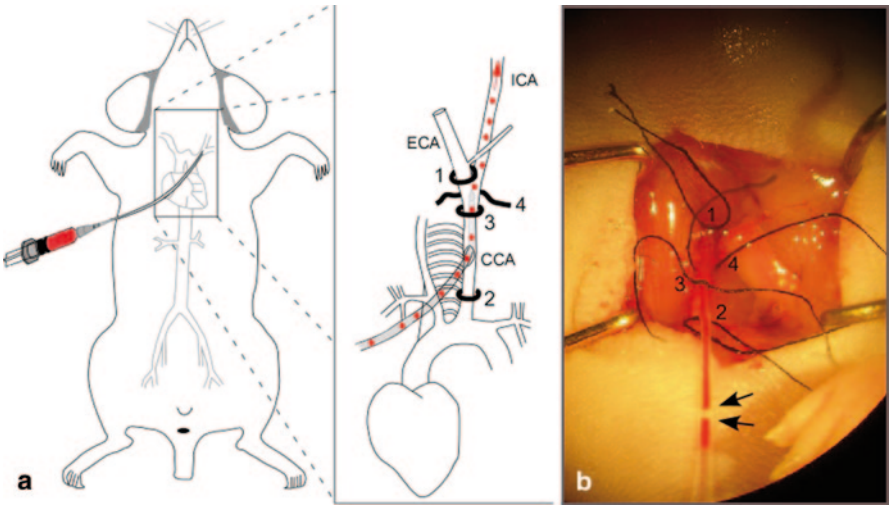

Fig. 5.3 Intracarotid tumor cell delivery. **a** Schematic diagram of intracarotid tumor cell delivery. The technique involves permanent ligation of the common and external carotid arteries after tumor cell inoculation and allows for efficient transport of tumor cells to the brain. **b** Photograph of a carotid artery preparation prior to tumor cell delivery. Ligatures *1–4* are visible. A cannula is inserted into the CCA and fixated with ligature 3. Note blood backflow in the cannula tubing (*arrows*) after removal of the microclamp

- The mouse is placed on the back and the head is stabilized. A longitudinal incision is made on the neck.
- Muscles are bluntly separated to expose the carotid sheath. The common (CCA), internal (ICA), and external (ECA) carotid arteries are dissected and separated from the vagal nerve and carotid vein.
- A 4-0 silk suture is placed under the ECA (1; see Fig. 5.3) and under the proximal part of the CCA (2; see Fig. 5.3) and tied tightly. Additionally, two further ligatures are placed under the common carotid artery distal to the expected injection site and tied loosely (3 and 4; see Fig. 5.3).
- A microclamp is used to clamp the CCA distal to the expected injection site before the CCA is nicked with a pair of microscissors and a cannula is inserted and fixated with ligature 3 (Fig. 5.3).
- Tumor cells are slowly delivered via a syringe connected to the cannula punctured upward into the CCA. After tumor cell injection, ligature 4 (Fig. 5.3) is tightened.
- The skin is closed with wound autoclips.

Artificial hematogenous delivery of tumor cells has been used to study selected steps of the multi-step process of metastasis formation in the brain, including arrest of tumor cells in brain capillaries, extravasation, and successful colonization of the brain [47].

5.2.3.2 Intracranial Metastasis Model

Alternatively to methods described above, tumor cells from tumor entities that are known to metastasize into the brain (e.g. lung, breast and melanoma) can be injected directly into the brain to monitor growth and angiogenesis of established metastasis [48]. Reproducibility of tumor cell inoculation in the brain can be achieved by using stereotactic guidance (Fig. 5.4).

- After disinfection of the skin, a small midline scalp incision using microsurgical tools is performed. Soft tissue attached to the skull is removed with fine forceps (Fig. 5.4a, b).
- A high-speed micro-drill is used to puncture the skull, thereby creating an opening for the injection of tumor cells (Fig. 5.4c).
- A syringe is loaded with the tumor cell suspension, while being careful to avoid creating air bubbles and is inserted into the brain by stereotactic guidance (Fig. 5.4d, e).
- Upon completing injection, the needle is left in place for another minute and is then slowly withdrawn to reduce tumor cell reflux. The skull opening is sealed with a thin layer of cyanoacrylate glue (Fig. 5.4f).
- A small animal stereotactic frame promotes consistent injection location of tumor cells (Fig. 5.4g). The coordinates for injection of tumor cells can vary according to the desired site for metastasis establishment. Common neuroanatomical locations include intracerebral injections [49].

5.2.3.3 Spontaneous in *Vivo* Brain Metastasis Models

Spontaneous mouse models of brain metastases that arise from a primary tumor are less frequent compared to experimental metastasis assays despite their high clinical relevance. They recapitulate the natural multi-step process of cell dissemination up to the formation of brain metastasis including local invasion of tumor cells from a primary tumor, intravasation into the blood vessels or lymphatics, survival in the circulation, arrest of tumor cells in brain capillaries, extravasation, and successful colonization of the brain. A complication of spontaneous brain metastasis assays is the uneven appearance of spontaneous metastases, which however mirrors the complexity of the metastatic cascade and reflects the heterogeneity observed in the clinic. Difficulties can be challenged by using a substantial number of mice per group. Careful and thorough planning of randomization into treatment groups is also needed; experiments are expensive and can be time-consuming. While there is a growing number of genetically modified mouse models that spontaneously develop tumors in specific tissues that frequently metastasize to other organs, there is currently no suitable genetically modified mouse model available for brain metastasis [50]. Spontaneous *in vivo* brain metastasis assays therefore require transplantation of the primary tumor. In this way, spontaneous metastatic spread to the CNS has been reported for a variety of cell lines after orthotopic transplantation of the primary tumor [51–53]. Additionally, tumor cell

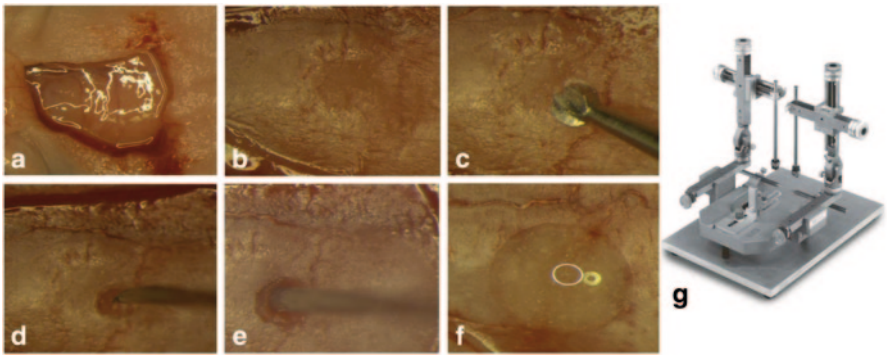

Fig. 5.4 Intracranial metastasis tumor model. Schematic diagram of intracranial stereotactic tumor cell injection. The intracranial metastasis model can be applied to study growth and angiogenesis of large, established brain metastatic lesions

sub-lines (brain metastatic variants) can be derived with a tropism to and for growth in the brain to increase and confine tumor cell dissemination to the CNS. In this respect, brain metastases resulting from tumor cell line injections can be harvested and subjected to multiple rounds of re-injection and harvesting resulting in an incidence of brain metastases in about 50 % [3, 54] or 80 % [55] of the mice. By this approach, CNS site-specific metastatic pathways can be identified by comparison of gene expression profiles of brain-tropic and parental cell lines [3]. *In vivo* recycling of a human melanoma cell line WM239A let to the establishment of a spontaneous melanoma brain metastasis model by orthotopic implantation and subsequent resection of the primary tumor, nicely reflecting the adjuvant setting [54]. Accordingly, breast cancer brain metastasis models also employ this strategy with human breast cancer cells MDA-MB-231BR that preferentially metastasize to the brain [56], which can be orthotopically injected into the fat pad. In this way, preclinical trail designs can be conducted to study differences in responsiveness of primary tumor and brain metastases to therapies in the adjuvant or neoadjuvant setting. Interestingly, spontaneous metastasis models allow for biochemical characterization of primary tumor and brain metastases. In this way, brain metastases and primary tumor can be harvested and gene and protein expression changes can be studied in matched samples.

5.3 Visualization and Quantification of Experimental Brain Metastases

Modeling CNS metastasis in mice requires assessment and analysis of the metastatic disease burden. Even though surrogate markers of tumor response, such as duration of survival or time to symptom onset can be monitored, the visualization and

Table 5.1 Imaging brain metastases in preclinical models: advantages and disadvantages

Imaging technique	Advantage	Disadvantage	Reference
Immunohistochemistry Confocal imaging	Practicability and feasibility	Non-repetitive, single time point *ex vivo* imaging at necropsy	[9, 42, 47, 86]
Magnetic resonance imaging	Repetitive *in vivo* imaging Whole brain imaging	Low resolution	[61]
Multiphoton (MPLSM)	Intravital, repetitive *in vivo* imaging of brain metastasis kinetics	Visualization of metastases restricted to cortical regions in up to 1 mm depths through a small cranial window	[5, 17]
	Microscopic resolution	Technically demanding	
Ultramicroscopy	Whole brain imaging Microscopic resolution	Non-repetitive, single time point *ex vivo* imaging at necropsy	[57]
Bioluminescence	Repetitive *in vivo* imaging in high throughput Whole brain imaging	Low resolution	[8, 48, 64]

quantification of brain metastasis formation is an indispensible component of any brain metastasis model system. Because intracranial metastasis growth cannot be measured through direct measurement, such as by use of calipers, many new brain imaging techniques have been developed in the last decades that can be employed to study the biology of brain metastasis formation and the response to therapy in a 3D environment.

The application and combination of novel and established imaging technologies should provide novel insights into brain metastasis development and response to therapies (Table 5.1).

5.3.1 Post Mortem Analysis

Standard histological sections and confocal imaging of the brain provide a valuable tool to study tumor cells in the brain parenchyma in high resolution, however 3D reconstructions are very laborious and hard to obtain. *Ex vivo* imaging by ultramicroscopy has not yet been used for brain tumor imaging but also has the potential to observe macroscopic specimens like whole brains with microscopic resolution [57]. Quantitative PCR-based methods might be applied to estimate precisely mice brain colonization by xenograft cancer cells [58, 59].

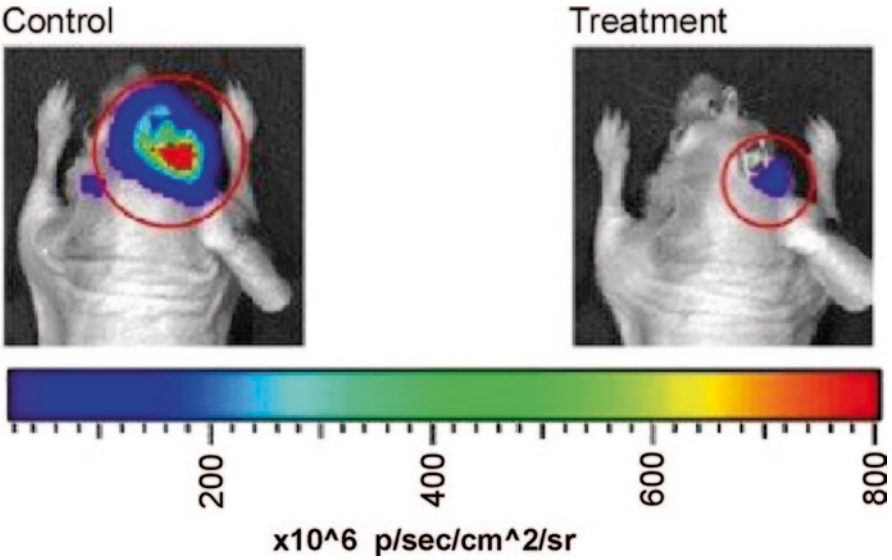

Fig. 5.5 Bioluminescence imaging. Non-invasive, high-throughput imaging of brain metastasis in mice using bioluminescence imaging. Heat map image representations show bioluminescence intensity for representative mice from control (*left*) and treatment (*right*) groups of a therapy response experiment

5.3.2 Intravital Non-Invasive Imaging Techniques

On a macroscopic scale, preclinical magnetic resonance imaging (MRI) allows for repetitive whole brain imaging but cannot resolve individual cells in high resolution [60], even though the sensitivity can be enhanced up to single cell detection capacity [61]. Quality of MRI can be further increased by specific labeling of cancer cells with ferumoxides–protamine sulfate [62], application of contrast-enhanced MRI approaches or combination with proton magnetic resonance spectroscopy H^1-MRS [63].

Bioluminescence imaging (Fig. 5.5) has been used for macroscopic brain tumor imaging [64] and can be employed to monitor metastasis evolution in the brain repetitively and non-invasively and to detect spontaneous or experimental metastases even at early stages of development [8, 48]. In additional to bioluminescent imaging, using cancer cells stably secreting Gaussia luciferase (Gluc) allows monitoring of metastases development by means of assessment of Gluc activity in the blood and urine (46). Rapid screening of multiple animals at a time and quantification of the signal obtained increases the potential for the use of bioluminescence imaging in preclinical trials.

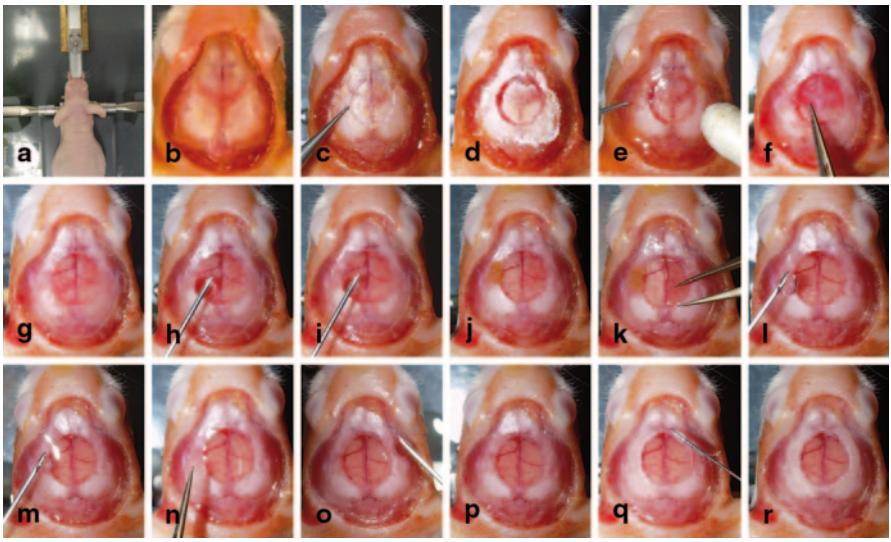

Fig. 5.6 Preparation of a cranial window. Serial images illustrating the preparation of a cranial window. The cranial window preparation, combined with the use of two-photon microscopy, is a very powerful tool to follow brain metastasis in real-time

5.3.3 Intravital Laser Scanning Multiphoton Microscopy (MPLSM)

On a microscopic scale, intravital multiphoton laser scanning microscopy (MPLSM) with a tissue penetration depths of 1 mm has begun to detail the process of brain colonization and interaction between tumor cells and the perivascular niche by repetitive imaging [5]. The ability to observe metastasis as a process rather than simply an end point using intravital multiphoton laser scanning microscopy has provided new insights into brain metastasis formation and represents a novel opportunity to experimentally address unanswered questions of metastasis research. Relevant techniques that are required for intravital imaging (e.g. preparation of a cranial window; *in vivo* microscopy) are further discussed.

Preparation of cranial window Multiphoton imaging of brain metastases requires the preparation of a cranial window. In this respect, craniectomies need to be performed that are closed by cover slips and cyanoacrylate glue (Fig. 5.6). Preparation steps that are described below were carried out using a dissecting microscope.

- The head of the mouse is stabilized by using a stereotactic mouse head holder including ear bars. To avoid drying-up, lotion can be used to cover the eyes of the mouse (Fig. 5.6a).
- After disinfection of the skin, a midline scalp incision using microsurgical tools is performed. Incision should extend approximately from the neck region to

the frontal area. Soft tissue attached to the skull is removed with fine forceps (Fig. 5.6b).

- A high-speed micro-drill (left side of the picture) is used to thin a circular area of skull (~6 mm in diameter) over the region of interest. Drilling should be done intermittently to minimize heat induced tissue injury (Fig. 5.6c).
- Drilling chips are washed away with sterile sodium chloride which is absorbed using cotton pads (Fig. 5.6d, e; right side of **e**).
- Craniectomy is performed (Fig. 5.6f). The island of bone within the drilled circle is lifted up with great caution using a pair of sharp forceps uncovering the open-skull region (Fig. 5.6g).
- Immediately after removing the 6 × 6 mm region of the skull, the brain surface is covered with sodium chloride to avoid drying-up (Fig. 5.6h, i).
- Removal of dura. The dura is punctured using a pair of sharp forceps and then carefully detached without affecting the superior sagittal sinus. Bleeding may occur but can be controlled by applying a sterile collagen sponge **(**Fig. 5.6, left side of **J** and **K**) with slight pressure. Cortex is rinsed with sterile sodium chloride throughout the preparation (Fig. 5.6j, k, l, m).
- A custom-made circular cover slip (6 mm diameter) is gently lowered to the open-skull region and sealed at the edge of the optical window with a thin layer of cyanoacrylate glue (Fig. 5.6n, o, p, q, r).

The cranial window technique allows to serially revisiting the same brain areas through the cranial window for up to months by using a coordinate-reading microscope, as well as using vascular pattern and unique branch points of the cortical vasculature as landmarks. Fluorescently labeled tumor cells can be administered intracarotidally to allow for efficient transport of tumor cells to the brain. Spontaneous brain metastasis models with a strong tropism to the brain can also be employed.

Intravital imaging using multiphoton microscopy Multiphoton imaging is now a well-established technique that can be used for high-resolution imaging by low photon toxicity in living animals [65]. Two-photon microscopy relies on the principle of simultaneous absorption; that is, two low-energy photons, when combined, provide sufficient energy to excite the fluorochrome [66]. In practice, two-photon excitation is generated by focusing a single pulsed laser through the microscope optics. As the laser beam is focused, the photons become more crowded (their spatial density increases), and the probability of two of them interacting simultaneously with a single fluorophore increases. The laser focal point is the only location along the optical path where the photons are crowded enough to generate significant occurrence of two-photon excitation. The capability to collect images up to 1 mm into biological living tissues provides an invaluable tool for studying cellular and subcellular processes in the context of tissues and organs in living animals. A typical multiphoton microscopy setup is shown in Fig. 5.7. The procedure is described in following protocol:

- Animals are secured in a mouse head holder and situated on the microscope stage.

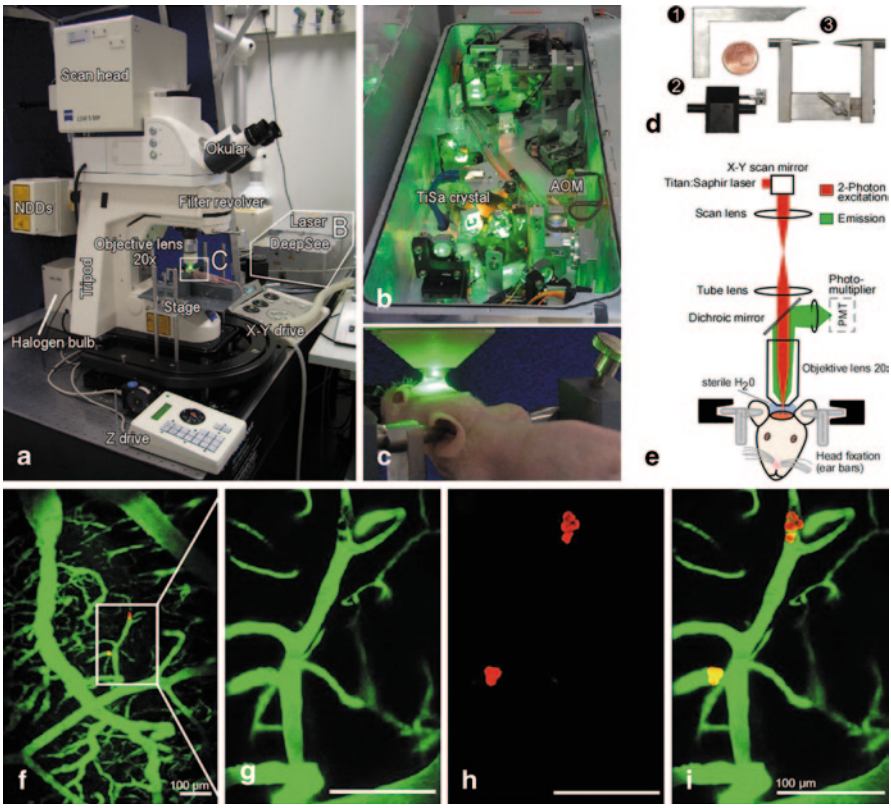

Fig. 5.7 Setup for multiphoton microscopy. A typical multiphoton microscopy setup consists of an upright laser scanning microscope **a** equipped with a two-photon laser **b** for *in vivo* MPLSM. For fluorescence detection two non-descanned detectors (NDDs) are used. **c** A custom-made microscopy stage contains an integrated stereotactic mouse head holder including ear bars and is used to prevent breathing artifacts during imaging and to allow for repeated positioning. **d** Head immobilization instruments including (1) teeth holder, (2) anesthesia mask, and (3) ear bars. **e** The excitation light is mirrored into the microscopical light path via mobile scan mirrors that produce a xy-movement of the light spot in the image plane and thereby scan the sample. Imaging is done by using a 20x water-immersion objective. Fluorescence is detected by photomultiplier tubes (PMT). **f–i** Visualization of fluorescently labeled tumor cells (*red*) adjacent to cerebral vessels (*green*). AOM, acousto-optic modulator

- Temperature is maintained at ~37 °C with a ventral heat pad (Harvard Apparatus).
- Images are acquired with a 10 or 40x aqueous immersion lens (Leica) to a depth of up to ~500 µm in the cortex.
- To visualize cerebral vessels, 100 µl of 10 mg ml^{-1} solution of FITC-labeled dextran (2M molecular weight, green) is injected into the tail vein of the mouse.
- Identical recording fields between sessions are identified by vascular anatomy and co-registry of the head holding device with the microscope stage.
- For image analysis of either single image stacks or 3-dimensional reconstructions appropriate software (e.g. AxioVision Rel. 4.6 software, Zeiss) can be used.

Intravital video microscopy can be used to follow dynamic processes such as tumor cell arrest, extravasation or interaction with the tumor microenvironment in real-time. In this respect, multiphoton microscopy was used to monitor live tumor cells in the brain for many weeks after hematogenous implantation into the carotid artery, thus revealing the vascular remodeling processes during early and late-stage tumor cell colonization [5]. In addition to capturing the live tumor cell extravasation through the BBB using intravital video microscopy, comparison of lung cancer and melanoma cells suggested that the divergent pathways of either co-opted microvascular remodeling or angiogenic growth account for different modes of tumor cell vascularization in the brain. It was furthermore possible to differentiate between dormant, regressing and proliferating (single) cells [5]. Future studies should aim at elucidating the molecular mechanisms underlying these tumor-vessel interactions to facilitate drug development for interference with the perivascular niche of tumor cells.

Interestingly, *in vivo* microscopy could also be used to study the prophylactic effects of VEGF-A (Vascular endothelial growth factor) blockade on the outgrowth of individual metastasizing lung cancer cells in the mouse brain [5]. One experimental group received the anti-VEGF-A antibody Avastin (Bevacizumab) just after tumor cell inoculation into the internal carotid artery. Avastin prevented early angiogenic events of micrometastases, and thereby induced prolonged dormancy of micrometastatic tumors (maximum 10 cells), which however switched to vessel co-option as an potential alternative growth mechanism in the brain [5, 14]. Effects on any other essential steps of the metastatic cascade (initial arrest at vascular branch points; early extravasation; perivascular position with close physical contact to a brain microvessel) were not observed. Avastin had no effect on the metastatic colonization of melanoma cells in the brain, which showed a non-angiogenic growth pattern under normal conditions. Further preclinical studies are required to determine how discontinued vs. prolonged inhibition of VEGF, and combination with other treatment modalities, influences the establishment and growth of micrometastatic disease.

After infiltration into the brain tissue, metastatic cells were reported to take advantage of unique properties of the brain microenvironment including microglia (the resident macrophages in the brain) and astrocytes [8, 9]. Real-time imaging offers the opportunity to study those interactions in real-time by using transgenic animals. These studies will support the development of novel strategies to target the unique microenvironment of brain metastasis.

5.4 Conclusion and Perspectives

Brain metastases cause progressive neurological deficits and symptoms of increased intracranial pressure that quickly deteriorate quality of life and limit the survival of cancer patients.

Advanced preclinical models of brain metastasis have made considerable progress in recent years to better understand spread to the CNS and brain colonization.

However, continuous progress in basic and translational science is urgently needed to develop novel treatment approaches that will turn this dismal diagnosis into a more manageable, maybe chronic disease.

Drug development should be aimed at improving the current standard of care (WBRT and SRS) while alleviating cognitive losses. In this regard, novel preclinical models covering aspects of radiation resistance of brain metastases and cognitive dysfunction are still needed. A proportion of patients receiving radiation therapy suffer from progressive, permanent cognitive impairment [67, 68]. New models analyzing cognitive dysfunction [69] are of great importance to study the preservation of cognition by radioprotectors [69–71]. Furthermore, testing of radiation sensitizing agents that increase the lethal effects of radiation without causing additional damage to normal tissue [72, 73] is needed in relevant brain metastatic models.

Further overall goals for future research include the development of treatment paradigms for established brain metastases or prevention strategies. An emphasis on research regarding the prevention of brain metastasis by prophylactic treatment is of considerable interest, as it is an appealing alternative to prevent the disease rather than to treat an already established metastasis. In fact, preclinical [5, 74, 75] and limited retrospective clinical data [24] also support the hypothesis that prevention of brain metastasis is more achievable than shrinkage of an established lesion. In a prevention scenario, a brain-permeable drug could potentially reach and control outgrowth of a more limited number of micrometastatic tumor cells compared to large established lesions. This underlies the need to identify patients at the highest risk of developing brain metastases as has already begun to be achieved by using a number of brain metastatic models [3, 29, 32, 76]. It is expected that continued mechanistic insight provided by preclinical models will identify additional druggable targets and reveal pathway signatures for CNS metastasis. The potential promise of a prevention setting also underscores the impact of strategies to circumvent the BBB. As a shielded “sanctuary site”, the brain harbors micrometastatic deposit that is protected from therapeutic drugs such as chemotherapy and large biological agents such as therapeutic antibodies [28]. Circumvention of the BBB can be achieved by physical and local disruption [77, 78], design of drugs that can be shuttled across the BBB using receptors that are naturally expressed on endothelial cells (EC) of the BBB [79–82] or by using drugs that are naturally brain-permeable [74, 75, 83–85].

It is increasingly evident that the unique brain tumor microenvironment, consisting of the perivascular niche and the inflamed neural brain parenchyma, plays a key role in the metastatic growth process, as well as in resistance to anti-tumor therapies. It is expected that this active tumor-host dynamic will stimulate further research regarding the unique brain tumor microenvironment as a key target for brain metastasis therapy.

Future drug development can attack the problem of brain metastasis by identifying meaningful targets for molecular therapeutic approaches, selecting optimal drugs and drug combinations, validating brain-permeable inhibitors, and rigorously evaluating existing, and inventing novel, preclinical models for a better understand-

ing of brain metastasis formation and drug responses. Hopefully in the future, the combination of advanced functional neuro-imaging and gene-expression profiling techniques will enable us to better identify the subgroup of patients who are at greatest risk for developing distant brain metastases and to personalize treatment of this devastating disease. Currently the following area of the brain metastasis research may be considered as critical:

- Establishment of novel preclinical models for brain metastasis formation that identify drugs as prevention or treatment agents: testing of agents given just after tumor cell inoculation as well as after micrometastases or large metastases have formed
- Molecular profiling of tumors and their brain-specific metastases to identify critical pathways mediating brain metastasis formation
- Identification of the most critical steps of brain metastasis formation, and of the steps that are the easiest to inhibit
- Determination of the influence of the brain microenvironment on metastasis
- Effective anticancer strategies for the brain as a "sanctuary site", identifying new molecular therapeutics that can cross the BBB
- Assays to detect and methods to improve drug accumulation in the CNS
- Prophylactic strategies for treatment of single dormant cells, or micrometastatic disease to prevent clinically relevant CNS metastases
- Identification and testing of radiation sensitizing agents that can enhance the results of radiation therapy ("Gamma knife" and WBRT)
- Behavioral tools for measuring long-term neurocognitive defects caused by different therapies

References

1. Patchell RA (2003) The management of brain metastases. Cancer Treat Rev 29(6):533–540
2. Gavrilovic IT, Posner JB (2005) Brain metastases: epidemiology and pathophysiology. J Neurooncol 75(1):5–14
3. Bos PD, Zhang XH, Nadal C, Shu W, Gomis RR, Nguyen DX, Minn AJ, van de Vijver MJ, Gerald WL, Foekens JA, Massague J (2009) Genes that mediate breast cancer metastasis to the brain. Nature459(7249):1005–1009
4. Chambers AF, Groom AC, MacDonald IC (2002) Dissemination and growth of cancer cells in metastatic sites. Nat Rev Cancer 2(8):563–572
5. Kienast Y, von Baumgarten L, Fuhrmann M, Klinkert WE, Goldbrunner R, Herms J, Winkler F (2010) Real-time imaging reveals the single steps of brain metastasis formation. Nat Med 16(1):116–122
6. Lorger M, Krueger JS, O'Neal M, Staflin K, Felding-Habermann B (2009) Activation of tumor cell integrin alphavbeta3 controls angiogenesis and metastatic growth in the brain. Proc Natl Acad Sci USA 106(26):10666–10671
7. Paget S (1889) The distribution of secondary growths in cancer of the breast. 1889. Cancer Metastasis Rev 8(2):98–101
8. Lorger M, Felding-Habermann B (2010) Capturing changes in the brain microenvironment during initial steps of breast cancer brain metastasis. Am J Pathol 176(6):2958–2971

9. Fitzgerald DP, Palmieri D, Hua E, Hargrave E, Herring JM, Qian Y, Vega-Valle E, Weil RJ, Stark AM, Vortmeyer AO, Steeg PS (2008) Reactive glia are recruited by highly proliferative brain metastases of breast cancer and promote tumor cell colonization. Clin Exp Metastasis 25(7):799–810
10. Zhang M, Olsson Y (1995) Reactions of astrocytes and microglial cells around hematogenous metastases of the human brain. Expression of endothelin-like immunoreactivity in reactive astrocytes and activation of microglial cells. J Neurol Sci 134(1–2):26–32
11. Patel RR, Mehta MP (2007) Targeted therapy for brain metastases: improving the therapeutic ratio. Clin Cancer Res 13(6):1675–1683
12. Chamberlain MC (2010) Brain metastases: a medical neuro-oncology perspective. Expert Rev Neurother 10(4):563–573
13. Takeshima H, Kuratsu J, Nishi T, Ushio Y (2002) Prognostic factors in patients who survived more than 10 years after undergoing surgery for metastatic brain tumors: report of 5 cases and review of the literature. Surg Neurol 58(2):118–123
14. Kienast Y, Winkler F (2010) Therapy and prophylaxis of brain metastases. Expert Rev Anticancer Ther 10(11):1763–1777
15. Fidler IJ, Yano S, Zhang RD, Fujimaki T, Bucana CD (2002) The seed and soil hypothesis: vascularisation and brain metastases. Lancet Oncol 3(1):53–57
16. Lockman PR, Mittapalli RK, Taskar KS, Rudraraju V, Gril B, Bohn KA, Adkins CE, Roberts A, Thorsheim HR, Gaasch JA, Huang S, Palmieri D, Steeg PS, Smith QR (2010) Heterogeneous blood-tumor barrier permeability determines drug efficacy in experimental brain metastases of breast cancer. Clin Cancer Res 16(23):5664–5678
17. Carbonell WS, Ansorge O, Sibson N, Muschel R (2009) The vascular basement membrane as "soil" in brain metastasis. PLoS ONE 4(6):e5857
18. Kusters B, Leenders WP, Wesseling P, Smits D, Verrijp K, Ruiter DJ, Peters JP, van Der Kogel AJ, de Waal RM (2002) Vascular endothelial growth factor-A(165) induces progression of melanoma brain metastases without induction of sprouting angiogenesis. Cancer Res 62(2):341–345
19. JuanYin J, Tracy K, Zhang L, Munasinghe J, Shapiro E, Koretsky A, Kelly K (2009) Noninvasive imaging of the functional effects of anti-VEGF therapy on tumor cell extravasation and regional blood volume in an experimental brain metastasis model. Clin Exp Metastasis 26(5):403–414
20. Leenders W, Kusters B, Pikkemaat J, Wesseling P, Ruiter D, Heerschap A, Barentsz J, de Waal RM (2003) Vascular endothelial growth factor-A determines detectability of experimental melanoma brain metastasis in GD-DTPA-enhanced MRI. Int J Cancer 105(4):437–443
21. Kim LS, Huang S, Lu W, Lev DC, Price JE (2004) Vascular endothelial growth factor expression promotes the growth of breast cancer brain metastases in nude mice. Clin Exp Metastasis 21(2):107–118
22. Leenders WP, Kusters B, Verrijp K, Maass C, Wesseling P, Heerschap A, Ruiter D, Ryan A, de Waal R (2004) Antiangiogenic therapy of cerebral melanoma metastases results in sustained tumor progression via vessel co-option. Clin Cancer Res 10(18 Pt 1):6222–6230
23. Novello O, Abrey LE, Grossi F (2009) Administration of sunitinib to patients with nonsmall cell lung cancer and irradiated brain metastases: A phase II trial. J Clin Oncol 27(15s (suppl., abstr 8077)):15s (suppl., abstr 8077)
24. Massard C, Zonierek J, Gross-Goupil M, Fizazi K, Szczylik C, Escudier B (2010) Incidence of brain metastases in renal cell carcinoma treated with sorafenib. Ann Oncol 21(5):1027–1031
25. Altaha R, Crowell E, Hobbs G, Higa G, Abraham J (2005) Increased risk of brain metastases in patients with HER-2/neu-positive breast carcinoma. Cancer 103(3):442–443
26. Stemmler HJ, Kahlert S, Siekiera W, Untch M, Heinrich B, Heinemann V (2006) Characteristics of patients with brain metastases receiving trastuzumab for HER2 overexpressing metastatic breast cancer. Breast 15(2):219–225
27. Yau T, Swanton C, Chua S, Sue A, Walsh G, Rostom A, Johnston SR, O'Brien ME, Smith IE: Incidence, pattern and timing of brain metastases among patients with advanced breast cancer treated with trastuzumab. Acta Oncol 2006;45(2):196–201

28. Palmieri D, Chambers AF, Felding-Habermann B, Huang S, Steeg PS (2007) The biology of metastasis to a sanctuary site. Clin Cancer Res 13(6):1656–1662
29. Grinberg-Rashi H, Ofek E, Perelman M, Skarda J, Yaron P, Hajduch M, Jacob-Hirsch J, Amariglio N, Krupsky M, Simansky DA, Ram Z, Pfeffer R, Galernter I, Steinberg DM, Ben-Dov I, Rechavi G, Izraeli S (2009) The expression of three genes in primary non-small cell lung cancer is associated with metastatic spread to the brain. Clin Cancer Res 15(5):1755–1761
30. Zhang C, Zhang F, Tsan R, Fidler IJ (2009) Transforming growth factor-beta2 is a molecular determinant for site-specific melanoma metastasis in the brain. Cancer Res 69(3):828–835
31. Ray PS, Wang J, Qu Y, Sim MS, Shamonki J, Bagaria SP, Ye X, Liu B, Elashoff D, Hoon DS, Walter MA, Martens JW, Richardson AL, Giuliano AE, Cui X (2010) FOXC1 is a potential prognostic biomarker with functional significance in basal-like breast cancer. Cancer Res 70(10):3870–3876
32. Nguyen DX, Chiang AC, Zhang XH, Kim JY, Kris MG, Ladanyi M, Gerald WL, Massague J (2009) WNT/TCF signaling through LEF1 and HOXB9 mediates lung adenocarcinoma metastasis. Cell 138(1):51–62
33. Xie TX, Huang FJ, Aldape KD, Kang SH, Liu M, Gershenwald JE, Xie K, Sawaya R, Huang S (2006) Activation of stat3 in human melanoma promotes brain metastasis. Cancer Res 66(6):3188–3196
34. Nam DH, Jeon HM, Kim S, Kim MH, Lee YJ, Lee MS, Kim H, Joo KM, Lee DS, Price JE, Bang SI, Park WY (2008) Activation of notch signaling in a xenograft model of brain metastasis. Clin Cancer Res 14(13):4059–4066
35. Gabos Z, Sinha R, Hanson J, Chauhan N, Hugh J, Mackey JR, Abdulkarim B (2006) Prognostic significance of human epidermal growth factor receptor positivity for the development of brain metastasis after newly diagnosed breast cancer. J Clin Oncol 24(36):5658–5663
36. Pestalozzi BC, Zahrieh D, Price KN, Holmberg SB, Lindtner J, Collins J, Crivellari D, Fey MF, Murray E, Pagani O, Simoncini E, Castiglione-Gertsch M, Gelber RD, Coates AS, Goldhirsch A (2006) Identifying breast cancer patients at risk for Central Nervous System (CNS) metastases in trials of the International Breast Cancer Study Group (IBCSG). Ann Oncol 17(6):935–944
37. Lin NU, Claus E, Sohl J, Razzak AR, Arnaout A, Winer EP (2008) Sites of distant recurrence and clinical outcomes in patients with metastatic triple-negative breast cancer: high incidence of central nervous system metastases. Cancer 113(10):2638–2645
38. Palmieri D, Fitzgerald D, Shreeve SM, Hua E, Bronder JL, Weil RJ, Davis S, Stark AM, Merino MJ, Kurek R, Mehdorn HM, Davis G, Steinberg SM, Meltzer PS, Aldape K, Steeg PS (2009) Analyses of resected human brain metastases of breast cancer reveal the association between up-regulation of hexokinase 2 and poor prognosis. Mol Cancer Res 7(9):1438–1445
39. Robey RB, Hay N (2005) Mitochondrial hexokinases: guardians of the mitochondria. Cell Cycle 4(5):654–658
40. Muller A, Homey B, Soto H, Ge N, Catron D, Buchanan ME, McClanahan T, Murphy E, Yuan W, Wagner SN, Barrera JL, Mohar A, Verastegui E, Zlotnik A (2001) Involvement of chemokine receptors in breast cancer metastasis. Nature 410(6824):50–56
41. Zlotnik A (2004) Chemokines in neoplastic progression. Semin Cancer Biol 14(3):181–185
42. Palmieri D, Bronder JL, Herring JM, Yoneda T, Weil RJ, Stark AM, Kurek R, Vega-Valle E, Feigenbaum L, Halverson D, Vortmeyer AO, Steinberg SM, Aldape K, Steeg PS (2007) Her-2 overexpression increases the metastatic outgrowth of breast cancer cells in the brain. Cancer Res 67(9):4190–4198
43. Eugenin EA, Berman JW (2003) Chemokine-dependent mechanisms of leukocyte trafficking across a model of the blood-brain barrier. Methods 29(4):351–361
44. Carbonell WS, Murase S, Horwitz AF, Mandell JW (2005) Migration of perilesional microglia after focal brain injury and modulation by CC chemokine receptor 5: an in situ time-lapse confocal imaging study. J Neurosci 25(30):7040–7047
45. Schackert G, Fidler IJ (1988) Development of in vivo models for studies of brain metastasis. Int J Cancer 41(4):589–594
46. Schackert G, Price JE, Zhang RD, Bucana CD, Itoh K, Fidler IJ (1990) Regional growth of different human melanomas as metastases in the brain of nude mice. Am J Pathol 1990;136(1):95–102

47. Fidler IJ, Schackert G, Zhang RD, Radinsky R, Fujimaki T (1999) The biology of melanoma brain metastasis. Cancer Metastasis Rev 18(3):387–400
48. Chung E, Yamashita H, Au P, Tannous BA, Fukumura D, Jain RK (2009) Secreted Gaussia luciferase as a biomarker for monitoring tumor progression and treatment response of systemic metastases. PLoS ONE 4(12):e8316
49. Winkler F, Kienast Y, Fuhrmann M, von Baumgarten L, Burgold S, Mitteregger G, Kretzschmar H, Herms J (2009) Imaging glioma cell invasion in vivo reveals mechanisms of dissemination and peritumoral angiogenesis. Glia 57(12):1306–1315
50. Rampetsreiter P, Casanovas E, Eferl R (2011) Genetically modiefied mouse models of cancer invasion and metastasis. Drug Discovery Today: Disease Models
51. Yang M, Jiang P, Sun FX, Hasegawa S, Baranov E, Chishima T, Shimada H, Moossa AR, Hoffman RM (1999) A fluorescent orthotopic bone metastasis model of human prostate cancer. Cancer Res 59(4):781–786
52. Yang M, Jiang P, An Z, Baranov E, Li L, Hasegawa S, Al-Tuwaijri M, Chishima T, Shimada H, Moossa AR, Hoffman RM (1999) Genetically fluorescent melanoma bone and organ metastasis models. Clin Cancer Res 5(11):3549–3559
53. Hayashi K, Yamauchi K, Yamamoto N, Tsuchiya H, Tomita K, Bouvet M, Wessels J, Hoffman RM (2009) A color-coded orthotopic nude-mouse treatment model of brain-metastatic paralyzing spinal cord cancer that induces angiogenesis and neurogenesis. Cell Prolif 42(1):75–82
54. Cruz-Munoz W, Man S, Xu P, Kerbel RS (2008) Development of a preclinical model of spontaneous human melanoma central nervous system metastasis. Cancer Res 68(12):4500–4505
55. Alterman AL, Stackpole CW (1989) B16 melanoma spontaneous brain metastasis: occurrence and development within leptomeninges blood vessels. Clin Exp Metastasis 7(1):15–23
56. Yoneda T, Williams PJ, Hiraga T, Niewolna M, Nishimura R (2001) A bone-seeking clone exhibits different biological properties from the MDA-MB-231 parental human breast cancer cells and a brain-seeking clone in vivo and in vitro. J Bone Miner Res 16(8):1486–1495
57. Dodt HU, Leischner U, Schierloh A, Jahrling N, Mauch CP, Deininger K, Deussing JM, Eder M, Zieglgansberger W, Becker K (2007) Ultramicroscopy: three-dimensional visualization of neuronal networks in the whole mouse brain. Nat Methods 4(4):331–336
58. Malek A, Catapano CV, Czubayko F, Aigner A (2010) A sensitive polymerase chain reaction-based method for detection and quantification of metastasis in human xenograft mouse models. Clin Exp Metastasis 27(4):261–271
59. Schneider T, Osl F, Friess T, Stockinger H, Scheuer WV (2002) Quantification of human Alu sequences by real-time PCR–an improved method to measure therapeutic efficacy of anti-metastatic drugs in human xenotransplants. Clin Exp Metastasis 19(7):571–582
60. Anderson SA, Frank JA (2007) MRI of mouse models of neurological disorders. NMR Biomed 20(3):200–215
61. Heyn C, Ronald JA, Ramadan SS, Snir JA, Barry AM, MacKenzie LT, Mikulis DJ, Palmieri D, Bronder JL, Steeg PS, Yoneda T, MacDonald IC, Chambers AF, Rutt BK, Foster PJ (2006) In vivo MRI of cancer cell fate at the single-cell level in a mouse model of breast cancer metastasis to the brain. Magn Reson Med 56(5):1001–1010
62. Song HT, Jordan EK, Lewis BK, Gold E, Liu W, Frank JA (2011) Quantitative T2* imaging of metastatic human breast cancer to brain in the nude rat at 3 T. NMR Biomed 24(3):325–334
63. Simoes RV, Martinez-Aranda A, Martin B, Cerdan S, Sierra A, Arus C (2008) Preliminary characterization of an experimental breast cancer cells brain metastasis mouse model by MRI/MRS. MAGMA 21(4):237–249
64. Hawes JJ, Reilly KM (2010) Bioluminescent approaches for measuring tumor growth in a mouse model of neurofibromatosis. Toxicol Pathol 38(1):123–130
65. Helmchen F, Denk W (2005) Deep tissue two-photon microscopy. Nat Methods 2(12):932–940
66. Göppert-Mayer M (1931) Elementary processes with two-quantum transitions
67. Chang EL, Wefel JS, Hess KR, Allen PK, Lang FF, Kornguth DG, Arbuckle RB, Swint JM, Shiu AS, Maor MH, Meyers CA (2009) Neurocognition in patients with brain metastases treated with radiosurgery or radiosurgery plus whole-brain irradiation: a randomised controlled trial. Lancet Oncol 10(11):1037–1044

68. Chang EL, Wefel JS, Maor MH, Hassenbusch SJ, III, Mahajan A, Lang FF, Woo SY, Mathews LA, Allen PK, Shiu AS, Meyers CA (2007) A pilot study of neurocognitive function in patients with one to three new brain metastases initially treated with stereotactic radiosurgery alone. Neurosurgery 60(2):277–283
69. Robbins ME, Payne V, Tommasi E, Diz DI, Hsu FC, Brown WR, Wheeler KT, Olson J, Zhao W (2009) The AT1 receptor antagonist, L-158,809, prevents or ameliorates fractionated whole-brain irradiation-induced cognitive impairment. Int J Radiat Oncol Biol Phys 73(2):499–505
70. Zhao W, Payne V, Tommasi E, Diz DI, Hsu FC, Robbins ME (2007) Administration of the peroxisomal proliferator-activated receptor gamma agonist pioglitazone during fractionated brain irradiation prevents radiation-induced cognitive impairment. Int J Radiat Oncol Biol Phys 67(1):6–9
71. Ramanan S, Kooshki M, Zhao W, Hsu FC, Riddle DR, Robbins ME (2009) The PPARalpha agonist fenofibrate preserves hippocampal neurogenesis and inhibits microglial activation after whole-brain irradiation. Int J Radiat Oncol Biol Phys 75(3):870–877
72. Rosenberg A, Knox S (2006) Radiation sensitization with redox modulators: a promising approach. Int J Radiat Oncol Biol Phys 64(2):343–354
73. Francis D, Richards GM, Forouzannia A, Mehta MP, Khuntia D (2009) Motexafin gadolinium: a novel radiosensitizer for brain tumors. Expert Opin Pharmacother 10(13):2171–2180
74. Palmieri D, Lockman PR, Thomas FC, Hua E, Herring J, Hargrave E, Johnson M, Flores N, Qian Y, Vega-Valle E, Taskar KS, Rudraraju V, Mittapalli RK, Gaasch JA, Bohn KA, Thorsheim HR, Liewehr DJ, Davis S, Reilly JF, Walker R, Bronder JL, Feigenbaum L, Steinberg SM, Camphausen K, Meltzer PS, Richon VM, Smith QR, Steeg PS (2009) Vorinostat inhibits brain metastatic colonization in a model of triple-negative breast cancer and induces DNA double-strand breaks. Clin Cancer Res 15(19):6148–6157
75. Gril B, Palmieri D, Bronder JL, Herring JM, Vega-Valle E, Feigenbaum L, Liewehr DJ, Steinberg SM, Merino MJ, Rubin SD, Steeg PS (2008) Effect of lapatinib on the outgrowth of metastatic breast cancer cells to the brain. J Natl Cancer Inst 100(15):1092–1103
76. Graesslin O, Abdulkarim BS, Coutant C, Huguet F, Gabos Z, Hsu L, Marpeau O, Uzan S, Pusztai L, Strom EA, Hortobagyi GN, Rouzier R, Ibrahim NK (2010) Nomogram to predict subsequent brain metastasis in patients with metastatic breast cancer. J Clin Oncol 28(12):2032–2037
77. Muldoon LL, Soussain C, Jahnke K, Johanson C, Siegal T, Smith QR, Hall WA, Hynynen K, Senter PD, Peereboom DM, Neuwelt EA (2007) Chemotherapy delivery issues in central nervous system malignancy: a reality check. J Clin Oncol 25(16):2295–2305
78. Bellavance MA, Blanchette M, Fortin D (2008) Recent advances in blood-brain barrier disruption as a CNS delivery strategy. AAPS J 10(1):166–177
79. Pardridge WM (2008) Re-engineering biopharmaceuticals for delivery to brain with molecular Trojan horses. Bioconjug Chem 19(7):1327–1338
80. de Boer JP, Abbink JJ, Brouwer MC, Meijer C, Roem D, Voorn GP, Lambers JW, van Mourik JA, Hack CE (1991) PAI-1 synthesis in the human hepatoma cell line HepG2 is increased by cytokines–evidence that the liver contributes to acute phase behaviour of PAI-1. Thromb Haemost 65(2):181–185
81. Lillis AP, Van Duyn LB, Murphy-Ullrich JE, Strickland DK (2008) LDL receptor-related protein 1: unique tissue-specific functions revealed by selective gene knockout studies. Physiol Rev 88(3):887–918
82. Pan W, Kastin AJ, Zankel TC, van KP, Terasaki T, Bu G (2004) Efficient transfer of receptor-associated protein (RAP) across the blood-brain barrier. J Cell Sci 117(Pt 21):5071–5078
83. Emanuel SL, Hughes TV, Adams M, Rugg CA, Fuentes-Pesquera A, Connolly PJ, Pandey N, Moreno-Mazza S, Butler J, Borowski V, Middleton SA, Gruninger RH, Story JR, Napier C, Hollister B, Greenberger LM (2008) Cellular and in vivo activity of JNJ-28871063, a nonquinazoline pan-ErbB kinase inhibitor that crosses the blood-brain barrier and displays efficacy against intracranial tumors. Mol Pharmacol 73(2):338–348
84. Kong LY, bou-Ghazal MK, Wei J, Chakraborty A, Sun W, Qiao W, Fuller GN, Fokt I, Grimm EA, Schmittling RJ, Archer GE, Jr., Sampson JH, Priebe W, Heimberger AB (2008) A novel

inhibitor of signal transducers and activators of transcription 3 activation is efficacious against established central nervous system melanoma and inhibits regulatory T cells. Clin Cancer Res 14(18):5759–5768
85. Hoffmann J, Fichtner I, Lemm M, Lienau P, Hess-Stumpp H, Rotgeri A, Hofmann B, Klar U (2009) Sagopilone crosses the blood-brain barrier in vivo to inhibit brain tumor growth and metastases. Neuro Oncol 11(2):158–166
86. Seike T, Fujita K, Yamakawa Y, Kido MA, Takiguchi S, Teramoto N, Iguchi H, Noda M (2011) Interaction between lung cancer cells and astrocytes via specific inflammatory cytokines in the microenvironment of brain metastasis. Clin Exp Metastasis 28(1):13–25

Chapter 6
Pulmonary Metastasis

Anastasia Malek

Abstract Metastases are the leading cause of death among cancer patients; furthermore, the lungs are the most common site of tumor dissemination. Better understanding of the molecular mechanisms underlying pulmonary colonization by circulating cancer cells could improve the quality of life and survival rate for patients. It definitely requires well-designed experimental systems.

This chapter presents a short review of the main biological aspects of pulmonary metastases and describes approaches to model metastatic processes in the lung *in vitro*, *ex vivo*, and *in vivo* with emphasis on experimental settings and applicability. In addition, the basic techniques for evaluation and analysis of experimental lung metastases are discussed. Finally, a qPCR-based method of detection and quantification of metastatic tumor burden in human xenograft models of pulmonary metastases is presented. Overall, the chapter content provides a methodological background for the experimental study of secondary lung cancer.

Abbreviations

CUP	Carcinoma of unknown primary
CT	Computed tomography
PET	Positron emission tomography
RFA	Radiofrequency ablation
SBRT	Stereotactic body radiotherapy
VP	Vascular permeability
V_C	Capillary volume
S_A	Alveolar surface area
GFP	Green fluorescent protein
NIR	Near infra-red
CTC	Circulating cancer cells
Luc	Luciferase
IHC	Immunihistochemistry
qPCR	Quantitative polymerase chain reaction

A. Malek (✉)
Department of Oncoendocrinology, Petrov Institute of Oncology, Sankt-Petersburg, Russia
e-mail: anastasia@malek.com

A. Malek (ed.), *Experimental Metastasis: Modeling and Analysis,*
DOI 10.1007/978-94-007-7835-1_6,

6.1 Introduction–Clinical Relevance of Pulmonary Metastasis

Approximately one out of 1,000 chest radiographs show the incidental finding of a pulmonary lesion caused by a tumor [1]. Unfortunately, only a small percentage (2-5 %) of lung tumors are of benign origin, e.g., lipomas, fibromas, hamartomas, and chondromas; the majority are malignant neoplasms, most commonly primary lung cancer, followed by metastases of extrapulmonary primary carcinomas. The lungs are among the most prominent target organs for metastatic disease. Most frequently, lung metastases originate from cancers of the breast, colon, head and neck, stomach, pancreas, kidney, bladder, the male and female genitourinary tract, and sarcomas. Lung metastases occur in approximately 30 % of patients dying of cancer and can reduce the quality of life for many patients living with advanced cancer. Pulmonary metastatic disease can be defined as a separate nosologic category since this condition requires specific diagnostic [2] and treatment approaches [3, 4].

Symptoms considered as clinical indications of secondary lung tumors are chest pain, dyspnea, cough, or hemoptysis. However, either an advanced metastatic process or specific localization of certain metastases may manifest by such symptoms, while the initial stages of pulmonary metastatic disease are usually silent clinically. A scenario that is not infrequently encountered is an incidental finding of secondary lung cancer of unknown origin, a so-called carcinoma of unknown primary (CUP), when patients are undergoing screening chest radiography, computed tomography (CT) scanning, or positron emission tomography (PET)/CT scanning. Radiographically, secondary lung tumors usually appear as discrete nodules (single or multiple), interstitial infiltrates, or endobronchial lesions with or without distal atelectasis or postobstructive pneumonitis. They often have a characteristic round appearance on chest radiographs.

Management of secondary lung cancer presents a challenge for the oncologist. There are a number of curative approaches including surgery, systemic chemotherapy or local chemo-perfusion, radiation, and immunotherapy; however, the most appropriate treatment plan depends on the number, location, and size of the metastases, the pathologic diagnosis of the primary tumor if known, and patient status. Several studies demonstrated a survival benefit from complete resection of all pulmonary metastases originating from breast [5] or colorectal cancers [6]. In some patients pulmonary metastasectomy may even be the only curative treatment option. Generally accepted rules for intended curative pulmonary metastasectomy are control of the primary tumor, technically completely resectable metastases, the exclusion of extrapulmonary metastases (except for potentially completely resectable hepatic metastases) and functional operability. The most important prognostic factors are complete resection, the exact entity of the tumor, and disease-free interval [3, 7]. The chemotherapeutic approach for lung metastases treatment is usually defined by the pathologic diagnosis of the primary tumor. However, many patients develop recurrent disease in the thorax despite the use of systemic chemotherapy, the dosage of which is limited by systemic toxicity. Similar to the basic principles of isolated limb and liver perfusion, isolated lung perfusion is an attractive and

promising surgical technique for the delivery of high-dose chemotherapy with minimal systemic toxicity [4]. Advanced techniques of localized radiotherapy, such as radiofrequency ablation (RFA) or stereotactic body radiotherapy (SBRT), may be considered as a method of choice or adjunctive therapy [8].

The appearance lung metastases defines the late (or disseminated) stage of cancer of any origin. Despite advanced curative approaches and individualized multimodal strategy applied for each patient, the prognosis of metastatic lung cancer is generally poor with only a slight difference among primary tumor types. The National Cancer Institute's (USA) statistics (2003–2009) for advanced cancer 5-years survival rate [9] provides the following numbers: breast cancer, 24.3 %; colorectal cancer, 12.5 %; bladder cancer, 5.4 %; pancreatic cancer, 2 %, and stomach cancer, 3.9 %. Considering the fact that the lungs are the primary site of distant metastases of these cancer types, the overall survival rate associated with pulmonary metastatic disease is currently disappointing. Among patients with cancer of unknown primary (CAP), pulmonary metastatic disease represents the most common cause of death with a median survival of 3 months [10].

6.2 General Consideration of Pulmonary Metastasis

Several factors could be considered to play a major role in pathogenesis of the lung metastasis: particularity of pulmonary blood circulation, adhesive properties and permeability of pulmonary endothelium mediating interaction with and extravasation of circulating tumor cells (CTC), local (pulmonary) specificity of host immune system.

6.2.1 Structure of the Vascular Bed

Detached tumor cells entre into the bloodstream through the venous drainage, after passing the right hart and arteries pulmonary, they reach the lungs and are retained in pulmonary capillaries. Thus, lung parenchyma is the most common site of bloodstream-mediated metastasis due to filtering capacity of pulmonary capillary net. Since blood oxygenation is a main physiological function of the lung, its vascular (arterial and venous) tree has an extremely branched structure. As it was estimated in early studies by integrated morphometric analysis, the human pulmonary arterial tree is comprised of 17 branch orders, from the main pulmonary artery (order 17) with a diameter of ~ 30 mm to more than 72 million order 1 arteries which range in diameter from 10–15 μm [11]. In context of this chapter, it is important to consider difference between human and rat lung. In contrast to the 15–17 orders of pulmonary artery branches in human lung, in smaller mammals such as rat, the pulmonary arterial tree is comprised of only 11–12 orders. As would be expected, the number of distal order 1 branches decreases with body mass. For example, in dog and rat lung the number of order 1 branches is estimated to be ~1 and 3 log orders less,

respectively, than that in human lung. However, the diameter of these distal precapillary order 1 branches is similar from human to rat lung [12].

One more specific feature of pulmonary vasculature is a density and spatial heterogeneity of the capillary net. Capillary networks adjacent to bronchovascular bundles and in the subpleural network are comprised of long tubular segments, similar in organization to those capillary networks seen in many systemic vascular beds. In contrast, shorter capillary segments are present in the much more dense capillary networks which occupy alveolar septal walls [13, 14]. This structural feature may be reflected by specific pattern of lung metastases distribution. There is also difference in lung capillary density among species. Thus, overall capillary loading or capillary density in the septal compartment in lung can be estimated by the ratio of total capillary volume (V_C) to total alveolar surface area (S_A). Based on data provided by Gehr and colleagues in their comprehensive assessment of scaling in the respiratory system, the V_C/S_A ratio increases from 1.18 in mouse lung to 1.24, 1.43, and 1.49 in rat, dog and human lung, respectively [15]. These data suggest that the alveolar capillary network is somewhat denser in larger mammals (human) that may result to higher predisposition to metastases development in comparison with laboratory animals.

In additional to anatomical/structural features of vascular bed, vascular permeability (VP) presents an essential and highly regulated factor implemented in metastatic process in the lung. Evidence suggests that cancer cells need to weaken the interendothelial junctions in order to cross the endothelial barrier. Several tumor-derived vasoactive compounds have been pointed out to drive increase in vascular permeability: VEGF, Angptl4, CCL2, SDF-1, etc [16, 17]. Src kinase of pulmonary endothelial cells was evaluated as a point of convergence for many of these regulatory pathways. An essential role of Src in extravasation of tumor cells from lung capillaries was demonstrated when direct intravenous injection of cancer cells resulted in a more than 2-fold reduction in lung tumor burden in src-null mice compared to control animals [18]. Results of this study, in both experimental metastasis and spontaneous metastasis models, revealed implication of Src-mediated VP in tumor metastasis to the lung.

6.2.2 Adhesive Properties and Cell-Cell Interaction

Besides vascular anatomy, proper characteristics of CTC can mediate pattern and intensity of metastatic process. As long ago as 1889, Stephen Paget proposed that metastasis depends on cross-talk between selected cancer cells (the ‘seeds’) and specific organ microenvironments (the ‘soil’) [19]. This hypothesis, so called “seed and soil”, still holds forth today [20]. As it is postulated now, the potential of a tumor cell to metastasize depends on its interactions with the homeostatic factors that promote tumor-cell growth, survival, angiogenesis, invasion and metastasis. In addition, some surface molecules of metastatic cells have affinity to capillary of certain tissue that defines preferential, not random, colonization of secondary organs.

Evidence for this phenomenon has been demonstrated in early studies by the preferential adhesion of metastatic tumor cells to vascular endothelial cells isolated from metastasized organs. For example, lung-metastatic tumor cells adhere preferentially to monolayers of lung-derived endothelial cells, whereas brain-metastatic glioma cells, liver-metastatic lymphoma cells, and ovary-metastatic teratoma cells adhere preferentially to endothelial cells isolated from brain, liver, and ovary, respectively [21, 22]. Structural and functional properties of various adhesive molecules and their implementation in the metastatic process are discussed explicitly in recent literature [23, 24].

Involvement of certain surface molecules in pulmonary metastasis is studied widely now. For instance, the chemokine receptor CXC4 was shown to be implicated in the lung specificity of breast tumor metastases, where the tissue-specific activity of its ligand CXCL12 allows chemokine-mediated signal activation [25]. Involvement of connexin-43 in colonization of the lung by circulating breast cancer cells was demonstrated in other study [26]. Mediation of lung metastasis of murine melanomas by a lung-specific endothelial cell adhesion molecule localazed on endothelia of distinct branches of lung blood vessels was demonstrated in early studies [27]. Role of integrins and selectins in lung—specific anchorage of colon cancer cells was analyzed recently by quantitative in vivo microscopy [28]. Translocation of oligosaccharides –binding lysosome associated membrane protein (LAMP1) to surface membrane and resulting over-representation of oligosaccharids (polylacNAc) specifically binding Galectin-3 was observed in melanoma cells. Since Gelectin-3 is expressed in highest amount in the lung as compared to other organs, this receptor-ligand interaction is considered to mediate lung-specific metastasis of melanomas [29].

Blood component may interact with CTC increasing their metastatic potency. For instance, CD154 expressed on and released from activated platelets induces an inflammatory response in endothelial cells and monocytes, including tissue factor production. CD154 has also been shown to activate platelets *in vitro* and promote thrombus stability *in vivo*. These CD154 effects may be mediated, at least in part, by CD40 signaling on platelets and vascular endothelial cells. Thus, Ingersoll and colleagues hypothesized that CD40 and CD154 promote lung metastases formation in experimental metastasis in mice [30]. The hypothesis was confirmed by observation that mice deficient in blood compartment CD40 had fewer lung nodules compared to wild-type mice and mice deficient in endothelial CD40. These results suggested an important contribution of the CD40/CD154 pathway to experimental lung metastasis. Furthermore, the data pointed to a selective role for peripheral blood cells in metastatic process.

6.2.3 Impact of Pulmonary Immune System

From an immunological point of view, various lymphocyte subsets have different requirements for trafficking to various organs including primary and secondary lymphoid tissues as well as non-lymphoid organs. It is possible that there are

organ-specific immune responses that might be able to eliminate a metastatic clone in one organ but not another. It has been shown that neutrophils may regulate lung metastasis development through physical interaction and anchoring of circulating tumor cells to endothelium [31]. In this study, human melanoma cells were i.v. injected into nude mice leading to the entrapment of many cancer cells. However, 24 h later, very few cancer cells remained in the lungs. In contrast, injection of human neutrophils an hour after tumor cell injection increased cancer cell retention by approximately 3-fold. Entrapped melanoma cells produced and secreted high levels of a cytokine, interleukin-8 (IL-8), attracting neutrophils and increasing tethering ß2-integrin expression by 75 to 100 %. As it was demonstrated, intercellular adhesion molecule-1 on melanoma cells and ß2-integrin on neutrophils interacted, promoting anchoring to pulmonary endothelium [31].

Moreover, the organ-specific NK cell subsets may play a critical role in organ-specific metastasis. In recent study of Ballas and colleagues, B16 murine melanoma cells readily colonized the lungs but not the liver after intravenous injection. Analysis of NK cell subsets, defined by the differential expression of a combination of CD27 and CD11b, indicated a significant difference in the distribution of NK cell subsets in the lung and liver with the mature subset being dominant in the lung and the immature subset being dominant in the liver. Several experimental approaches, including adoptive transfer, clearly indicated that the immature hepatic NK cell subset, CD27+CD11b–, was protective against liver metastasis; this subset mediated its protection by a perforin-dependent cytotoxic mechanism. In contrast, the more mature NK cell subsets were more efficient at reducing pulmonary tumor load. These data indicated that organ-specific immune responses may play a pivotal role in determining the permissiveness of a given organ for the establishment of a metastatic niche. [32]

Role of macrophages was investigated by Jordan and colleagues [33]. It was shown that activation of macrophages by natural anti-neoplastic compound (Cordyceps sinensis) reduces lung metastasis occurrence in a surgical excision model of metastatic mammary carcinoma while does not influence on primary tumor growth. This result suggested that pulmonary macrophages are also involved in control of lung colonization by cancer cells [33]

Taken together, these data reveals complex and intricate mechanism of lung—specific metastasis, suggesting an active role of cancer cells, lung endothelia and residual immune cells. Recent gene-expression studies that profiled metastases established in mouse models after injection of human cancer cells have shown striking difference between populations of the cells that colonize distinct organs, suggesting that many potential factors, in addition to surface molecules, may determine organ-specific metastasis [34, 35]. Obviously, better understanding of main mechanisms and factors governing lung metastasis development will improve recent curative strategies and increase life quality for many cancer patients. Study of pulmonary metastasis requires well-established experimental models.

6.3 In *Vitro* Approaches to Recapitulate Certain Steps of Metastatic Process

6.3.1 Conventional Cell Culture Methods

Attempts to experimentally model metastasis begin with rudimentary *in vitro* assays designed to recapitulate individual facets of the metastatic process such as cell adhesion, motility and invasion. Adhesive properties of cancer cells can be investigated by treating cells with anti-bodies binding specifically certain adhesion molecules on cancer cell surface. In some setting such *in vitro* experiments may closely reflect an *in vivo* situation [36]. Resistance cells to anoikis is being evaluated by culturing cells on non-adherent surface while colony forming ability can be estimated by plating sell at low density on adherent surface or in soft agar. Results of these assays may be correlated with certain *in vivo* properties of cancer cells [37]. The cell motility, for instance, can be observed by videomicroscopy or measured by so-called "wound-healing" assay. The cellular invasion is often measured using a Boyden chamber (or transwell chamber) which constitutes a barrier in culture through which cellular invasion can be monitored and estimated qualitatively. Basic *in vitro* approaches are described in details in Chapter 3 of this issue and elsewhere in cell culturing manuals. However, it should be considered that these assays do not reflect specificity of lung tissue architecture as well as specific aspects of lung metastasis.

6.3.2 Lung Organotypic 3D Models

The complex three-dimensional architectural structure of lung parenchyma assumes connections of alveolar units to airways and the close proximity of capillary network. Considering specific sponge-like texture of lung tissue, simple co-culturing of alveolar and endothelial cells is not sufficient to mimic it. 3D lung organotypic model can be created by using collagen or gelatin sponge (Gelfoam) that may serve as a scaffold for organotypic cells co-culture and may be used to study initial events of lung metastasis development. The porous structure of the Gelfoam provide with possibility of microscopic imaging and histological analysis of co-culture. This approach was successfully realized in several studies of lung tissue regeneration, angiogenesis and lung metastasis [38, 39], however this method is quite laborious. Co-culturing lung-derived cells and cancer cells assumes their syngenic nature. Xenograft cancer/immuno-deficient host setting is theoretically acceptable as well; however no data are published so far. In their study, Martin and colleagues used lung-derived cell mixture from FVB mice and syngenic cancer cell line R221A previously isolated from a mammary tumor in the fat pad of a MMTV-PyVT transgenic mouse in the FVB/n background [40]. Cancer cells were labeled with green

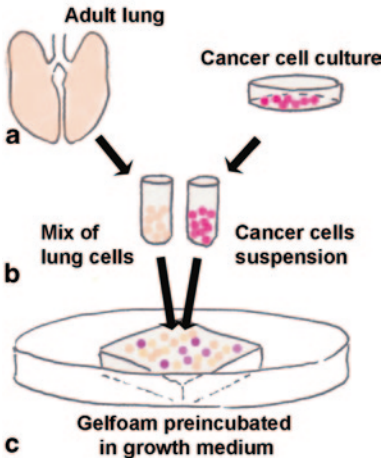

Fig. 6.1 Setup of the 3D lung organotypic co-culture assay. After the lung cells are completely dissociated **a** and most of the red cells are removed, cells suspension is washed and placed on top of the Gelfoam sponge in parallel with suspension of cancer cells **b** in a tissue culture dish containing media. **c** Prolonged incubation allow cells to penetrate inside of Gelfoam and form co-culture mimicking lung tussue.

fluorescent protein (GFP). Protocol of the procedure is adopted from [39] with minor modifications. Setup of the assay is presented in Fig. 6.1**.**

- To construct the cultures, lungs are taken from 6−8 week old mice and completely dissociated overnight at 30°C in digestion solution
- Gelfoam is aseptically cut into 2cm^2 squares and placed into 35 mm culture dishes
- Small needles were placed at two points in the sponge to serve as positional markers for subsequent imaging experiments
- Cancer cells (1.5×10^6) in PBS in a volume of 20 µl are inoculated onto the top of the scaffold
- The digested lung mixture is washed in PBS, while red blood cells are lysed in a solution of PharmLyse (BD Biosciences, San Jose, CA) in PBS.
- The lung cells mixture then is again washed once more in PBS, and 2×10^6 cells in PBS in a volume of 20 µl are also inoculated onto the top of the scaffold.
- The co-cultures is placed at 37°C to allow the cells to soak into the scaffolds.
- One ml appropriate culture media with 15% FCS supplemented with fungizone and antibiotic should then be added to the cultures, and they are placed back into a 37°C incubator
- Culture media is changed daily throughout the experiments
- Before cultures were imaged using confocal microscopy, they are inverted such that the surface of the scaffold where the cells were seeded is flush against the glass surface of the dish.

6.3.3 Ex Vivo Pulmonary Metastasis Assay [41]

Assay was developed quite long ago [42] and modified recently for lung metastasis study [41]. It is still not widely accepted, however it provides with exceptional

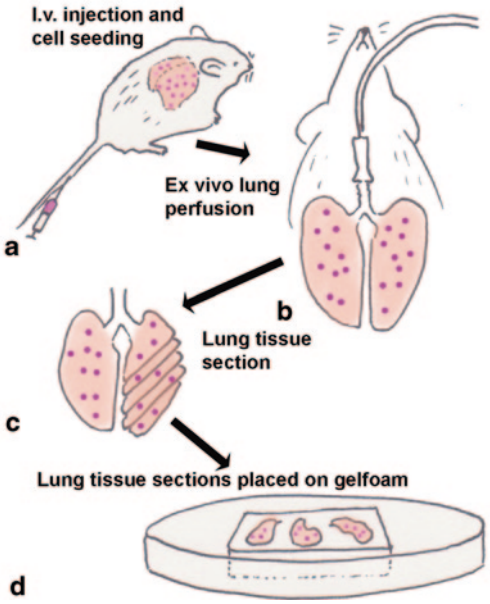

Fig. 6.2 Workflow of ex vivo pulmonary metastasis assay. **a** Fluorescent-labeled tumor cells are delivered to mice by tail-vein injection. **b** Following euthanasia, the trachea is cannulated and attached to a gravity perfusion apparatus. The lungs are infused in the vertical position under a constant 20 cm H2O hydrostatic pressure. The lungs were allowed to cool at 4°C for 20 min to solidify the agarose medium solution. **c** Complete transverse serial sections (1–2 mm in thickness) are gently sliced from each lobe with a scalpel, yielding 16–20 lung slices per pair of lungs. **d** 4–5 lung sections were placed on the sterile Gelfoam sections bathing in culture media

opportunity of real-time assessment of progression from single metastatic cells to multicellular colonies in the lung. The approach allows maintain native lung architecture with all cellular components including migratory cells, type I and type II pneumocytes, alveolar macrophages, vascular endothelial cells, red blood cells, airway-associated epithelial cells, and stromal cells for over three weeks. This assay can be easily applied to study interaction of tumor cells with components of lung tissue as well as for screening of novel anti-metastatic agents at several dose and schedule combinations. As a previous one, this approach assumes utilization clonally related lung tissue and GFP-labeled metastatic cancer cells. Workflow of the assay is schematically shown in Fig. 6.2 while protocol of the procedure is short-cut and adopted from initial publication [41]:

- GFP-positive tumor cells (2×10^5) are delivered by tail-vein injection to mice circulation
- Within 15 min of tumor injection, the mice are euthanized by CO2 inhalation
- Using sterile surgical conditions in a laminar flow hood, the mice are placed in dorsal recumbency. The sternum is removed to expose the lung. The trachea is then cannulated with a 20-gauge intravenous catheter and attached to a gravity perfusion apparatus under constant 20 cm H2O hydrostatic pressure or by syringe infusion of 1.2 ml of well-mixed culture medium/agarose solution at 40°C
- The trachea, lungs, and heart are then carefully removed and immediately placed in a cold solution of PBS containing antibiotics streptomycin at 4°C for 20 min to solidify the agarose/medium solution
- Complete transverse sections (1–2 mm in thickness) are made from each lobe using a n.21 scalpel blade, yielding 16–20 lung sections

- Then 4–5 lung sections are placed on a single 1.5 × 0.7-cm sterile Gelfoam section that had been preincubated for 2 hours in a 6-cm tissue culture dish with culture medium
- Lung sections are incubated at 37°C in humidified conditions of 5 % CO2. Fresh culture medium should be replaced and lung tissue sections are turned over with a sterile iris thumb forceps every other day.

Serum-free conditions on the base of M-199 medium is used for lung culture were described in initial study [42], Mendoza and colleagues proposed some modifications of the media [41] applied for lung perfusion and for farther culturing of lung tissue sections. A critical aspect of the assay is the insufflation of 0.6 % agarose to the lung that is necessary to maintain lung structure. However, technical sophistication of the method is justified by possibility to closely recapitulate *in vivo* condition. Mendoza et al. in their article [41] provides with results of parallel *in vivo* and *ex vivo* assays that confirmed validity of the proposed method.

6.4 In Vivo Models of Lung Metastasis

6.4.1 Spontaneous Metastasis from Orthotopic Xenograft or Syngenic Tumor

The complex nature of metastatic processes and certain endurance of metastases development dictate the need for *in vivo* experimental methods that implement all supportive and regulatory systems in the whole organism setting and for a longer duration to compare to *in vitro*/*ex vivo* experiments. The laboratory mouse traditionally represents the most relevant and useful system for these types of studies. Several approaches to model the metastatic process in mouse are utilized, and there are advantages and disadvantages to each.

Optimal recapitulation of the metastatic process, starting from the initial event of cancer cells detaching from the tumor and entering the bloodstream, may be achieved in models with orthotopically growing primary tumors, either xenografts or syngenic. Example of the xenograft model of the human osteosarcoma developing pulmonary metastases was established by Luu and co-workers [43]. The authors used three osteosarcoma cell lines derived from the same osteosarcoma patient; thus, they had a similar genetic background. The parental cells were transformed with the chemical carcinogen (N-methyl-N'-nitro-N-nitrosoguanidine, MNNG) or with the Ki-RAS oncogen. The derivative cell lines exhibited various *in vitro* characteristics in terms of motility, invasion capacity and anchorage independent growth. When these cells were orthotopically injected into the proximal tibia of athymic mice, it was observed that only Ki-RAS-transformed cells were able to metastasize efficiently from the primary site and develop numerous pulmonary metastases; MNNG –transformed cells produced pulmonary metastases only occasionally, whereas pa-

rental cell lines never developed any lung metastases. Thus, by using these three cancer cell lines, a clinically relevant animal model of lung-metastasizing cancer was established. Such a model can facilitate the investigation of different stages of cancer progression and elucidate the potential role of particular molecular factors in lung metastases development.

However, the using of immunocompromised animals does not allow consideration of the impact of the host immune system in cancer progression and metastases development. This factor is particularly important in cases of pulmonary metastatic disease, where certain components of immune system, such as alveolar macrophages or pulmonary dendritic cells, may play a crucial role. Thus, Miretti and co-authors [44] developed a syngenic model of osteosarcoma metastasizing to the lungs using a cell line derived from a spontaneous osteosarcoma in a Balb/c mouse. In contrast to the study described in the previous paragraph, this study found that increased metastatic potency of the cells *in vivo* does not correlated with an increase of motility, invasion ability or anchorage-independent growth capacity assayed *in vitro*. This observation suggests a role of some endogenous host factors, most likely the immune system, in the process of modeling metastases formation. A shortcoming of the syngenic model is a paucity of endogenously originating metastases in the mouse, compared to those associated with human cancer. In some cases, multiple re-injections of the cells into the mice followed by in vitro passages are utilized to select the most aggressive cancer cell clone and to augment the metastatic potential of the cancer cell population [45]. Increased numbers of cancer cells or repeated injections can be used to improve the reproducibility of the experimental model. Alternative way to increase metastatic potential of injected cancer cells is preliminary whole-body irradiation of mice resulting to suppression of host immune activity; however, such an approach will reduce the competence of the syngeneic model.

6.4.2 Pulmonary Tumor Dissemination from Non-Orthotopic Sides/Tail Vein Injection

In some case orthotopic inoculation of tumor cells is neither possible nor necessary. If the first steps of the metastatic process are of scientific interest, a primary tumor can be grown wherever it is relevant or readily accomplished. For instance, cancer cells can be injected into the location of a typical locally-spreading of tumor, such as the peritoneal cavity for rabdomyosarcomas and ovarian cancers [46]. The simplest way to model distant tumor metastases into the lung is formation of a primary tumor in subcutaneous tissue. All the aforementioned models are considered to closely reflect a real metastatic process; however, they are considerably time-consuming and not always adequately reproducible.

The classic approach to model the later stages of metastatic process is an injection of cancer cells directly into the venous bloodstream followed by evaluation of their ability to colonize the lung. Cancer cells can be either syngenic or xenografts. As it is widely accepted, the syngenic model will reflect tumor-host interactions, while the

xenograft model can be used to study specific characteristics of cancer cells. Some technical aspects must be considered if tumor cells are injected directly into the tail vein for both physiological and ethical reasons. The total number of injected cells usually does not exceed 200–300 thousand, the cells must be well-suspended and not form visible conglomerates, the maximum injected volume should not exceed 150–200 μl, and the injection must be given slowly with the mouse kept in a comfortable position to allow sufficient respiration. This technique is routinely used in many labs for a variety of experimental settings. The conventional protocol is included in this chapter because it closely models metastatic dissemination in the lungs. Some practically important aspects and relevant illustrations can be found in the methodological chapter published by Box and Eccles in their Methods in Molecular Biology series [47]. The following protocol is partially adopted from their publication:

- Place a mouse in the restrainer.
- Disinfect the whole tail using an alcohol-dampened swab.
- Gently mix the tumor cell suspension and load into syringe without needle
- Attach a sterile needle and, expel any air bubbles leaving the intended volume for injection
- Rotate the tail to locate one of the two lateral tail veins.
- With the needle bevel facing upward and on the same plane as the tail vein, slide the needle in 2 mm. A slight pull on the syringe plunger should reveal a flash of blood in the needle
- hub confirming correct entry
- Push the plunger in very slowly and deliver the cell suspension. The vein will change from dark to light as the cell suspension temporarily replaces the blood. Any resistance or blanching will indicate the needle is not in the vein.
- Remove the needle from the vein and with a sterile gauze swab, apply slight pressure to the injection site until bleeding has stopped.
- Remove the mouse from the restrainer and return to its cage. Observe the mouse for 5–10 min to ensure no recurrent bleeding or acute respiratory disfunction. Control the mice condition over one hour to exclude any ill effects.

Repeat using a fresh needle and new cell suspension for each mouse (loading a syringe with sufficient cells for multiple mice can lead to blood clotting in the needle between injections)

6.5 Evaluation of Experimental Lung Metastasis in In Vivo Models

6.5.1 Vital (whole body) Visualization

Growth of metastases in the lung of laboratory mice can be visualized *in vivo* by imaging techniques, like conventional radiography, computed tomography (CT), positron emission tomography (PET), bioluminescence (BLU) or fluorescence (FLU)

imaging. These methods require the using of specific contrasting reagents [48, 49], cancer cells expressing luciferase (Luc) or fluorescent protein (GFP, NIR) [44, 50]. An optimal combination of mentioned techniques can considerably increase sensitivity and allow an accurate detection and 3-dimensional localization pulmonary metastases with several mm of size [51]. All these methods are well established however details of procedures can be slightly variable depending on experimental setting. More precise and even semiquantitative analysis of cancer cells in animal lung can be done by intravital fluorescence video microscopy of the mechanically ventilated lungs after tracheotomy [28]. This approach allows even visualize and analyze the process of tumor cells adhesion on the endothelial wall.

6.5.2 Ex Vivo Approaches of Lung Metastasis Evaluation

Ex vivo lung metastases can be visualized with various resolutions. The rough analysis can be done after infusion of the lung samples with India ink solution followed by destaining with Fakete's solution. The tumor nodules do not absorb India ink, which results in the normal lung tissue staining black while the tumor nodules remain white [44]. Alternative approach is staining with Bouin's fluids that provides a contrast of white lesions against yellow lung tissue [52]. Contrasted metastatic nodules can be easily counted and measured (Fig. 6.3a, b). These methods are well accepted for determining tumor load on the lungs, however supposes relative low accuracy and resolution.

Much more sensitive method of ex-vivo visualization of lung metastasis was described recently [53, 54]. By using tumor cells stably expressing the lacZ gene encoding the bacterial enzyme β-galactosidase, authors supposed possibility of even single detection (Fig. 6.3c). This is a low-cost and not equipment-intensive, however, relatively laborious method. Cancer cells should be stably transfected with the lacZ gene encoding the bacterial enzyme β-galactosidase that metabolizes the chromogenic substrate 5-bromo-4-chloro-3-indolyl-beta-D-galactopyranoside (X-Gal) to an insoluble indigo blue dye. It allows highly sensitive and selective histochemical blue staining of tumor cells in mouse tissue ex vivo down to the single cell level. More precise detection of small metastases in the lung tissue can be performed by light microscopy after routine histological H&E staining (Fig. 6.4a) or IGH for human- or tumor- specific markers (Fig. 6.4b).

6.6 Quantitative Real-Time PCR-Based Assay of Xenograft Lung Metastasis Model

Despite thier wide establishment, methods described in previous paragraphs do not allow a quantitative analysis. PCR-based techniques could represent a valid option for sensitive detection of metastatic human cancer cells in mouse tissues and several authors have applied PCR for specific cell detection. For instance, Nitsche and

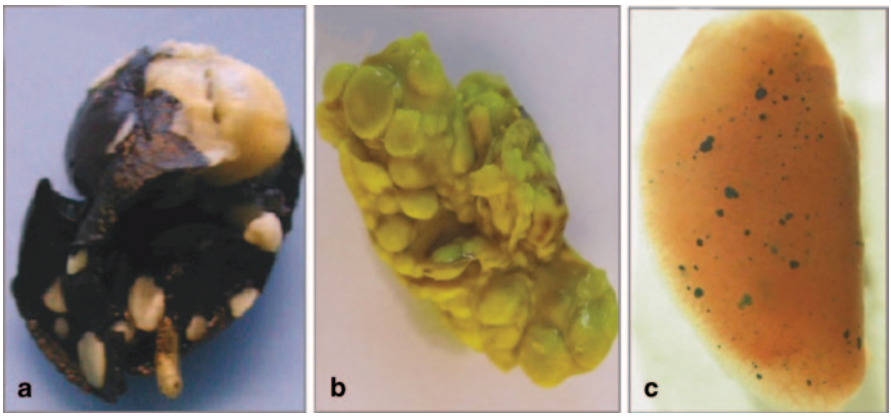

Fig. 6.3 Macroscopic detection of experimental lung metastases. **a** India ink staining (adopted from [44]) **b** Bouin's solutions staining (adopted from [52]) and **c** X-Gal staining for lacZ—expressing cancer cells (adopted from [53])

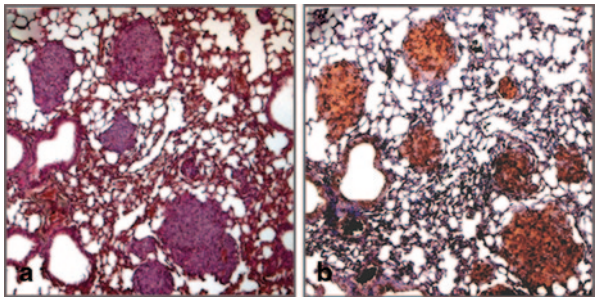

Fig. 6.4 Microscopic detection of experimental lung metastases. Lung metastases developed after i.v. injection of human melanoma cells 1205Lu in nude mice. **a** conventional H&E **b** IHC staining with antibodies against S-100A1 protein

co-authors have described the simultaneous human- and mouse-specific real-time PCR amplification using two different reporter fluorescent dyes to detect xenograft human cells [55]. This method was designed for analysis of blood samples but could be adjusted for any others tissue. However, the threshold of detection was 2 % of human cells, which is barely sufficient in case of solid tumor dissemination. Later, the same group proposed a real-time PCR method based on the amplification of human-specific highly repetitive a-satellite DNA sequences [56]. While the high sensitivity of this technique allowed the detection of one human cell in 10 million mouse cells, it relied on a highly repetitive target sequence in the human genome and thus did not allow reproducible quantification. Likewise, methods based on amplification of the highly repetitive Alu sequence by means of conventional [57] or real-time PCR [58] have the same drawback, since the human genome harbors about 1.1 million copies of the Alu element in a variety of locations and some of them remain actively mobile. This makes it difficult to get equal and reproducible PCR amplification when using primers complementary to the Alu sequence, thus hampering precise quantification. A more accurate detection system was based on an amplification of

Table 6.1 Primers for quantitative real-timePCR assay

(Hu)-specific primers, forward	5′-ctgttttgtggcttgttcag-3′
(Hu)-specific primers, reverse	5′-aggaaaccttccctcctcta-3′
Mouse (Mo)-specific, forward	5′-ttggttgagaagcagaaaca-3′
Mouse (Mo)-specific, reverse	5′-cacacagtcaagttcccaaa-3′

exogenous sequences introduced into the human cell genome prior to the experiment [59]. However, this assay requires a monoclonal population of human cancer cells stably transfected with a specific plasmid, which might interfere with the cell biological properties. Furthermore, the data from this assay must be corrected for the variable number of genomic copies of the plasmid introduced in the cells.

Precise quantification of xenograft metastatic cells in mouse tissue can be done by method described recently [37]. There, species-specific, non-transcribed and conserved regions of the human and mouse genome are selected as targets for PCR amplification. Genomic DNA from the tissue of interest serves as a template for two parallel real-time PCR, and the amount of human cells in a given mouse tissue sample is calculated on the basis of the differences in amplification rates. This method allows highly reproducible detection and quantification of xenograft metastatic cells with the limit of detection below 0.001 % of the total cell number. Method can be applied for almost any type of tissue with consideration of tissue amount taken for analysis. For evaluation of pulmonary metastasis in each experimental animal, it is recommended to use half organ (e.g. right lung) for DNA extraction followed by qPCR analysis and half organ (e.g. left) for routine H&E staining or IHC that allow rough control of the results.

6.6.1 Method Setup

Human (Hu) and mouse (Mo) specific primers for real-time PCR are generated to amplify species-specific, non-transcribed and conserved regions in xenograft (human) and host (mouse) genome. Human (Hu)-specific primers for amplification of 122-bp fragment of a region 7p15-p12 and mouse (Mo)-specific primers for amplification of 181-bp fragment of a region 2F1-F3 of the human and mouse genome, correspondently, are proved and presented in Table 6.1.

These are non-transcribed regions of the human β-actin and mouse β-2-microglobin genes, respectively. One can design other primers pair with consideration of species types (rat, chicken) and optimal length of amplified fragment. Primer specificity must be controlled by conventional PCR before setting of described qPCR-based approach (Fig. 6.5a).

The correlation between the amount of human and mouse DNA in the samples and the amplification efficiency for each primer pair should be estimated to fit the curve and to define equation for experimental data estimation. Any kind of genomic DNA from two species of interest can be utilized for setup the method.

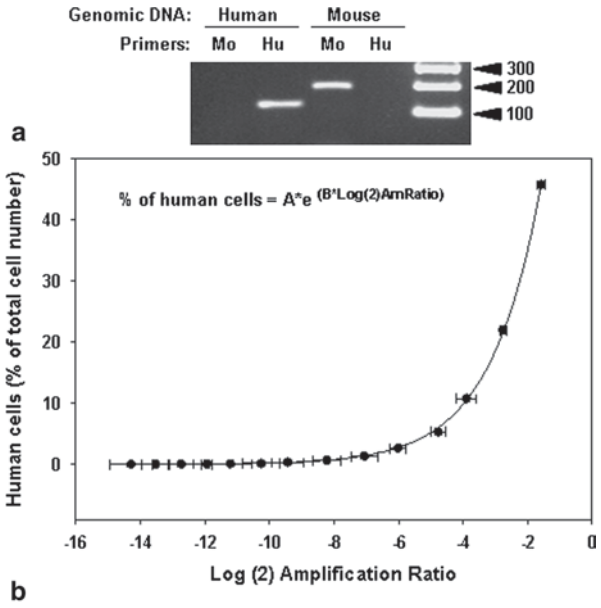

Fig. 6.5 q PCR method setup. **a** Conventional PCR was done with human or mouse genomic DNA and human or mouse -specific primers to confirm the species specificity of both primer pairs. **b** Curve fitting of qPCR data for human and mouse genomic DNA standards. *Y-axis*: Content of human genomic DNA expressed as percentage of human cells (see Table 1 for details). *X-axis*: qPCR quantification shown as mean log(2) Amplification Ratio +/− SD determined in triplicate samples. Adopted from [37]

- A series of standards containing human and mouse genomic DNA with mass percentages of human DNA gradually decreasing from 50 to 0.006 % are prepared (Table 6.2, line 3).
- In order to express the results as percentage of human cells instead of percentage of DNA mass, input data are adjusted for the difference in the size between of the human (~ 3.2 billion bp) and mouse (~ 2.7 billion bp) genomes (Table 6.2, line 4).
- Real-time PCR reactions are performed in parallel with Hu and Mo specific primers with amount of 250–500 ng of DNA mix. Example of resulting Ct are presented in Table 6.2, line 5-6
- The ratios of Hu and Mo amplification rates ('Amp Ratio', Table 6.2, line 7) is calculated as $2^{(CT[Hu]—CT[Mo])}$. The Amplification Ratios underwent $Log_{(2)}$ transformation for easier analysis of samples with low amounts of human DNA (line 8).
- Since standard reactions are performed in three independent experiments, at this stage the average $Log_{(2)}$ Amp Ratio +/− SD for the three paired reactions is calculated (Table 6.2, lines 9–10)
- The results are fitted using a non-linear (logarithmic) regression equation with the amount of human genomic DNA in the sample as the input variable on the x-axis and the $Log_{(2)}$ Amp Ratio on the y-axis (Fig. 6.5b). The value of the independent coefficients A (125.05) and B (0.635) can be determined using SigmaPlot 10.0 software. These coefficients can vary depending on the qPCR kit, equipment, assay conditions and primers, and thus have to be determined for each specific experimental setup.
- To quantify the human cell metastatic load, the initial equation was reversed into a two parameter exponential function ($y=A*exp^{(B*x)}$) where y is the percentage of human cells or human genomic DNA in the sample and x is the Log(2) Amp Ratio.

Table 6.2 Setup of qPCR method

Preparation of standards														
1. Human DNA (ng/μL)	125.00	62.50	31.25	15.63	7.81	3.91	1.95	0.98	0.49	0.24	0.12	0.06	0.03	0.02
2. Mouse DNA (ng/μL)	125.00	187.50	218.75	234.38	242.19	246.09	248.05	249.02	249.51	249.76	249.88	249.94	249.97	249.98
3. Human DNA (% of total)	50.000	25.000	12.500	6.250	3.125	1.563	0.781	0.391	0.195	0.098	0.049	0.024	0.012	0.006
4. Human cells (% of total)	*45.763*	*21.951*	*10.757*	*5.325*	*2.650*	*1.322*	*0.660*	*0.330*	*0.165*	*0.082*	*0.041*	*0.021*	*0.010*	*0.005*
qPCR results and calculations														
5. Ct with human primers	21.780	22.480	23.230	24.040	25.170	26.100	27.190	28.960	29.320	30.470	30.920	31.450	32.770	32.910
6. Ct with mouse primers	20.170	19.650	19.390	19.120	19.200	19.260	19.280	19.460	19.100	19.020	18.920	18.710	18.970	18.920
7. Amplification Ratio	0.328	0.141	0.070	0.033	0.016	0.009	0.004	0.001	0.001	0.000	0.000	0.000	0.000	0.000
8. Log(2) Amp Ratio	−1.610	−2.830	−3.840	−4.920	−5.970	−6.840	−7.910	−9.500	−10.22	−11.45	−12.00	−12.74	−13.80	−13.99
9. Log(2) Amp Ratio mean	−1.577	−2.763	−3.893	−4.770	−6.013	−7.057	−8.220	−9.433	−10.26	−11.21	−11.94	−12.73	−13.52	−14.29
10. Standard deviation (SD)	0.133	0.107	0.304	0.210	0.248	0.419	0.315	0.208	0.173	0.669	0.384	0.230	0.254	0.866
Reverse calculations														
11.Human cells (%)	*46.071*	*21.736*	*10.629*	*6.102*	*2.777*	*1.435*	*0.687*	*0.319*	*0.189*	*0.104*	*0.065*	*0.039*	*0.024*	*0.015*

- Comparison of the experimental data from this reverse calculation with the starting percentage of human cells in the reactions (Table 6.2, line 11 and 4) should show a close correlation, indicating that the method gives correct values over a wide range of human DNA percentage.

6.6.2 DNA Extraction and Real-Time PCR

Any suitable method of genomic DNA isolation and quantitative real-time PCR may be applied. However, considering high sensitivity of PCR it's strongly recommended to stick to the same DNA isolation technique and real-time PCR kit/machine over all steps of the single assay as well as for various experiments are planned to be compared. For the same reason, it is expectable to obtain results variability between experimental animals, therefore using the groups at least for 10 mice is recommended.

- Experimental metastases-bearing mice are harvested, whole lungs are extracted and either froze down with liquid nitrogen or immediately used for DNA isolation.
- Lung tissues is homogenized in urea lysis buffer (2% (w/v) SDS, 10mM EDTA, 0.35M NaCl, 0.1M Tris-HCl, pH 8.0, 7M urea).
- Genomic DNA is extracted (optimally with the standard phenol-chloroform method) and diluted in TE buffer, pH 8.0.
- Real-time PCR is carried out in any suitable LightCycler using the SYBR-Green PCR Master Mix (Applied Biosystems Inc, Foster City, USA) according to the manufacturer's protocol with 250 ng of total genomic DNA. PCR conditions were: 95° for 1 min, 56° for 45 s and 72° for 45 s for 30 cycles, with a first cycle 95° for 10 min.
- In parallel, it is recommended to reproduce several points of standard curve by performing qPCR with several Hu/Mo DNA standard mixtures.

6.6.3 Data Analysis and Statistics

In order to estimate the amounts of human cells in mouse tissues, paired real-time qPCR should be done in triplicate for each sample. Amplification Ratios is determined from the cycle threshold (Ct) according to the formula $R = 2^{(CT[Hu] - CT[Mo])}$ and transformed into $Log_{(2)}R$ for each paired reactions. The percentage of human cells was calculated from the mean values of $Log_{(2)}R$ using the exponential function $Y = A*exp^{(B*X)}$. The A and B constants were determined as described in the section 6.6.1 (see Table 6.2). Results are averaged for each animal.

Averaged results for experimental group of animals are calculated by conventional method. Differences between groups of animals may be assessed with an unpaired two-tailed t-test. Figure 6.6 demonstrate correlation of qPCR (for group of 10 animals) and IHC (one representative example)—based estimation of xeno-

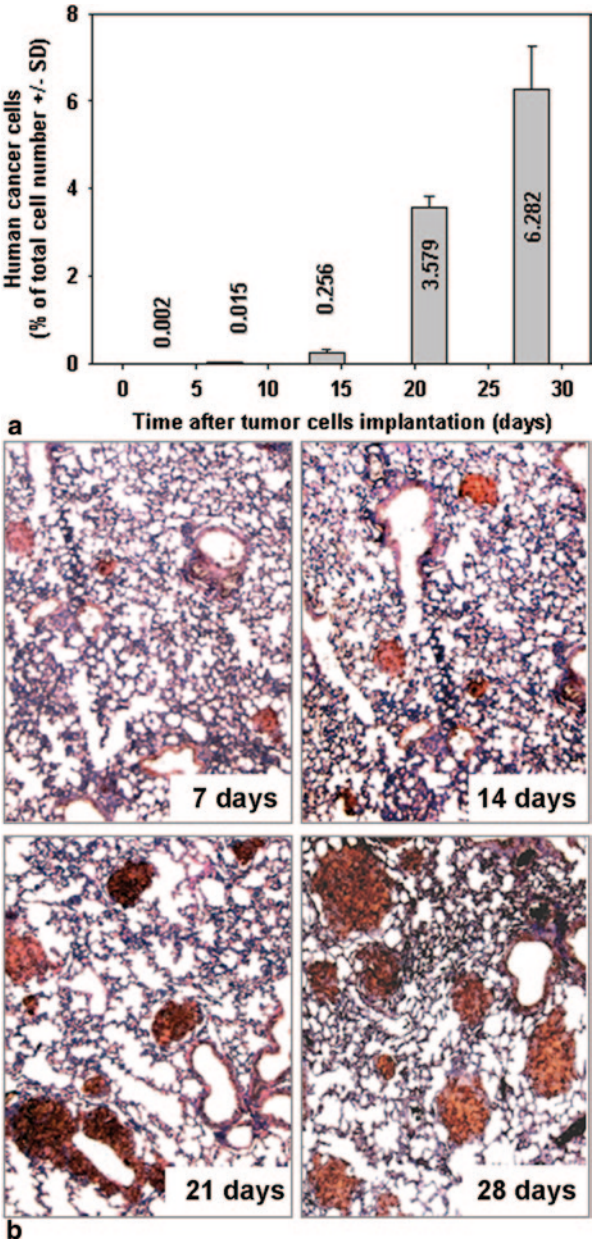

Fig. 6.6 Lung metastases burden estimated by qPCR and IHC. **a** Amounts of metastatic cells in mouse lungs after intravenous injection of human melanoma 1205Lu cells determined by qPCR at 3, 7, 14, 21 and 28 days after cell injection. Results are shown as mean per group ± SD. **b** Tissue sections were prepared from paraffin-embedded specimens of mouse lungs obtained at the same days after cell injection. IHC staining was performed using an anti S-100A1 antibody

graft metastasis burden in lung of nude mice after intravenous injection with human melanoma cells 1205 Lu. Both methods, qPCR and IHC, revealed progressive colonization of lung by tumor cells, however only qPCR approach allow quantification. After being first described in various experimental settings [37], this method was used in others studies by our [60] and others [61] groups.

6.7 Conclusion

As it was mentioned in introduction, metastatic dissemination of lung faces a challenge for practical oncology regardless localization and histological type of primary tumor. Survival rate is currently disappointing, quality of life for patients with advanced secondary cancer of lung is still low while therapeutic approaches are rather palliative.

In parallel with farther investigation of biology of various cancer types that tend to pulmonary colonization, study of proper lung metastasis process is essential and may lead to development of relevant preventive and curative approaches. With considering specific anatomic and physiologic features of the lung that are briefly discussed in this chapter, experimental in *vitro/ ex vivo/ in vivo* models may provide with new insights into general mechanism of pulmonary metastasis. This chapter systematically describes main experimental approaches applied for lung metastasis research with hope to provide researchers with useful theoretical and practical information.

References

1. Ott S, Geiser T (2012) [Epidemiology of lung tumors]. Ther Umsch 69:381–388
2. Schueller G, Herold CJ (2003) Lung metastases. Cancer Imaging 3:126–128
3. Dresler CM, Goldberg M (1996) Surgical management of lung metastases: selection factors and results. Oncology (Williston Park) 10:649–655. (discussion 655–646, 659)
4. Van Schil PE, Hendriks JM, van Putte BP, Stockman BA, Lauwers PR, et al (2008) Isolated lung perfusion and related techniques for the treatment of pulmonary metastases. Eur J Cardiothorac Surg 33:487–496
5. Kycler W, Laski P (2012) Surgical approach to pulmonary metastases from breast cancer. Breast J 18:52–57
6. Vodicka J, Spidlen V, Simanek V, Safranek J, Treska V, et al (2012) [Surgical therapy of pulmonary metastases of colorectal cancer–ten-year results]. Rozhl Chir 91:81–86
7. Osei-Agyemang T, Ploenes T, Passlick B (2012) [Pulmonary metastasectomy: indication and technique]. Zentralbl Chir 137:234–241
8. Schlijper RC, Grutters JP, Houben R, Dingemans AM, Wildberger JE, Raemdonck DV, Cutsem EV, Haustermans K, Lammering G, Lambin P, Ruysscher DD (2013) What to choose as radical local treatment for lung metastases from colo-rectal cancer: Surgery or radiofrequency ablation? Cancer Treat Rev. doi: 10.1016/j.ctrv.2013.05.004
9. Surveillance epidemiology and end results (SEER)—Statistical reports provided by National Cancer Institute (NCI) / U.S. National Institute of Health (NIH) on web site: http://seer.cancer.gov/statistics/
10. Hemminki K, Riihimaki M, Sundquist K, Hemminki A (2013) Site-specific survival rates for cancer of unknown primary according to location of metastases. Int J Cancer 133:182–189
11. Horsfield K (1978) Morphometry of the small pulmonary arteries in man. Circ Res 42:593–597
12. Townsley MI (2012) Structure and composition of pulmonary arteries, capillaries and veins. Compr Physiol 2:675–709
13. Guntheroth WG, Luchtel DL, Kawabori I (1992) Functional implications of the pulmonary microcirculation. an update. Chest 101:1131–1134

14. Guntheroth WG, Luchtel DL, Kawabori I (1982) Pulmonary microcirculation: tubules rather than sheet and post. J Appl Physiol 53:510–515
15. Gehr P, Mwangi DK, Ammann A, Maloiy GM, Taylor CR, et al (1981) Design of the mammalian respiratory system. V. Scaling morphometric pulmonary diffusing capacity to body mass: wild and domestic mammals. Respir Physiol 44:61–86
16. Garcia-Roman J, Zentella-Dehesa A (2013) Vascular permeability changes involved in tumor metastasis. Cancer Lett 335:259–269
17. Claesson-Welsh L, Welsh M (2013) VEGFA and tumour angiogenesis. J Intern Med 273:114–127
18. Criscuoli ML, Nguyen M, Eliceiri BP (2005) Tumor metastasis but not tumor growth is dependent on Src-mediated vascular permeability. Blood 105:1508–1514.
19. Stephen Paget S (1889) The distribution of secondary growths in cancer of the breast. Lancet 133(3421):571–573
20. Mendoza M, Khanna C (2009) Revisiting the seed and soil in cancer metastasis. Int J Biochem Cell Biol 41:1452–1462
21. Auerbach R, Lu WC, Pardon E, Gumkowski F, Kaminska G, et al (1987) Specificity of adhesion between murine tumor cells and capillary endothelium: an in vitro correlate of preferential metastasis in vivo. Cancer Res 47:1492–1496
22. Nicolson GL, Belloni PN, Tressler RJ, Dulski K, Inoue T, et al (1989) Adhesive, invasive, and growth properties of selected metastatic variants of a murine large-cell lymphoma. Invasion Metastasis 9:102–116
23. Okegawa T, Pong RC, Li Y, Hsieh JT (2004) The role of cell adhesion molecule in cancer progression and its application in cancer therapy. Acta Biochim Pol 51:445–457
24. Saiki I (1997) Cell adhesion molecules and cancer metastasis. Jpn J Pharmacol 75:215–242
25. Muller A, Homey B, Soto H, Ge N, Catron D, et al (2001) Involvement of chemokine receptors in breast cancer metastasis. Nature 410:50–56
26. Elzarrad MK, Haroon A, Willecke K, Dobrowolski R, Gillespie MN, et al (2008) Connexin-43 upregulation in micrometastases and tumor vasculature and its role in tumor cell attachment to pulmonary endothelium. BMC Med 6:20
27. Zhu DZ, Cheng CF, Pauli BU (1991) Mediation of lung metastasis of murine melanomas by a lung-specific endothelial cell adhesion molecule. Proc Natl Acad Sci U S A 88:9568–9572
28. Gassmann P, Kang ML, Mees ST, Haier J In vivo tumor cell adhesion in the pulmonary microvasculature is exclusively mediated by tumor cell–endothelial cell interaction. BMC Cancer 10:177
29. Krishnan V, Bane SM, Kawle PD, Naresh KN, Kalraiya RD (2005) Altered melanoma cell surface glycosylation mediates organ specific adhesion and metastasis via lectin receptors on the lung vascular endothelium. Clin Exp Metastasis 22:11–24
30. Ingersoll SB, Langer F, Walker JM, Meyer T, Robson T, et al (2009) Deficiencies in the CD40 and CD154 receptor-ligand system reduce experimental lung metastasis. Clin Exp Metastasis 26:829–837
31. Huh SJ, Liang S, Sharma A, Dong C, Robertson GP (2010) Transiently entrapped circulating tumor cells interact with neutrophils to facilitate lung metastasis development. Cancer Res 70(14):6071–6082
32. Ballas ZK, Buchta CM, Rosean TR, Heusel JW, Shey MR (2013) Role of NK cell subsets in organ-specific murine melanoma metastasis. PLoS One 8:e65599
33. Jordan JL, Nowak A, Lee TD (2010) Activation of innate immunity to reduce lung metastases in breast cancer. Cancer Immunol Immunother 59:789–797
34. Lee H, Lin EC, Liu L, Smith JW (2003) Gene expression profiling of tumor xenografts: In vivo analysis of organ-specific metastasis. Int J Cancer 107:528–534
35. Montel V, Huang TY, Mose E, Pestonjamasp K, Tarin D (2005) Expression profiling of primary tumors and matched lymphatic and lung metastases in a xenogeneic breast cancer model. Am J Pathol 166:1565–1579
36. Tuscano JM, Kato J, Pearson D, Xiong C, Newell L, et al (2012) CD22 antigen is broadly expressed on lung cancer cells and is a target for antibody-based therapy. Cancer Res 72:5556–5565

37. Malek A, Catapano CV, Czubayko F, Aigner A (2010) A sensitive polymerase chain reaction-based method for detection and quantification of metastasis in human xenograft mouse models. Clin Exp Metastasis 27:261–271
38. Andrade CF, Wong AP, Waddell TK, Keshavjee S, Liu M (2007) Cell-based tissue engineering for lung regeneration. Am J Physiol Lung Cell Mol Physiol 292:L510–518
39. Martin MD, Fingleton B, Lynch CC, Wells S, McIntyre JO, et al (2008) Establishment and quantitative imaging of a 3D lung organotypic model of mammary tumor outgrowth. Clin Exp Metastasis 25:877–885
40. Martin MD, Carter KJ, Jean-Philippe SR, Chang M, Mobashery S, et al (2008) Effect of ablation or inhibition of stromal matrix metalloproteinase-9 on lung metastasis in a breast cancer model is dependent on genetic background. Cancer Res 68:6251–6259
41. Mendoza A, Hong SH, Osborne T, Khan MA, Campbell K, et al (2010) Modeling metastasis biology and therapy in real time in the mouse lung. J Clin Invest 120:2979–2988
42. Siminski JT, Kavanagh TJ, Chi E, Raghu G (1992) Long-term maintenance of mature pulmonary parenchyma cultured in serum-free conditions. Am J Physiol 262:L105–110
43. Luu HH, Kang Q, Park JK, Si W, Luo Q, et al (2005) An orthotopic model of human osteosarcoma growth and spontaneous pulmonary metastasis. Clin Exp Metastasis 22:319–329
44. Miretti S, Roato I, Taulli R, Ponzetto C, Cilli M, et al (2008) A mouse model of pulmonary metastasis from spontaneous osteosarcoma monitored in vivo by Luciferase imaging. PLoS One 3:e1828
45. Jia SF, Worth LL, Kleinerman ES (1999) A nude mouse model of human osteosarcoma lung metastases for evaluating new therapeutic strategies. Clin Exp Metastasis 17:501–506
46. Daniel L, Durbec P, Gautherot E, Rouvier E, Rougon G, et al (2001) A nude mice model of human rhabdomyosarcoma lung metastases for evaluating the role of polysialic acids in the metastatic process. Oncogene 20:997–1004
47. Box GM, Eccles SA (2011) Simple experimental and spontaneous metastasis assays in mice. Methods Mol Biol 769:311–329
48. Denoyer D, Greguric I, Roselt P, Neels OC, Aide N, Taylor SR, Katsifis A, Dorow DS, Hicks RJ (2010) High-contrast PET of melanoma using (18)F-MEL050, a selective probe for melanin with predominantly renal clearance. J Nucl Med 51(3):441–447
49. Nimmagadda S, Pullambhatla M, Stone K, Green G, Bhujwalla ZM, Pomper MG (2010) Molecular imaging of CXCR4 receptor expression in human cancer xenografts with [64Cu] AMD3100 positron emission tomography. Cancer Res 70(10):3935–3944
50. Hanyu A, Kojima K, Hatake K, Nomura K, Murayama H, et al (2009) Functional in vivo optical imaging of tumor angiogenesis, growth, and metastasis prevented by administration of anti-human VEGF antibody in xenograft model of human fibrosarcoma HT1080 cells. Cancer Sci 100:2085–2092
51. Deroose CM, De A, Loening AM, Chow PL, Ray P, et al (2007) Multimodality imaging of tumor xenografts and metastases in mice with combined small-animal PET, small-animal CT, and bioluminescence imaging. J Nucl Med 48:295–303
52. Yang F, Huang W, Li Y, Liu S, Jin M, et al (2013) Anti-tumor effects in mice induced by survivin-targeted siRNA delivered through polysaccharide nanoparticles. Biomaterials 34:5689–5699
53. Arlt MJ, Born W, Fuchs B (2012) Improved visualization of lung metastases at single cell resolution in mice by combined in-situ perfusion of lung tissue and X-Gal staining of lacZ-tagged tumor cells. J Vis Exp:e4162
54. Hauser S, Bickel L, Weinspach D, Gerg M, Schafer MK, et al (2011) Full-length L1CAM and not its Delta2Delta27 splice variant promotes metastasis through induction of gelatinase expression. PLoS One 6:e18989
55. Nitsche A, Becker M, Junghahn I, Aumann J, Landt O, et al. (2001) Quantification of human cells in NOD/SCID mice by duplex real-time polymerase-chain reaction. Haematologica 86:693–699.
56. Becker M, Nitsche A, Neumann C, Aumann J, Junghahn I, et al. (2002) Sensitive PCR method for the detection and real-time quantification of human cells in xenotransplantation systems. Br J Cancer 87:1328–1335.

57. Kim J, Yu W, Kovalski K, Ossowski L (1998) Requirement for specific proteases in cancer cell intravasation as revealed by a novel semiquantitative PCR-based assay. Cell 94:353–362.
58. Schneider T, Osl F, Friess T, Stockinger H, Scheuer WV (2002) Quantification of human Alu sequences by real-time PCR–an improved method to measure therapeutic efficacy of anti-metastatic drugs in human xenotransplants. Clin Exp Metastasis 19:571–582.
59. Eckhardt BL, Parker BS, van Laar RK, Restall CM, Natoli AL, et al. (2005) Genomic analysis of a spontaneous model of breast cancer metastasis to bone reveals a role for the extracellular matrix. Mol Cancer Res 3:1–13.
60. Malek A, Nunez LE, Magistri M, Brambilla L, Jovic S, et al. (2012) Modulation of the activity of Sp transcription factors by mithramycin analogues as a new strategy for treatment of metastatic prostate cancer. PLoS One 7:e35130.
61. Milanesi A, Lee JW, Li Z, Da Sacco S, Villani V, et al. (2012) beta-cell regeneration mediated by human bone marrow mesenchymal stem cells. PLoS One 7:e42177.

Chapter 7
Liver Metastases

Ann F. Chambers and Jason L. Townson

Abstract The liver is a common site of metastases that originate from diverse types of primary tumors, second only to lymph nodes as the most frequent metastatic site. As a vital organ with a number of varied functions, organ damage due to metastatic disease is associated with profound morbidity and mortality. The multiple functions, large blood volume as well as the unique anatomy (dual blood supply, fenestrated endothelium and sinusoids) of the liver play an important role in the frequency of liver metastasis. Yet, while a substantial knowledge base has been generated regarding the liver as a metastatic site, development of therapeutic options to treat liver metastases has not progressed as rapidly. Though metastasis is often studied in models that reduce the system to individual steps, a fully integrated understanding of the process, and the critical steps that may be targeted by therapy, remains incomplete and is likely necessary to develop suitable therapies. Towards this goal, in this chapter we describe the process of metastasis, liver anatomy and function, and models of liver metastasis and analysis.

Abbreviations

(CAM)	chorioallantoic membrane
(HCC)	hepatocellular carcinoma
(IVVM)	intravital videomicroscopy
(MRI)	magnetic resonance imaging
(PCR)	polymerase chain reaction
(PET)	positron emission tomography
(SPECT)	single photon emission computed tomography

A. F. Chambers (✉)
London Regional Cancer Program and Department of Oncology,
University of Western Ontario, London, Canada
e-mail: Ann.Chambers@lhsc.on.ca

J. L. Townson
The University of New Mexico, Center for Micro-Engineered Materials, Albuquerque, USA

A. Malek (ed.), *Experimental Metastasis: Modeling and Analysis,*

DOI 10.1007/978-94-007-7835-1_7,

7.1 Introduction—Metastasis and the liver

As with the detection of metastatic cancer in most organs, incidence of liver metastasis is correlated with short survival times [1–6]. This frequently poor outcome prevails despite an expansive and rapidly growing body of literature detailing the underlying causes and mechanisms that control cancer progression, and corresponding (though not as rapid) improvements in cancer therapies that have led to increased survival rates for multiple types of cancer. Yet many aspects of cancer progression, including cancer metastasis, remain incompletely understood. This is in part due to the complex, multistep nature of the metastatic process, during which a significant number of intrinsic variables play a role in progression. This includes the tissue of metastatic cell origin as well as destination, route of travel, normal host and metastatic cell genetic and protein expression variations [7–10]. As such, what may be considered a significant regulatory mechanism at one particular step in the metastatic process, which may allow or inhibit progression at that particular step, may be inconsequential if the cell is incapable of overcoming later steps in the metastatic cascade. Further, as metastatic spread has often occurred at the time of diagnosis and initial treatment, a focus on later (and highly inefficient) steps in the metastatic process is often necessary [11]. In addition to the expanding knowledge regarding cancer progression mechanisms, earlier detection and improved therapeutic interventions have been credited with increased survival, mainly due to treatment prior to the occurrence of overt metastatic cancer [12]. However, this is once again an incomplete explanation, as grade and size are correlated with metastatic disease but are not the sole determinant. This incomplete understanding of the metastatic process, and a corresponding lack of translation of known mechanisms to effective systemic treatment options specifically designed for metastatic disease, highlight the need for research specifically focused on further elucidation of the metastatic process and design of suitable, and more efficacious, treatment options.

While the individual steps that a cancer cell must take (detailed further below) in order to successfully form a metastatic tumor are generally understood, a comprehensive and integrated understanding of the entire process for all cells within a given population remains incomplete. The limited overall efficacy of a number of therapies that were expected to specifically inhibit specific steps in the metastatic process (e.g. matrix metalloproteinase inhibitors, angiogenesis inhibitors, etc.) highlight the need for improved understanding and better ability to translate experimental findings to the clinical setting [13]. Indeed, a number of basic principles remain far from understood, including the concepts of parallel and serial metastatic progression, the nature and roles of cancer stem cells or other metastatic cell subpopulations, the microenvironment etc. [14–18]. Further complicating the issue is the heterogeneous nature of metastatic progression among individual patients and even among cells originating from the same primary tumor [19]. Finding appropriate models to recapitulate such complexity, and understanding the data they yield, is a significant challenge. In order to facilitate such research, here we present an overview of basic concepts of metastasis, focusing on the liver as a secondary site,

while also examining experimental models that have allowed a significant knowledge base to be generated.

The overall process of metastasis itself has been well documented and at its most basic can be described as consisting of cells leaving a primary tumor, invading local tissue, intravasation into blood or lymph vessels, circulation and survival in these vessels, arrest in a secondary tissue, extravasation, initiation and continuation of growth and angiogenesis [7–10, 20]. Indeed, breaking down the process into such steps has allowed for identification of factors contributing to, and mechanisms controlling, various steps of the process [21–26]. Yet despite this understanding of individual steps that control specific steps of the metastatic process, an integrated and complete understanding of the mechanisms controlling all steps in this process remains incomplete.

Metastasis in general remains a significant clinical problem. However, some organs are more prone to development of clinically apparent metastatic tumors than others [7, 20]. In particular, the liver is a frequent site of metastasis from multiple primary cancers including colorectal, pancreatic, breast, melanoma (skin and uveal), esophageal, gastric and liver cancer itself [27–29]. Considering the number of critical roles the liver plays, disruption of normal liver function can have significant effects on normal body function and ultimately on survival. Additionally, while the full role of the microenvironment on metastatic progression is still far from completely understood, the diverse range of functions performed by the cells of the liver may produce niche microenvironments that spatially and temporally affect disease progression. In order to provide a context for the nature of metastatic progression in the liver we provide a brief overview of the anatomy and function of the liver before describing models of liver metastasis. A number of anatomical and physiological factors including the unique vasculature, size, diverse functions and location all likely play an important role in not only metastatic progression, but in the design and analysis of in vivo models of metastasis. As with any model system, each has specific advantages, disadvantages and limitations and thus the model should be chosen carefully with full regard to the ability of answer the specific questions and hypotheses being addressed. This is of particular importance in models of a process as complicated as metastasis, as too broad a focus can easily be paid to a mechanism or step that may not ultimately be a significant rate limiting step in progression, or a suitable candidate for therapeutic intervention.

7.2 Anatomy of the Liver

The liver is located immediately below the diaphragm in the upper part of abdominal cavity. As both the largest internal organ and gland, it performs a number of vital functions including blood filtration, detoxification, bile production, glycogen storage, protein synthesis, hormone production and regulation of immune responses [28]. As a whole, the liver is traditionally described as divided into 4 lobes (left, right, caudate and quadrate), each divided by a number of ligaments and overlying the gallbladder.

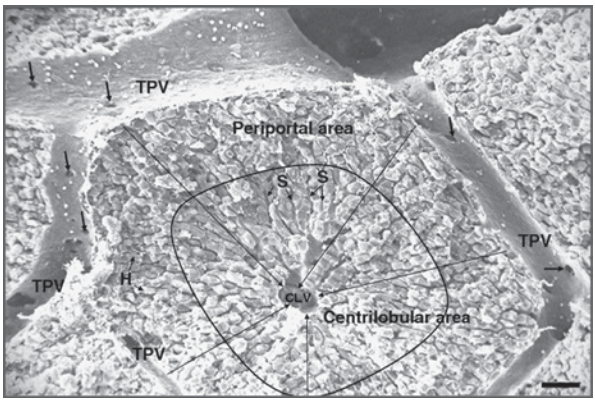

Fig. 7.1 Liver morphology, as seen by scanning electron microscopy. Terminal portal veins (*TPV*) surround hepatic lobules. The hepatocytes (*H*) are arrayed in flat plates surrounding a centrilobular vein (*CLV*). The sinusoids (*S*) provide a microvasculature within the lobules. Blood flows through openings in the terminal portal veins (arrows) into and through the sinusoids, and is collected by centrilobular veins (*CLV*), and then to interlobular veins and to the suprahepatic vein (not shown). Also not shown, perilobular arteries, lymphatic vessels, nerve fibers and bile ducts, which also contribute to the portal tracts occupied by the TPV. *Bar: 50 μm* (reprinted with permission from [116])

The lobes themselves are further subdivided into functional areas that are primarily defined as regions of tissue fed by a branch of the portal vein. At the histological level, the liver is divided into lobules that are hexagonal in structure and composed of branches of the terminal portal vein and artery, bile ducts, liver sinusoids and hepatic venules (Fig. 7.1). The primary structural organization of the lobules are the liver sinusoids, which themselves are composed of diverse types of cells including hepatocytes, endothelial cells, and macrophages/Kupffer cells, which are responsible for the equally diverse functions completed by the liver.

Having a vital role in metabolism and maintenance of blood composition, and of particular significance in terms of haematogenous dissemination of metastatic cells, the liver is supplied by two major vascular branches; the hepatic artery and portal vein. Of the two, the portal vein is responsible for the majority (~70%) of the blood delivered to the liver [30–32]. It should thus be of little surprise that a number of organs drained by the vessels feeding into the portal vein (including the colon, stomach, pancreas, esophagus and spleen) are common sites from which liver metastases originate. In contrast, the arterial blood delivered via the hepatic artery does not directly originate from upstream organs, but is instead oxygenated blood delivered from the heart via the abdominal aorta. As such, blood arriving via the hepatic artery is filtered through capillaries of several organs, including the lung, prior to arriving in the liver. Studies that have examined the growth of metastases from cells originating from the portal vein or hepatic artery have found that greater than 70% of liver metastases likely arrive in the liver via the portal vein [33–36] (Table 7.1). However, the presence of breast, melanoma (skin and uveal), renal, ovarian and

Table 7.1 Incidence of liver metastasis via the portal vein and hepatic artery

Primary site	Incidence rate	Route
Liver	49% [36]	Portal vein
Colon	78% [36]	Portal vein
Rectum	71% [36]	Portal vein
Esophageal	52% [36]	Portal vein
Gastric	39% [36]	Portal vein
Pancreas	85% [36]	Portal vein
Melanoma	58% [117]	Hepatic artery
Breast	30% [36]–32%	Hepatic artery
Lung	16% [36]	Hepatic artery
Ovarian	13% [36]	Hepatic artery or peritoneal spread
Prostate	4 [36]–9% [33]	Hepatic artery

lung cancer metastases in the liver indicate that the frequency of metastatic growth in the liver is not only due to the sheer number of cells that arrive directly in the liver via the portal vein system, but also due to the relatively hospitable "soil" of the liver.

The exact role of a number of the unique anatomical features (e.g. sinusoids, fenestrated and phagocytic endothelium, etc.) and the complex and diverse metabolic functions of the liver on the progression of metastasis remain to be further explored. For example, how do the blood flow pattern, nutrient or toxin levels at various times post injection, specific cellular metabolic functions and the local cell and microenvironment heterogeneity, etc., influence metastatic cell fate and progression? Additionally, taking into account that the liver is large, highly dynamic and multifunctional organ, would specific factors both promote and inhibit metastases in the same organ at different times? In any case, because the liver is a vital organ, compromise of liver function by growth of metastases can lead to significant quality of life consequences for patients, and can results in patient death.

7.3 Experimental Models of Metastasis

The inefficiency of the metastatic process, by which few of the cells that leave a primary tumor successfully form a macroscopic metastasis, has been well validated by clinical data and experimental models [7, 37, 38]. The overall inefficiency of this stepwise process highlights the fact that individual steps within the process are regulated by a variety of cancer cell and micro-environment influenced mechanisms which the majority of cells shed from a primary tumor are not suitably equipped to overcome. In general, the methods used to understand and quantify metastasis reflect this multistep nature and examine only specific steps of the process. The use of mice with primary tumor formation and subsequent metastatic cell dissemination due to genetic modification, spontaneous growth or chemically induced tumors, allows for monitoring progression of cancer cells throughout the process [39]. However, limited availability, accessibility, significant variability and the often extended experimental time required to study spontaneous models makes them less attractive

and less frequently used than experimental metastasis models. As such, both models of metastasis in general, and liver metastasis in particular, are most frequently performed using in vitro surrogate models or in vivo experimental models generally using mice, or in some cases rats or avian embryos. While any number of avian embryos and small or large mammals can be used as models, due to their common use (well characterized), reasonable cost and general availability we will primarily focus on mouse and chick embryo models.

7.3.1 In Vitro Models of Steps in the Metastatic Process

The multistep and multi-organ nature of metastasis essentially precludes the study of the entire process in vitro and thus necessitates that in vitro assays be used in a greatly minimized and focused manner in order to study specific steps in the process. Indeed, a number of assays have been developed which are meant to quantify and understand specific steps in the process including invasion, migration etc. [40–45]. However, as these models do not recapitulate the anatomical and functional complexity of the liver and are more general in nature, detailed description of these techniques and assays can be found in literature focused on that particular subject. In a general context, the effect of the microenvironment on cancer cell growth is applicable to all metastatic sites. Multiple in vivo studies using mice for experimental models of liver and lung metastasis have revealed that the fate of individual cells is diverse, with some remaining dormant, many undergoing apoptosis and only a small subset forming micrometastases and eventually large metastases [7, 46–49]. Along these lines, studies using 3D in vitro models in which cells are grown in basement membrane matrix gel (e.g. Matrigel™ and Cultrex®) have demonstrated that the growth of cells in 3D more closely replicates in vivo growth than 2D culture [40, 50–53]. This includes the observation that mixed cell populations in which extended periods of single cell dormancy, frequently observed in vivo but not in 2D culture, are observed in various proportions of the cells dependent on cell line. Co-culture methods and custom fabrication of tuneable (size, shape, modulus) microenvironments for 3D culture may present an opportunity to build increasingly complex microenvironments, however significant functional diversity observed in the liver would still be absent [42, 54–59].

7.3.2 General Consideration of in Vivo Metastasis Models

In the same way that the majority of in vitro ‘metastasis assays’ essentially isolate individual steps of metastasis in order to examine the mechanisms of that specific step (often in a greatly simplified way), liver metastasis models can be modified in order to recapitulate only certain steps in the process. Spontaneous metastasis models are models in which cells naturally disseminate from a primary tumor to secondary site, regardless of the nature of the primary tumor (chemically induced,

genetic, transplanted tissue, injected cells etc.) [39]. As such, cells complete all steps of metastasis, including primary tumor growth, migration from primary tumor intravasation into the circulation/lymphatics, delivery to secondary sites, extravasation and growth. In comparison, experimental metastasis models commence by injection of cells directly into the vasculature (blood or lymph) feeding a secondary tissue in order to introduce cells systemically or target cells to a particular site.

In the case of experimental liver metastasis models, a broad definition would include injection and arrival of cells via arterial blood flow, direct injection of the cells into the liver, or more commonly, via the portal vein system (either directly or injection via organs draining into the portal system such as the spleen) [39]. While spontaneous models may offer the benefit of recapitulating the entire process of metastasis, they are generally highly variable and require longer experimental times. Additionally, a number of experimental models have demonstrated that cell death leading to inefficiency of the metastatic process can occur after cell arrival in a secondary site [7, 46–49, 60]. As such, while experimental metastasis captures only the steps in the metastatic process following intravasation, steps following extravasation have been shown to be highly inefficient and thus elucidating the factors responsible for cell progression, or conversely loss of cells, may lead to development of logical therapeutics. Additionally, experimental models of liver metastasis offer a higher degree of control over the cell population being introduced into the liver, including the number and timing of cells injected, co-injection of other cells and/or particles, genetic or protein expression modification of the cells and pre-labelling with imaging contrast agents. As the vast majority of cells injected via the portal vein into the liver have been shown to arrest in the liver, the direct introduction of cells vs spontaneous dissemination from a primary tumor also allows for extended periods of observation that can be limited by primary tumor induced endpoints (size or morbidity) [46, 61, 62]. In the context of mimicking natural disease progression, introduction of cancer cells to the liver via the portal vein follows the natural path of many types of cancer, including colon, gastric and esophageal, for which embedding these cells in their natural site of origin would add significant technical complication. Loss of the influence of the organ of primary tumor growth may have an effect on growth in a secondary site, however most experimental animal models do not actually recapitulate normal primary tumor progression, largely negating this factor. While tumors originating from primary cancers such as breast and melanoma are not believed to arrive in the liver via the portal system, the hepatic artery and portal vein converge at the level of the liver sinusoid. This ensures that while the route of travel is not identical, the microenvironment of arrest is appropriate [29, 63].

7.3.3 Avian Embryo Models—Chick Chorioallantoic Membrane (CAM)

Avian embryo models, and in particular the chick chorioallantoic membrane (CAM), have been well characterized for their use as a model tumor progression, including

metastasis and angiogenesis [64–67]. While used less frequently than some other animal models (i.e. mice and rats), chick embryo models offer a number of practical advantages including relatively simple housing and maintenance requirements and lower overall cost [64, 68–70]. From a technical perspective, avian models of tumor progression have additional advantages relative to both in vitro and other in vivo models. Compared to in vitro models, avian embryos (depending on their embryonic development when used experimentally) provide a complex in vivo environment (diverse cell types, vasculature, blood flow, filtering organs etc.) that allows multiple steps of metastasis to be studied sequentially. In comparison to larger mammalian animal models, chick embryos are easier to house and maintain, provide an accessible surface for imaging (the CAM generally or deeper tissue using near infrared (NIR) imaging techniques), are naturally immunodeficient until late in embryo development, and can be used in large number to facilitate higher throughput experiments. Some limitations of the embryo model include the sensitivity of the developing embryo to cytotoxic therapeutics, the closed system (i.e. no elimination administered chemicals) and shorter observation period that can reduce the ability to determine therapeutic efficacy in this model. As a model for metastatic progression however, the ability to image at the sub-cellular level is a distinct benefit.

Chicken embryos develop for 21 days before hatching. The embryo itself is protected and nourished by three membranes, the yolk sack membrane, the amnion and the chorioallantoic membrane, all of which are naturally enclosed by the egg shell. Experimental tumor models using the chicken embryo can be performed either in the egg shell (in ovo) or after removing the egg shell (ex ovo). Detailed protocols for both methods have been described in detail previously [64, 65, 67, 68, 71–73], with videos of the technique also available [73–75]. The general experiments that can be performed using either method are similar, with the most significant difference between the two methods being simply the presence or absence of the egg shell and the corresponding decreased viability and increased surface access (to the CAM) using the ex ovo method. This surface access allows for a large area on which multiple tumors can be implanted and imaged longitudinally at high resolution [67, 76]. While the CAM and its dense vasculature are most commonly used as the site of tumor cell growth and arrest, liver metastasis models can be performed using the chick embryo model via either spontaneous metastasis or injection of cells via the CAM vasculature [72]. Indeed, blood returning to the embryo form the CAM drains into the portal system and first passes through the liver of the embryo, arresting most of the cells and facilitating use as a liver metastasis model [77–78]. Analysis of liver metastasis has been performed by a number of methods including electron microscopy, polymerase chain reaction (PCR) based techniques to detect human cells within the liver, recovery of the cells from the embryo (via tissue dissociation and selective pressure) or by using fluorescent cell lines or histological techniques in order to visualize the metastases [64, 70, 73, 77–81]. The proximity of the embryo to the surface in the ex ovo model may also allow for direct observation of metastasis using tissue penetrating imaging techniques including near infrared (NIR) excitation and emission or multiphoton microscopy [82]. While the chick embryo has been used primarily to study progression and liver metastasis of solid

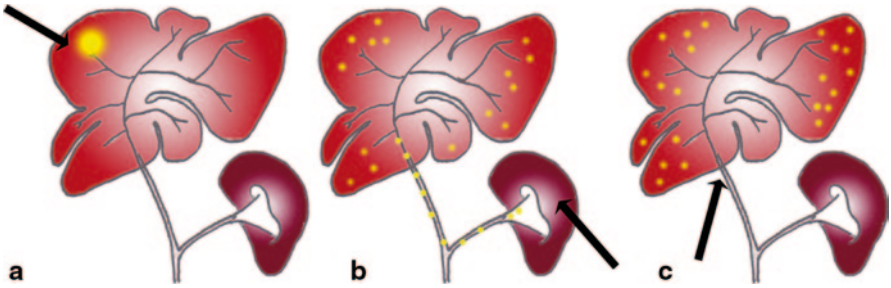

Fig. 7.2 Establishment of single and disseminated liver metastases. The model of single liver macrometastasis is established by subcapsular injection of tumour cells or implantation of tumour tissue (**A**). The model of disseminated liver micrometastases is established by intrasplenic (**B**) or intraportal (**C**) injection of cancer cells

tumors, this model has also been used to study progression of human leukemia cell lines that were found to form granulocytic sarcomas in the CAM and were detected in the liver and other organs by PCR. Interestingly, tumor engraftment was rapid and occurred in 100 % of eggs injected via the vasculature or amnion, but not the yolk sack or direct CAM implantation [81].

7.3.4 Rodent Models

Rodent models, and in particular mouse models, have been used extensively in order to study the process of liver metastasis [62, 83–88]. The method of introducing cancer cells into the liver however varies significantly with the most common injection routes including direct injection into one or more lobes of the liver, via the portal vein system or indirectly through injection of cells into the spleen [46, 63, 83, 84, 89–91] (Fig. 7.2). As with any experimental model, each has distinct advantages and disadvantages and should be chosen in the context of the experiment and hypothesis to be addressed. For instance, while direct injection into the liver is a simpler surgery, it recapitulates only the last steps of metastatic progression (from most primary tumors), sustained growth and angiogenesis. As such, this model would be limited to experiments examining the effect of treatment on large metastatic tumors. Additionally, while the size of cell clusters has been shown to influence metastatic progression, cell clusters that arrive in the liver via the blood vasculature would not be expected to aggregate as a dense population of millions of cells present following direct liver injections. The significant exception to this is that the most frequent site of metastasis for hepatocellular carcinoma (HCC) is the liver itself, making direct injection of cells into the liver a reasonable model of primary orthotopic HCC growth with subsequent local metastases [36]. Overall, a significant advantage of rodent, and in particular mouse models of liver metastasis, is the wealth of publications that detail the growth of a wide variety of cell lines, both mouse and human, in multiple strains (and with different immune status) of

mice [62, 83–86, 88, 90]. As with any mouse experiments, the ability to genetically engineer mice in order to examine the influence of specific molecules and host cell types, or express reporter genes (e.g. fluorescence), allows for an expanded level of control over the microenvironment.

As the primary methods of introducing cells into the liver for metastasis models, the use of splenic injection and portal vein injections (Fig. 7.2) have a number of similarities and subtle differences that require discussion. The primary similarity between the two methods is arrival of the cells via the portal vein. Despite this, the rate and proportion (of injected population) of cancer cells, and accompanying cell types in the case of splenic injections, differ. Given the influence of the microenvironment on cancer progression and metastasis, this should not be overlooked. Indeed, studies examining liver metastases following splenic injections have found that cells from the mouse spleen are co-localized with the injected cancer cells in the liver and that in certain cell lines splenic injections are more efficient [92]. While the exact mechanism of this increased efficiency is unknown, it is likely similar to studies demonstrating that clusters of cells injected into the portal vein yield more metastases than individually injected cells [87]. Additionally, it has been suggested that cancer cells coated with red blood cells/platelets may exhibit increased metastatic efficiency [93]. As a method of cell injection, cannulation of the portal vein has also been reported, allowing for subsequent injection of systemic therapy directly to the liver as is sometimes done clinically [94].

Injection of cells via cardiac or intravenous injection can also be used to deliver cells systemically, including to the liver. These injection routes will however result in arrest of the vast majority of cells in the organ in which they the first encounter a capillary bed (e.g. lung for intravenous injections; multiple arterially supplied organs for intracardiac injections) [7, 95]. The ease of intravenous injection would make this method preferred for high throughput studies and indeed would be the logical method of injection for cells that pass through other organs prior to arriving in the liver (breast, lung, melanoma etc.). Indeed, some melanoma cell lines have been found to survive or grow primarily or exclusively in the liver following i.v. injections [85]. While a technically simpler method of introducing cells into the liver, cell lines that grow well in the lung (or any other site) will limit the observation period as most will arrest and grow in this site. Intracardiac injections via the right side of the heart would be similar to intravenous injections. However, injection into the left side of the heart would be expected to deliver cells to organs proportionally to blood flow patterns. In this case a significant proportion of cells would be expected to be delivered to the digestive system, including to the liver [7, 95]. Preferential growth in the liver would then be a function of the liver “soil” [20].

7.4 Imaging and Analysis Techniques

A significant challenge when trying to dissect the entire metastatic process is the simultaneous need to image a large number of metastatic cells in multiple diverse cell microenvironments at a molecular to organ or even whole animal level. These com-

peting requirements often force the decision to monitor either small subpopulations of cells with high resolution (generally by optical microscopy of tissue sections or in vivo using intravital videomicroscopy (IVVM) or the entire population of cells via non-invasive imaging methods (e.g. magnetic resonance imaging (MRI), ultrasound, whole body fluorescence (FLU) or bioluminescence (BLU), radio labelling etc.) [67, 83, 86, 96]. The location of the liver provides additional challenges for imaging as the large size of the organ, its internal location and constant movement all pose technical hurdles. These challenges have in large part been overcome by advances in gating and surgical techniques, contrast agents and imaging hardware, but are not yet routine or simple. The decision to monitor smaller numbers of cells with high resolution, larger populations at lower resolution, at single time points (histology) or longitudinally must still be made in most cases. With continuing advances in imaging hardware and the availability of multi-purpose, multi-modal imaging contrast agents (and diagnostics and drug delivery vehicles), the technical capability to serially or simultaneously deliver therapeutics and image the same population of cells via multiple imagining methods exists, however is still technically challenging in vivo [97–99].

7.4.1 Optical Microscopy

Optical microscopy has the advantage of resolution at the sub-cellular (sub micrometer) level, but this is counter balanced by the currently limited depth of penetration, significant image degradation due to motion artifacts and limited field of view. Yet, as metastatic progression is controlled at the cellular (both intra and inter) level, microscopy has and continues to be indispensible in identifying many basic characteristics and mechanism of the metastatic process. For analysis of liver metastasis at a single time point, microscopy is often used to image and quantify cells or tumors in thin or thick sections (with various cell stains or fixation methods) of tissue. In order to image the metastatic process in vivo, IVVM has been well documented with detailed techniques described previously [65, 67, 71, 74, 95].

The ability to section and stain liver tissue to be analyzed by microscopy has a number of advantages including technically simple (can reduce background signal and no motion) imaging procedures and a large number of stains that can be used to label different cells types in order to facilitate identification and quantification. However, limitations exist in the type of information that can be gathered from what is essentially a snapshot of a dynamic process. As a measure of quantification of the fate of cells, or the effect of treatment on progression and size of metastases, analysis of histological sections is still a preferred method. Indeed, significant data regarding metastatic cell fate following arrest in the liver has been generated via thin or thick section analysis of tissue [46, 62, 88]. These studies have revealed that the majority of cells arriving in the liver undergo apoptosis, while smaller proportions, dependent on cell type, remain in the liver as dormant cells (so-called dormant cancer cells, DCC) or begin proliferating to form metastases [46, 47, 62, 88].

A wide variety of contrast agents (often fluorescent), labels and stains exist and are suitable for in vivo use. The choice of cell label is significant as it can considerably alter the type of information that can be obtained from the experiment. While somewhat more limited than options for staining histological samples, a number of methods can be used to highlight specific anatomy (commonly vascular dyes—variable "leakiness") or label metastatic cells. This includes cell lines stably expressing fluorescent (FLU) or bioluminescent (BLU) proteins or labelled with inorganic particles or dyes of various excitation and emission properties, e.g. [83, 88, 100, 101]. Cells can be labelled transiently with fluorescent particles prior to injection in order to facilitate their tracking by optical microscopy or in combination with other modalities such as MRI [83, 88, 90, 100]. Advantages of nano or micron sized particles are their often increased optical properties including brightness, stability and defined excitation and emission spectra. Additionally, many novel nanoparticles are being designed to act as contrast agents for multiple imaging modalities simultaneously [97, 98, 102].

Though the maximum resolution for optical microscopy is currently higher than other imaging modalities (nano scale for super resolution techniques), in vivo imaging of the liver is complicated by its internal location and constant movement. However, a number of techniques for stabilization and tissue access have been published, including exposing and securing the liver to underlying cover glass or using a surgically implanted window to image micrometastases and even solitary cells [95, 103]. In the context of understanding and quantifying the fate of individual metastatic cells, portal vein injections have an advantage of delivering nearly all cells, and cell sized particles, directly to the liver to be arrested in the vasculature. This physical arrest of cells and particles by size has been used in order to account for cells by co-injection of fluorescent reference particles [46, 62, 95]. In this way the fate of cells in reference to particles can be quantified.

Overall, the greatest current advantage of optical microscopy analysis of liver metastasis is the ability to directly image intra- and inter-cellular events that may be obscured by imaging larger tumors or indirect cell indicators (e.g. iron oxide for MRI). As much of the cell-microenvironment is different by location within the liver, it is probably ultimately necessary to use such high resolution imaging in order understand metastatic progression and the subcellular/intracellular events controlling progression mechanism. However, the addition of whole animal molecular imaging may capture large scale differences in growth, blood flow patterns, metabolic activity etc., which would not be apparent with the limited field of view possible using optical microscopy.

7.4.2 Whole Animal Imaging Techniques

Advances in the field of non-invasive whole animal imaging, with an emphasis on molecular imaging, have continued to improve the resolution of a number of imaging modalities to the point that they are able to detect smaller tumors, and in some

cases individual cancer cells within an intact organ or animal [83, 90, 96, 100, 104–107]. It should be noted that while molecular or single cell imaging non-invasive imaging is indicative of the presence or activity of cells, it is generally not truly at the molecular level per cell but the average of many cells (e.g. PET, SPECT tracers), the minimum number and characteristics of which differ based on the contrast agent and sensitivity of the particular modality. Though not directly imaging the subcellular events of individual cells, a possibly significant benefit of non-invasive whole animal imaging is the lack of invasive surgery that could have effects on tumor progression. This is due to experimental and clinical studies in which results indicate invasive surgery may have an effect on shedding of cells from the primary tumor as well as subsequent growth [108–110].

Most common and clinically used imaging modalities are available and have specifically designed hardware for imaging of small animals including mice. This includes MRI, SPECT/CT, PET and ultrasound. The advantages and limitations of these common imaging modalities, including their cost, contrast agents and resolution have been reviewed thoroughly elsewhere [105]. It is worth noting however that in all cases, resolution using small animal equipment is now generally sufficient to detect the presence of micrometastases, if not single metastatic cells. This resolution can vary significantly though and requires substantial optimization of gating techniques, pulse sequences, image reconstruction algorithms and the choice/availability of contrast agents. An example of advances in the convergence of hardware, software and contrast agents for multimodality imaging is highlighted by the use of dual magnetite (for MR) and fluorescent (optical) particles that have facilitated quantification of solitary metastatic cells in multiple organs, including the liver, using both modalities [90, 100]. However, in this situation optical microscopy is still used to validate the presence of solitary cells as detected by signal voids (due to iron oxide) in MRI images. This is because the majority of contrast agents for non-invasive imaging are indicative of the presence of the contrast agent and not a metastatic cell. Retention of pre-loaded (in or on the cell) contrast agent, or preferential co-localized of post injected contrast agent are therefore assumed and must be validated.

As with the model of metastasis used, the choice of imaging modality should be chosen based on experimental questions to be answered. An illustration of the tradeoffs that must be made when choosing an imaging modality for analysis of liver metastasis growth is highlighted by a comparison of data obtained for B16F1 murine melanoma metastasis growth in the liver by MRI or ultrasound. Whole animal or organ imaging by MRI has been shown to be able to detect and quantify nearly the entire population of metastatic cells (single cells, micro and macrometastases), and a comparison of this technique vs traditional histological analysis is presented in Fig. 7.3 [83]. However, analysis by MRI requires expensive and customized hardware, pulse sequence optimization, use of contrast agent (for single cell imaging) and can require long image acquisition times. In comparison, imaging metastases by high frequency ultrasound (Fig. 7.4) is relatively inexpensive, requires no contrast agent and images can be acquired relatively quickly. Yet the ability to detect single cells and very small micrometastases, as well as image liver beneath the

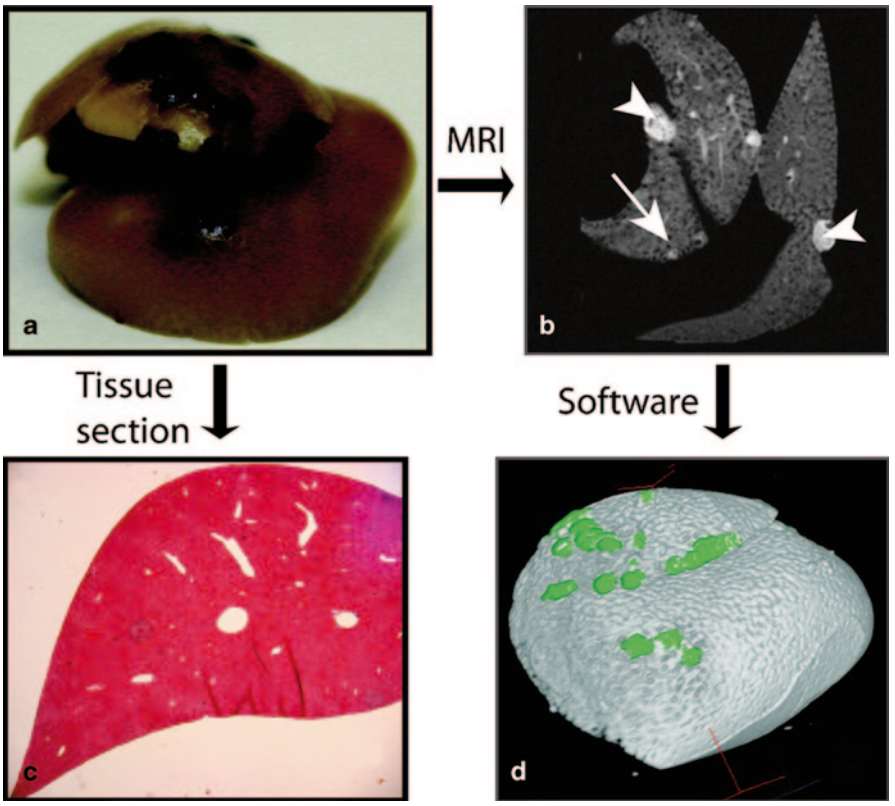

Fig. 7.3 Analysis of liver metastases via MRI. MR images from a whole mouse liver can be used to quantify tumor numbers and volumes, as well as volumes of solitary (dormant) cells. Whole livers (A) were scanned by MRI to generate a series of two-dimensional images, from which areas representing metastatic B16F1 murine melanoma tumors as well as dormant solitary cells are calculated (B). These sections, from the full liver volume, were used to render three-dimensional images (C) and used to calculate tumor volume for the whole liver. In contrast, standard histology (D) samples only a small subset of the full liver volume. Image modified from Townson et al., Cancer Research 2009 [83].

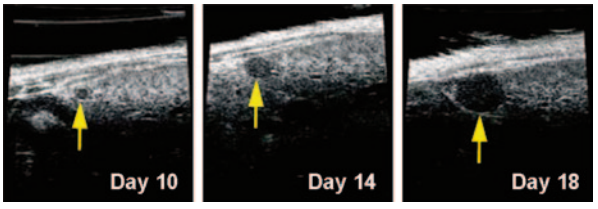

Fig.7.4 Analysis of liver metastasis via ultrasound. Growth of an individual B16F1 murine melanoma metastasis in liver. Calculated metastasis volumes at three times after mesenteric vein injection of cells: day 10 (0.06 mm3); day 14 (0.61 mm3); day 18 (3.79 mm3). Bar, 1.0 mm. Image modified from Graham et al., Cancer Research 2005 [86].

ribs, is currently limited [86]. While practical limitations generally result in the use of the imaging modality that is most readily available, the ability to image different populations (single cells, micrometastases and large metastases), surface antigens vs metabolic activity, blood flow etc., by various imaging modalities makes it realistic to image the entire level with cellular level resolution. Additionally, the use of multimodal contrast agents that also function as drugs or experimental cargo (e.g. shRNA etc.) delivery vehicles are beginning to allow for experimental manipulation and simultaneous imaging.

7.5 Conclusion

In most cases metastases, not local, non-invasive primary tumors, are responsible for cancer related deaths. The dual high volume blood supply to the liver, "unfiltered" in the case of the portal vein, in combination with what appears to be a relatively permissive tumor growth microenvironment make the liver a common site of lethal metastases. Advances in surgery, radiation therapy and systemic therapies have significantly increased survival following diagnosis of liver metastases, however prognosis is still generally poor. This is primarily due to the collateral damage/non-specific toxicity and technical complexity of treating multiple (spatially and temporally) metastases via surgery or radiation to a deep tissue vital organ. Considering the possibility of the presence of occult and perhaps dormant metastases that can emerge following removal of all clinically identifiable tumors (primary or metastatic at first treatment), it is likely that to make further significant advances in survival, advances in systemic therapy will be required. In order to achieve this, a better understanding of metastatic growth in liver is required. As a metastatic site for cells delivered via both arterial and portal vein blood, the liver provides a suitable microenvironment for determining the effect of site of growth based on preferred soil vs frequency of distribution. Additionally, multiple direct (portal vein system, directly into liver tissue) and indirect (intracardiac, intravenous, splenic injection) are available to recapitulate arrival via different routes as would be seen in patients.

Advances in systemic therapy including identification of surface ligands, molecular targeted therapy and nanoparticle drug delivery vehicles may offer a number of promising advantages for treatment of metastatic liver disease, including specificity and reduced toxicity [102, 111–113]. These include the ability to directly target surface receptors, deliver drug intracellular and exploit advances in non-cytotoxic therapies [114–115]. These combined properties may make molecular or cellular targeted therapies (vs treating the entire tumor as a single entity) capable of eliminating occult or dormant cells responsible for recurrent disease. Additionally, most therapeutics, including novel nanoparticles, normally accumulate in the liver, and elucidation of methods to take advantage of this effect, while avoiding Kupffer or endothelial cell uptake, could possibly provide a therapeutic opportunity. However, in order to develop novel systemic therapies for such applications, further knowledge regarding the fate of individual metastatic cells and population heterogene-

ity need to be understood. While acknowledging that the models and techniques outlined here are far from ideal and continue to evolve, when combined with other experimental advances a number of basic questions remain to be answered. The effect of the complex functional diversity of the liver, and its influence on the also heterogeneous metastatic cell population, is likely of particular importance. Corresponding to the diverse function of the liver, it has been well documented that even within a structure as small as the lobule, extensive variance with respect to specific molecular uptake, secretion and oxygen levels are observed. Would such niche environment provide a survival advantage for cells as has been documented in bone? It is hoped that the information presented here provide a basis to facilitate this required research and continue the necessary development on these models, integration of imaging techniques.

References

1. Tomlinson JS et al (2007) Actual 10-year survival after resection of colorectal liver metastases defines cure. J Clin Oncol 25:4575–4580. doi:25/29/4575 [pii] 10.1200/JCO.2007.11.0833
2. Adam R et al (2009) Patients with initially unresectable colorectal liver metastases: is there a possibility of cure? J Clin Oncol 27:1829–1835. doi:JCO.2008.19.9273 [pii] 10.1200/JCO.2008.19.9273
3. Peters S et al (2006) Intra-arterial hepatic fotemustine for the treatment of liver metastases from uveal melanoma: experience in 101 patients. Ann Oncol 17:578–583. doi:mdl009 [pii] 10.1093/annonc/mdl009
4. Chua TC, Saxena A, Liauw W, Chu F & Morris DL (2011) Hepatic resection for metastatic breast cancer: a systematic review. Eur J Cancer 47:2282–2290. doi:S0959-8049(11)00428-X [pii] 10.1016/j.ejca.2011.06.024
5. Kerkar SP, Kemp CD & Avital I (2010) Liver resections in metastatic gastric cancer. HPB (Oxford) 12:589–596. doi:10.1111/j.1477-2574.2010.00224.x
6. Nguyen KT, Gamblin TC & Geller DA (2009) World review of laparoscopic liver resection-2,804 patients. Ann Surg 250:831–841. doi:10.1097/SLA.0b013e3181b0c4df
7. Chambers AF, Groom AC. & MacDonald IC (2002) Dissemination and growth of cancer cells in metastatic sites. Nat Rev Cancer 2:563–572. doi:10.1038/nrc865 nrc865 [pii]
8. Pantel K & Brakenhoff RH (2004) Dissecting the metastatic cascade. Nat Rev Cancer 4, 448–456. doi:10.1038/nrc1370 nrc1370 [pii]
9. Gupta GP & Massague, J (2006) Cancer metastasis: building a framework. Cell 127:679–695. doi:S0092–8674(06)01414–0 [pii] 10.1016/j.cell.2006.11.001
10. Steeg PS (2006) Tumor metastasis: mechanistic insights and clinical challenges. Nat Med 12:895–904. doi:nm1469 [pii] 10.1038/nm1469
11. Chambers AF, MacDonald IC, Schmidt EE, Morris VL & Groom AC (2000) Clinical targets for anti-metastasis therapy. Adv Cancer Res 79:91–121
12. Karim-Kos HE et al (2008) Recent trends of cancer in Europe: a combined approach of incidence, survival and mortality for 17 cancer sites since the 1990s. Eur J Cancer 44:1345–1389. doi:S0959–8049(07)01028–3 [pii] 10.1016/j.ejca.2007.12.015
13. Patricia S Steeg et al (2009) Preclinical drug development must consider the impact on metastasis. Clin Cancer Res 15:4529–4530
14. Visvader JE & Lindeman GJ (2008) Cancer stem cells in solid tumours: accumulating evidence and unresolved questions. Nat Rev Cancer 8:755–768. doi:nrc2499 [pii] 10.1038/nrc2499
15. Klein CA (2009) Parallel progression of primary tumours and metastases. Nat Rev Cancer 9:302–312. doi:nrc2627 [pii] 10.1038/nrc2627

16. Joyce JA & Pollard JW (2009) Microenvironmental regulation of metastasis. Nat Rev Cancer 9:239–252. doi:nrc2618 [pii] 10.1038/nrc2618
17. Uhr JW & Pantel K (2011) Controversies in clinical cancer dormancy. Proc Natl Acad Sci USA 108, 12396–12400. doi:1106613108 [pii] 10.1073/pnas.1106613108
18. Morgan SC & Parker CC (2011) Local treatment of metastatic cancer–killing the seed or disturbing the soil? Nat Rev Clin Oncol 8:504–506. doi:nrclinonc.2011.88 [pii] 10.1038/nrclinonc.2011.88
19. Rodenhiser DI, Andrews JD, Vandenberg TA & Chambers AF (2011) Gene signatures of breast cancer progression and metastasis. Breast Cancer Res 13:201. doi:bcr2791 [pii] 10.1186/bcr2791
20. Fidler IJ (2003) The pathogenesis of cancer metastasis: the 'seed and soil' hypothesis revisited. Nat Rev Cancer 3:453–458. doi:10.1038/nrc1098 nrc1098 [pii]
21. Chambers AF & Matrisian LM (1997) Changing views of the role of matrix metalloproteinases in metastasis. J Natl Cancer Inst 89:1260–1270
22. Deryugina EI & Quigley JP (2006) Matrix metalloproteinases and tumor metastasis. Cancer Metastasis Rev 25:9–34. doi:10.1007/s10555–006-7886–9
23. Condeelis J & Pollard JW (2006) Macrophages: obligate partners for tumor cell migration, invasion, and metastasis. Cell 124:263–266. doi:S0092-8674(06)00055-9 [pii] 10.1016/j.cell.2006.01.007
24. Erler JT et al (2006) Lysyl oxidase is essential for hypoxia-induced metastasis. Nature 440:1222–1226. doi:nature04695 [pii] 10.1038/nature04695
25. Chaudary N & Hill RP (2007) Hypoxia and metastasis. Clin Cancer Res 13:1947–1949. doi:13/7/1947 [pii] 10.1158/1078-0432.CCR-06-2971
26. Folkman J (2002) Role of angiogenesis in tumor growth and metastasis. Semin Oncol 29:15–18. doi:10.1053/sonc.2002.37263 S0093775402503353 [pii]
27. Tang ZY et al (2004) A decade's studies on metastasis of hepatocellular carcinoma. J Cancer Res Clin Oncol 130:187–196. doi:10.1007/s00432-003-0511-1
28. Brodt P (2011) Liver metastasis: biology and clinical management. In Cancer Metastasis—Biology and Treatment 446 (Springer, 2011)
29. Burnier JV et al (2011) Type IV collagen-initiated signals provide survival and growth cues required for liver metastasis. Oncogene 30:3766–3783. doi:onc201189 [pii] 10.1038/onc.2011.89
30. Vollmar B & Menger MD (2009) The hepatic microcirculation: mechanistic contributions and therapeutic targets in liver injury and repair. Physiol Rev 89:1269–1339. doi:89/4/1269 [pii] 10.1152/physrev.00027.2008
31. Schenk WG, Jr., Mc DJ, Mc DK & Drapanas T (1962) Direct measurement of hepatic blood flow in surgical patients: with related observations on hepatic flow dynamics in experimental animals. Ann Surg 156:463–471
32. Rappaport AM (1980) Hepatic blood flow: morphologic aspects and physiologic regulation. Int Rev Physiol 21:1–63
33. Bubendorf L et al (2000) Metastatic patterns of prostate cancer: an autopsy study of 1,589 patients. Hum Pathol 31:578–583
34. Elias D et al (1998) Resection of liver metastases from a noncolorectal primary: indications and results based on 147 monocentric patients. J Am Coll Surg 187:487–493. doi:S1072-7515(98)00225-7 [pii]
35. Selzner M, Morse MA, Vredenburgh JJ, Meyers WC & Clavien PA (2000) Liver metastases from breast cancer: long-term survival after curative resection. Surgery 127:383–389. doi:S0039606000128053 [pii]
36. Hess KR et al (2006) Metastatic patterns in adenocarcinoma. Cancer 106:1624–1633. doi:10.1002/cncr.21778
37. Tarin D, Vass AC, Kettlewell MG & Price JE (1984) Absence of metastatic sequelae during long-term treatment of malignant ascites by peritoneo-venous shunting. A clinico-pathological report. Invasion Metastasis 4:1–12
38. Weiss L (1990) Metastatic inefficiency. Adv Cancer Res 54:159–211

39. Welch DR (1997) Technical considerations for studying cancer metastasis in vivo. Clin Exp Metastasis 15:272–306
40. Albini A et al (1987) A rapid in vitro assay for quantitating the invasive potential of tumor cells. Cancer Res 47:3239–3245
41. Kumar S. & Weaver VM (2009) Mechanics, malignancy, and metastasis: the force journey of a tumor cell. Cancer Metastasis Rev 28:113–127. doi:10.1007/s10555-008-9173-4
42. Yates C et al (2007) Novel three-dimensional organotypic liver bioreactor to directly visualize early events in metastatic progression. Adv Cancer Res 97:225–246. doi:S0065-230X(06)97010-9 [pii] 10.1016/S0065-230X(06)97010-9
43. Kim JB, Stein R & O'Hare MJ (2004) Three-dimensional in vitro tissue culture models of breast cancer—a review. Breast Cancer Res Treat 85, 281–291. doi:10.1023/B:BREA.0000025418.88785.2b 5266910 [pii]
44. Auerbach R, Lewis R, Shinners B, Kubai L & Akhtar N (2003) Angiogenesis assays: a critical overview. Clin Chem 49:32–40
45. Kleinman HK & Jacob K (2001) Invasion assays. Curr Protoc Cell Biol Chapter 12, Unit 12 12. doi:10.1002/0471143030.cb1202s00
46. Luzzi KJ et al (1998) Multistep nature of metastatic inefficiency: dormancy of solitary cells after successful extravasation and limited survival of early micrometastases. Am J Pathol 153:865–873. doi:S0002-9440(10)65628-3 [pii] 10.1016/S0002-9440(10)65628-3
47. Townson JL, Naumov GN & Chambers AF (2003) The role of apoptosis in tumor progression and metastasis. Curr Mol Med 3:631–642
48. Townson JL & Chambers AF (2006) Dormancy of solitary metastatic cells. Cell Cycle 5:1744–1750. doi:2864 [pii]
49. Cameron MD et al (2000) Temporal progression of metastasis in lung: cell survival, dormancy, and location dependence of metastatic inefficiency. Cancer Res 60:2541–2546
50. Bissell MJ et al (1999) Tissue structure, nuclear organization, and gene expression in normal and malignant breast. Cancer Res 59:1757–1763; discussion 1763–1764
51. Lee GY, Kenny PA, Lee EH & Bissell MJ (2007) Three-dimensional culture models of normal and malignant breast epithelial cells. Nat Methods 4:359–365. doi:nmeth1015 [pii] 10.1038/nmeth1015
52. Barkan D et al (2008) Inhibition of metastatic outgrowth from single dormant tumor cells by targeting the cytoskeleton. Cancer Res 68:6241–6250. doi:68/15/6241 [pii] 10.1158/0008-5472.CAN-07-6849
53. Barkan D, Green JE & Chambers AF (2010) Extracellular matrix: a gatekeeper in the transition from dormancy to metastatic growth. Eur J Cancer 46:1181–1188. doi:S0959-8049(10)00154-1 [pii] 10.1016/j.ejca.2010.02.027
54. Kaehr B, Allen R, Javier DJ, Currie J & Shear JB (2004) Guiding neuronal development with in situ microfabrication. Proc Natl Acad Sci USA 101:16104–16108. doi:0407204101 [pii] 10.1073/pnas.0407204101
55. Kaehr B et al (2006) Direct-write fabrication of functional protein matrixes using a low-cost Q-switched laser. Anal Chem 78:3198–3202. doi:10.1021/ac052267s
56. Kaehr B & Shear JB (2007) Mask-directed multiphoton lithography. J Am Chem Soc 129:1904–1905. doi:10.1021/ja068390y
57. Kaehr B & Shear JB (2008) Multiphoton fabrication of chemically responsive protein hydrogels for microactuation. Proc Natl Acad Sci USA 105:8850–8854. doi:0709571105 [pii] 10.1073/pnas.0709571105
58. Nielson, R., Kaehr, B. & Shear, JB (2009) Microreplication and design of biological architectures using dynamic-mask multiphoton lithography. Small 5:120–125. doi:10.1002/smll.200801084
59. Knopeke MT et al (2011) Building on the foundation of daring hypotheses: Using the MKK4 metastasis suppressor to develop models of dormancy and metastatic colonization. FEBS Lett 585:3159–3165. doi:S0014-5793(11)00672-7 [pii] 10.1016/j.febslet.2011.09.007
60. Hedley BD & Chambers AF (2009) Tumor dormancy and metastasis. Adv Cancer Res 102:67–101. doi:S0065-230X(09)02003-X [pii] 10.1016/S0065-230X(09)02003-X.

61. Chambers AF, Naumov GN, Vantyghem SA & Tuck AB (2000) Molecular biology of breast cancer metastasis. Clinical implications of experimental studies on metastatic inefficiency. Breast Cancer Res 2:400–407
62. Naumov GN et al (2003) Ineffectiveness of doxorubicin treatment on solitary dormant mammary carcinoma cells or late-developing metastases. Breast Cancer Res Treat 82:199–206. doi:10.1023/B:BREA.0000004377.12288.3c
63. Wu Y et al (2010) Insulin-like growth factor-I regulates the liver microenvironment in obese mice and promotes liver metastasis. Cancer Res 70:57–67. doi:0008-5472.CAN-09-2472 [pii] 10.1158/0008-5472.CAN-09-2472
64. Chambers AF, Shafir R & Ling V (1982) A model system for studying metastasis using the embryonic chick. Cancer Res 42:4018–4025
65. Chambers AF, Schmidt EE, MacDonald IC, Morris VL & Groom AC (1992) Early steps in hematogenous metastasis of B16F1 melanoma cells in chick embryos studied by high-resolution intravital videomicroscopy. J Natl Cancer Inst 84:797–803
66. Vargas A, Zeisser-Labouebe M, Lange N, Gurny R & Delie F (2007) The chick embryo and its chorioallantoic membrane (CAM) for the in vivo evaluation of drug delivery systems. Adv Drug Deliv Rev 59:1162–1176. doi:S0169-409X(07)00172-X [pii] 10.1016/j.addr.2007.04.019
67. Leong HS et al (2010) Intravital imaging of embryonic and tumor neovasculature using viral nanoparticles. Nat Protoc 5:1406–1417. doi:nprot.2010.103 [pii] 10.1038/nprot.2010.103
68. Chambers AF, Wilson SM, Tuck AB, Denhardt GH & Cairncross JG (1990) Comparison of metastatic properties of a variety of mouse, rat, and human cells in assays in nude mice and chick embryos. In Vivo 4:215–219
69. Subauste MC et al (2009) Evaluation of metastatic and angiogenic potentials of human colon carcinoma cells in chick embryo model systems. Clin Exp Metastasis 26:1033–1047. doi:10.1007/s10585-009-9293-4
70. Goulet B et al (2011) Nuclear localization of maspin is essential for its inhibition of tumor growth and metastasis. Lab Invest 91:1181–1187. doi:labinvest201166 [pii] 10.1038/labinvest.2011.66
71. MacDonald IC, Schmidt EE, Morris VL, Chambers AF & Groom AC (1992) Intravital videomicroscopy of the chorioallantoic microcirculation: a model system for studying metastasis. Microvasc Res 44:185–199. doi:0026-2862(92)90079-5 [pii]
72. Wilson SM & Chambers AF (2004) Experimental metastasis assays in the chick embryo. Curr Protoc Cell Biol Chapter 19, Unit 19 16. doi:10.1002/0471143030.cb1906s21
73. Palmer TD, Lewis J & Zijlstra A (2011) Quantitative analysis of cancer metastasis using an avian embryo model. J Vis Exp. doi:2815 [pii] 10.3791/2815
74. Cho CF, Ablack A, Leong HS, Zijlstra A & Lewis J (2011) Evaluation of nanoparticle uptake in tumors in real time using intravital imaging. J Vis Exp. doi:2808 [pii] 10.3791/2808
75. Dohle DS et al (2009) Chick ex ovo culture and ex ovo CAM assay: how it really works. J Vis Exp. doi:1620 [pii] 10.3791/1620
76. Lewis, JD. et al (2006) Viral nanoparticles as tools for intravital vascular imaging. Nat Med 12:354–360. doi:nm1368 [pii] 10.1038/nm1368
77. Kim J, Yu W, Kovalski K & Ossowski L (1998) Requirement for specific proteases in cancer cell intravasation as revealed by a novel semiquantitative PCR-based assay. Cell 94, 353–362. doi:S0092-8674(00)81478-6 [pii]
78. Locker J, Goldblatt PJ & Leighton J (1970) Ultrastructural features of invasion in chick embryo liver metastasis of Yoshida ascites hepatoma. Cancer Res 30:1632–1644
79. Endo Y, Sasaki T, Harada F & Noguchi M (1990) Specific detection of metastasized human tumor cells in embryonic chicks by the polymerase chain reaction. Jpn J Cancer Res 81:723–726
80. Zijlstra A et al (2002) A quantitative analysis of rate-limiting steps in the metastatic cascade using human-specific real-time polymerase chain reaction. Cancer Res 62:7083–7092
81. Taizi M, Deutsch VR, Leitner A, Ohana A & Goldstein RS (2006) A novel and rapid in vivo system for testing therapeutics on human leukemias. Exp Hematol 34:1698–1708. doi:S0301-472X(06)00443-7 [pii] 10.1016/j.exphem.2006.07.005

82. Wyckoff J, Gligorijevic B, Entenberg D, Segall J & Condeelis J (2011) High-resolution multiphoton imaging of tumors in vivo. Cold Spring Harb Protoc 2011. doi:2011/10/pdb.top065904 [pii] 10.1101/pdb.top065904)
83. Townson JL et al (2009) Three-dimensional imaging and quantification of both solitary cells and metastases in whole mouse liver by magnetic resonance imaging. Cancer Res 69:8326–8331. doi:0008-5472.CAN-09-1496 [pii] 10.1158/0008-5472.CAN-09-1496
84. Townson, J. L. et al (2011) The synthetic triterpenoid CDDO-Imidazolide suppresses experimental liver metastasis. Clin Exp Metastasis 28, 309–317. doi:10.1007/s10585-011-9374-z
85. Logan PT et al (2008) Single-cell tumor dormancy model of uveal melanoma. Clin Exp Metastasis 25:509–516. doi:10.1007/s10585-008-9158-2
86. Graham KC et al (2005) Three-dimensional high-frequency ultrasound imaging for longitudinal evaluation of liver metastases in preclinical models. Cancer Res 65, 5231–5237. doi:65/12/5231 [pii] 10.1158/0008-5472.CAN-05-0440
87. Enomoto, T. et al (2006) Consistent liver metastases in a rat model by portal injection of microencapsulated cancer cells. Cancer Res 66:11131–11139. doi:66/23/11131 [pii] 10.1158/0008-5472.CAN-06-0339
88. Naumov, GN. et al (2002) Persistence of solitary mammary carcinoma cells in a secondary site: a possible contributor to dormancy. Cancer Res 62:2162–2168
89. Rajendran S. et al (2010) Murine bioluminescent hepatic tumour model. J Vis Exp. doi:1977 [pii] 10.3791/1977
90. Shapiro EM, Sharer K, Skrtic S & Koretsky AP (2006) In vivo detection of single cells by MRI. Magn Reson Med 55:242–249. doi:10.1002/mrm.20718
91. Morris VL et al (1993) Early interactions of cancer cells with the microvasculature in mouse liver and muscle during hematogenous metastasis: videomicroscopic analysis. Clin Exp Metastasis 11:377–390
92. Bouvet M et al (2006) In vivo color-coded imaging of the interaction of colon cancer cells and splenocytes in the formation of liver metastases. Cancer Res 66:11293–11297. doi:66/23/11293 [pii] 10.1158/0008-5472.CAN-06-2662
93. Kirstein JM et al (2009) Effect of anti-fibrinolytic therapy on experimental melanoma metastasis. Clin Exp Metastasis 26:121–131. doi:10.1007/s10585-008-9221-z
94. Vrancken Peeters MJ, Perkins AL & Kay MA (1996) Method for multiple portal vein infusions in mice: quantitation of adenovirus-mediated hepatic gene transfer. Biotechniques 20:278–285
95. MacDonald IC, Groom AC & Chambers AF (2002) Cancer spread and micrometastasis development: quantitative approaches for in vivo models. Bioessays 24:885–893. doi:10.1002/bies.10156
96. Heyn C et al (2006) In vivo MRI of cancer cell fate at the single-cell level in a mouse model of breast cancer metastasis to the brain. Magn Reson Med 56:1001–1010. doi:10.1002/mrm.21029
97. Kim J et al (2008) Multifunctional uniform nanoparticles composed of a magnetite nanocrystal core and a mesoporous silica shell for magnetic resonance and fluorescence imaging and for drug delivery. Angew Chem Int Ed Engl 47:8438–8441. doi:10.1002/anie.200802469
98. Lee JE, Lee N, Kim T, Kim J & Hyeon T (2011) Multifunctional mesoporous silica nanocomposite nanoparticles for theranostic applications. Acc Chem Res 44:893–902. doi:10.1021/ar2000259
99. Bardhan R, Lal S, Joshi A & Halas NJ (2011) Theranostic nanoshells: from probe design to imaging and treatment of cancer. Acc Chem Res 44:936–946. doi:10.1021/ar200023 ×
100. Heyn C et al (2006) In vivo magnetic resonance imaging of single cells in mouse brain with optical validation. Magn Reson Med 55:23–29. doi:10.1002/mrm.20747
101. Tsuji K et al (2006) Dual-color imaging of nuclear-cytoplasmic dynamics, viability, and proliferation of cancer cells in the portal vein area. Cancer Res 66:303–306. doi:66/1/303 [pii] 10.1158/0008-5472.CAN-05-2958
102. Ashley CE et al (2011) The targeted delivery of multicomponent cargos to cancer cells by nanoporous particle-supported lipid bilayers. Nat Mater 10:389–397. doi:nmat2992 [pii] 10.1038/nmat2992

103. Yang M et al (2002) Direct external imaging of nascent cancer, tumor progression, angiogenesis, and metastasis on internal organs in the fluorescent orthotopic model. Proc Natl Acad Sci USA 99:3824–3829. doi:10.1073/pnas.052029099052029099 [pii]
104. Foster-Gareau P, Heyn C, Alejski A & Rutt BK (2003) Imaging single mammalian cells with a 1.5 T clinical MRI scanner. Magn Reson Med 49:968–971. doi:10.1002/mrm.10417
105. Weissleder R & Pittet MJ (2008) Imaging in the era of molecular oncology. Nature 452:580–589. doi:nature06917 [pii] 10.1038/nature06917
106. Condeelis J & Weissleder R (2010) In vivo imaging in cancer. Cold Spring Harb Perspect Biol 2, a003848. doi:cshperspect.a003848 [pii] 10.1101/cshperspect.a003848
107. O'Neill K, Lyons SK, Gallagher WM, Curran KM & Byrne AT (2010) Bioluminescent imaging: a critical tool in pre-clinical oncology research. J Pathol 220:317–327. doi:10.1002/path.2656
108. Thaker PH et al (2006) Chronic stress promotes tumor growth and angiogenesis in a mouse model of ovarian carcinoma. Nat Med 12:939–944. doi:nm1447 [pii] 10.1038/nm1447
109. Hofer SO, Shrayer D, Reichner JS, Hoekstra HJ & Wanebo HJ (1998) Wound-induced tumor progression: a probable role in recurrence after tumor resection. Arch Surg 133:383–389
110. Demicheli R, Retsky MW, Hrushesky WJ, Baum M & Gukas ID (2008) The effects of surgery on tumor growth: a century of investigations. Ann Oncol 19:1821–1828. doi:mdn386 [pii] 10.1093/annonc/mdn386
111. Lo A, Lin CT & Wu HC (2008) Hepatocellular carcinoma cell-specific peptide ligand for targeted drug delivery. Mol Cancer Ther 7:579–589. doi:7/3/579 [pii] 10.1158/1535-7163.MCT-07-2359
112. Farokhzad OC et al (2006) Targeted nanoparticle-aptamer bioconjugates for cancer chemotherapy in vivo. Proc Natl Acad Sci USA 103:6315–6320. doi:0601755103 [pii] 10.1073/pnas.0601755103
113. Peer D et al (2007) Nanocarriers as an emerging platform for cancer therapy. Nat Nanotechnol 2:751–760. doi:nnano.2007.387 [pii] 10.1038/nnano.2007.387
114. Davis ME, Chen ZG & Shin DM (2008) Nanoparticle therapeutics: an emerging treatment modality for cancer. Nat Rev Drug Discov 7:771–782. doi:nrd2614 [pii] 10.1038/nrd2614
115. Byrne JD, Betancourt T & Brannon-Peppas L (2008) Active targeting schemes for nanoparticle systems in cancer therapeutics. Adv Drug Deliv Rev 60:1615–1626. doi:S0169-409X(08)00225-1 [pii] 10.1016/j.addr.2008.08.005
116. Vidal-Vanaclocha F (2008) The prometastatic microenvironment of the liver. Cancer Microenviron 1:113–129. doi:10.1007/s12307-008-0011–6

Chapter 8
Malignant Pleural Effusion

Antonia Marazioti and Georgios T. Stathopoulos

Abstract Malignant pleural effusion (MPE) poses a significant clinical problem annually affecting two million patients worldwide. MPE is most commonly caused by pleural metastasis of lung, breast, gastrointestinal, and other tumors, as opposed to the development of primary pleural-based malignancies, which are more infrequent. The appearance of a MPE in a patient with cancer signals systemic disease, short survival, and poor quality of life. Under normal conditions, the pleural space contains small amounts of fluid that are dynamically regulated by production via systemic blood vessel filtration and by lymphatic absorption. Any tumor-induced distortion of the pleural fluid production, circulation, and clearance process may result in MPE. Until recently, tumor-mediated obstruction of normal pleural fluid absorption was considered to be the most important path to MPE. However, recent advancements in experimental modeling of MPE indicate that tumor-induced inflammation, angiogenesis, and vascular hyperpermeability critically drive MPE formation independent from anatomical blockade of pleural fluid turnover. In this regard, different research groups have established novel experimental models mimicking human pleural malignancies, including models of human cancer induced-MPE in immunocompromized animals as well as mouse cancer-induced MPE in immunocompetent mice. These modeling approaches have expanded the field of pleural cancer research and will be addressed in detail in the present chapter.

Abbreviations

MPE	Malignant pleural effusion
CAM	Chorioallantoic membrane
MPM	Malignant pleural mesothelioma
VEGF	Vascular rndothelial growth factor
IL	Interleukin
TNF	Tumor necrosis factor
CCL2	Chemokine ligand 2
VEGFR1	Vascular endothelial growth factor receptor 1

A. Marazioti (✉) · G. T. Stathopoulos
Department of Physiology, Faculty of Medicine, University of Patras, Patras, Greece
e-mail: amarazioti@upatras.gr

G. T. Stathopoulos
e-mail: gstathop@upatras.gr

A. Malek (ed.), *Experimental Metastasis: Modeling and Analysis,*
DOI 10.1007/978-94-007-7835-1_8,

PCNA	Proliferating cell nuclear antigen
TUNEL	Terminal deoxynucleotidyl nick-end labelling
SCID	Severe combined immunodeficient mice
LLC	Lewis lung adenocarcinoma cells
FITC	fluoroisothiocynate
NF-κB	Nuclear factor kappa (-light-chain-enhancer of activated) B

8.1 Introduction—Clinical Relevance

Pleural cancers affect approximately 500–700 patients per million population and are among the most lethal and poorly treatable malignancies. Patients with pleural carcinomatosis often live only few months after diagnosis, and most have a poor quality of life greatly impaired by dyspnea, cough, and/or chest pain. Constitutional symptoms including weight loss, anorexia, malaise and fatigue accompany respiratory symptoms, culminating in poor patient functional status.

Pleural carcinomatosis most commonly represents metastatic disease. This can either be from a distant site, as with breast and colon cancer, or loco regional, as with lung cancer. In either case the diagnosis of pleural malignancy signifies the spread of cancer beyond the organ of origin, and hence end-stage disease. Because of the diffuse nature of the disease that affects all intrathoracic structures, survival is limited and surgery is not a stand-alone treatment option. Thoracentesis, chemical and mechanical pleurodesis, and tunneled indwelling pleural catheters are considered only in patients with prolonged life expectancy and only provide palliation by means of pleural fluid drainage and prevention of pleural fluid reaccumulation.

Pleural malignancies mainly include primary malignant pleural mesothelioma (MPM) and secondary pleural metastasis of various tumors resulting in malignant pleural effusion (MPE). MPM is infrequent with an annual incidence ranging from 7–40 per million population. Most cases of MPM are occupation-induced [1, 2]. MPE is more frequent affecting 500–700 people per million population every year [3, 4]. About 80 % of MPEs are caused by adenocarcinomas of the lung, breast, and ovary or by lymphomas [5], with metastatic adenocarcinoma being the most common histological type. Other causes include malignancies of the genitourinary tract or gastrointestinal tract, with 5–10 % of patients having unknown primary cancer sites.

Knowledge on the pathophysiology of malignant pleural diseases remains limited, and in part accounts for the relative lack of novel therapies. Improved understanding of pathogenesis will likely provide more effective approaches to prevent and manage pleural malignancies.

8.2 Pleural Structure

The lungs are the essential organs of respiration that expand during inhalation and deflate during exhalation. For the protection and function of the lungs, the thorax is shaped like a bellow with the diaphragm as the moving part at the caudal and widest part and the trachea at the upper and narrowed part. The outer surface of the lung and the inner surface of the thoracic cage have evolutionally become covered by an elastic, serous, and lubricating surface to form the pleural cavity. This decreases friction between lung, thoracic wall and diaphragm during movement. In humans, the right and left pleural cavities are separated from one another by the mediastinum.

The pleural space is enclosed by a smooth lubricating membrane, the pleura. The pleural membrane is thin, moist, and has two layers, visceral and parietal. The visceral pleura cover the entire surface of the lungs. Extensions of visceral pleura into the underlying lung form fissures that divide the lungs into lobes. The parietal pleura cover the inner surface of the thoracic cage, including the mediastinal surfaces and diaphragm. It is further subdivided into four anatomical regions: (i) The mediastinal pleura that is adherent to the pericardium; (ii) The diaphragmatic pleura that covers the convex surface of the diaphragm; (iii) the costal pleura that lines the inner surface of the ribs; and (iv) the cervical pleura that is the continuation of the costal and mediastinal parts of the pleura over the apex of the lung. Visceral and parietal pleura coalesce at the hilae, where they are penetrated by the major airways and pulmonary vessels.

The visceral and parietal pleura consist of a single cellular layer and four subcellular layers. Starting at the pleural space the layers are: (i) a single layer of mesothelial cells, that are always adhered to one another via tight junctions; (ii) a thin subendothelial connective tissue layer, including a basal lamina; (iii) a thin superficial and elastic layer, that is fused with the second layer; (iv) a loose connective tissue layer, that contains nerves, blood vessels and lymphatics; and (v) a deep fibroelastic layer, that is adhered tightly to the underlying tissue. The surface area of the mesothelial cell layer is substantially increased by the presence of microvilli. Microvilli enmesh glycoproteins rich in hyaluronic acid that lubricate the pleural surface and decrease the friction between the lung and the thorax.

The normal pleural space contains a thin film of liquid that is called pleural fluid. The volume and characteristics of this serous fluid is determined by a combination of dynamic phenomena involving the pulmonary and systemic circulation, the lymphatic drainage, the mechanic movement of the thoracic cage and the movement of the heart [6]. Pleural fluid is produced by filtration from the systemic circulation, and production occurs in the region where blood vessels are closest to the mesothelial layer [7]. The volume of the fluid remains steady via reabsorption through the lymphatic drainage.

8.3 Pleural Fluid Dynamics

The pleural fluid carries out the important function of providing mechanical coupling between the chest wall and the lung. It also provides lubrication during the movement of the lungs during breathing. For the effective coupling between lung and chest wall the volume of pleural liquid required for lubrication must be kept down to a minimum. The volume and composition of the normal pleural fluid is subject to control by a number of regulatory mechanisms [8, 9].

Under normal conditions, the pleural space contains a small amount of fluid, quantified in humans to be 0.26 ± 0.1 ml/kg of body weight [6]. This small amount of liquid separates the pleural membranes over the entire surface of the lungs [10]. The pleural fluid, in a manner similar to other bodily fluids, flows into the pleural space by filtration from systemic vessels and is absorbed into lymphatics.

The systemic sources of liquid lie in the adjacent pleural membranes. The major source of normal pleural fluid is thought to be the systemic blood supply of the parietal pleura. The parietal pleural vessels are very close to the pleural space and have a high microvascular pressure due to their drainage into systemic venules. Once the liquid filters across the systemic vessels, it can then flow along a pressure gradient across the mesothelial layer into the pleural space. The flow rate of the pleural fluid is approximately 0.5 ml per hour in adults [11–13].

There are three different mechanisms of excess fluid removal from the pleural space: (i) a lymphatic drainage through the stomata of the parietal pleura; (ii) an absorptive pressure gradient through the visceral pleura; and (iii) cellular mechanisms. In case of an abnormality of one or more of the mechanisms of pleural fluid turnover, a pleural effusion occurs.

The majority of pleural fluid exits the pleural space by bulk flow and not by diffusion or other routes. With bulk flow via lymphatics, liquid and protein are removed at the same rates and the protein concentration of the remaining liquid does not change. Lymphatic absorption of fluid from the pleural space takes place on the parietal side. Communication between lymphatics and the pleural space occurs via openings of small diameter that are called stomata. Stomata are formed between adjoining mesothelial cells and are situated only in the anterior lower thoracic wall and diaphragm. The opening of the stomata is stretched to a larger diameter with inspiration and expansion of the chest wall, leading to an increase of the absorption flow from the pleural space and lymphatic flow through costal, mediastinal and diaphragmatic pleura. [9, 14, 15].

The amount of fluid in the pleural cavity is also regulated by the hydrostatic-osmotic pressure relationship in the visceral pleura. Liquid is absorbed according to Starling forces through the mesothelium and the adjacent pulmonary capillaries. Nevertheless, absorption that flows through the visceral pleura is normally negligible, so that, under normal conditions, the pleural space and the pulmonary interstitium are two functionally separate compartments [9, 14].

Sodium channels and other ion transport have been implicated in fluid absorption from the pleural space. Under physiological conditions the vesicular

transport of liquid and protein from the pleural space seems to contribute to overall fluid removal from this space. [16]. On the other hand, water channels have been implicated as a possible way of clearance of pleural fluid. The presence of aquaporins in mesothelial cells seems to participate in the movement of pure water [17].

8.4 Pathogenesis of Malignant Pleural Effusion

An important and classically recognized role in the pathogenesis of MPE is definitely played by tumor-associated blockade of local lymphatic outflow that leads to a decreased rate of pleural fluid drainage. Thus, the fluid is accumulated in the pleural cavity leading to a malignant effusion. If the lymphatic clearance is normal, excess fluid that enters the pleural space can usually be removed, since the maximum capacity of the lymphatics for fluid removal is up to 30 times the normal rate of fluid formation [7]. Indeed, clinical observations has shown that the clearance of fluid from the pleural space is decreased in patients with MPE [18]. The blockade of the lymphatic network occurs in two ways. First, through parietal pleural infiltration that culminates in obstruction of the stomata, from where the pleural fluid is normally cleared form the pleural cavity. Second, through metastasis to mediastinal lymph nodes, where the drainage of the pleural lymphatic nodes takes place, hindering the drainage of the fluid from the pleural cavity [18].

On the other hand, an increase in pleural fluid formation also appears to contribute significantly to the development of a MPE [19]. There are several possible explanations for this. The presence of a primary tumor or metastases in the lung may increase the amount of interstitial fluid, which would then lead to increased pleural fluid formation. Furthermore, the presence of mediastinal lymph node involvement might decrease lymphatic flow from the lung and lead to increased amounts of fluid entering the pleural space by traversing the visceral pleura. Finally, it seems that the presence of pleural metastases may increase the permeability of the capillaries in the visceral and/or parietal pleura. This would also explain why malignant effusions are exudates.

It is yet unknown whether the increased vascular permeability observed with MPE involves primarily the neoplastic intratumoral blood vessels, or the adjacent, seemingly normal, pleural capillaries. The mechanism by which cancer cell infiltration of the pleura causes increased vascular permeability is also not fully elucidated. Studies have shown that is due to increased production of angiogenic and inflammatory mediators from cancer cells into the pleural cavity. Tumor-elaborated mediators that seem to be important in the pathogenesis of MPE by increasing vascular permeability are vascular endothelial growth factor (VEGF), interleukin (IL)-6, tumor necrosis factor (TNF), chemokine ligand 2 (CCL2) and others [20–24].

Indeed, levels of VEGF, IL-6, TNF and other angiogenic and inflammatory mediators are higher in pleural fluid of patients with MPE than in their serum [25]. VEGF and other cytokines are potent factors that increase angiogenesis

and endothelial permeability, thereby contributing directly to the development of MPE [26]. Apart from direct induction of blood vessel leakiness, cancer-elaborated signalling molecules likely trigger inflammatory responses in the host. In this regard, these mediators attract granulocytes, monocytes, and lymphoid cells, which in turn may participate in local production of angiogenic and inflammatory mediators [27, 28].

Malignant diseases cause pleural effusions through different mechanisms, direct and/or indirect. A prerequisite for the development of a MPE is entering of tumor cells into the pleural cavity with subsequent formation of pleural metastatic foci [20]. The route of metastasis to the pleura varies according to the location of the primary tumor. Adenocarcinoma of the lung spreads to the parietal pleura from the visceral pleura along existing pleural adhesions. Tumor cells migrate to the visceral pleura from underlying pulmonary capillaries (haematogenous spread). Pleural metastases from a primary site other than the lung result from haematogenous or lymphatic spread. Neoplastic involvement of the lymphatic drainage system, either in the parietal pleura and/or in the mediastinum, is the primary mechanism by which pleural metastases cause pleural effusions. Specifically, malignant effusions secondary to breast cancer and lymphomas arise through chest wall lymphatics. Moreover, pleural metastases of gastric origin are usually the result of pulmonary arterial embolism. Other neoplasms that are often detected in the pleural cavity may occur after intermediate metastasis to the liver (hepatic metastasis) [18].

Another mechanism for the development of a MPE from various cancers is bronchial obstruction. The presence of exophytic endobronchial mass can lead to obstruction of a segmental bronchus and atelectasia and/or pneumonia, leading to a further increase in negative pressure to the affected hemithorax and enhancement of pleural fluid accumulation. Finally, cancer cell invasion to the pericardium also causes pleural effusion, either by increasing the pressure in systemic and pulmonary circulation or by direct drainage of fluid from the pericardial to the pleural space [29].

8.5 Modeling Pleural Malignancies

8.5.1 A Historic Perspective

Animal models in cancer research have been developed to simulate human carcinogenesis. Although the ideal animal model does not exist, many models can emulate aspects of human carcinogenesis. Although modern tissue, organ and cell culture procedures, computer-aided modelling and other non- animal research tools have reduced the dependence on animals, they cannot completely replace experimental animal models.

The development of various animal models has been important in the study of the pathogenesis of pleural malignancies. They have proven essential in investigating

physiologic changes in the pleural space in health and disease and in assessing the efficacy and safety of novel therapeutic drugs. For example, animal studies have assessed the efficacy and adverse effects of various anti-cancer agents and chemical pleurodesis agents, which are used for the induction of pleural inflammation and fibrosis aimed at obliterating the pleural space.

As detailed above, MPE is more commonly induced by secondary cancer metastasis to the pleura. Until recently, the mechanisms underlying the pathogenesis of MPE were poorly understood. Therefore, it has been essential for clinically relevant *in vivo* models to be established. In this regard, animal models of MPE have been developed and have provided novel insights into the mechanisms of effusion formation. Most animal studies on MPE have been performed using laboratory mice, which feature several advantages including small size, similarities to humans and an entirely sequenced genome.

The majority of animal models of MPE have been developed in immune-deficient animals. In a landmark study, Yano and coworkers reported on a MPE model using athymic nude mice. Human PC14 lung adenocarcinoma cells were injected intravenously and produced lesions in the lung parenchyma and invaded the pleura causing MPE [20]. Similarly, another research group caused effusions in nude mice by injecting intravenously as well as intraperitoneally human PC14PE6/AS2 lung adenocarcinoma cells [30]. Intravenous injection of tumor cells induces a pattern of hematogenous metastases but a defined primary tumor as a source of metastatic spread is missing. Therefore, orthotopic implantation of tumor cells could be more relevant. Boehle et al established a model of orthotopic xenotransplantation of human lung cancer with subsequent MPE formation. Specifically, they injected intrapulmonary and intrapleurally human adeonocarcinoma, squamous cell carcinoma and undifferentiated large cell carcinoma cells in severe combined immunodeficient (SCID/bg) mice [31]. A similar model of orthotopic implantation in SCID mice was used for inducing MPE [32]. Human mesothelioma cell lines were intrapleurally implanted in SCID mice and tumor growth as well as malignant pleural effusion was observed. Orthotopic model systems were also set up in immunodeficient rats, which developed MPE after inoculation of human PC-14 lung adenocarcinoma cells in intrapleural and subpleural sites [33].

Currently, only one animal model of MPE generation by genetically-induced carcinogenesis exists [34]. To accomplish this, the investigators generated combined conditional knockout mice with pleural mesothelial cells specifically deficient in genes frequently altered in human mesothelioma (Nf2, INKA4/ARF locus and p53 tumor suppressor). When NF2- deficient mice were crossed with either INKA4/arfdeficient or p53 deficient mice, a high incidence of malignant pleural mesothelioma ensued.

Both athymic nude mice and animal xenograft models that use human tumor cell lines have been used to increase our understanding of MPE. However, recent information regarding the key influence of the tumor microenvironment on tumor progression and growth has led to greater reliance on immunocompetent models. Kimura et al. Implanted meth A fibrosarcoma into the pleural space of wild type Balb/c mice [35]. An MPE model has also been established in immunocompetent

New Zealand white rabbits by intrapleural introduction of rabbit VX2 sarcoma [36–38]. Another relevant and highly reproducible animal model was developed by the authors of this chapter and involves the intrapleural injection of Lewis lung carcinoma (LLC) cells to syngeneic wild type C57BL/6 mice [22].

In recent years, work on relevant animal models of MPE has started paving the road for elucidating the molecular pathogenesis of pleural malignancies. Basic aspects of MPE pathobiology have been determined and potential therapeutic targets have been established. Continuous work for modification and improvement of the above models could hopefully lead to the development of therapies that will halt or even prevent MPE formation in patients with cancer.

8.5.2 In Vitro Models

The development of a MPE by cancer invading the pleural space is a complex phenomenon potentially involving resident mesothelial, inflammatory, endothelial, pulmonary, and/or malignant cells. Pleural vascular hyperpermeability, new vessel formation (angiogenesis) as well as inflammation that are regulated by interplay between host- and tumor-derived mediators present important elements of MPE pathobiology. Although suboptimal, some *non-animal* models for the isolated study of the above constituents of MPE pathogenesis have been developed.

8.5.2.1 Chick Embryo Chorioallantoic Membrane (CAM) Assay

To study angiogenesis, the chick embryo chorioallantoic membrane (CAM) can be used. CAM is an extraembryonic membrane, which serves as a gas exchange surface and its function is supported by a dense capillary network. CAM has been used to study morphofunctional aspects of the angiogenic process and can be adapted very easily to study angiogenesis. Also, because of the lack of a developed immune system in the chick embryo, CAM represents a host tissue for tumor engrafting suitable to study the angiogenic and metastatic potential that characterizes human malignancies. Eggs are incubated at 37 °C and a window is opened on the egg's shell on day 4 of incubation, exposing the CAM. The window is covered with tape and the implant (e.g. tumor cells, tumor-conditioned medium) can be applied onto a specific area of the CAM (restricted by a plastic ring, methylcellulose disc, collagen and gelatin sponge etc.) on Day 9 of embryo development (Fig. 8.1a). After 48–72h, CAM is fixed in situ and excised from the eggs. Blood vessels can be counted under a stereomicroscope and digitally quantified (Fig. 8.1b). The CAM assay is relatively simple, reliable, quick, inexpensive and thus suitable for large-scale screening. The major disadvantage of this assay is that the CAM contains already a well-developed vascular network, which makes it difficult to discriminate between new capillaries and old ones [39, 40].

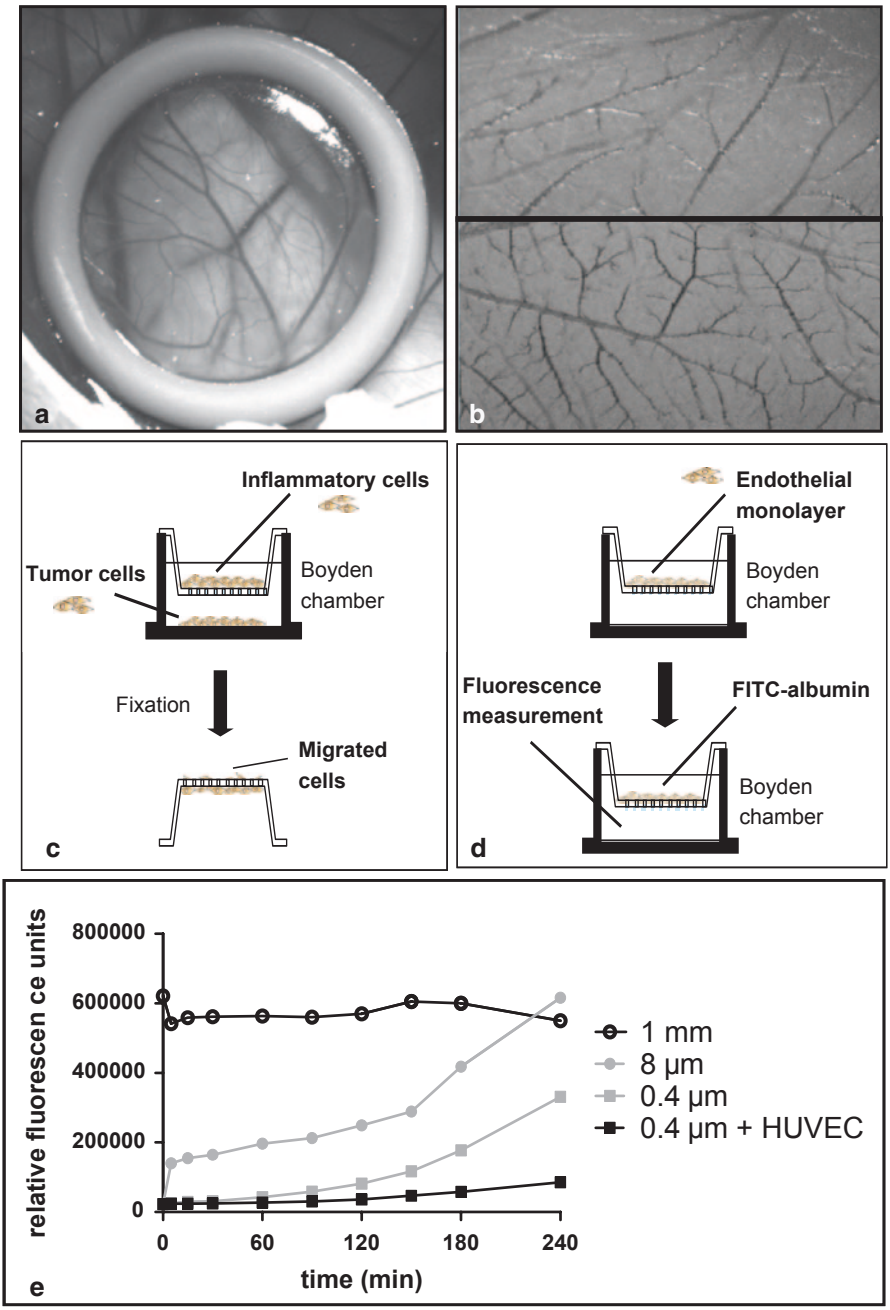

Fig. 8.1 CAM assay **a** Eggshell window and plastic ring area used for the study of new vessel formation. **b** Typical results without (*top*) or with (*bottom*) application of angiogenic stimulus. Boyden chamber assays **c** Schematic representation of chemotaxis assay chamber. **d** Schematic representation of in vitro vascular permeability assay chamber. **e** Typical results obtained from permeability assay chambers according to pore size (small pores make the membrane tighter) and the presence of endothelial cells, which makes the membrane relatively impermeable to FITC-labeled albumin

8.5.2.2 Boyden Chamber Assay

To study tumor-induced inflammation, chemotaxis assays may be useful. Tumor cells located in the pleural space secrete inflammatory mediators that result in the influx of host inflammatory cells in this region. Chemotaxis can be examined in a Boyden chamber, which consists of an upper and lower well separated by a membrane filter. Inflammatory cells are seeded onto the top compartment and tumor cells are placed in the bottom compartment of the Boyden chamber (Fig. 8.1c). The compartments are divided by a membrane with varying pore diameter. Eight-μm-pore size is appropriate for mononuclear chemotaxis assays. After a period of incubation (usually 24 h) the porous membrane is removed, inverted, air dried and stained with May-Gruenwald-Giemsa, after mechanical removal of cells in the top compartment. Cells that have migrated toward the chemotactic stimulus are counted on the fixed and stained bottom surface of the membrane using light microscopy [24, 41].

8.5.2.3 In Vitro Vascular Permeability Assay

This is a sensitive and efficient technique for investigating endothelial barrier function and the mechanisms that control permeability. Disruptions of endothelial barrier integrity or looseness of the mesothelial cell sheet can result in vascular hyper-permeability, a situation that takes place during MPE formation. The permeability chamber (Boyden chamber) consists of a well and an insert (Fig. 8.1d). The inserts contain 1.0 μm pores within a transparent polyethylene membrane. Mesothelial or endothelial cells (2×10^4 cells per well) are seeded onto commercially available collagen-coated inserts and are left to grow for four days at 37ºC in 5% CO2. The upper and lower chambers contain 200 μL and 800 μL growth medium, respectively. On the day of the experiment the formed confluent cell monolayer occludes the membrane pores. The reagents of interest (e.g. cytokines, growth factors, tumor conditioned medium) are added in the serum-free medium of the upper chamber for 15–30 min. After treatment, a tracer molecule is added on top of the cells as an index of macromolecular diffusion across the formed monolayer. One hour incubation allows the tracer to permeate through the cell monolayers. Common tracer molecules are radiolabeled or FITC-labelled albumin and FITC-labelled Dextran. The extent of permeability is determined by measuring the fluorescence intensity or count the radioactivity in the bottom compartments (Fig. 8.1e) [41, 42].

While *in vitro* studies can provide information on the functions of isolated cell types during MPE development, MPE is a complex phenomenon that can only be accurately reproduced *in vivo*. In MPE, tumor-host cross-talk takes place in the pleural space that leads to local increases in the relative abundance of inflammatory cells and mediators, in the formation of new blood vessels in and around pleural tumors, and in hyper permeability of existing and newly formed blood vessels. The integer of these phenomena is pleural fluid accumulation in the pleural space. Therefore, *in vivo* modeling is required for the study of MPE pathobiology.

8.5.3 Animal Models

Only one animal model of genetically induced MPE exists at present [34].All other available models are developed by introduction of tumor cells or tissue into the recipient animal. The different models vary in terms of host species used, its immune status, the type of tumor employed, the site of tumor inoculation and the interspecies relationship between host and tumor.

8.5.3.1 Choice of Animal Species

The establishment of a successful MPE model is primarily based on the appropriate animal species. Many different animal models using different species have been employed in the investigation of pleural diseases. The choice of the right experimental animal is very important so as to have an effective tool for the study of all aspects of MPE. For instance, small animals (e.g. mice) usually cost less and are easier to handle. On the other hand, larger animals (e.g. rabbits) are more easily manipulated experimentally and provide adequate amount of biologic material for examination. Furthermore, there are animals that appear to have incomplete mediastina (e.g. mice, dogs) and/or have a thin visceral membrane leading to perplexions in fluid transport across the pleura (e.g. rabbits, rats).

Animal choice for MPE modeling is often based on the knowledge of the genomic sequence of the species, by the availability of reagents to analyze samples and tools to manipulate gene expression in animals. The most common used animal species for MPE modeling is mice. Occasionally, rabbits and rats have been used. The following general characteristics of mice make them ideal for the present malignant model:

- Genetically best characterized of all mammals
- The mouse genome shares sufficient homology with that of humans
- A wide array of genetically engineered mice are available
- The large litter size of mice makes breeding timelier and easier
- A wide variety of available analytical reagents (e.g. Antibodies, elisa kits etc.)
- High tumor incidence, rapid tumor growth as well as the highest number of syngeneic tumor models
- High-throughput genotyping methods (e.g. Using genomic DNA from tail fragments) have been developed for the mouse
- Many inbred strains of mice have been isolated over the years. Inbred animals share a great degree of genetic identity, reducing experimental variability. Moreover, histocompatibility within inbred strains allows tumor transplantation.

Due to the above advantages, several constitutive and conditional gene knockout and knockin mice have been used in pleural disease investigations, and the development of systems that facilitate conditional and site-specific gene overexpression or silencing in the adult mouse, such as the tetracycline on–off models and Cre-Lox recombination system respectively, is expected to greatly enhance research in this area.

8.5.3.2 Methods of Cancer Cells Delivery

Various methods have been used to deliver tumor cells or tissue in the animal used in order to develop malignant pleural effusion. Malignant cells can be implanted into the pleural space directly by surgery or intrapleural injection or indirectly from metastases from tumors implanted in the lungs.

Thoracotomy has been used for the orthotopic implantation of freshly isolated human adenocarcinoma tissues into nude mice. This method offer a high take up rate of the cancer with local and regional spread [43, 44]. However, thoracotomy remains an invasive and painful method that can disturb the respiratory mechanism of the mice.

- Before implantation, patient tumor specimens are sewn together (5–10 pieces, 1–1.5 mm^3 per piece).
- Mice are anesthetized with isoflurane. A skin and muscle incision is made and the chest wall is opened.
- Tumor is tied into the visceral and parietal pleura or directly to the lung.
- After closing the chest wall the remaining air in the cavity can be withdrawn with a 2 ml syringe.

Intravenous injection Delivery of tumor cells to the pleural space can be achieved by intravenous injection with subsequent blood-borne translocation to lung vasculature and lung/pleural outgrowth [20, 21, 31]. Indeed, intravenous injection of human adenocarcinoma cells produces numerous lung lesions, pleural metastases and effusions [20, 45]. Below usual tail vein injection procedure s described.

- Mice are exposed to heating lamp for tail vein dilation (4–5 min).
- Then they are placed unanesthetized into a restrainer and slight pressure is applied to straighten the tail and further dilate the lateral vein.
- The needle is gently forced through the skin (at a slight angle) and then positioned parallel into the vein. When the vein is canulated, the 26G needle is advanced into the lumen an additional 5 mm and tumor cell injection of 100–300 μl volume (approximately 2.5×10^5 to 1×10^6 cells/ml, depending on the metastatic potential of the cells) is performed slowly into the lateral tail vein.

Intrapleural injection Tumors or cancer cells can also be injected directly into the pleural space using fine needles (27G). Commercially available cancer cell lines are grown in cell culture conditions and are titrated before injection to standardize the tumor load per mouse. A volume of 50–100 μl of 1×10^5–1×10^6 tumor cells is usually injected into an adult mouse.

- Mice are anesthetized with by gas anesthesia (3 % isoflurane) or by intraperitoneal injection of ketamine (100 mg/kg)/xylazine (5 mg/kg) using a 25G needle.
- The skin overlying the posterior and lateral thoracic wall is shaved and disinfected, and a 5-mm-long transverse skin incision is made on the left posterolateral thoracic area at the xiphoid level (Fig. 8.2a).

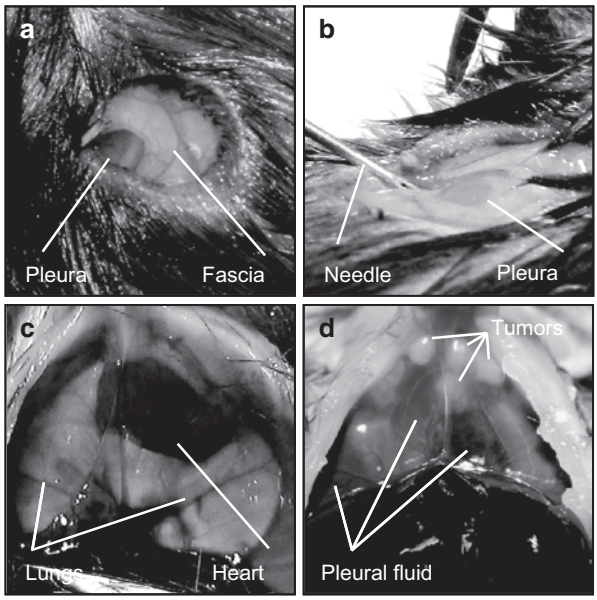

Fig. 8.2 Mouse modeling of MPE **a** Skin incision made for intrapleural injection of tumor cells. **b** Intrapleural injection. **c** Transdiaphragmatic view of untreated C57/BL6 mouse. **d** Transdiaphragmatic view of C57/BL6 mouse 12 days after intrapleural LLC cell injection

- Thoracic wall is exposed by retraction of fascia and muscle, leaving the parietal pleura intact.
- The tip of a 1.2 cm 27G needle is advanced under visual control through the translucent pleura at the seventh intercostal space at the midaxillary line into the pleural cavity where the tumor cell suspension is released slowly (Fig. 8.2b).
- The skin incision is closed using a suture and the animals are placed on a heating pad or under a heat lamp until complete recovery.

The procedure is not associated with mortality or morbidity. Pneumothoraxes never occur; however, even large volumes of air instilled into the murine pleural cavity are spontaneously absorbed within a matter of seconds to few minutes (unpublished observations). This intrapleural approach does not resemble human cancer metastasis to the pleura [18], but gives the opportunity to study the ability of tumor cells to trigger a MPE when homed to the pleural cavity, dissecting out the steps of vascular, pulmonary and pleural invasion.

A number of studies have used intratracheal, intrabronchial, intrapulmonary, or subpleural injection of the tumor cells with subsequent outgrowth into the pleural space [31, 33, 46]. Additionally, different research groups have employed intraperitoneal introduction of tumors [21, 47]. However, the behavior of tumor cells in the peritoneal and pleural cavities may be different, as the mechanisms of pleural and peritoneal fluid clearance are different [48] and pleural mesothelial cells may differ from peritoneal ones [49] In addition, morbidity and mortality of animals after intrapleural tumor delivery is different than what occurs after intraperitoneal inoculation [47]. Therefore, intrapleural orthotopic implantation models prevail for the study of MPE.

8.5.3.3 Consideration of Animal Immune Status

The genetic background of the animal used may deeply influence tumor growth and progression in vivo. The majority of animal models of MPE have been developed in immune-deficient hosts that allow the development of pleural metastases by xenogenic tumor cells. Various human cancer cell lines, especially adenocarcinomas, have been successfully introduced into the pleural space of immunodeficient mice, which give rise to MPE. The immune-deficient animals used in these models include severe combined immunodeficient (SCID) [31, 32] and athymic mice (nude; natural cytotoxicity receptor, NCR-deficient) [20, 21, 50] as well as immune-deficient rats [33]. The complexity of the human tumor is reliably mimicked in these models, being appropriate for predicting drug response in human tumors. Moreover, human tumor xenografts grown in immunodeficient mice become useful when tracing mediators back to the host or tumor, as these derive from different species [48]. The shortcoming of these models is that the lymphocyte-mediated response to the tumor is lost, e.g. nude mice lose certain T-cell responses and SCID mice lose both their T-and B-cell responses.

It is well known that MPE development is the result of a complex interaction between tumor and host immune response. Tumor cells secrete mediators that attract host inflammatory cells which, in turn, may impact tumor progression. Hence immunocompromised models have a serious limitation when applied to simulate MPE. An attractive alternative are immunocompetent hosts implanted with syngeneic tumors.

Different groups developed such models to study MPE, including intrapleural injection of metha fibrosarcoma to Balb/c mice or pleural implantation of VX2 tumors into New Zealand White rabbits [35, 36]. We developed a murine model of MPE in wild type, immune-intact mice, by intrapleural injection of syngeneic LLC lung adenocarcinoma cells [22]. The latter model appears to be highly relevant to human disease and 100% reproducible since all animals develop an MPE. These models have the advantage that mice are immunocompetent, such that the tumor microenvironment can be mirrored as much as possible and the role of specific molecules and genes in tumor development and progression can be explored at all stages. A major disadvantage is that they use mouse tumors and may be difficult to predict what will happen in the human tumor with regard to therapeutic response.

All preclinical trials of potential therapies against MPE need evaluation of toxicity; in this regard, the host inflammatory response is implicated in mechanisms of toxicity and should be intact [51, 52]. Immuno-deficient in contrast to immuno-intact models is impaired in terms of evaluation of toxicity. However, these immunological deficits can be partly overcome by grafting human tumors onto ‘humanized’ NOD/SCID mice [53].

8.5.3.4 Implanted Substance

A successful animal model of MPE depends on the form of tumor implanted in the pleural cavity, tissue or cells. In order to retain cell membrane integrity and

cell-to-cell contact to provide tumor architecture relevant to the original tumor, *intact tumor fragments* are implanted in the parietal and visceral pleura. Moreover, tying of cancerous tissues in the pleural space of animals offers the advantage of combined transplantation of tumor cells and stroma, as the latter seems to play an important role in the biologic behavior of tumor development [54]. However, intrapleural injection of *tumor cell suspensions* is easier, less time-consuming and more reproducible. Tumor cells grow in the pleural cavity and invade contiguous structures, including mediastinum, lung parenchyma and diaphragm. These local implantations are followed by induction of MPE with appearance of cachexia and dyspnea [22, 55].

Additionally, tumors of different origin appear to exhibit different behavior as far as development of an MPE is concerned. Some tumors lead to MPE formation in a few weeks, mimicking an advanced stage of human disease [56], whereas other mouse tumors are incompetent for MPE formation. The reason for this specific tumor phenotype (MPE induction) is a focus of intense investigations in our laboratory.

Occasionally, asbestos fibers have been used, instead of tumors, as carcinogens for induction of pleural diseases. Fibers are usually introduced to the pleural cavity of various animal species either via the respiratory tract (inhalation exposure) or by direct intrapleural injection. Fibers cause the growth of deformed malignant cells that begin reproducing at an uncontrollable rate, causing inflammation of the pleura. This symptom often triggers the production of excess fluid in the area, resulting in pleural effusion [1, 57, 58].

8.5.4 Assessment of MPE Formation and Progression

Several parameters such as weight loss, pleural fluid accumulation and tumor enumeration are commonly used as end-points related to MPE formation and tumor progression. Survival is another definitive endpoint. Pleural fluid and tissues are being collected at necropsy performed at varying time intervals after the tumor injections and processed for analysis using various techniques.

8.5.4.1 General Status of Animals

MPE formation in experimental animals leads to *cachexia*, a sign of tumor progression [23]. As MPE develops mice lose weight, specifically there is a rapid loss of adipose and muscle tissue, as well as present impaired physical function. Mice are weighted on the day of the intrapleural injection of tumor cells and every seven days until the harvest day. Determination of mice body weight at the harvest day and its change compared with initial weight can be a quantification of developing cachexia [24].

At the progressed stages of MPE mice appear to have severe dyspnea, weakness and decreased locomotor activity. Indeed, induction of MPE facilitates mortality of

the animal, as suppression of pleural fluid accumulation leads to increase of survival rate. Thus, *survival* of mice after tumor cell injection should be determined by daily observation of experimental animal till moribund.

8.5.4.2 Pleural Effusion and Pleural Tumor Progression

Most animal models use the presence of pleural fluid and/or determination of *pleural fluid volume* as the primary end-point [20, 22, 36, 59]. This is done by fine needle aspiration with or without chest opening and is easy in mice that have incomplete mediastinal separations. Pleural fluid volume above the normal amount of pleural fluid of mice (20 μl) is considered to represent a pleural effusion (Fig. 8.2c, d). Carcinomatous pleural effusions typically are exudative, with bloody appearance. Pleural fluid collection allows the study of pathologic mediators and biological pathways implicated in MPE formation.

Pleural tumor dissemination can be assessed by counting the number as well as the size of pleural tumor implantations at necropsy (Fig. 8.3d). Because pleural tumors are evenly distributed between visceral and parietal pleural surfaces, usually only visceral implantations are enumerated under a dissecting microscope, excluding primary tumors at the site of the injection that occurs occasionally. Macroscopically detectable metastases (e.g. Lungs, heart, kidney etc) are also harvested for microscopic and histological examination. A more robust method for pleural tumor evaluation involves stereological methods. Thoracic sections sampled randomly are stained with simple stains after determination of total thoracic volume by saline immersion. The relative to total thoracic volume and absolute thoracic tumor volume can be then determined by point counting [60]. Furthermore, as far as xenograft models are concerned, a relatively new and simple method for evaluation of tumor burden has been established. Specifically, Malek et all. devised a simple and universal real-time PCR-based method for quantitative detection of human tumor cells disseminated in mouse tissues. The method relies on the parallel amplification of unique, species-specific, conserved and non-transcribed sequences in the mouse and human genomes. This highly sensitive and reproducible method can easily be applied for the accurate quantification of human tumor cells into the thoracic cavity of mice [61].

Monitoring of pleural fluid accumulation and tumor growth in living animals is important for MPE research. Several imaging techniques have become available for small animals. Unlike necropsy, non invasive imaging techniques allow the measurement of tumor burden or the presence of fluid in the pleural cavity without the need to sacrifice the animal. Imaging modalities include computed tomography (CT), magnetic resonance imaging (MRI) and positron emission tomography (PET). In vivo bioluminescent (BLU)/biofluorescent (FLU) imaging is another imaging modality with a multitude of applications in MPE research (Fig. 8.3a). This technique requires the respective luminescent or fluorescent tumor cell reporter to be introduced to the host or the tumor cells prior to imaging. It should be noted

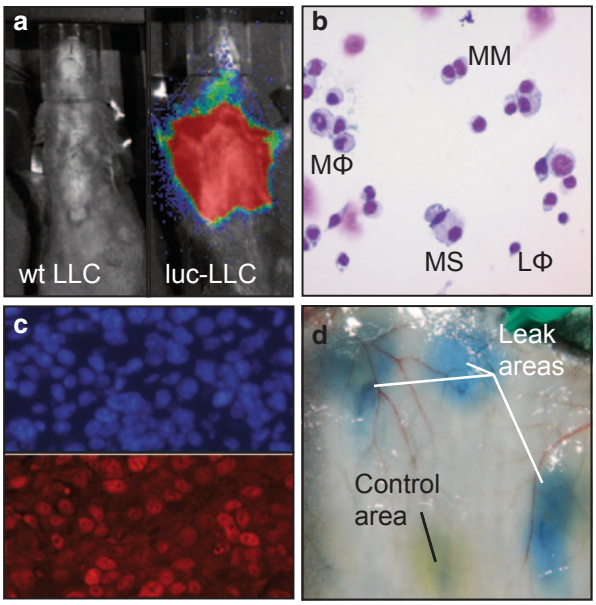

Fig. 8.3 Experimental end-points in the mouse model of LLC-induced MPE in C57BL/6 mice. **a** Bioluminescent detection of luciferase-expressing LLC tumor cells in vivo. Shown are bioluminescent images from live C57BL/6 mice 12 days after intrapleural injection of *wt* (*left*) and luciferase expressing (*right*) *LLC* cells. **b** Cytocentrifugal specimen of MPE cells with cells most likely representing mesothelial (*MS*), young mononuclear (*MM*), macrophage (*MΦ*), and lymphocytic (*LΦ*) cells. **c** Fluorescent microphotographs of pleural tumor tissue stained with Hoechst 33342 (*top*; *blue* color indicates nuclei) and immunolabeled with anti-PCNA antibody (bottom; red color indicates nuclear immunoreactivity for PCNA, a marker of cell proliferation). **d** Inverted C57BL/6 mouse dermis showing areas of no hyperpermeability (*control area*) and areas of enhanced Evans blue extravasation (*leak areas*)

that certain imaging approaches are better suited for specific applications over others. Specifically, tomographic approaches, such as CT and MRI, that provide high spatial resolution, are well suited for morphological detection of tumors with anatomical details. In comparison, PET and bioluminescent (BLU)/biofluorescent (FLU) imaging present high sensitivity and are better suited for monitoring tumor cell burden, viability and metabolism. Imaging approaches reliant on γ- and X-ray detection are not ideal for frequent imaging, as the animal becomes exposed to cumulatively significant doses of radiation. On the other hand, bioluminescent (BLU)/biofluorescent (FLU) imaging has the disadvantage that luminescent/fluorescent light emission is greatly attenuated with increased tissue depth [62]. Taken together, increased availability of small animal imaging modalities have undoubtedly facilitated the progress in the variety of ways that tumor biology can be visualized noninvasively in living mice.

8.5.4.3 MPE-Induced Host Reactions

Recent studies from our group have shown that tumor angiogenesis, pleural vascular hyper-peremability and induced tumor induced host inflammation have a prominent role in MPE formation [22, 63]. Therefore, determinations relevant to these biologic processes constitute additional end-points in animal models of MPE.

MPE development is accompanied by inflammatory cell recruitment. Most of the nucleated cells in pleural fluid are lymphocytes, monocytes and tumor cells; more than 50% of the cellular content is monocytes but there are occasions that neutrophils may predominate. *Inflammation* is measured in the pleural space, tumor tissue and blood of animals with MPE. Measurements in the pleural and vascular compartments are straightforward. Fifty thousand pleural fluid cells are used for cytocentrifugal specimen (cytospin) preparation. The slides are stained with modified May-Grunwald-Giemsa stain and distinct inflammatory cell types are enumerated as a percentage of cells on the slide using a light microscope (Fig. 8.3b). Measurements in tumor tissue are more complex; inflammatory cell tracking requires specific immunolabeling of mononuclear (e.g. F4/80, Ly6C), neutrophilic (e.g. GR1, E4, etc.), or other cell surface markers and flow cytometric analysis using [24].

Angiogenesis is an important end-point in experimental MPE, as it is intimately linked with the pathogenesis. New vessel formation in pleural tumor is evaluated by immune labeling with the endothelial marker factor VIII-related antigen, the anti-cluster of differentiation 31 antibody or hematopoietic stem cell antigen CD34, with subsequent assessment of the amount/density of new vessels in pleural tumor tissues. When the tumor is vascularized, it grows to clinically recognizable size and the balance of tumor cell apoptosis and proliferation are shifted towards proliferation. Therefore, pleural tumor tissue can also be examined for proliferation and apoptosis rates by immune-labeling for proliferating cell nuclear antigen (PCNA) or Ki67 and terminal deoxynucleotidyl nick-end labeling (TUNEL) respectively (Fig. 8.3c). In addition, the concentration of angiogenic mediators (i.e. VEGF, IL-6, CXCL-1) in tumor tissue, pleural fluid, or peripheral blood can be determined, providing an additional outcome measure in experimental MPE.

Pleural *vascular hyperpermeability* is regulated by a complex interplay between host and tumor derived mediators and presents an important feature in MPE pathobiology, as it constitutes the biologic event directly leading to fluid accumulation. Quantification of plasma leakage from pleural vessels in experimental MPE can be obtained by comparing total protein content of pleural fluid and serum. The higher the pleural fluid/serum protein ratio is, the higher the extent of the vascular permeability. Moreover, a well established method for measuring vascular permeability is the Miles assay, also known as the Evan's blue dye method. Evan's blue is a marker that specifically binds to albumin, allowing for a quantification of vascular leakage into the pleural cavity. The accumulated dye can be quantified by the use of a spectrophotometer. MPE levels of color per unit of time reflect the rate of vascular permeability. According to another approach, called modified Miles assay, vascular leakiness is determined by injecting MPE fluid in the mouse dermis followed by intravenous delivery of albumin tracer (e.g. Evans' blue). Local albumin

extravasation indicates the degree of vascular leakiness (Fig. 8.3d). This assay is also very useful for investigating the pro-permeability potential of any individual vasoactive mediator contained in a MPE [24].

8.6 Mechanisms Of Pleural Tumor Progression In The Immunocompetent Mouse Model Of Lewis Lung Carcinoma-Induced MPE

Published observations from harvesting studies, in various tumor progressive time points, support that the formation of experimental MPE after intrapleural injection of syngeneic Lewis Lung Carcinoma (LLC) cells in C57BL/6 mice [22] occurs via four distinct stages of tumor progression, which are detailed below:

- *Tumor implantation phase* (*days 0–4*). At the first day of the experiment (Day 0) the intrapleural injection of LLC cells into the mice takes place. The concentration of LLC cells injected per mice is 3×10^6 cells/ml. Cells in culture are counted and resuspended in the appropriate volume of PBS. The total volume injected is 50 μl/mouse (15×10^4 tumor cells). The following days (days1–4) intrapleural propagation of the tumor cells occurs. LLC cells home to the pleural surfaces, start to proliferate and to form microscopic tumor foci. At these early time points (up to day 4) initial tumor foci are detectable in the surface of visceral and parietal pleura only by means of microscopy. However, there are no gross pleural tumors and no accumulation of pleural fluid during this phase.
- *Inflammatory phase* (*days 5–8*). Tumors continue to grow and trigger an intact host immune response. Specifically, LLC tumors secrete inflammatory and angiogenic cytokines and chemokines that chemoattract a mixed inflammatory cell population. This is evident by differential cell counting of the inflammatory cell component in pleural fluid after harvesting mice at Day 8. Pleural exudates start forming very slowly and at this phase the fluid volume is still very low. Therefore, this phase is mainly characterized by a low volume of pleural fluid containing very high concentrations of tumor and host derived inflammatory mediators and immune cell populations.
- *Vascular hyperpermeability phase* (*days 8–12*). Well-established pleural tumor foci secrete VEGF, TNF, CCL2, and other powerful inducers of vascular permeability, rendering vessels hyperpermeable. This leads to extravasation of plasma fluid and proteins into the pleural cavity. In this phase, significant accumulation of pleural fluid takes place in an exponential fashion. Pleural effusions become clearly visible using CT scanning and radiography. The pleural fluid is initially straw-colored as in humans with MPE, but starts appearing hemorrhagic with time, as occurs in humans with very advanced disease. This shift in fluid appearance is thought to occur because of the pattern of hyperpermeability: initially, only plasma leaks into MPE; hovewer, the development of abnormal, disorganized blood vessels within progressive tumor-related angiogenesis leads

to leakage of blood cells, including red blood cells. MPE fluid, however, is not hemothorax as it does not coagulate and the hematocrit level rises gradually rather than abruptly. Due to the acute increase of pleural fluid volume during this phase, the inflammatory cells and mediators in the pleural cavity are diluted and, despite continued production/recruitment, their relative abundance is gradually reduced, as compared to the previous phase.

- *Phase of accelerated tumor progression* (*day12-death*). In this phase the pleural fluid acts as a giant vessel that feeds established tumor foci thereby facilitating their accelerated growth and pleural spread. Larger pleural tumors form bridges between the lung parenchyma and the thoracic cage and infiltrate neighboring anatomic structures, including lung, chest wall, mediastinum and diaphragm. Lungs are severely compressed in size by the abundant tumor formation leading to respiratory distress and dyspnea. Mice present severe weight loss, cachexia and eventually die.

The above characterized model of MPE is similar in many aspects to human MPE. Like human MPE, MPEs in this model are exudates with high levels of serum proteins, cytokines and chemokines that are produced locally in the pleural cavity of the mouse. Tumor growth triggers a host immune response, followed by a mixed inflammatory cell component in the pleural fluid that resembles the inflammatory cell phenotype found in human MPE. New vessel formation within tumors and increased vascular permeability, mechanisms involved in human MPE pathogenesis, are also present in this mouse model of MPE. Therefore, this model can be a useful tool to investigate the mechanisms and treatment of MPE.

8.7 Translational Contributions Of Experimental Models

Translational research in MPE is necessary to further our understanding on the mechanisms involved in disease development and to evaluate and establish innovative and targeted therapeutic alternatives. Significant progress accomplished in recent years has been reviewed elsewhere and will be briefly outlined here [28].

Studies in animal models of MPE have generated an improved understanding of pleural tumor pathobiology. The insights gained have identified new therapeutic targets, including VEGF, IL-6/Stat3, and TNF/NF-κb signaling [20–23, 50]. Although most older work on MPE has been performed in immunodeficient mice [43], the development of immunocompetent models represents a significant step forward for translational pleural research. Using these models the role of important mediators and biologic pathways in effusion formation has been uncovered. VEGF levels have been found to be significantly elevated in MPE and its receptor 1 (VEGFR1) was implicated in the angiogenic effects of VEGF in MPE progression [50, 64]. Expression of interleukin 6 with subsequent activation of Stat3 in cancer

cells was also mechanistically shown to participate in adenocarcinoma-associated MPE formation [30]. On the other hand, pleural fibrinolytic activity and MYO18B gene repression were proven to be important pathways in the pathogenesis of sarcoma- and mesothelioma-associated MPE [32, 37, 38]. Use of immunocompetent models led to the identification of an important role for NF-κb activation in lung adenocarcinoma cells in MPE formation and progression. The transcription factor was found to act via promotion of TNF secretion by tumor cells, which led in an autocrine manner to further NF-κb activation and enhanced VEGF elaboration [23]. Recently, another NF-κb-dependent mediator secreted by adenocarcinoma cells was identified, which is critical in the ability of these cells to trigger MPE formation, namely monocyte chemotactic protein-1 (MCP-1, also known as CCL2) [27]. Furthermore, angiopoietin/Tie2 signaling was pin-pointed as an important component of MPE pathogenesis, as its blockade significantly reduced pleural fluid volume and pleural tumor foci [65]. Using the LLC model different groups identified important roles for tumor-derived osteopontin in MPE formation as well as efficacy of vinorelbine in improving outcome [41, 59]. Moreover, host-derived interleukin-5 was found to promote experimental MPE induced by both lung and colon adenocarcinoma [66] whereas aquaporin-1 (AQP1) was recently implicated in increased volume of MPE [67].

In addition, studies have examined the efficacy of novel therapies, and have provided insights into potential future therapies against MPE. In this regard, synergism of interleukin IL-12 and IL-15 blockade was discovered and shown to be beneficial against experimental MPE [35], inhibitors of topoisomerase II were applied [55] and VEGF-receptor tyrosine kinase inhibition was performed [20] at the preclinical level. Bortezomib (an indirect inhibitor of NF-κb activation) and zoledronic acid (an aminobiphosphonate that exerts potent antitumor effects) were also found to exert beneficial effects against mouse MPE by inhibiting tumor-specific NF-κβ and Ras signaling, respectively [68, 69]. Recent studies using a sulindac derivative showed promising effects on intrapleural tumor dissemination via down-regulation of pleural vascular permeability [70].

These mechanistic and therapeutic studies provided significant insights on disease pathogenesis and identified potential therapeutic targets.

8.8 Conclusions

MPE is a common problem for cancer patients, especially those suffering from lung cancer. MPE pathogenesis is not adequately understood and more research efforts are needed to further unveil tumor-host interactions that take place during cancerous involvement of the pleura. However, several steps towards better understanding MPE pathobiology have already been accomplished, which will hopefully lead to therapeutic improvements in the future.

References

1. Robinson BW, Lake RA (2005) Advances in malignant mesothelioma. N Engl J Med 353:1591–1603
2. Scherpereel A, Astoul P, Baas P, Berghmans T, Clayson H, et al (2010) Guidelines of the european respiratory society and the european society of thoracic surgeons for the management of malignant pleural mesothelioma. Eur Respir J 35:479–495
3. Lee YC, Light RW (2004) Management of malignant pleural effusions. Respirology 9:148–156
4. Antony VB, Loddenkemper R, Astoul P, Boutin C, Goldstraw P, et al (2001) Management of malignant pleural effusions. Eur Respir J 18:402–419
5. Henschke CI, Yankelevitz DF, Davis SD (1991) Pleural diseases: multimodality imaging and clinical management. Curr Probl Diagn Radiol 20:155–181.
6. Noppen M, De Waele M, Li R, Gucht KV, D'Haese J, et al (2000) Volume and cellular content of normal pleural fluid in humans examined by pleural lavage. Am J Respir Crit Care Med 162:1023–1026
7. Broaddus VC, Wiener-Kronish JP, Berthiaume Y, Staub NC (1988) Removal of pleural liquid and protein by lymphatics in awake sheep. J Appli Physiol 64:384–390
8. Agostoni E (1972) Mechanisms of the pleural space. Physiol Rev 52:57–128.
9. Zocchi L (2002) Physiology and pathophysiology of pleural fluid turnover. Eur Respir J 20:1545–1558
10. Albertine KH, Wiener-Kronish JP, Bastacky J, Staub NC (1991) No evidence for mesothelial cell contact across the costal pleural space of sheep. J Appli Physiol 70:123–134
11. Albertine KH, Wiener-Kronish JP, Staub NC (1984) The structure of the parietal pleura and its relationship to pleural liquid dynamics in sheep. Anat Rec 208:401–409
12. Albertine KH, Wiener-Kronish JP, Staub NC (1985) Blood supply of the caudal mediastinal lymph node in sheep. Anat Rec 212:129–131, 154–125
13. Lai-Fook SJ (2004) Pleural mechanics and fluid exchange. Physiol Rev 84:385–410
14. Miserocchi G (1997) Physiology and pathophysiology of pleural fluid turnover. Eur Respir J 10:219–225
15. Wang NS (1975) The preformed stomas connecting the pleural cavity and the lymphatics in the parietal pleura. Am Rev Respir Dis 111:12–20
16. Agostoni E, Bodega F, Zocchi L (2002) Albumin transcytosis from the pleural space. J Appli Physiol 93:1806–1812
17. Song Y, Yang B, Matthay MA, Ma T, Verkman AS (2000) Role of aquaporin water channels in pleural fluid dynamics. Am J Physiol—Cell Physiol 279:C1744–C1750
18. Meyer PC (1966) Metastatic carcinoma of the pleura. Thorax 21:437–443
19. Light R (1997) Diseases of the pleura. Curr Opin Pulm Medicine 3:303–304
20. Yano S, Shinohara H, Herbst RS, Kuniyasu H, Bucana CD, et al (2000) Production of experimental malignant pleural effusions is dependent on invasion of the pleura and expression of vascular endothelial growth factor/vascular permeability factor by human lung cancer cells. Am J Pathol 157:1893–1903
21. Yeh HH, Lai WW, Chen HH, Liu HS, Su WC (2006) Autocrine IL-6-induced Stat3 activation contributes to the pathogenesis of lung adenocarcinoma and malignant pleural effusion. Oncogene 25:4300–4309
22. Stathopoulos GT, Zhu Z, Everhart MB, Kalomenidis I, Lawson WE, et al (2006) Nuclear factor-kappaB affects tumor progression in a mouse model of malignant pleural effusion. Am J Respir Cell Mol Biol 34:142–150
23. Stathopoulos GT, Kollintza A, Moschos C, Psallidas I, Sherrill TP, et al (2007) Tumor necrosis factor-α promotes malignant pleural effusion. Cancer Res 67:9825–9834
24. Stathopoulos GT, Psallidas I, Moustaki A, Moschos C, Kollintza A, et al (2008) A central role for tumor-derived monocyte chemoattractant protein-1 in malignant pleural effusion. J Natl Cancer Inst 100:1464–1476

25. Ishimoto O, Saijo Y, Narumi K, Kimura Y, Ebina M, et al (2002) High level of vascular endothelial growth factor in hemorrhagic pleural effusion of cancer. Oncology 63:70–75
26. Collins PD, Connolly DT, Williams TJ (1993) Characterization of the increase in vascular permeability induced by vascular permeability factor in vivo. Br J Pharmacol 109:195–199
27. Stathopoulos GT, Psallidas I, Moustaki A, Moschos C, Kollintza A, et al (2008) A central role for tumor-derived monocyte chemoattractant protein-1 in malignant pleural effusion. J Nat Cancer Inst 100:1464–1476
28. Stathopoulos G (2011) Translational advances in pleural malignancies. Respirology 16:53–63
29. Light R (2007) Pleural disease. In: Evidence-based respiratory medicine, 2nd edn. Blackwell, London
30. Yeh HH, Lai WW, Chen HHW, Liu HS, Su WC (2006) Autocrine IL-6-induced Stat3 activation contributes to the pathogenesis of lung adenocarcinoma and malignant pleural effusion. Oncogene 25:4300–4309
31. Boehle AS, Dohrmann P, Leuschner I, Kalthoff H, Henne-Bruns D (2000) An improved orthotopic xenotransplant procedure for human lung cancer in SCID bg mice. The Annals of Thoracic Surgery 69:1010–1015
32. Edakuni N, Ikuta K, Yano S, Nakataki E, Muguruma H, et al (2006) Restored expression of the MYO18B gene suppresses orthotopic growth and the production of bloody pleural effusion by human malignant pleural mesothelioma cells in SCID mice. Oncol Res 16:235–243
33. Ohta Y, Kimura K, Tamura M, Oda M, Tanaka M, et al (2001) Biological characteristics of carcinomatosa pleuritis in orthotopic model systems using immune-deficient rats. Int J Oncol 18:499–505
34. Jongsma J, van Montfort E, Vooijs M, Zevenhoven J, Krimpenfort P, et al (2008) A conditional mouse model for malignant mesothelioma. Cancer cell 13:261–271
35. Kimura K, Nishimura H, Matsuzaki T, Yokokura T, Nimura Y, et al (2000) Synergistic effect of interleukin-15 and interleukin-12 on antitumor activity in a murine malignant pleurisy model. Cancer Immunol Immunother 49:71–77
36. Hatton MWC, Southward SMR, Ross BL, Legault K, Marien L, et al (2002) Angiostatin II is the predominant glycoform in pleural effusates of rabbit VX-2 lung tumors. J Lab Clin Med 139:316–323
37. Hatton MWC, Southward SMR, Legault KJ, Ross BL, Clarke BJ, et al (2004) Fibrinogen catabolism within the procoagulant VX-2 tumor of rabbit lung in vivo: effluxing fibrin(ogen) fragments contain antiangiogenic activity. J Lab Clin Med 143:241–254
38. Hatton MWC, Southward SMR, Ross BL, Clarke BJ, Singh G, et al (2006) Relationships among tumor burden, tumor size, and the changing concentrations of fibrin degradation products and fibrinolytic factors in the pleural effusions of rabbits with VX2 lung tumors. J Lab Clin Med 147:27–35
39. Tufan AC, Satiroglu-Tufan NL (2005) The chick embryo chorioallantoic membrane as a model system for the study of tumor angiogenesis, invasion and development of anti-angiogenic agents. Curr Cancer Drug Targets 5:249–266
40. Ribatti D (2012) Chicken chorioallantoic membrane angiogenesis model. Methods Mol Biol 843:47–57
41. Psallidas I, Stathopoulos GT, Maniatis NA, Magkouta S, Moschos C, et al. (2013) Secreted phosphoprotein-1 directly provokes vascular leakage to foster malignant pleural effusion. Oncogene 32(4):528–535
42. Slack-Davis JK, Atkins KA, Harrer C, Hershey ED, Conaway M (2009) Vascular cell adhesion molecule-1 is a regulator of ovarian cancer peritoneal metastasis. Cancer Res 69:1469–1476
43. Astoul P, Colt HG, Wang X, Hoffman RM (1993) Metastatic human pleural ovarian cancer model constructed by orthotopic implantation of fresh histologically-intact patient carcinoma in nude mice. Anticancer Res 13:1999–2002
44. Wang X, Fu X, Kubota T, Hoffman RM (1992) A new patient-like metastatic model of human small-cell lung cancer constructed orthotopically with intact tissue via thoracotomy in nude mice. Anticancer Res 12:1403–1406
45. Elkin M, Vlodavsky I (2001) Tail vein assay of cancer metastasis. Curr Protoc Cell Biol 19:2

46. Mase K, Iijima T, Nakamura N, Takeuchi T, Onizuka M, et al. (2002) Intrabronchial orthotopic propagation of human lung adenocarcinoma–characterizations of tumorigenicity, invasion and metastasis. Lung Cancer 36:271–276
47. Heike Y, Takahashi M, Ohira T, Naruse I, Hama S, et al. (1997) Genetic immunotherapy by intrapleural, intraperitoneal and subcutaneous injection of IL-2 gene-modified Lewis lung carcinoma cells. Int J Cancer 73:844–849
48. Zocchi L (2002) Physiology and pathophysiology of pleural fluid turnover. Eur Respir J 20:1545–1558
49. Michailova KN, Usunoff KG (2006) Serosal membranes (pleura, pericardium, peritoneum). Normal structure, development and experimental pathology. Adv Anat Embryol Cell Biol 183:i-vii, 1–144. (back cover)
50. Yano S, Herbst RS, Shinohara H, Knighton B, Bucana CD, et al (2000) Treatment for malignant pleural effusion of human lung adenocarcinoma by inhibition of vascular endothelial growth factor receptor tyrosine kinase phosphorylation. Clin Cancer Res 6(3):957–965
51. Monk JP, Phillips G, Waite R, Kuhn J, Schaaf LJ, et al (2006) Assessment of tumor necrosis factor alpha blockade as an intervention to improve tolerability of dose-intensive chemotherapy in cancer patients. J Clin Oncology 24(12):1852–1859
52. Abushamaa AM, Sporn TA, Folz RJ (2002) Oxidative stress and inflammation contribute to lung toxicity after a common breast cancer chemotherapy regimen. Am J Physiol Lung Cell Mol Physiol 283:L336–345
53. Richmond A, Su Y Mouse xenograft models vs GEM models for human cancer therapeutics: Dis Model Mech. 2008 Sep-Oct;1(2–3):78–82
54. Kim K-U, Wilson SM, Abayasiriwardana KS, Collins R, Fjellbirkeland L, et al (2005) A novel in vitro model of human mesothelioma for studying tumor biology and apoptotic resistance. pp. 541–548
55. Kraus-Berthier L, Jan M, Guilbaud N, Naze M, Pierré A, et al (2000) Histology and sensitivity to anticancer drugs of two human non-small cell lung carcinomas implanted in the pleural cavity of nude mice. Clin Cancer Res 6:297–304
56. Antunes G, Neville E, Duffy J, Ali N (2003) BTS guidelines for the management of malignant pleural effusions. Thorax 58:ii29–ii38
57. Kroczynska B, Cutrone R, Bocchetta M, Yang H, Elmishad AG, et al (2006) Crocidolite asbestos and SV40 are cocarcinogens in human mesothelial cells and in causing mesothelioma in hamsters. Proc Nat Acad Sci 103:14128–14133
58. Kleymenova EV, Bianchi AA, Kley N, Pylev LN, Walker CL (1997) Characterization of the rat neurofibromatosis 2 gene and its involvement in asbestos-induced mesothelioma. Molecular Carcinogenesis 18:54–60
59. Cui R, Takahashi F, Ohashi R, Yoshioka M, Gu T, et al (2009) Osteopontin is involved in the formation of malignant pleural effusion in lung cancer. Lung cancer (Amsterdam, Netherlands) 63:368–374
60. Hsia CC, Hyde DM, Ochs M, Weibel ER (2010) An official research policy statement of the American thoracic society/European respiratory society: standards for quantitative assessment of lung structure. Am J Respir Crit Care Med 181:394–418
61. Malek A, Catapano CV, Czubayko F, Aigner A (2010) A sensitive polymerase chain reaction-based method for detection and quantification of metastasis in human xenograft mouse models. Clin Exp Metastasis 27:261–271
62. Lyons SK (2005) Advances in imaging mouse tumour models in vivo. J Pathol 205:194–205
63. Stathopoulos GT, Sherrill TP, Han W, Sadikot RT, Yull FE, et al. (2008) Host nuclear factor-kappaB activation potentiates lung cancer metastasis. Mol Cancer Res 6:364–371
64. Zebrowski BK, Yano S, Liu W, Shaheen RM, Hicklin DJ, et al. (1999) Vascular endothelial growth factor levels and induction of permeability in malignant pleural effusions. Clin Cancer Res 5(11):3364–3368
65. Moschos C, Psallidas I, Kollintza A, Karabela S, Papapetropoulos A, et al. (2009) The angiopoietin/Tie2 axis mediates malignant pleural effusion formation. Neoplasia 11:298–304

66. Stathopoulos GT, Sherrill TP, Karabela SP, Goleniewska K, Kalomenidis I, et al (2010) Host-derived Interleukin-5 Promotes Adenocarcinoma-induced Malignant Pleural Effusion. Am J Respir Crit Care Med 182:1273–1281
67. Zhang J, Xie C, Zhu Z, Huang H, Zeng Z Potential role of AQP1 and VEGF in the development of malignant pleural effusion in mice. Med Oncol 2012 29(2):656–662
68. Stathopoulos GT, Moschos C, Loutrari H, Kollintza A, Psallidas I, et al (2008) Zoledronic Acid Is Effective against Experimental Malignant Pleural Effusion. Am J Respir Crit Care Med 178:50–59
69. Psallidas I, Karabela SP, Moschos C, Sherrill TP, Kollintza A, et al (2010) Specific effects of bortezomib against experimental malignant pleural effusion: a preclinical study. Mol Cancer 9:56
70. Moschos C, Psallidas I, Cottin T, Kollintza A, Papiris S, et al (2011) A sulindac analogue is effective against malignant pleural effusion in mice. Lung Cancer 73:171–175

Chapter 9
Mathematical Modeling of the Metastatic Process

Jacob G. Scott, Philip Gerlee, David Basanta, Alexander G. Fletcher, Philip K. Maini and Alexander R. A. Anderson

Abstract Mathematical modeling in cancer has been growing in popularity and impact since its inception in 1932. The first theoretical mathematical modeling in cancer research was focused on understanding tumor growth laws and has grown to include the competition between healthy and normal tissue, carcinogenesis, therapy and metastasis. It is the latter topic, metastasis, on which we will focus this short review, specifically discussing various computational and mathematical models of different portions of the metastatic process, including: the emergence of the metastatic phenotype, the timing and size distribution of metastases, the factors that influence the dormancy of micrometastases and patterns of spread from a given primary tumor.

Abbreviations

MCs	Markov chains
CA	Cellular automata
EMT	Epithelial-mesenchymal transition
CTCs	Circulating tumor cells
ODEs and PDEs	Ordinary and partial differential equations

J. G. Scott (✉) · D. Basanta · A. R. A. Anderson
Integrated Mathematical Oncology, H. Lee Moffitt Cancer Center and Research Institute, Tampa, FL, USA
e-mail: jacob.g.scott@gmail.com

J. G. Scott · A. G. Fletcher · P. K. Maini
Wolfson Centre for Mathematical Biology, Mathematical Institute, Oxford University, Oxford, UK

P. Gerlee
Mathematical Sciences Division, University of Gothenburg, Gothenburg, Sweden

Chalmers University of Technology, Gothenburg, Sweden

A. Malek (ed.), *Experimental Metastasis: Modeling and Analysis,*
DOI 10.1007/978-94-007-7835-1_9,

9.1 Introduction—Why Use Mathematical Models?

Metastasis accounts for 90 % of cancer related deaths [1], and the shift from localized to metastatic disease represents a paradigm shift for clinicians and patients alike as the strategy for therapy changes from aggressive and localized, to systemic and generally palliative. Despite its importance, this complex multi-step process remains poorly understood. With the exception of studies showing genetic correlations between primary sites and sites of metastatic arrest [2, 3], there is little understanding of the driving principles behind this process. Our lack of knowledge is, for example, reflected in the fact that self-seeding, a process whereby a primary tumor releases metastatic cells that return to the primary tumor and accelerate its growth, is hypothesized to be a driver of primary growth [4], yet our current knowledge of the metastatic cascade is insufficient to determine the validity of this claim. For such a multi-faceted process, only through a combination of experimental and theoretical investigations can we hope to gain a comprehensive mechanistic understanding, and therefore uncover sensitive points where we can intervene and prolong the life of affected patients.

9.2 Where Experiments Cannot Go: Opportunities for Mathematical Models

The strength of experimental model systems is their ability to provide clear answers to specific questions. The strength of mathematical models is their ability to combine disparate experimental data and coalesce them into a coherent framework, which can then be used to predict the overall dynamics of the system in question. In particular, mathematical models allow for identification of the parameters to which the system is the most sensitive, and also allow for logical reasoning beyond what experiments can provide. In this sense, mathematical models of metastasis should be playing a larger role in the research in this area as experimentation is typically limited to one or a few steps in the cascade. Many mathematical models to date, however, have also concentrated on only a subset of the steps of the cascade. While these models are useful, as they have quantified the impact of parameters within the models of each step, they have yet to yield any fundamental additions to our knowledge of the process itself.

To definitively answer questions in biology, the burden of proof falls on the experimental scientists. To connect the disparate experimental ‘truths’ into a coherent framework however, is within the purview of theorists. Further, when theory has been established, but necessary experimental techniques have yet to be developed, theory can again step in to advance science by making specifically testable predictions—vastly shrinking the set of possible experiments. This dual role is best understood by thinking of where mathematical/computational science fits into the scientific method. The place of theory, typically called mathematical or theoretical

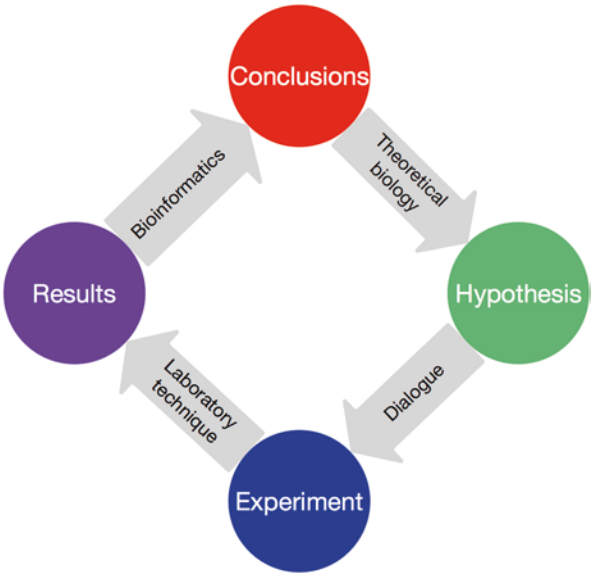

Fig. 9.1 An overview of the scientific method, and where theoretical/computational scientists fit into this process in the life/medical sciences and biology. Theoretical biology is the science of putting together existing knowledge into specific theoretical frameworks which can be used to make predictions and generate further hypotheses. Bioinformatics is a statistical science used for helping scientists make conclusions when faced with large data sets and non-linear relationships. Dialogue between multi-disciplinary scientists helps shape meaningful experiments. Laboratory technique translates experimental constructs into meaningful results

biology, lies between biological conclusions and new hypotheses (Fig. 9.1). The central goal of this discipline is to create rigorous frameworks, beyond linear 'cartoon' models of mechanism, through which specific predictions and hypotheses can be generated. Bioinformatics, another computational field in biology, largely works between experiment and conclusion, helping to make sense of the vast amounts of data that come out of modern day experiments. This review will focus on models from the field of theoretical biology.

9.2.1 Model Types: Descriptive vs. Mechanistic Models

Mathematical models of biological systems tend to fall into two broad camps: descriptive and mechanistic. A descriptive model seeks to succinctly encapsulate the behavior of a system so that future behaviors can be predicted, without regard to the underlying processes. These types of models can often be 'fit' in their final form by using any one of a number of optimization methods. A mechanistic model, on the other hand, is one that begins by trying to capture the processes driving a complex system and then builds up towards the measurable results. These types of models are more commonly 'parameterized' with low-level experimental data rather than fit to large-scale outcomes.

Both approaches can provide useful insights but since we want to connect directly with experimental measurement and drive novel experimentation, mechanistic models are where we need to focus our attention. This does not mean that we should build all-encompassing mechanistic models of every process that we think is important in metastasis—since this would only provide us with a complex caricature of the real system with no additional understanding. Instead, we need to consider key processes and describe them in a level sufficient to gain insight, which should be tied to the resolution of the experimental data that might be used to drive and validate such models in the first place. Mirroring experimental observation should always be a key part of model validation but ultimately if a model is to be useful it should also make predictions that go beyond current observations, and further drive our understanding and inquiry.

To this end, our group, and others, have begun to build models more like those typically built to understand complex engineering systems, into which the more detailed models can eventually be embedded when the time comes for specific predictions to be made. Until that time, these higher level models serve to shed light on areas of our knowledge which are most severely lacking, and provide experimental questions to fill those gaps in a systematic manner.

9.2.2 A Note on Mathematical Tools: Stochastic vs. Deterministic Models

Like experimentalists, mathematical modelers have many tools at their disposal. These tools comprise a wide spectrum, ranging from classical 'pen and paper' models, to those requiring powerful computers to iterate, and everything in between. There are many ways to distinguish these models from each other, but likely the most telling dichotomy is the difference between stochastic and deterministic models.

A deterministic model is one in which there is no randomness: the model will behave exactly the same way each time it is solved. This does not mean that the model is necessarily predictable: indeed, many deterministic models exhibit wild fluctuations and even chaotic results, exhibiting strong dependence on even small changes in initial conditions or parameter values. The strength of these models is that they allow us to understand all the possible behaviors of a system and in which parameter regimes those behaviors occur. Examples of deterministic models discussed in this review include ordinary and partial differential equations (ODEs and PDEs), which describe how key quantities of interest, such as chemical concentrations or cell densities, vary continuously with one (in the case of ODEs) or many (for PDEs) independent variables. Well-mixed systems, where space is not considered, are typically modeled with ODEs where the dependent variables evolve in time; PDEs are utilized when there is also spatial heterogeneity, or differences in 'age' or differentiation status across the population modeled.

A stochastic model, on the other hand, has randomness written in to the system itself. This randomness can be incorporated into the model in many different ways. Models can represent many individual entities which can interact with one another or move in ways defined by probabilities. Alternatively, noise terms may be explicitly incorporated into existing deterministic descriptions. As compared to their deterministic counterparts, these sorts of models are often better representations of the underlying biological processes, which do seem to be governed at some level by randomness, and the results of any given simulation of a model can be quite different from another, again mimicking biology. Gaining a deep understanding of these models through analysis is, however usually much more difficult, and we must often rely upon averages of many realisations to gain an understanding of the system, or on analysing the average ("mean-field") behavior of the system, effectively returning to a deterministic description. Examples of the types of stochastic model discussed in this review include Markov chains (MCs), cellular automata (CA) and Moran processes. MCs are stochastic processes in which a population is subject to a time-independent series of transitions, from one state to another in a 'memoryless' fashion, that is without regard to the history of the system [5]. CA are discrete time and discrete 'cell' based models. Individual cells, often called 'agents', are programmed with simple rules and simulated as they interact in a computational domain. Complex behaviors often can emerge from simple rule sets and limited numbers of agents [6], and while these models are not necessarily stochastic by nature, the ones described in this review are, by virtue of their rules. The Moran process [7] is a stochastic process of birth and death in which a well-mixed population of two (or more) species compete in a manner meant to mimic Darwinian selection.

In the science of metastasis, all of these model types have been, and will continue to be, utilized for different applications. This is particularly relevant as there are a number of steps in the metastatic cascade (outlined in Fig. 9.2) which span multiple scales, both spatial and temporal. In the remainder of this brief review, we will cover the most relevant mathematical models of the metastatic cascade and highlight the ways in which these models have affected our knowledge, future experiments and clinical decision making. We will begin by describing a series of mathematical models built around a specific experimental murine metastasis model which was able to give insight into several key, unmeasurable parameters. We will then describe a series of models focussed on the genetic emergence of metastasis which generates a number of hypotheses, but can not yet be tied to experimental data. We then discuss models aimed at understanding the size distribution of metastases at the time of diagnosis, several of which offer the possibility of connecting to patient-specific data. We then review several models aimed at understanding the temporal patterns of recurrence through the dormancy mechanism, and we conclude by reviewing some recent network models of metastasis aimed at understanding the anatomic patterns of metastatic spread within the body.

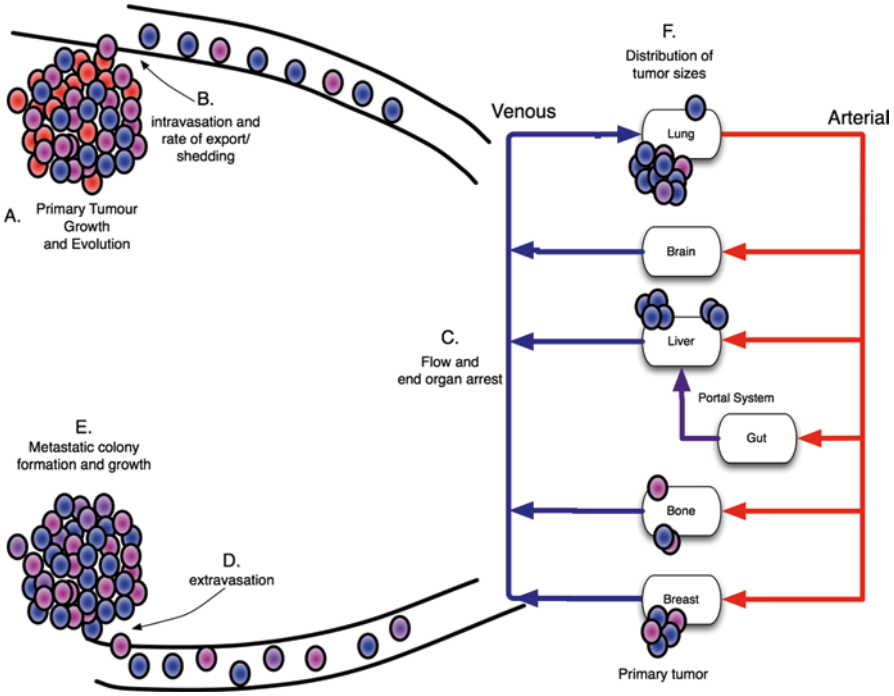

Fig. 9.2 An overview of the metastatic process. Each step in the cascade represents an opportunity for experimental systems to be designed. Understanding the temporal dynamics within each step, and how the steps join together, however, is a challenge that also requires mathematical modeling. Cells from typically heterogeneous primary tumors grow (**a**) and some (*blue* and *purple*) are able to intravasate (**b**). Once in the vascular system, cells are subject to physical forces and selection of flow and filtration (**c**) until they extravasate (**d**) and colonise a foreign tissue bed (**e**). Tumors at this final stage will be distributed in size based on temporal and other factors (**f**) and will be made up of only certain clones from the primary tumor dependent on biological factors

9.3 Models of Experimental Systems

One of the first attempts to model the metastatic process is described in a series of papers by Liotta and colleagues [8–10]. In this work, the authors built an experimental system and mathematical models in parallel in an attempt to better define the parameters of each step in the process. The experimental system considered was a mouse model of fibrosarcoma that readily formed pulmonary metastases, via both implantation and intravenous injection. In this way, the authors were able to accurately control many parameters, and use the results to obtain estimates for those that could not be measured directly.

The authors derived an ODE model to describe how the population of tumor cells changes in time in each of several key ‘compartments’ as a result of flux between them. Each of the compartments in their mathematical model represents a discrete phase of the metastatic cascade, illustrated schematically by the blue boxes

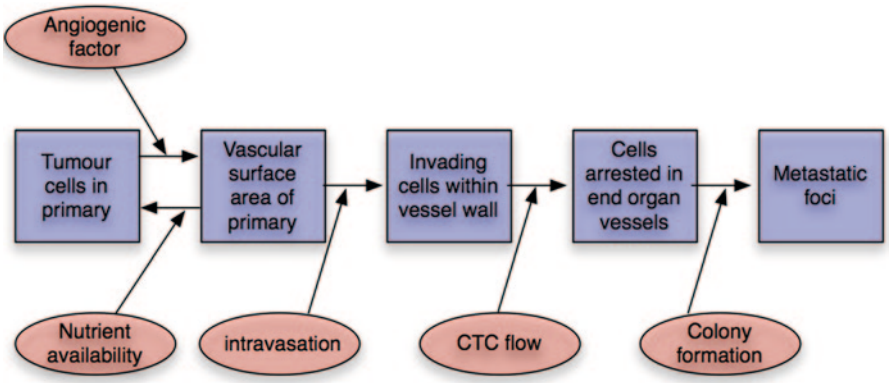

Fig. 9.3 Compartment model developed by Saidel et al. [8]. Each of the blue boxes represent measurable quantities from the *in vivo* model, while the ovals represent quantities inferred from the model

in Fig. 9.3 [8]. Numbers of cells measured from the murine experimental system were used to parameterize this mathematical model. The model was then used to predict the effect of a number of perturbations to the system including: tumor resection, tumor trauma, vessel growth inhibition, lung vessel damage and inhibition of intravasation. Each of these perturbations was simulated to predict response and the experimental system was then assayed with good correlation, giving significant insight into the otherwise unmeasurable aspects of the system and the mechanisms driving the response to the perturbations.

As discussed previously, biological systems are often ruled by stochastic processes at the cellular level, and in the case of metastasis, this is certainly the case. To this end, Liotta et al. developed and analysed a MC model of a subset of the above system [9]. The authors additionally considered that cancer cells do not only travel and arrest as single cells, but are found in clumps of varying size [11]. The model contains three compartments: tumor cell clumps in the circulation, tumor cell clumps arrested in the pulmonary capillary bed, and pulmonary metastatic foci. In agreement with experimental data, the model assumes that the entry rate of clumps is size-dependent, following a decaying power-law (i.e. the number of clumps of size n scales as $n^{-\alpha}$, $\alpha = 2$), that the clump death rate is inversely proportional to size, and the colonisation rate increases linearly with clump size. The validation was carried out in the fibrosarcoma mouse model, where cancer cells were injected intravenously and the animals were sacrificed 10–30 days post-implant. The model showed good agreement both with respect to the number of macroscopic metastatic foci as a function of time, and the time-dependent probability of finding a metastasis-free animal. An interesting conclusion from the study was that larger clumps have a strong impact on metastasis formation, and hence that disassociating agents that reduce clump size could have therapeutic effect.

A follow-up study further simplified this mathematical model to account only for arrest and foci formation, without regard to clump size [10]. Interestingly, the sharp transition in the metastasis-free probability remained, suggesting that this phenomenon is due only to the stochastic nature of arrest and foci formation. If these results can be extended to patients they could represent a novel method for assessing the likelihood of micrometastatic lesions that eventually could become clinically relevant.

9.4 Models as Abstractions: Insights into Unmeasurable Processes

In the previously discussed models, each portion of the model corresponded directly to an aspect of an experimental system. In this way, the authors were able to use the strength of each system to gain a deeper understanding of the mechanisms driving each portion of the well-controlled process. Many aspects of the metastatic process in the clinic, however, are not amenable to this sort of methodology, and cannot be measured/quantified directly. This situation, where measurements are not yet able to be made, is one where mathematical models can play an influential role and relieve the impasse at which we would otherwise be. A specific case of this is in tumor genomics: we know that genetic mutations play a role, but we are not yet able to measure the dynamic changes of a tumor genome within a patient over time.

9.4.1 Evolutionary Models: Emergence of Metastatic Clones

The emergence of metastatic disease has largely been attributed to cells gaining functions specific to intravasation (Fig. 9.2). This gain of function has been linked to genetic mutation, with large numbers of specific genes being implicated. More generally, the epithelial-mesenchymal transition (EMT) has been identified as a process (likely polygenic) involved in the acquisition of metastatic potential [12].

Experimental studies have shown that EMT (among other phenotypic changes) is important for the development of metastatic clones [13], but as measuring the individual mutations within a patient's tumor over time remains beyond the scope of experimental science, understanding the dynamics of this process is a ripe question for theoreticians. To this end, a number of models have employed a stochastic description called the Moran process [7] to study the genetic landscape of a tumor's cellular population over time. In this process, populations of constant size consisting of individual agents (cells), usually of two distinct (geno)types, are grown in competition with one another under selection. The Moran process was originally designed to mimic Darwinian selection, where cells of a given type are chosen randomly to divide or die based on an ascribed fitness, usually linked to division rate. The population dynamics are then simulated, with the aim of understanding long-term behavior (coexistence or dominance by one population). These models serve as ex-

cellent platforms through which to understand the emergence of new clones within a population, much like the emergence of EMT, or any other metastasis-specific trait.

To study the dynamics of the emergence of the metastatic phenotype, Michor et al. [14] proposed a model of tumor growth, based on the Moran process, that took account of mutation to a metastatic phenotype. The authors modeled a heterogeneous tumor made up initially of cells without the ability to metastasize (type-0, fitness r_0). At each time step, a cell is randomly chosen to divide (biased by fitness) at which time the cell has a probability u of producing mutated offspring that can metastasize (a type-1 cell) with fitness r_1 (where a fitness of 1 is neutral). This mutated offspring also now has a probability q of being 'exported' from the population to initiate a metastatic tumor of their own (Fig. 9.4). Results for a range of parameter combinations were calculated both analytically and by exact stochastic simulation. The authors found that initiating tumors with different parameter combinations could lead to qualitatively different outcomes: the model predicted that metastatic clones are most likely the result of advantageous mutations that will occupy the majority of the primary tumor. Indeed, for a mutation that confers metastatic potential and simultaneously a lower fitness in the primary tumor, there must be approximately a million-fold increase in metastatic potential for it to generate the same number of metastases in a patient.

Dingli et al. [15] extended the previous model by Michor et al. [14] by allowing tumors to grow above a constant size, and incorporating a dependence on tumor size in the export probability. The authors suggested that certain types of mutations confer a fitness advantage ($r_1 > 1$) and metastatic ability (e.g. mutations in RAS and MYC), and can dominate the tumor and seed many metastases; while other types of mutations (such as MSG) have a lower relative fitness as compared to non-mutants ($r_1 < 1$) and can therefore co-exist only in small populations and can even be 'exported' entirely, depending on the export rate (q). This insight provides an explanation for the situation in which there exists metastatic disease without evidence for cells with metastatic potential in the primary, or in the more extreme case where there is no evidence of a primary tumor at all [16].

To consider this model in a more clinically grounded context, Haeno and colleagues [17] studied a new metric, total tumor burden, which they tied to survival. In this study, the aforementioned model was extended and the timing of interventions, which included surgery (removal of a fraction of type-0 and type-1 cells; those residing in the primary tumor) and chemotherapy (affecting birth and death rates for all cells) was incorporated. The authors used threshold values for total tumor burden to correlate with time of diagnosis and patient death and investigated the effect of each of the therapies. They found that, depending on how a simulated patient's tumor was situated in parameter space (the relative rates of acquisition of the metastatic phenotype, u, 'export' of the metastatic cells to foreign stroma, q, and the birth-death balance (r_0, r_1) of each cell type), qualitatively different outcomes could be obtained from therapies given at different times. While currently beyond our abilities to tie to clinical data, this model served to illustrate how such a technique could shed light on the metastatic processes in play for a patient, and potentially influence treatment choice.

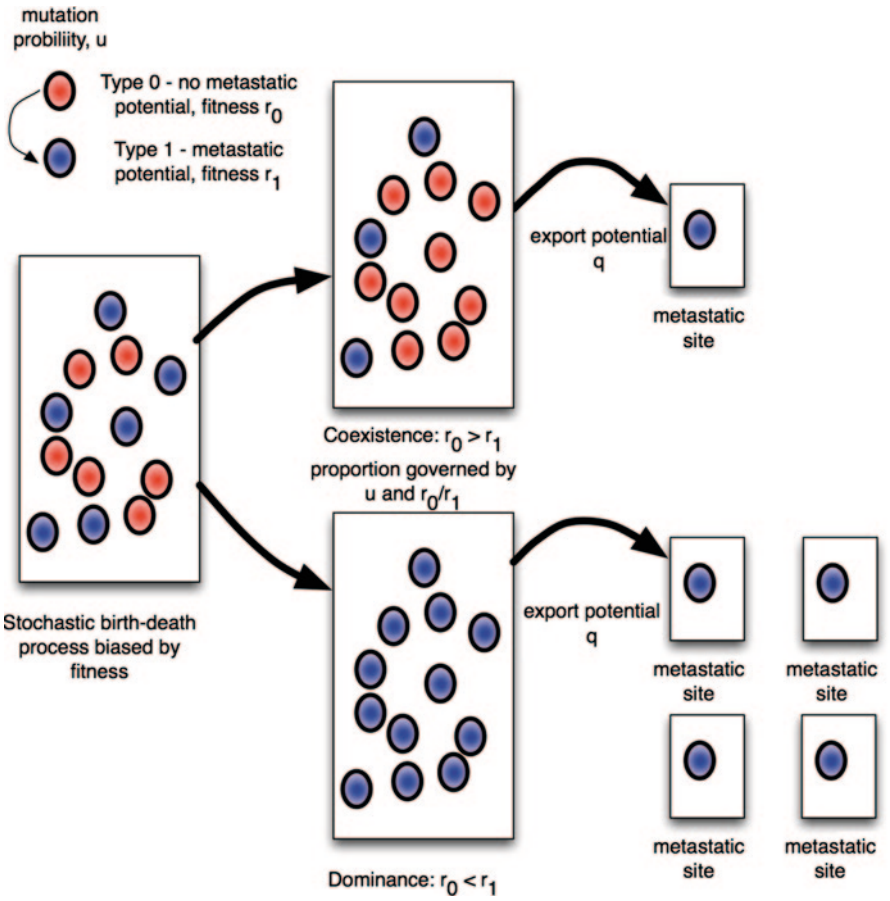

Fig. 9.4 The Moran process as utilized to study the emergence of metastasis [14–16]. The primary tumor (*left*) is allowed to grow and turn over, the population changing based on the probability of mutation, u, and the relative fitness of the two cell types, r_0 and r_1. As cells gain the ability to metastasize (mutate into *type 1* cells) they also have the opportunity, at rate q, to be exported and begin their own colonies. At steady state, the primary tumor can be composed of either all type 1 cells (dominance, when $r_1 > r_0$) or a coexistence with the proportions of cells governed by the mutation u and the fitness ratio r_1/r_0

9.4.2 Metastatic Colony Size Distribution

At present there is a single designation in the standard clinical cancer staging system (the TNM system, which describes the primary *T*umour, any positive lymph *N*odes and any *M*etastasis) to describe metastatic disease: either M0 for a patient with no observable metastasis, or M1 for a patient with *any amount* of metastatic

disease; yet there can be great variation in both size and location of metastases from one patient to another. Historically, patients with any amount of metastatic disease have only been offered localized treatment at those metastatic sites if they caused a specific problem, but not with curative intent (with several specific exceptions, e.g. solitary brain metastasis in lung cancer). This paradigm is beginning to change with the advent of the concept of 'oligometastasis' describing the situation where a patient may have only a small number of metastases, a number worth treating. While only a small number of trials have been conducted [18, 19], this approach is gaining in popularity with the increased availability of highly targeted, minimally invasive therapeutic modalities such as stereotactic body radiation therapy. The main problem confronting this movement, however, is our lack of understanding of which situations represent 'oligometastasis'. That is, which patient with one obvious metastatic lesion actually has many other, subclinical ones, and which does not? To answer this question, a number of mathematical models have been developed in an attempt to understand the distribution of sizes of metastatic lesions in time.

One such study is that of Iwata et al. [20], in which computed tomography (CT) images of spatially separated colonies of hepatocellular carcinoma in a patient's liver were fit to a novel PDE model of colony size. In their system the population of tumors was modeled as a distribution of colony size over time. Each colony was assumed to grow by a saturating growth function (specifically Gompertzian growth, though any growth law could have been used [21]) and release metastatic cells at a rate proportional to the volume of the colony raised to some power, effectively representing the fractal dimension of the blood supply of the tumor [22, 23].

Using three successive scans of the patient's tumor progression without therapy, and several after initiation of chemotherapy, the model parameters were fit and predictions about the pre-diagnosis time course could be made. Further, and likely of greater import, predictions about subclinical metastatic burden at the time of diagnosis were made. This sort of information, which is currently not available to clinicians, represents a class of personalized information about a patient's disease that does not rely on genomic information, and could be measured for any patient who already has scans taken during the course of standard therapy. This approach, of using scans which are 'standard of care', is being utilized in primary glioblastoma and is approaching clinical trials [24], but the model of Iwata et al. represents the only such attempt, to our knowledge, in metastatic disease.

The same question that was addressed with a deterministic model by Iwata et al. [20] has been addressed using a number of stochastic modeling techniques. Bortoszyinski et al. [25], Hanin et al. [26] and Xu et al. [27] used similar growth laws as discussed by Iwata et al. and then derived expressions called joint distribution functions, which predicted the probability of there being a given distribution of metastatic colony sizes at a given time. The authors then each validated their models against a single patient's data. The models, after fitting, were also able to predict several salient features about the patients' pre-diagnosis condition and the natural history of their disease.

9.4.3 Understanding Temporal Recurrence Patterns

9.4.3.1 Tumor Dormancy

The mechanisms and timing of distant recurrence of cancers after treatment of the primary tumor remain difficult to study in the clinic. It is widely believed that most patients have sub-clinical micrometastatic disease at the time of diagnosis, the distribution of which we discussed in the previous section, but that only some of them will go on to develop overt metastasis. The reasons for this are largely unknown even though there is a large literature [28], both experimental and theoretical, surrounding the period of so-called 'tumor dormancy'.

After definitive therapy for most primary cancers, the majority of distant recurrences occur in the first two years, mostly due to micrometastatic disease that was undetected at the time of primary therapy that eventually grew to a detectable size. Demicheli and colleagues [29] however, noted a bimodal distribution of relapse times for patients treated in the Milan trial of primary surgery for breast cancer. One peak was in the expected range, at 18 months, while the other was a broader peak centered at 60 months after surgery. To understand this long lag time, Retsky, Demicheli and colleagues [30, 31] proposed a new mechanism of cancer dormancy and recurrence. They posited that micrometastases that exist at the time of surgery can be activated by the subsequent inflammation into a non-dormant state. To illustrate their hypothesis they built a stochastic model of micrometastasis dormancy in which metastatic sites exist in one of three states: dormant single cells, colonies arrested at the avascular limit, and growing colonies. In their simulations they allowed for stochastic transitions between these states (assuming the transition was to a larger state) and showed that this model could recapitulate the unexpected bimodal distribution of the large clinical trial—but only if they allowed for a transition 'bonus' added at the time of surgery (Fig. 9.5). Their results have been used to argue for differing chemotherapy schedules as well as suppression of inflammation at the time of primary surgery [32, 33].

Another explanation for variable dormancy times is related to the cancer stem cell hypothesis. This well-known hypothesis has been modeled extensively for a number of different tumors (for a review, see Michor [34]), but has only received limited attention in connection to dormancy and metastasis. Enderling and colleagues pioneered this work and showed, using a stochastic model of cellular hierarchy within a tumor, that single cancer stem cell-driven solid microtumors may undergo long periods of dormancy despite cellular activity [35]. The length of the dormancy period depends on the complex interplay between stem cells and their non-stem cancer cell counterparts. Specifically, they found that impaired cancer stem cell migration, as well as large numbers of non-stem cancer cells, increase population dormancy times. Higher non-stem cancer cell death rates were correlated with shorter dormancy times and, paradoxically, with increased tumor growth in the long term [35–37]. This 'tumor growth paradox' was also explored in an analytical model by Hillen et al. [38] and was put forward as an explanation for some of the failures of therapy [39].

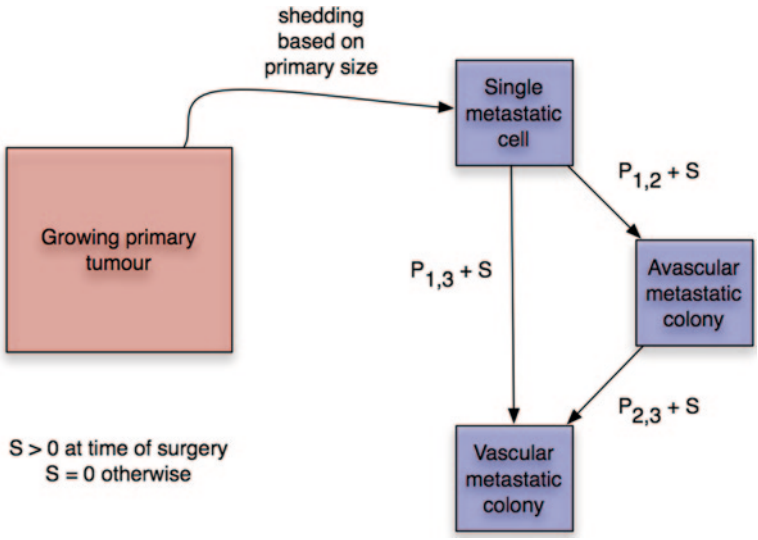

Fig. 9.5 The model posited by Retsky et al. [30]. The primary tumor (*red*) is allowed to grow and randomly seed single metastatic cells. The single cells can switch state stochastically to become growing colonies which are constrained by an avascular limit ($P_{1,2}$) or which are vascularized ($P_{1,3}$). In order to fit the results of this model to bimodal recurrence pattern of the Milan trial [29], they needed to effect a 'bonus' to the transition probabilities at the time of surgery (S), which led to the hypothesis that there is a metastasis promoting role by peri-surgical inflammation

9.4.3.2 Primary-Secondary Communication

The idea that primary tumor factors can affect the growth of metastases has also been modeled by considering communication between the primary tumor and secondary metastatic deposits. Boushaba and colleagues [40, 41] considered an anti-angiogenic factor secreted by the primary which would keep spatially separated, yet local, metastases in a dormant state and reported a critical distance window in which this effect was active. This result is difficult to interpret in hematogenous metastasis as the idea of a diffusion 'distance' for any factor secreted by the primary is not trivially understood because of the fluid dynamics involved in blood flow as compared to diffusion through tissue. A different study, by Eikenberry et al. [42], considered the effect of the primary on metastatic deposits through interactions mediated by the immune system. They modeled the removal of the primary as a decrease in immune stimulus, which in turn could promote metastatic growth. A mechanism-agnostic model analyzed by Diego et al. showed primary-secondary communication to have an effect on metastatic growth, but only in a very small region of parameter space [43], suggesting that, while possible, this is a rare phenomenon. While there is a growing theoretical literature on this subject, the clinical data to support its import are lacking and the data in biological model systems have been shown in only a few studies, reviewed by Peeters et al. [44], and therefore it is difficult to draw any solid conclusions at this time.

9.5 Making Sense of Existing Data on Patterns of Spread

We have now discussed mathematical models built with specific experimental systems in mind, ones designed to help explain some unmeasurable quantities in existing patients and ones for which no experiments can yet be done. The final class of models that we will discuss were derived in order to analyze existing, population level data of metastatic spread, with the aim of making predictions about the most likely routes of spread. The aim of these models is not to examine and quantify the involved substeps (such as the models by Liotta et al. [8–10]), but instead they focus on the 'global' system dynamics.

9.5.1 Metastasis Dynamics on Networks

Understanding the patterns of spread of a particular primary tumor can help guide clinicians in their decision making for patients. This knowledge is useful for follow up purposes in that we can target our interrogations to the organs most likely at risk so as to minimize testing and maximize our chances of early detection of recurrence. Further, understanding the temporal patterns of recurrence helps us to structure our follow up schedule and to understand when to employ the greatest vigilance, as early detection of recurrence gives the best chance of successful salvage therapy.

This temporal aspect of metastatic spread was captured in a model by Chen et al. [45], which made use of a large database of Medicare claims. The data were such that, for each patient with a primary tumor, a temporal sequence of metastatic events labeled according to anatomical location were recorded. The authors analyzed the data by calculating a time-dependent hazard as a function of the primary and metastatic site, and could observe how, given a primary in a certain location, the risk of developing certain metastatic lesions developed over time. They also formulated a statistical model with the ability to predict the location of the primary tumor given a sequence of metastatic sites, and the reverse: given a certain primary, predicting the most typical sequence of metastatic sites. The accuracy of the above predictions is, however, not yet of a quality that makes them a clinically relevant tool (the true positive rate of primary site prediction was 51 %), although the study shows the potential of this kind of temporal data when mixed with a network based approach.

In another effort to better understand the patterns and timing of metastasis, Newton et al. built and analyzed a MC model of metastatic patterns of primary lung cancers [46, 47]. By focusing on a specific cancer, rather than patterns overall, the authors hoped to be able to infer more about the mechanisms of metastasis than simply quantifying the patterns. When building this model, they began by constructing a network of connected organs and made the assumption that any transition is possible as a direct step, that is: a cancer can move directly from any organ to any other organ (the network connectivity is 'all to all'). Once this network was built, an

iterative, random method called the Monte Carlo method [48] was used to solve for a series of transition probabilities, which would then lead to the steady state defined by a large autopsy study of untreated patients [49]. The quantitative understanding provided by these studies goes beyond the empirical understanding clinicians have about patterns of spread from retrospective studies, and allows for a more detailed analysis of the parameters and the dynamics than is possible without these methods.

The most important insight gained from this approach was that certain sites, in the case of primary lung cancer, act differently than others, and that these differences affect the metastatic patterns of the disease as a whole. Specifically, Newton et al. [47] identify the adrenal gland and kidney as 'spreaders', which, when colonized by metastases, significantly increase the probabiliy of further organs becoming involved. They also identified regional lymph nodes, the liver and bone as 'sponges', temporally suppressing metastasis in other sites when colonized.

9.5.2 Embedding Anatomically Correct Connectivity

Each of the previous studies which has utilized a network-theoretic approach has assumed 'all to all' connectivity. In the case of hematogenous metastasis however, there is a simple and conserved network architecture (that of the vasculature) that significantly reduces the complexity of the problem and further, and more importantly, offers the possibility for patient specific modeling and prediction—something that the previous models are unable to do. Specifically, the human vascular network can be written down very simply as a directed network which is weighted by relative blood flow and capillary bed filtration. Scott and colleagues recently postulated a series of hypotheses based on this anatomically informed network [50]: that the specific filtration characteristics of each organ, modulated by the biology of the circulating tumor cells (CTCs), would significantly affect the half-life of CTCs in the circulation; that one could solve for metastatic patterns by knowing a patient's specific filtration characteristics, much like one could solve for quantities within an electric circuit; and that treatment could be personalized, based on CTC measurements from each of the vascular compartments, and knowledge of the primary tumor location.

In subsequent theoretical work, Scott et al. examined the self-seeding hypothesis [51] and showed that direct self-seeding (i.e. the primary tumor shedding cells that directly returned to the primary), which they dubbed 'primary seeding', was many orders of magnitude less likely than 'secondary seeding', the process by which cells from the primary metastasize to a secondary location, grow and then re-shed progeny into the vasculature which then return to the primary. This distinction, while difficult or currently impossible to measure in the clinic, is of chief importance, as it suggests that there are levels of detail about extant disease that are not captured in the previous models. Specifically that the direct organ-organ 'transitions' that were suggested by Newton et al. [47] could instead be meta-phenomena reflecting more

than one transition, meaning that information could be missed concerning the location of metastatic colonies.

While we learn about the population-level propensity and temporal dynamics of spread from the models of Chen [45] and Newton [46, 47], what is lacking is a framework by which these models could be applied to an individual patient. In order to make these models applicable to individual patients, and not just more accurate statements about population level data, we have to be able to tie them to clinical measurements. While the model of Scott and colleagues is based on a highly heterogeneous selection of experiments [51], the underlying framework is one that can be utilized in a patient-specific manner, a non-genetic application of the concept of 'personalized medicine'. Specifically, measurements of CTCs could be taken from the individual compartments (arterial, venous and portal venous, respectively, red, blue and purple in Fig. 9.6) and used to infer the existence of subclinical metastatic disease. This information would provide a better understanding of the overall tumor burden and would allow for clinical trials to test the utility of organ directed therapy or localized therapies, depending on the patient specific clinical data.

9.6 The Way Forward: Communication and Iterative Multi-Disciplinary Science

Mathematical models have several roles to play in the clinical and biological sciences. The models presented in this review have highlighted a disparate set of these roles, including generation of novel hypotheses, explanation of phenomena which could not be described with existing, 'cartoon' models, and prediction of patterns of spread. We have specifically discussed a number of models of the metastatic process which lend insight to several different aspects of the process. These insights include: the dynamics of the emergence of metastatic potential, the distribution of size of metastases through time, the possible mechanisms responsible for tumor dormancy, the patterns of spread of primary tumors, and possible mechanisms driving these patterns.

These theoretical models never stand alone in the scientific process, but they do represent an underutilized tool in the biological sciences, and particularly in the study of metastasis. Metastasis remains the most important, lethal, and enigmatic part of cancer, and while we have been 'waging war' against this disease for nearly 50 years, our progress has been limited. Indeed, the limited scope of this review, which covers all of the theoretical work, to our knowledge, in this critical component of cancer progression, highlights the dire need for more work in this area. More and more we are finding that scientists working alone are not able to make as much progress as they could working together—and indeed this has been the case in metastasis. Going forward, scientists from disparate fields, including the

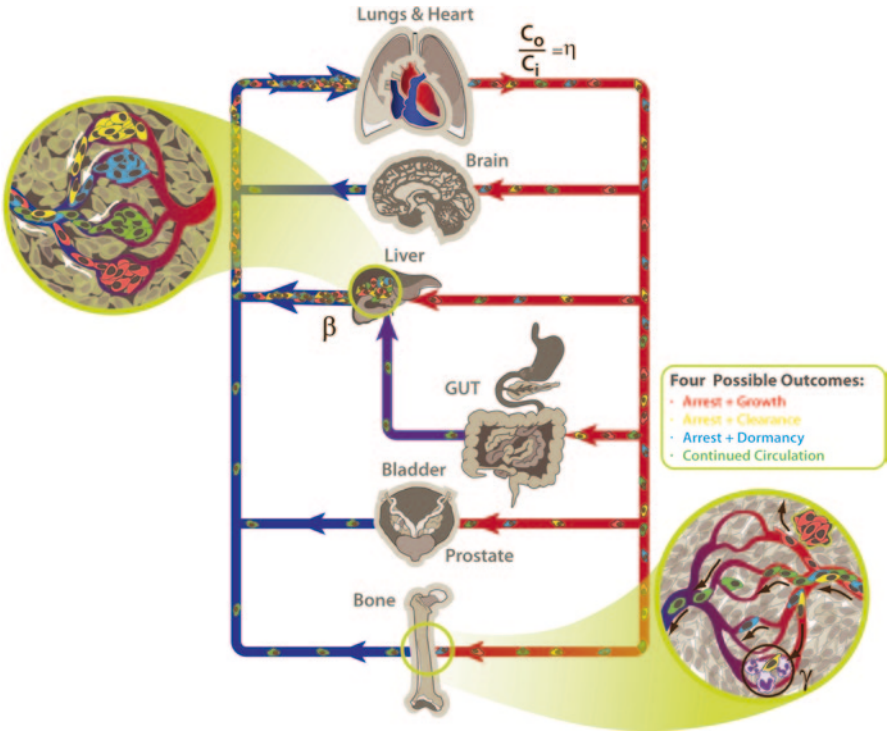

Fig. 9.6 The human vascular system represented as a network to illustrate the filter/flow perspective. From this perspective, several new quantities can be calculated for an individual patient which could be used to tailor therapy in a personalized way. Specifically: η, the filtration fraction, which is the proportion of CTCs that are able to traverse a given capillary bed; β, the shedding rate of an individual tumor; and, the number of CTCs in the each of the three distinct compartments (arterial, *red*; port venous, *purple*; and, systemic venous, *blue*). A knowledge of each of these could, for an individual patient, be used to better understand the individual's risk of metastatic spread

mathematical/theoretical disciplines, must open and foster dialogues between one another, for if we aim to understand, and therefore interrupt, this complex and nonlinear process, we have to work integrate and work together [52].

Acknowledgment The authors would like to thank Katya Kadyshevskaya at the Scripps Institute for help in preparing Fig. 9.6. JGS would like to thank the NIH Loan Repayment Program for support. AGF is funded by the EPSRC and Microsoft Research, Cambridge through grant EP/I017909/1. PG, DB, ARAA and JGS gratefully acknowledge funding from the NCI Integrative Cancer Biology Program (ICBP) grant U54 CA113007 and the PM thanks Physical Sciences in Oncology Centers U54 CA143970.

References

1. Britta W, Peterse JL, van't Veer LJ (2005 Aug) Breast cancer metastasis: markers and models. Nat Rev Cancer 5(8):591–602
2. Bos PD, Zhang XH-F, Nadal C, Shu W, Gomis RR, Nguyen DX, Minn AJ, van de Vijver MJ, Gerald WL, Foekens JA, Massagu J (2009 June) Genes that mediate breast cancer metastasis to the brain. Nature 459(7249):1005–1009
3. Minn AJ, Gupta GP, Siegel PM, Bos PD, Shu W, Giri DD, Viale A, Olshen AB, Gerald WL, Massagu J (2005 July) Genes that mediate breast cancer metastasis to lung. Nature 436(7050):518–524
4. Norton L, Massagu J (2006 August) Is cancer a disease of self-seeding? Nat Med 12(8):875–878
5. Norris J (2008) Markov Chains. Cambridge University Press
6. von Neumann J, Burks AW (1966) Theory of Self-Reproducing Automata. University of Illinois Press
7. Moran PAP (1962) The statistical processes of evolutionary theory. Clarendon, Oxford
8. Saidel GM, Liotta LA, Kleinerman J (1976 February) System dynamics of metastatic process from an implanted tumor. J Theoret Biol 56(2):417–434
9. Liotta LA, Saidel GM, Kleinerman J (1976 September) Stochastic model of metastases formation. Biometrics 32(3):535–550
10. Liotta LA, Delisi C, Saidel G, Kleinerman J (1977 September) Micrometastases formation: a probabilistic model. Cancer letters 3(3–4):203–208
11. Liotta LA, Kleinerman J, Saidel GM (1974 May) Quantitative relationships of intravascular tumor cells, tumor vessels, and pulmonary metastases following tumor implantation. Cancer Res 34(5):997–1004
12. Chaffer CL, Weinberg RA (2011 May) A perspective on cancer cell metastasis. Science 331(6024):1559–1564
13. Thiery JP (2003 Dec) Epithelial-mesenchymal transitions in development and pathologies. Curr Opin Cell Biol 15(6):740–746
14. Michor F, Nowak MA, Iwasa Y (2006 June) Stochastic dynamics of metastasis formation. J Theoret Biol 240(4):521–530
15. Dingli D, Michor F, Antal T, Pacheco JM (2007 March) The emergence of tumor metastases. Cancer Biol Therap 6(3):383–390
16. Greco FA (2012 Aug) Cancer of unknown primary site: evolving understanding and management of patients. Clin Adv Hematol Oncol 10(8):518–24
17. Haeno H, Michor F (2010 March) The evolution of tumor metastases during clonal expansion. J Theor Biol 263(1):30–44
18. Milano MT, Zhang H, Metcalfe SK, Muhs AG, Okunieff P (2009 June) Oligometastatic breast cancer treated with curative-intent stereotactic body radiation therapy. Breast Cancer Res Treat 115(3):601–8
19. Milano MT, Katz AW, Zhang H, Okunieff P (2012 July) Oligometastases treated with stereotactic body radiotherapy: long-term follow-up of prospective study. Int JRadiat Oncol Biol Phys 83(3):878–86
20. Iwata K, Kawasaki K, Shigesada N (2000 March) A dynamical model for the growth and size distribution of multiple metastatic tumors. J Theor Biol 203(2):177–186
21. Gerlee P (2013 Feb) The model muddle: in search of tumour growth laws. Cancer Res 73(8):2407–2411
22. Baish JW, Jain RK (1998 Sep) Cancer, angiogenesis and fractals. Nat Med 4(9):984
23. Baish JW, Jain RK (2000 July) Fractals and cancer. Cancer Res 60(14):3683–8
24. Neal ML, Trister AD, Cloke T, Sodt R, Ahn S, Baldock AL, Bridge CA, Lai A, Cloughesy TF, Mrugala MM, Rockhill JK, Rockne R C, Swanson KR (2013) Discriminating survival outcomes in patients with glioblastoma using a simulation-based, patient-specific response metric. PLoSOne 8(1):e51951

25. Bartoszyński R, Edler L, Hanin L, Kopp-Schneider A, Pavlova L, Tsodikov A, Zorin A, Yakovlev AY (2001 June) Modeling cancer detection: tumor size as a source of information on unobservable stages of carcinogenesis. Math Biosci 171(2):113–42
26. Hanin L, Rose J, Zaider M (2006 Dec) A stochastic model for the sizes of detectable metastases. J Theor Biol 243(3):407–417
27. Xu JL, Prorok PC (1998 Sept) Estimating a distribution function of the tumor size at metastasis. Biometrics 54(3):859–864
28. Piez D, Labonte MJ, Bohanes P, Zhang W, Benhanim L, Ning Y, Wakatsuki T, Loupakis F, Lenz H-J (2013 Feb) Cancer dormancy: a model of early dissemination and late cancer recurrence. Clin Cancer Res 18(3):645–53
29. Demicheli R, Abbattista A, Miceli R, Valagussa P, G Bonadonna (1996) Time distribution of the recurrence risk for breast cancer patients undergoing mastectomy: further support about the concept of tumor dormancy. Breast Cancer Res Treat 41(2):177–85
30. Retsky MW, Demicheli R, Swartzendruber DE, Bame PD, Wardwell RH, Bonadonna G, Speer JF, Valagussa P (1997 Sept) Computer simulation of a breast cancer metastasis model. Breast Cancer Res Treat 45(2):193–202
31. Demicheli R, Retsky MW, Swartzendruber DE, Bonadonna G (1997 Nov) Proposal for a new model of breast cancer metastatic development. Ann Oncol 8(11):1075–80
32. Demicheli R, Retsky MW, Hrushesky WJM, Baum Michael (2007 Dec) Tumor dormancy and surgery-driven interruption of dormancy in breast cancer: learning from failures. Nat Clin Pract Oncol 4(12):699–710
33. Retsky M, Demicheli R, Hrushesky WJm, Forget P, De Kock M, Gukas I, Rogers RA, Baum M, Pachmann K, Vaidya JS (2012) Promising development from translational or perhaps antitranslational research in breast cancer. Clin Transl Med 1(1):17
34. Michor F (2008 June) Mathematical models of cancer stem cells. J Clin Oncol: Offic J Am Soc Clin Oncol 26(17):2854–2861
35. Enderling H, Anderson ARA, Chaplain MAJ, Beheshti A, Hlatky L, Hahnfeldt P (2009 Nov) Paradoxical dependencies of tumor dormancy and progression on basic cell kinetics. Cancer Res 69(22):8814–8821
36. Enderling H, Hahnfeldt P, Hlatky L, Almog N (2012 May) Systems biology of tumor dormancy: linking biology and mathematics on multiple scales to improve cancer therapy. Cancer Res 72(9):2172–5
37. Enderling H (2013) Cancer stem cells and tumor dormancy. Adv Exp Med Biol 734:55–71
38. Hillen T, Enderling H, Hahnfeldt P (2013 Jan) The tumor growth paradox and immune system-mediated selection for cancer stem cells. Bull Math Biol 75(1):161–84
39. Gao X, McDonald JT, Hlatky L, Enderling Heiko (2013 Jan) Acute and fractionated irradiation differentially modulate glioma stem cell division kinetics. Cancer Res 73(5):1481–1490
40. Boushaba Khalid, Levine HA, Nilsen-Hamilton M (2006 Oct) A mathematical model for the regulation of tumor dormancy based on enzyme kinetics. Bull Math Biol 68(7):1495–526
41. Kim Y, Boushaba K (2013) Regulation of tumor dormancy and role of microenvironment: a mathematical model. Adv Exp Med Biol 734:237–59
42. Eikenberry S, Thalhauser C, Kuang Y (2009 Apr) Tumor-immune interaction, surgical treatment, and cancer recurrence in a mathematical model of melanoma. PLoS ComputBiol 5(4):e1000362
43. Diego D, Calvo GF, Prez-Garca VM (2012 July) Modeling the connection between primary and metastatic tumors. J Math Biol:1–36
44. Peeters CFJM, de Waal RMW, Wobbes T, Ruers TJM (2008 Nov) Metastatic dormancy imposed by the primary tumor: does it exist in humans? Ann Surg Oncol 15(11):3308–15
45. Chen LL, Blumm N, Christakis NA, Barabsi A-L, Deisboeck TS (2009 Sept) Cancer metastasis networks and the prediction of progression patterns. Br J Cancer 101(5):749–758
46. Newton PK, Mason J, Bethel K, Bazhenova LA, Nieva J, Kuhn P (2012) A stochastic Markov chain model to describe lung cancer growth and metastasis. PloS one 7(4):e34637

47. Newton PK, Mason J, Bethel K, Bazhenova L, Nieva J, Norton L, Kuhn P (2013 Feb) Spreaders and sponges define metastasis in lung cancer: A Markov chain mathematical model. Cancer Res 73(9):2760–2769
48. Diaconis P (2009 April) The markov chain monte carlo revolution. Bullet Am Math Soc 46(2):179–205
49. Disibio Guy, French SW (2008 June) Metastatic patterns of cancers: results from a large autopsy study. Arch Pathol Lab Med 132(6):931–939
50. Scott J, Kuhn P, Anderson ARA (2012 July) Unifying metastasis–integrating intravasation, circulation and end-organ colonization. Nat Rev Cancer 12(7):445–6
51. Scott JG, Basanta D, Anderson ARA, Gerlee P (2013) A mathematical model of tumour self-seeding reveals secondary metastatic deposits as drivers of primary tumour growth. J Royal Soc, Interface/Royal Soc 10(82):20130011
52. Anderson ARA, Quaranta V (2008) Integrative mathematical oncology. Nat Reviewscancer 8(3):227–234

Index

A. Malek (ed.), *Experimental Metastasis: Modeling and Analysis,*
DOI 10.1007/978-94-007-7835-1,